Elucidating regulators of red blood cell development in health and disease

Sen, Taha

2021

Document Version:
Publisher's PDF, also known as Version of record

Elucidating regulators of red blood cell development in health and disease

Taha Sen

LUND
UNIVERSITY

DOCTORAL DISSERTATION

by due permission of the Faculty of Medicine, Lund University, Sweden.
To be defended at I1345, BMC, Lund University
2021, November 17th, 13.00.

Faculty opponent
Professor James Palis
University of Rochester Medical Center,
Rochester, NY, USA

Organization
LUND UNIVERSITY
Division of Molecular Medicine and Gene Therapy
Institution of Laboratory Medicine
Author Taha Sen

Document name

Date of issue

Sponsoring organization

Elucidating regulators of red blood cell development in health and disease

Red blood cells are are plentiful, flexible and essential. They are the most abundant cell in our body and their main object is to carry oxygen, which is essential for cellular respiration. The formation of red blood cells is called erythropoiesis. Erythropoiesis is intimately coupled to cell division and mitochondrial function. Aberrations in these two processes are often associated with red blood cell disorders, which result in anemia. Anemia is characterized by the lack of red blood cells and/or reduced hemoglobin concentrations resulting in reduced oxygen transport to the tissue and inevitable to reduced quality of life and increased mortality. My aim in this thesis has been to deepen our understanding of how erythropoiesis is regulated in health and disease

In the first paper we demonstrated that anemia caused by pRb deficiency was due to disrupted differentiation with underlying impairment to mitochondrial function at the orthochromatic erythroblast stage. The MDS-like phenotype of pRb deficient mice could be rescued by enhanced PPAR pathway signaling, an important signaling axis in mitochondrial biogenesis, in vivo either genetically or therapeutically.

In the second paper we translated our findings in the mouse to a human setting by inhibiting PPAR signaling. We demonstrated that perturbed PPAR signaling in human hematopoietic stem/progenitor cells from both bone marrow and cord blood results in impaired formation of early erythroid progenitors and delayed terminal erythroid differentiation in vitro. We showed that PPAR signaling is important for iron, heme and globin homeostasis. Furthermore we demonstrated that PPAR signaling affects cell cycle exit indicating that there is a mutual regulation between cell cycle progression and mitochondrial function during terminal erythropoiesis.

In the third paper we demonstrated that Ypel4, which is highly expressed in orthochromatic erythroblasts, is important for the integrity of red blood cell membrane. Ypel4 null erythroblast had reduced deformability and were cleared at an increased rate. The phenotype resembled defects normally observed in human hereditary membrane disorders.

Overall the papers included in this thesis highlight mechanisms and genes important for terminal erythropoiesis specifically in the orthochromatic erythroblast. We further described disease associated with the different perturbations to erythropoiesis. The work presented here could therefore be important in developing novel treatments for red blood cell disorders.

Key words Erythropoiesis, anemia, mitochondria, MDS, membrane disorders

Classification system and/or index terms (if any)

Supplementary bibliographical information		Language English
ISSN 1652-8220		ISBN 978-91-8021-128-4
Recipient's notes	Number of pages 81	Price
	Security classification	

Signature  Date 2021-10-14

Elucidating regulators of red blood cell development in health and disease

Taha Sen

LUND
UNIVERSITY

Coverphoto by Hamit Sen

Lund University, Faculty of Medicine, Department of Laboratory Medicine
Lund Stem Cell Center, Division of Molecular Medicine and Gene Therapy

Lund University, Faculty of Medicine Doctoral Dissertation Series 2021:121
ISBN 978-91-8021-128-4
ISSN 1652-8220

Printed in Sweden by Media-Tryck, Lund University
Lund 2021

To my parents

Table of Contents

Papers included in thesis

Paper I

Enhancing mitochondrial function in vivo rescues MDS-like anemia induced by pRb deficiency

Taha Sen, Mayur Jain, Magnus Gram, Alexander Mattebo, Shamit Soneji, Carl R. Walkley, Sofie Singbrant

Experimental Hematology, Volume 88, 2020, Pages 28-41

Paper II

Decreased PGC1β expression results in disrupted human erythroid differentiation, impaired hemoglobinization and cell cycle exit

Taha Sen, Jun Chen & Sofie Singbrant

Scientific Reports, Volume 11, Article number: 17129 (2021)

Paper III

Yippee like 4 (Ypel4) is essential for normal mouse red blood cell membrane integrity

Alexander Mattebo, **Taha Sen**, Maria Jassinskaja, Kristýna Pimková, Isabel Prieto González-Albo, Abdul Ghani Alattar, Ramprasad Ramakrishnan, Stefan Lang, Marcus Järås, Jenny Hansson, Shamit Soneji, Sofie Singbrant, Emile van den Akker, and Johan Flygare

Scientific Reports, Volume 11, Article number 15898 (2021).

Abbreviations

AGM	Aorta-Gonad-Mesonephros
BasoE	Basophilic Erythroblast
BFU-E	Burst Forming Unit Erythroid
BM	Bone Marrow
CDK	Cyclin Dependent Kinase
CFC	Colony Forming Cell
CFU-E	Colony Forming Unit Erythroid
CLP	Common Lymphoid Progenitor
CKI	Cyclin Dependent Kinase Inhibitors
CMP	Common Myeloid Progenitor
E	Embryonic Day (mouse)
EHT	Endothelial-to-Hematopoietic Transition
EMP	Erythro-Myeloid Progenitor
EPO	Erythropoietin
EpoR	Erythropoietin Receptor
ESA	Erythropoiesis Stimulating Agents
ETC	Electron Transport Chain
FACS	Fluorescence-Activated Cell Sorting
FL	Fetal Liver
GC	Glucocorticoid
GM-CSF	Granulocyte/Macrophage Colony Stimulating Factor
GMP	Granulocyte/Macrophage Progenitor
HE	Hemogenic Endothelium
HIF	Hypoxia-Inducible Factor
HSC	Hematopoietic Stem Cell
HSPC	Hematopoietic Stem and Progenitor Cell
IL	Interleukin
MDS	Myelodysplastic Syndromes
MEP	Megakaryocyte/Erythroid Progenitor
MPP	Multipotent Progenitor

mtDNA	Mitochondrial DNA
OrthoE	Orthochromatic Erythroblast
OXPHOS	Oxidative phosphorylation
PGC1b	PPAR gamma coactivator 1b
PolyE	Polychromatophilic Erythroblast
PPAR	Peroxisome proliferator-activated receptors
pRb	Retinoblastoma protein
ProE	Proerythroblast
RARS	Refractory Anemia with Ring Sideroblasts
RBC	Red Blood Cell
ROS	Reactive Oxygen Species
SCF	Stem Cell Factor
TCA	Tricarboxylic Acid
TPO	Thrombopoietin
Tf	Transferrin
WT	Wild Type
YS	Yolk Sac

Preface

Is it not incredible that by the time you have finished this sentence your body will have produced approximately 10.000.000 new red blood cells? It is truly overwhelming when you then realize that red blood cells have a relatively slow turnover rate of 120 days compared to intestinal epithelium cells, which in turn renew every couple of days. Despite this, hematopoietic cells and specifically red blood cells have by far the highest turnover rate by weight, which places enormous responsibility on the precursor hematopoietic stem and progenitor cells that give rise to all the different lineages of blood cells. In the simplest terms, the main function of red blood cells is to carry oxygen to all your other hard working cells, from the brain to the skin on your toes. In a fashion quite similar to a roller coaster ride your red blood cells drop of the previous returning passengers (carbon dioxide) and pick up fresh passengers (oxygen) in the lung. To give you an idea on how important this analogy of a roller coaster ride is, your body would sustain severe damage within 5 minutes of this ride being out of service. For such a simple task, red blood cells do indeed have a vital role.

The significance of blood was recognized before the advent of "modern" laboratory studies. Already in ancient times, blood was described as '*the gift of life',* then often in religious context. From drinking the blood of your adversaries to bathing in blood as a rejuvenating tonic, blood has had many perplexing roles in our ancestors' lives. Although the mystical role of blood has somewhat vanished in today's society we are nevertheless left in awe when reminded of the biological complexities in both steady state production and sometimes, unfortunately, the perturbed maintenance due to certain diseases. In this thesis, I will try to give further insight into the key components of erythropoiesis, the production of red blood cells, propose novel treatment options for perturbed erythropoiesis and what role mitochondrial function has in all of this. I took on this challenge about 5 years ago having no clue why mitochondrial function was particularly important for red blood cell production. Now 5 years later I would like to share my insights on the importance of mitochondrial function in erythropoiesis.

Populärvetenskaplig sammanfattning

Våra röda blodkroppar lever i genomsnitt 120 dagar och bryts därefter ner av makrofagerna, immunsystemets medfödda städare av både främmande och egna celler. De röda blodkropparnas uppgift är att transportera syre från lungorna till kroppens olika vävnader och föra tillbaka koldioxid. Men vad händer om de röda blodkropparna bryts ner ovanligt snabbt eller helt enkelt inte produceras i tillräckligt snabbt takt med den mängd som försvinner efter 120 dagars cirkulering i våra blodkärl? Då uppstår vad vi i dagligt tal kallar blodbrist, eller anemi, och det kännetecknas av bristen på röda blodkroppar och/eller bristen på viktiga komponenter som hemoglobin. Hemoglobin är det syrebindande proteinet och är grundläggande för de röda blodkropparnas funktion.

Anemi kan uppstå på grund av en rad olika anledningar och det vanligaste är att vi inte får tillräckligt med näringsämnen som järn och vitaminer från vår föda. Med rätt förutsättningar är det en ganska enkel behandling i de fallen. Patienter med anemi upplever andfåddhet och allmän trötthet eftersom blodet saknar de syretransporterande cellerna. Mitt arbete har fokuserat på de mer svårbehandlade anemierna som uppstår i samband med defekter under produktionen av röda blodkroppar. Produktionen av röda blodkroppar regleras av erytropoietin, en proteinmolekyl som är viktig för utvecklingen och underhållet av röda blodkroppar. Extra tillskott av erytropoietin tillsammans med blodtransfusioner är de vanligaste behandlingsalternativen för patienter med anemi. Upprepade blodtransfusioner kan dock ha allvarliga biverkningar. Dessutom har de flesta patienter med kronisk anemi redan höga nivåer av erytropoietin vilket resulterar i att kroppen inte svarar på ytterligare tillskott av proteinet.

Mitt huvudsakliga forskningsmål har varit att få nya inblick i produktionen av röda blodkroppar och hur det regleras. På så vis kan man hitta nya sätt att behandla anemi. Produktionen av röda blodkroppar är väldigt beroende av en väl fungerade celldelning. Retinoblastoma proteinet (pRb) är viktig i regleringen av cellcykeln och avsaknaden av pRb orsakar därför anemi hos möss. Myelodysplastiska syndrom är en grupp av heterogena pre-leukemiska sjukdomar som orsakas av onormal utveckling i benmärgen. Patienter med dessa sjukdomar lider vanligtvis av

svårbehandlade anemier. Forskning föreslår alltmer att icke funktionella mitokondrier kan vara en av de bakomliggande orsakerna till hämmad produktion av röda blodkroppar. Utöver deras funktion som cellens kraftverk så har mitokondrierna andra viktiga roller, särskilt för bildandet av röda blodkroppar, bland annat sker tillverkningen och regleringen av hemoglobin inom mitokondrierna.

I avhandlingen presenterar jag tre studier som förklarar orsaker till hämmad blodbildning och funktion. I **studie I** demonstrerar våra resultat att icke-funktionella mitokondrier i vår musmodell orsakar MDS-liknande anemi. Genom att överuttrycka proteinet PGC1b, ett viktigt protein för mitokondriernas nybildning, kunde vi förbättra anemin. Vidare syftar vårt arbete till att hitta kliniskt mer relevanta sätt att förbättra anemi. I detta ändamål studerade vi kemiska substanser som aktiverar samma proteinkomplex som PGC1b. En i synnerhet, Bezafibrate, visade sig vara en mycket intressant kandidat eftersom den på samma sätt kunde förbättra anemi genom att normalisera antalet röda blodkroppar till friska motsvarigheter när den inkorporerades i maten till sjuka möss.

För att undersöka om resultaten från vår första studie kunde översättas till den mänskliga miljön använde vi oss av friska mänskliga blodstamceller. I **studie II** inhiberade vi uttrycket av PGC1b i blodstamcellerna och kunde där bekräfta att det resulterar i en försenad utveckling av röda blodkroppar med brister i hemoglobinproduktion, cellcykelreglering och storleken på unga röda blodkroppar. Dessa resultat tyder på att det finns en ömsesidig reglering mellan mitokondrier och cell cykeln under bildandet av röda blodkroppar. I **studie III** undersökte vi ett annat protein , YPEL4, som har ökat uttryck i föregångarna till röd blodkroppar. Möss som saknar *Ypel4* genen har inte anemi i sin vanliga bemärkelse. Däremot verkar YPEL4 proteinet vara viktig i bevarandet av röda blodkroppars integritet. Röda blodkroppar som saknar YPEL4 städas undan snabbare än deras friska motsvarigheter för att de är större och har sämre deformerbarhet, en viktig egenskap för röda blodkroppar då de måste färdas genom trånga kärl.

Sammanfattningsvis presenterar den här avhandlingen viktiga aspekter av bildandet och funktionen av röda blodkroppar. Studie I och II visar att mitokondriernas funktion faktiskt har en viktig roll i nybildningen av röda blodkroppar, både hos möss och också människor. Med studie III identifierade vi att Ypel4 är viktigt för röda blodkroppars struktur vilket är ett viktigt första steg för potentiell framtida behandling av anemi som istället orsakas av strukturella svagheter i cellernas membran.

Özet

Kırmızı kan hücreleri ortalama 120 gün hayatta kalır, ardından bağışıklık sistemimizin doğuştan gelen 'temizleyici hücreleri' olan makrofajlar tarafından parçalanırlar. Kırmızı kan hücrelerinin görevi, akciğerlerden vücudun çeşitli dokularına oksijen taşımak ve akciğerlere karbondioksiti getirmektir. Peki kırmızı kan hücreleri olması gerektiğinden daha yavaş üretilir veya daha hızlı parçalanarak dolaşımda bulunmaları gereken 120 günlük süre içinde tüketilirse ne olur? Bu durumda, kırmızı kan hücrelerinin ve/veya hemoglobin gibi önemli bileşenlerin eksikliği ile karakterize edilen ve halk dilinde kansızlık olarak bilinen anemi ortaya çıkar. Hemoglobin, oksijenin kanda taşınmasını sağlayan bir proteindir ve kırmızı kan hücrelerinin fonksiyonu için oldukça önemlidir.

Anemi birçok nedenle ortaya çıkabilir fakat en yaygın sebep vücudumuzun tükettiğimiz besinlerden demir ve vitamin gibi bileşikleri yeterli miktarda alamamasıdır. Bu tür durumlarda alınacak demir takviyesi kolay bir tedavi yöntemidir. Anemi hastaları, kanda oksijen taşıyan hücrelerin eksikliğinden dolayı nefes darlığı ve genel bir yorgunluk hali yaşarlar. Ben bu çalışmamda, kırmızı kan hücrelerinin üretim aşamasındaki kusurlardan kaynaklanan ve tedavisi nispeten daha zor olan anemilere odaklandım. Eritropoetin; kırmızı kan hücrelerini düzenleyen, gelişimleri ve sürdürülmeleri için gerekli olan bir hormondur. Kan transfüzyonuna ek olarak eritropoetin takviyesi anemi hastaları için en yaygın tedavi seçeneğidir. Fakat tekrarlanan kan transfüzyonları ciddi yan etkilere sebep olabilir. Ayrıca, kronik anemi hastalarının çoğunda eritropoetin hali hazırda yüksek seviyelerde bulunur, bu durumda vücut ek hormon takviyesine yanıt veremez.

Araştırmamdaki ana hedefim, kırmızı kan hücrelerinin üretimi ve düzenlenmesi üzerine yeni anlayışlar kazandırmak, bu sayede anemi tedavisine yeni yaklaşımlar sunabilmekti. Kırmızı kan hücrelerinin üretimi, doğru işleyen hücre bölünmeleriyle yakından ilişkilidir. Retinoblastoma proteini (pRb), hücre döngüsünün düzenlenmesi için oldukça önemlidir ve eksikliği farelerde anemiye neden olur. Miyelodisplastik sendrom (MDS), kemik iliğindeki anormal gelişimden kaynaklanan heterojen bir hastalık grubudur. MDS hastaları, tedavisi zor olan inatçı bir anemiden muzdariptir. Günden güne artan mevcut araştırmalar, mitokondrideki

işlev bozukluğunun, kırmızı kan hücrelerinin üretiminde kusurlara neden olabileceğini ileri sürmektedir. Mitokondriler, hücrenin güç merkezi olmalarının yanında kırmızı kan hücrelerinin üretilmesinde önemli rol oynarlar. Hemoglobin üretimi ve düzenlenmesi mitokondriler içinde gerçekleşir.

Tezimde sunduğum üç çalışmayla, kırmızı kan hücrelerinin üretimini ve fonksiyonunu bozan mekanizmaları açıklıyorum. İlk çalışmadaki sonuçlarımız, fonksiyonunu kaybeden mitokondrinin farelerde MDS benzeri anemiye sebep olduğunu göstermektedir. Yeni mitokondri üretimini destekleyen PGC1b geninin ifadesinin artırılmasıyla mevcut anemiyi tedavi edebildik. Çalışmamızın amacı anemiyi iyileştirebilmek için klinik olarak daha uygun yollar bulabilmekti. Bu sebeple, PGC1b ile aynı protein kompleksini aktive eden kimyasal maddeler üzerine çalıştık. Özellikle Bezafibrat bu amaçta oldukça ilginç bir aday olduğunu kanıtladı çünkü hasta farelerin öğünlerine dahil edildiğinde kırmızı kan hücrelerinin sayısını sağlıklı farelerdekine benzer şekilde normalize ederek anemiyi iyileştirdi.

Bir sonraki araştırmamızda, ilk çalışmamızdaki sonuçların insanlar üzerinde uygulanabilirliğini görmek için sağlıklı insanlardan alınan kök hücreleri inceledik. İkinci çalışmada, kök hücrelerdeki PGC1b genini baskıladık. Bu sayede bu protein üretiminin engellenmesinin; hemoglobin üretimi, hücre döngüsü ve genç kırmızı kan hücrelerinin boyutundaki kusurlara bağlı olarak yetişkin kırmızı kan hücrelerinin gelişiminde gecikmeye sebep olduğunu doğruladık. Bu sonuçlar, mitokondri ve hücre döngüsünün karşılıklı olarak kırmızı kan hücrelerinin üretimini düzenlediğini göstermiştir.

Üçüncü çalışmada, öncül kırmızı kan hücrelerinde ifadesi artan YPEL4 proteinini inceledik. YPEL4 eksikliği olan fareler anemi teşhisi almazlar, yine de kırmızı kan hücrelerinin bütünlüğünü korumada önemli bir protein gibi görünmektedir. YPEL4 proteininden yoksun kırmızı kan hücreleri daha büyük oldukları ve dar damarlardan geçebilmelerine olanak sağlayan ‘deforme olabilme’ özelliğine daha az sahip oldukları için, bu proteini kodlayan emsallerinden daha hızlı tükenirler.

Özet olarak tezim, kırmızı kan hücrelerinin üretimi ve işlevselliği üzerine önemli yaklaşımlar ortaya koymaktadır. İlk iki çalışma, mitokondri işlevselliğinin hem insan hem farelerde yeni kırmızı kan hücrelerinin oluşumunda önemli rol oynadığını göstermektedir. Üçüncü çalışmayla birlikte, Ypel4 geninin kırmızı kan hücrelerinin yapısı için önemli olduğunu gösterdik. Bu sonuç, hücre zarındaki yapısal zayıflıklardan kaynaklanan aneminin tedavisi için önemli bir adım olacaktır.

1. Hematopoiesis

Hematopoiesis, from the greek haima (blood) and poiesis (to make), is the continuous formation of blood cellular components. The hematopoietic stem cells (HSC), formed during embryogenesis, are what sustains this continuous production of blood in adult mammals. Hematopoiesis is well underway already at embryonic development, and can be divided into three distinct waves, primitive, transitory and definitive hematopoiesis. Although the specific time and place in which HSC's emerge is still debated, their ability to generate all blood cell types is undeniable. The hallmarks of a stem cell is its ability to self-renew and differentiate.

In a complex multi-step process HSC differentiate into intermediate progenitors, which become committed to specialized blood lineages. With each differentiation step, lineage commitment is further restricted, finally giving rise to mature cells. The mature specialized cells each have their own function such as oxygen transport (erythrocytes), immune response (macrophages, granulocytes, lymphocytes) and blood coagulation to stop excess blood loss from damaged vessels (platelets).

To understand adult hematopoiesis one also needs to comprehend the hematopoiesis during embryonic development. For instance, erythropoiesis, the production of red blood cells similarly has three different waves during embryogenesis with considerable differences in the final cell product. The importance of understanding the developmental biology of erythropoiesis is critical knowledge as dyserythropoiesis can manifest already during fetal development. By distinguishing similarities and dissimilarities between fetal and adult hematopoiesis one becomes better equipped in treating disrupted hematopoiesis, regardless of disease origin. In this thesis, I will describe important regulators of red blood cell production and propose novel ways to treat dyserythropoiesis in relation to specific diseases.

HSC-independent primitive hematopoieis

Distinction between the different waves of hematopoiesis during early development is important as it occurs in multiple niches with different origins. Primitive hematopoiesis is, as the name suggests, the earliest and most primitive form of hematopoiesis during early embryonal development. It is a little bit strange, because we have blood cells before we have any vasculature to carry it. With the onset of gastrulation, mesodermal precursor cells at the primitive streak give rise to the hemangioblasts, which is at the heart at of the vascular and hematopoietic system [1]. The first site of vasculogenesis and hematopoiesis occurs in the extraembryonic tissue, the yolk sac (YS). The so called "blood islands" formed by the hemangioblasts can be observed in the murine embryo already at day 7.5 (E7.5) post conceptus [2]. As the blood islands grow, they are lined with endothelial cells that eventually form the umbilical veins with the central cells giving rise to the primitive erythroblasts [3]. Unlike the adult red blood cells (RBC), primitive RBC are composed differently. Primitive erythroblasts are larger, nucleated, and express different fetal globin [4] with increased oxygen-carrying capacity and gas exchange efficiency [5]. Primitive hematopoiesis therefore reveals how essential oxygen transport is, even in the earliest stages of life. However, primitive hematopoiesis is not about RBCs only. Coincident with primitive erythroid progenitors, primitive macrophages and megakaryocyte progenitors also develop from unipotent progenitors within the blood islands of the YS. In the mouse, primitive hematopoiesis is extremely short-lived and goes on for approximately 24 hours after which the first multilineage erythro-myeloid progenitors (EMP) appear at day E8.5.

HSC-independent definitive hematopoiesis

Following the short-lived unipotent progenitors that give rise to primitive erythroblasts, macrophages and megakaryocytes within the blood islands the multilineage erythro-myeloid progenitors (EMP) appear around day E8.5 in the mouse [6]. EMPs are responsible for the second transient wave of hematopoiesis prior to HSC emergence. The EMP progenitors are Runx1 dependent and express c-Kit, CD41 and CD16/32 surface markers [7-10], differentiating them from their more primitive counterparts in the YS. EMPs are produced through a process termed endothelial-to-hematopoietic transition. Runx1 plays an essential role in this transformation of hemogenic endothelial cells within both progenitors and definitive

HSCs. Through extrinsic factors, a gene regulatory network provided by transcription factors and mechanical force, hemogenic endothelial cells undergo endothelial-to-hematopoietic transition, where they lose their cell polarity, break their tight junctions to neighboring endothelial cells and take on the rounder form of a hematopoietic cell [11-14]. The emerging EMPs then migrate to and colonize the fetal liver (FL) where they rapidly differentiate, giving rise to a second wave of erythroid progenitors that this time more closely resembles their adult counterparts [10]. The migration of EMPs begins to decline by day E10.5, however their progeny can support the survival of the embryo until birth, even in the absence of HSC [15].

HSC emergence

The concept of a HSC was developed around 60 years ago in studies that aimed to characterize radiation sensitivity. Heavily irradiated mice were transplanted with cells from the bone marrow (BM) of syngeneic donors. While the recipient's hematopoietic system was ablated due to irradiation, hematopoiesis could be reconstituted with the help from non-irradiated BM cells. The donor derived colonies formed in the spleen were macroscopically studied and determined to be of multiple hematopoietic lineages [16, 17]. Although HSCs had not yet been identified, it paved the way for continued characterization of these colony forming progenitor cells. Two very important characteristics of HSC were determined when studying the colonies, their ability to give rise to multiple hematopoietic lineages (multipotency) and their ability to retain parental characteristics (self renewal) [18]. However, the question regarding their origin still remained.

The existence of vascular endothelial cells with hemogenic properties have been hypothesized for over a century, described within several different vertebrate species [19]. Studying the chick embryo and later confirmed in mouse it was instead suggested that adult hematopoiesis was initiated in the YS and that the YS derived extraembryonic progenitors then colonized the intraembryonic sites of definitive hematopoiesis [20-22]. This was at the time most likely considered plausible due to primitive hematopoiesis taking place in the YS. However this model would be challenged by the experiments done on avian embryos where early chick yolk sacs were transplanted onto quail embryos. [23] Since the blood cells of these two species can be distinguished under the microscope it was determined that the progeny of the quail derived cells contributed to the hematopoietic cells. Furthermore, hematopoietic activity was shown to be present only in the ventral part of the aorta

[24], with this the intraembryonic vasculature would once again be called back to attention as the site of definitive hematopoietic stem cells formation.

With YS derived transitory hematopoiesis still ongoing, HSCs start to emerge at day E10.5 in the developing aorta, specifically in the aorta-gonad-mesonephros (AGM) region. The AGM region was determined to possess the ability of *de novo* HSC production, which has been demonstrated in mouse by different studies including explant studies [25, 26], in vivo imaging [27], fate tracing [28] and complemented with studies in other vertebrates such as zebrafish [29, 30]. Similar to the EMP progenitor, HSC bud off from the endothelial cells of the AGM region by the endothelial-to-hematopoietic transition [11]. HSC initially colonize the liver where they expand and then go on at E15 to colonize the main site of adult hematopoiesis, the bone marrow **(Figure 1)**.

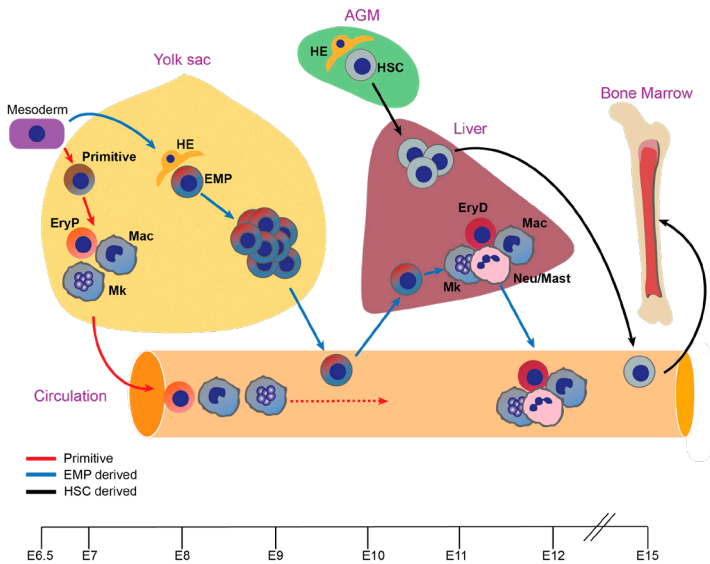

Figure 1 Sites of hematopoiesis. The yolk sac is the site where both primitive and definitive progenitors emerge from. The definitive EMP progenitors then colonize the liver where they expand. Simultaneously HSC start to emerge at the AGM region who also colonize the liver, expand, and then travel to their final resting place in the bone marrow. The color of the arrows indicates origin and the axis in the bottom show murine embryonic days at which these processes occur (Adapted from J. Palis 2016)[6].

Factors regulating hematopoiesis

The emergence, maintenance, and differentiation of hematopoietic stem and progenitor cells are finely regulated by both extrinsic and intrinsic factors. Extrinsic factors refer to extracellular ligands (cytokines) and their related receptors. Intrinsic factors are the DNA modulating and modifying elements namely transcription factors and epigenetic regulators respectively. The identification of these essential regulators in hematopoiesis has been made possible by studying genetically modified animals and loss of function approaches. Although we understand that the presence and function of these factors are important their roles are not yet fully elucidated. These factors form connected reciprocal regulatory networks and are involved in many aspects of biological functions governing survival, differentiation and proliferation of cells.

Intrinsic factors

Transcription factors (TF) are proteins that regulate the process of DNA transcription. TFs have DNA-binding domains that bind to enhancer or promotor sequences by which genes distal from the regulatory sequence are either activated or repressed. With the support of coactivators, corepressors or chromatin/DNA – modifiers TFs form complexes essential for the commitment of cells to specific lineages. Throughout the years, several genes that encode TFs have been targeted in an effort to permanently or conditionally prevent their expression. This approach, also known as gene knockout, has been extremely useful in determining which and to what extent certain genes are important for the emergence and regulation of the hematopoietic system. The main TFs, essential for definitive hematopoiesis, controlling HSC emergence and regulation are GATA2 [31-35], FLI1 [36], SCL [37, 38], LMO2 [39, 40], RUNX1 [41, 42], ERG [36, 43], CBFB [44, 45]. These transcriptional regulators form multiprotein complexes **(Figure 2)**, resulting in a multifaceted regulatory circuitry with RUNX1 in the centre at the time of HSC emergence [41, 46-49]**.** Three GATA factors are important for early murine hematopoietic progenitors, GATA-1, GATA-2 and GATA-3. While GATA-2 is essential for the emergence, function and early myelo-erytroid progenitor differentiation of HSCs [50-55], GATA-3 is also expressed in the regions where HSCs emerge indicating that they might be functionally compensatory [56]. Conversely, GATA1 has a more important role during erythroid differentiation and will therefore be discussed in depth in chapter 3 covering erythropoiesis.

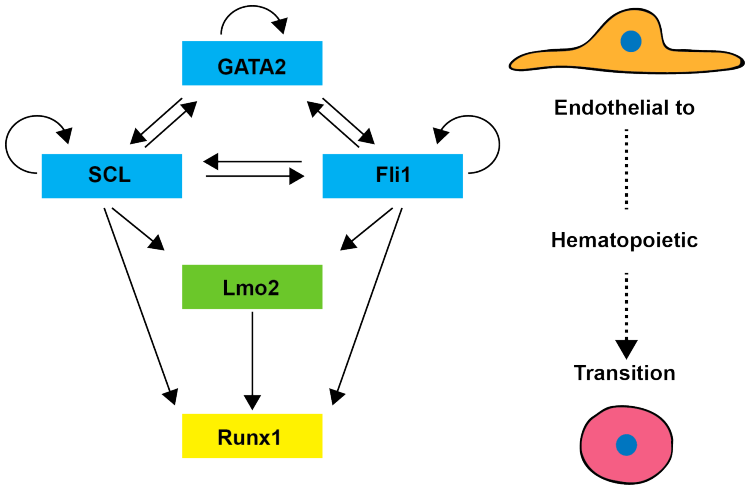

Figure 2 Regulatory circuit of TFs, at the ontogeny of hematopoiesis. These transcription factors form a "transcription factor heptad" that is essential for the initiation on EHT and the emergence of HSCs

Extrinsic factors

Cytokines of the hematopoietic system are extracellular ligands that bind to and activate structurally and functionally conserved receptors. They are produced in varying tissues and cell types [57]. The cytoplasmic domain of these receptors generate biological responses that promote proliferation, differentiation, survival or activation.

Stem cell factor (SCF) and its corresponding ligand tyrosine kinase receptor (KIT) are crucial for the maintenance of HSC [58]. KIT is expressed in the HSC, multipotent progenitors as well as the more committed progenitors such as BFU-Es. In the fetal initiation of hematopoiesis however, HSC emergence is not dependent on KIT expression [59]. As demonstrated by heterozygous KIT mutants, partial loss of KIT signalling is associated with disrupted reconstitution of several lineages in the peripheral blood, including RBCs [60]. Thrombopoietin (TPO) and its related receptor, MPL, is quite similar to KIT in terms of being expressed on multipotent HSC as well as more committed progenitors downstream of the hematopoietic hierarchy. TPO was originally described as a humoral factor, a factor transported by the circulatory system, able to increase platelet production in patients with Thrombocythemia [61, 62]. Further characterization of TPO and its receptor, MPL, remained elusive until the discovery of a retrovirus that caused acute leukemia and polycythemia [63]. Apart from its originally discovered role as a regulator of platelet

production MPL signaling is also important for HSC maintenance [64-66] and erythropoiesis [67].

While some cytokines are lineage specific (e.g. Epo), others have a broader regulatory effect on multiple lineages. IL-3 and GM-CSF are two additional cytokines that act on multiple lineages throughout the hematopoietic hierarchy [68]. IL-3 is a multi-lineage stimulating factor and has been reported to play a role in the proliferation of stem cells during differentiation [69]. Injection of bacterially synthesized recombinant IL-3 into mice has been demonstrated to increase the frequency of several lineages including erythrocytes, megakaryocytes and monocytes, indicating that it is an important and potent stimulant of the hematopoietic system [70]. Interestingly, IL-3 and GM-CSF receptors belong to the same subfamily of class I hematopoietin receptors [71]. While both receptors are expressed broadly, they are differentially expressed. IL-3 receptor is expressed earlier and promotes expansion and proliferation whereas the GM-CSF receptor preferentially induces differentiation [72].

As briefly mentioned, some factors are involved in differentiation towards specific lineages. In this thesis the work has been focused on the erythroid lineage,. Coincidentally, all of the above mentioned cytokines are important for erythroid development in one form or another. Erythropoietin (Epo), which is the main hormone with regards to erythropoiesis, will be described in next chapter.

2. Erythropoiesis

The formation of red blood cells (RBC) is called erythropoiesis. The main function of circulating RBCs, also known as erythrocytes, is to carry oxygen to and expel carbon dioxide from the different tissues in our body. Oxygen is an absolute requirement for the function of all our organs. When we look for water on other planets as an indication of potential life, it is because the principal components of water, oxygen and protons (hydrogen), act as electron acceptors during cellular respiration. For most life forms, oxygen is key in the release of chemical energy and essential for the cells to fuel cellular activity. The RBCs are highly specialized cells, easily distinguished under the microscope, and are by far the most common cell in the body. RBC numbers are in a continuous fluctuation with about 2 million cells generated every second in the adult human to accommodate for the corresponding amount simultaneous cleared in the spleen with the help of macrophages [73]. They have a biconcave discoid shape making them capable of enduring extreme mechanical forces as they are passed through the smallest of blood vessels, i.e. capillaries [74, 75]. The lack of a nucleus is therefore an advantage when traveling through said capillaries. They are packed with haemoglobin, an iron-containing protein, which gives the blood its distinctive red color and is instrumental for the ability of hemoglobin to bind to oxygen.

Stem cell to red blood cell

Erythropoiesis can broadly be divided into three stages; 1) the generation and differentiation of committed erythroid progenitors, 2) terminal differentiation which is associated with considerable morphologic changes, and 3) final maturation in the circulation [76]. The earliest committed erythroid progenitors that start to express the erythropoietin receptor (EpoR), critical for the development of RBC, are the burst-forming unit-erythroid (BFU-E), and the following colony-forming unit-erythroid (CFU-E) [77-79]. These progenitors are characterized by their ability to produce colonies in semisolid medium. Colonies produced by BFU-Es consist of

approximately thousand cells indicating that the BFU-E cells are 12 cell divisions upstream of an orthochromatic erythroblast. CFU-Es on the other hand undergo 4-5 division and give rise to much smaller colonies [80]. Although their generation is independent of EpoR expression [81], the progenitors themselves are Epo-dependent when forming colonies.

In the second stage, erythroblasts undergoing terminal differentiation are more responsive to erythropoietin (Epo), express Glycophorin A and transferrin receptor (TfR, CD71), which decreases as they mature (**Figure 3)**. Terminal erythroid differentiation is dependent on symmetrical cell division and starts with the proerythroblast progressing into basophilic, polychromatophilic and orthochromatic erythroblast, which are all morphologically distinct under the microscope [82]. During the terminal differentiation, erythroblasts gradually accumulate more hemoglobin [83], decrease in cell size and condense their nuclei [84], to finally extrude the nuclei following a cell cycle exit to become reticulocytes [85]. Flow cytometric analyses have been extensively developed for the progressive isolation of different erythroblast subpopulations, both in human and mouse [82, 84, 86-88], facilitating the study of differences between individual subpopulations.

Transcriptional analysis has provided information on the stage-specific complexity during terminal differentiation, revealing that the greatest changes in gene expression occur between the proerythroblasts to basophilic erythroblasts, and polychromatophilic to orthochromatic erythroblasts populations [89, 90]. Erythroid differentiation occurs in the bone marrow, in a niche of macrophages surrounded by erythroblasts named “erythroblast islands” [91]. Finally, enucleated reticulocytes emerge in the peripheral blood to make final changes to their RNA content, membrane assembly and cytoskeleton [92-95] leading to the biconcave discoid shape of a mature RBC. Mature RBCs have a lifetime of approximately 120 days in humans [96] after which they are cleared by macrophages. Disruption of any of these processes can lead to anemia.

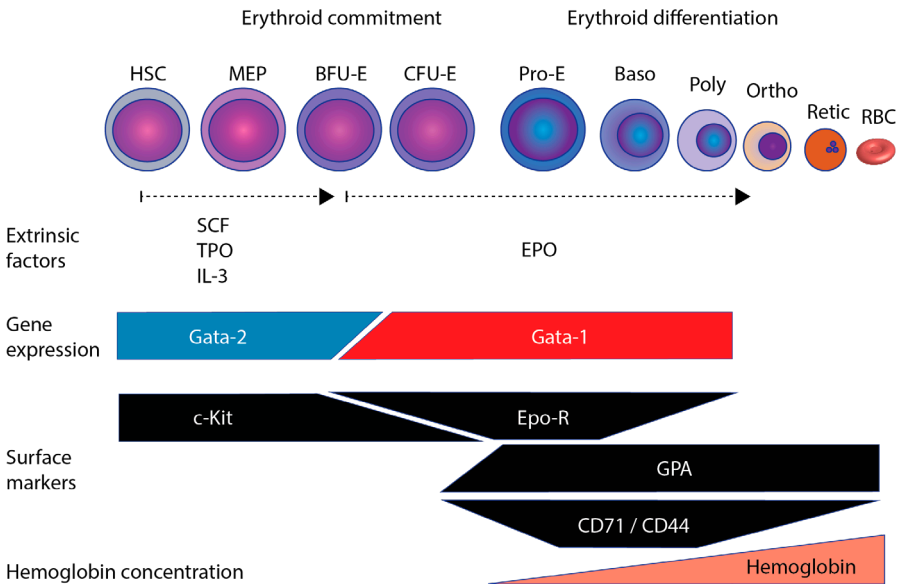

Figure 3 Schematic description of adult erythroid differentiation in the mouse.

Factors regulating erythropoiesis

Intrinsic factors

Among the erythroid lineage restricted transcriptional regulators, none is more essential than GATA-1. Originally identified as a protein that binds the regulatory sequences within the globin gene loci [97, 98], it has since been shown to regulate practically all erythroid specific genes [99-102]. Ablation of GATA-1 therefore results in arrested development at the proerythroblast stage [103-105]. GATA-1 associated cofactors modulate gene expression through several multiprotein complexes formed by FOG1, SCL, LMO2, KLF1, LDB1 and GFI1B [106-108] . Decreased expression of any of these GATA1 associated cofactors leads to defects in primitive and/or definitive erythropoiesis [40, 109-115]. GATA2 is expressed prior to GATA1 in more immature hematopoietic stem and progenitor cells (HSPC). Starting with the bipotential erythroid/megakaryocytic progenitors (EMP), GATA1 expression is increased and the GATA factors have overlapping expression [116].

This combinatorial signalling of GATA2 and GATA1 is important for their ability to perform a transcriptional switch where GATA1, with its partner FOG1, represses GATA2 expression resulting in a mutually exclusive expression pattern [117, 118]. GATA switching is essential for the terminal differentiation of erythroblasts. Thus, the GATA1 associated factors have both gene repressive (FOG1, GFI-1B) and inducing (SCL, LMO2, KLF, LDB1) roles.

SCL/TAL1, with its ubiquitous expression throughout hematopoiesis, is essential for both YS derived hematopoiesis as well adult hematopoiesis, where its absence results in disrupted erythropoiesis [38, 111, 112]. SCL/TAL1 forms a pentameric complex with LMO2, LDB1, E47/E2A and GATA1 **(Figure 4)**. This complex binds to regulatory elements of many erythroid genes and transcription factors such as KLF1 [108, 119, 120]. KLF1 is similarly known to be erythroid restricted, regulating genes important for hemoglobinization, globin switching, mitochondrial function and cell cycle exit [121-126] .

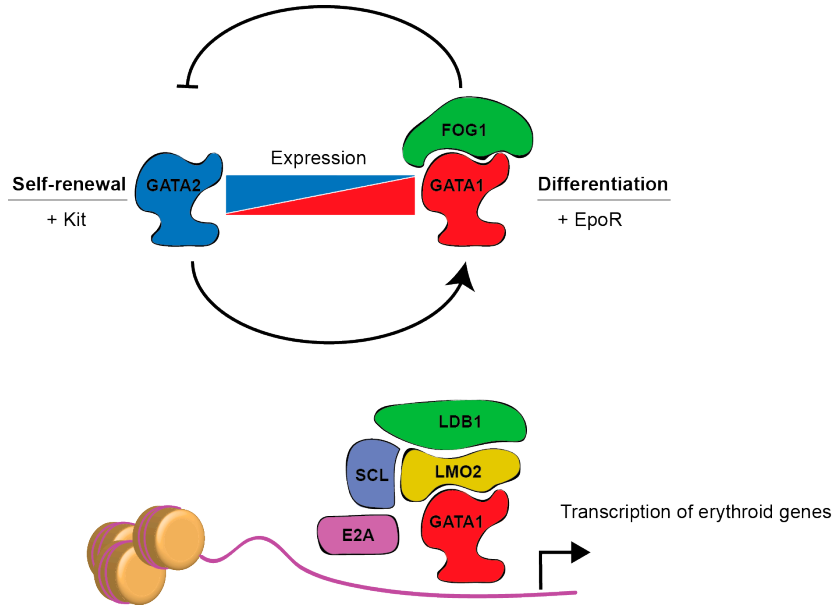

Figure 4 GATA1 and GATA2 expression during erythropoiesis. Adapated from Bresnick, 2018[116]. GATA2 targets are associated with erythroid commitment in HSPCs whereas GATA1 regulates genes associated with red cell function in erythroblasts.

Erythropoietin and other extrinsic factors

During early stages of HSCP commitment, the more primitive cells in the myelo-erythroid progenitor hierarchy, are dependent on a variety of cytokines and growth factors including SCF, IL-3, TPO and glucocorticoids (GC) [68]. KIT and its ligand SCF support the expansion of HSCs [127], but also the proliferation and expansion of BFU-Es during recovery from acute anemia [128, 129]. IL-3 has been shown to have synergistic effects with Epo and GM-CSF on cycling rates [130]. Additionally, inhibition of TPO by the disruption of its receptor in progenitors resulted in reduction of cells in multiple lineages including the erythroid [131].

After the BFU-E stage, Kit expression starts to diminish and EpoR takes over (**Figure 3)**. Epo is essential in for RBC survival[132], proliferation[133], terminal differentiation [134] and its role in the activation of erythroid specific genes is well established [135, 136]. During development, Epo is produced in the fetal liver at the site where definitive erythropoiesis first takes place. Mice lacking Epo/EpoR signalling therefore die by E13.5 due to severely inhibited definitive erythropoiesis [81, 137]. In the adult however, the main site of Epo production is the kidney [138].

Epo signalling is mediated by its cognate receptor EpoR whose expression is activated by GATA-1[139, 140]. The dimerization of EpoR upon Epo binding results in the downstream signalling of multiple signal transduction pathways including JAK2/STAT5, PI3K/AKT/mTOR and MAPK pathways. Disruption of the components in these three pathways have been shown to negatively affect erythrocyte progenitor proliferation[141], maturation[142], survival[143-145], iron metabolism [145-147], translation of mitochondria related genes[148], and responsiveness to Epo [144].

Steady state erythropoiesis is a dynamic process that at any given time is ready to adjust RBC production in response to anemia. The main way in which the erythropoietic capacity can be elevated is through increased Epo expression [77, 149]. At normoxia hypoxia-inducible transcription factors (HIF) are degraded by the activity of prolyl hydroxylase (PHD) enzymes. During hypoxic conditions (i.e. anemia) the lack of oxygen results in the accumulation of HIF-a and the subsequent raise in Epo expression by the dimerization of HIF-a and HIF-b

Conditions of acute anemia can induce a physiological stress response through hypoxia [129] and is distinct from steady state erythropoiesis. This so-called stress erythropoiesis takes place in the spleen, which is seeded with activated early progenitors from the BM [150, 151]. The stress progenitors are regulated

differently, are defined by specific surface markers [152] and more closely resemble the fetal erythroid progenitors[153].

Cortisol, a glucocorticoid (GC) hormone is another factor that has been demonstrated to be important for early erythroid committed progenitors during stress erythropoiesis[154]. Under these circumstances, GCs has been shown support stress erythropoiesis by promoting self-renewal of BFU-E progenitors [155-158]. Most likely through the induce expression of Kit, Lmo2 and inhibition Gata1 expression [155, 159].

Cell cycle and erythropoiesis

The cells in our body reproduce in a tightly regulated sequence of events, where the components of the cell are duplicated and then divided into two new cells. This cycle of duplication and division is called the cell cycle. The active cell cycle can be divided into 4 different cell cycle phases the G1, S, G2 and M phase [160]. Eukaryotic cells have developed a complex network of proteins that control this system to ensure that progression past a checkpoint only occurs when everything is favourable [161]. The first checkpoint is the start point in late G1-phase. Here the cell decides if it wants to commit to cell cycle entry and the progression into S-phase where DNA is duplicated. Retinoblastoma protein (pRb) is the critical regulator of the G1-S1 progression. Favourable mitogenic signals during G1 phase induce the activation of CDKs (CDK4/6). Phosphorylation of pRb by these CDKs results in the “release” of E2F transcription factors which are crucial for the expression G1/S genes (**Figure 5**) [162-165]. Therefore, the classical view of pRb is as the cell cycle regulator by its interaction with the E2F transcription family

It is widely accepted that differentiation is associated with cell cycle arrest. Consequently, proliferation and differentiation are generally mutually exclusive processes [166-168]. In erythropoiesis however, terminal differentiation is coupled to proliferation. Two distinct cell cycle mechanisms takes place during erythropoiesis, namely renewal divisions of committed progenitors and differentiation divisions of erythroblasts [169]. While renewal divisions follow standard cell cycle features such as size control [170], the initiation of differentiation divisions results in reduced time spent in G1 phase resulting in reduced size [171, 172]. The loss of cyclins and CDKs involved in G1 phase results in disrupted terminal erythropoiesis [173-175]. As an example, E2F4 deficient mice exhibit

normal renewal divisions, but display disrupted differentiation divisions, resulting in macrocytic erythrocytes [176].

The distinct division programs occurring in erythropoiesis are accomplished by rapid change in cell cycle regulators. For terminal erythroid differentiation divisions to take place, EpoR dependence of CFU-Es marks a commitment step in erythropoiesis which is dependent on S-phase progression and the downregulation of p57 which subsequently results in downregulation of the GATA-1 antagonist, PU.1 [177].

Erythropoiesis therefore has an indisputable relationship with the cell cycle. During terminal differentiation, erythroid progenitors undergo 4-5 differentiation divisions, followed by pRb-promoted cell cycle exit in the terminally differentiating erythroblasts to produce mature RBCs [178, 179].

The cell cycle is tightly controlled by the cyclical synthesis and degradation of proteins at specific cell cycle stages, particularly of cyclins, cyclin dependent kinases and their inhibitors. This is generally done through E2F dependent transcription and conversely by pRb mediated repression of E2Fs. The E2F transcription family can broadly be subdivided into two categories, the activating E2Fs (E2F1, E2F2, E2F3a/b) and the repressive E2Fs (E2F4,E2F5,E2F6, E2F7, E2F8) [180-183]. pRb is a multi-domain protein with several partner-specific binding sites [184]. Describing pRb as a E2F dependent cell cycle regulator is therefore an oversimplification as approximately 50 different proteins has been suggested to bind to pRb and only 8 of these are from the E2F family [165]. Indeed pRb is known to have E2F independent mechanisms in cell cycle regulation, most notable the indirect role of pRb in the degradation of the CDK inhibitor p27 [185], and induction of apoptosis at the mitochondria [186]. Therefore, gene targeting approaches where pRb is concerned is not a matter of presence or absence. With pRb there is a complex regulatory network, which has not completely been elucidated yet [187].

Apart from its role in cell cycle progression, pRb has since been implicated in many other cellular functions including differentiation, apoptosis, cell cycle arrest, and mitochondrial biogenesis [188, 189] , all important aspects of erythropoiesis.

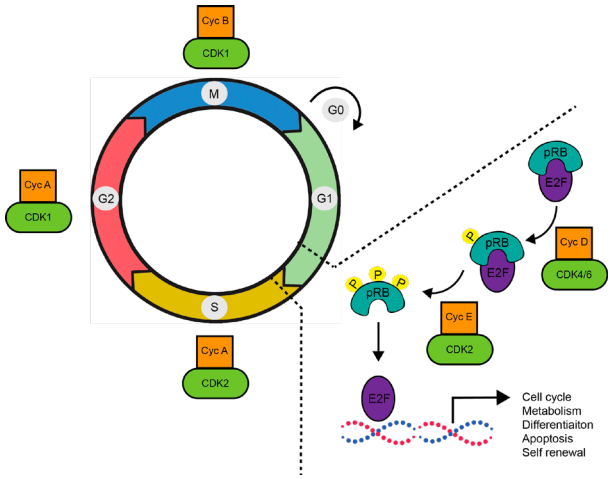

Figure 5 Cell cycle checkpoint at G1 and the regulation of pRb. CDK4/6 mediate the initial hypo phosphorylation of pRb and CDK2 finalizes the complete phosphorylation of pRb and the consequent release of E2F transcription factors which have a broad downstream transcriptional effect. CDKs are presented with their corresponding cyclins.

The role of pRb in erythroid differentiation

pRb and E2F proteins have been implicated in the cell fate regulation of multiple tissues including myogenic, neural, and hematopoietic stem cell lineages [190-194]. Although pRb deficient mice embryos die at E13.5 due to inefficient erythropoiesis, doubt still remained as to whether these effects were intrinsic to the erythroid cells [188, 195]. In chimeric mice transplanted with pRb deficient embryonic stem cells it was demonstrated that pRb deficient cells significantly contributed to the erythroid lineage with intact differentiation potential [196, 197]. Additionally, healthy extraembryonic tissue was suggested to be sufficient for rescuing the erythroid defect and lethality in pRb deficient embryos [193, 198], collectively suggesting that the erythroid defects were non-cell intrinsic. However in vitro erythroid culture experiments [179] and conditional gene targeting approach in the erythroid compartment [189] later confirmed that pRb conclusively has cell intrinsic role in erythropoiesis.

Several cell cycle related and pRb associated factors have been implicated in terminal differentiation of erythroblasts including E2Fs [124, 199-204], Cyclins [173], Cyclin dependent kinases (CDK), Cyclin-dependent kinase inhibitors (CKI) [185, 205], Histone modifiers [206], and other transcription factors such as the E2F

dimerization partners [207] and the GATA1 associated PU.1 [208, 209]. Collectively the ablation of these factors are associated with cell cycle and maturation related defects often with pRb at the heart of each signalling pathway, clearly demonstrating an important role for pRb in erythroid differentiation.

Disrupted erythropoiesis due to aberrant pRb signalling has been attributed to failed cell cycle exit [189], disrupted mitochondrial biogenesis [189], stress erythropoiesis [203, 210, 211], hypoxic stress [212], oxidative stress [213, 214], GATA1 repression [209] and stressed DNA replication [215]. These defects associated with absent or deregulated pRb signalling could be separated into two major groups, namely cell cycle regulation and cell metabolisms. While the role of pRb in cell cycle regulation has been extensively studied, its connection to cell metabolism is not entirely understood. The major questions remaining are how cell metabolism is controlled downstream of pRb, and if/how metabolic cues and mitochondrial function can regulate cell cycle progression. Furthermore, while previous studies have implicated that pRb is essential for normal erythropoiesis, the exact erythroid terminal subpopulations mainly affected have remained largely unknown.

Coupling metabolism and cell cycle

HSC function and differentiation is known to be regulated by metabolic cues [216]. The HSC niche in the BM is a hypoxic environment [217], and as such HSCs are largely independent of oxidative metabolism. However, environmental oxygen availability does not completely drive metabolic preferences. Rather there are cell intrinsic mechanisms mediated in part by high expression of HIF1a [218] and inactive mitochondria [219]. Indeed, HSCs homeostasis is exquisitely dependent on anaerobic glycolysis, which is mediated through the HIF1a-PDK system. Conversely, progenitors increasingly rely on oxidative metabolism as they differentiate.

When generating ATP, mitochondria can make use of three specific metabolic pathways; glucose, lipid or protein metabolism (**Figure 6**). Glycolysis and the tricarboxylic acid cycle (krebs cycle) can produce ATP independently of the electron transport chain (ETC, or OXPHOS), however this occurs less efficiently compared to that of ETC driven oxidative phosphorylation which produces ATP at a higher yield [220]. Stem cells and progenitor cells prefer different ATP producing pathways implicating metabolic states to cell fate decisions. Commitment of HSCs

into the erythroid lineage and erythroid terminal differentiation has been shown to be dependent on metabolic rearrangements, affecting the glycolytic, lipid as well as the glutamine pathway [221-225].

Interestingly the cell cycle machinery, particularly pRb mediated mechanisms, has been demonstrated to have multiple connections to cell metabolism including effects on lipid metabolism [226], insulin secretion [227], glutamine catabolism [228, 229], reduction/oxidation balance [230-233] and autophagy [234, 235], which indirectly also affects metabolism. Proteomic changes analyzed in pRb ablated colon and lungs tissue of mice revealed mitochondrial dysfunction with reduced mitochondrial mass, oxidative phosphorylation and altered tricarboxylic acid (TCA) cycle [232]. In *Drosophila*, G1-S transition during cell cycle has also been shown to have mitochondria actively participating in the G1-S transition through unique structural changes that increasing membrane potential which in turn triggers cyclin E expression [236, 237].

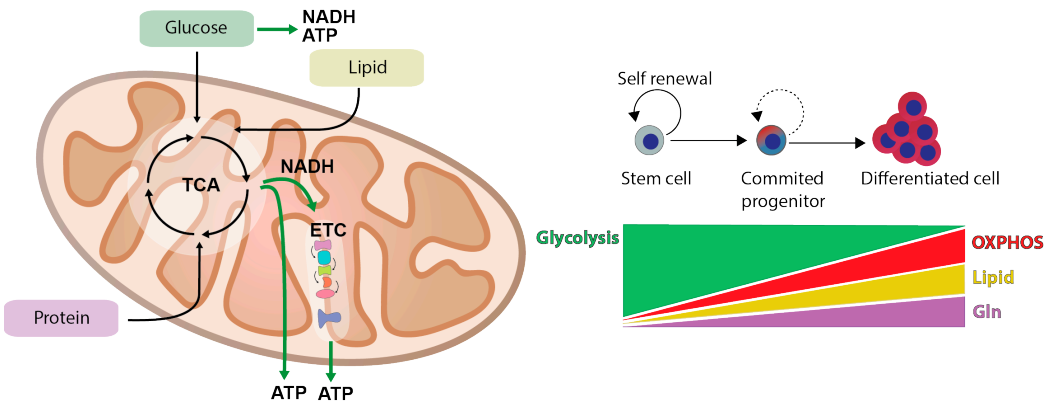

Figure 6. Schematic representation of mitochondrial ATP generation and preferred metabolic pathway in HSC and differentiated progenitors. Adapted from Ito & Suda (2014) [207]

3. Mitochondria and red blood cells

For a long time mitochondria were simply considered as ATP generating power plants. However, recent scientific advances have paved the way for a more nuanced perspective on mitochondrial function and its role in varied cellular processes. It is widely accepted today that mitochondria play an essential role in programmed cell death, stem cell regulation, innate immunity and iron & heme homeostais [238]. Particularly, iron and heme homeostasis is of special interest in the context of this thesis since they are essential for proper RBC function and mitochondrial defects are increasingly being associated with haematological diseases in general and dyserythropoiesis in particular.

Metabolic changes in the mitochondria are known to affect HIF factor regulation. Reactive oxygen species (ROS), a by-product of mitochondrial oxidative phosphorylation, are known to stabilize HIF and thereby promote Epo expression [239]. Interestingly Epo has been shown to induce ROS during the early stages of terminal erythroid differentiation, indicating a reciprocal regulation of mitochondria and Epo [240]. Furthermore, Epo has been demonstrated to induce mitochondrial biogenesis in cardiomyocytes [241]. However, this function remains to be validated in erythroid cells.

Heme and Iron

The daily production of approximately 200 billion RBCs requires immense amounts of iron to sustain hemoglobin production. To satisfy the needs of new RBC production, the macrophages degrade aged RBC to recycle the iron. Iron recycling is by and large enough to maintain the iron bioavailability needed for RBC production. However, without the absorption of iron by duodenal enterocytes there would be no iron pool to begin with. Indeed, the most prevalent cause of anemia is due to nutritional iron deficiency. Collectively mechanisms controlling uptake, storage and utilization of the iron pool are extremely important for erythropoiesis and disruptions of these mechanisms often result in anemia [242-254].

Iron uptake is mediated by transferrin (Tf) proteins, which have two high-affinity sites for ferric iron (FeIII), and their receptors TfR [255, 256]. With the endocytosis of Iron-Tf-receptor complex, iron is shuttled to the mitochondria for its utilization in the heme biosynthetic pathway and Iron-sulphur cluster synthesis which is important for the electron transport chain (**Figure 7)**. The metabolism and utilization of iron at the mitochondria starts with its transportation into mitochondria via mitoferrin 1 (MFN1) [247, 250]. In the mitochondria iron is either incorporated into protoporphyrin IX (PPIX) by ferrochelatase (FECH) to produce heme [257], or used for the Iron-Sulphur (Fe-S) cluster synthesis, which is important for the electron transport chain. When not used in the mitochondria, Fe-S clusters are transported out of the mitochondria by ABCB7 [258] to become incorporated into other client proteins. Heme synthesis starts with ALAS2 [259] inside the mitochondria (erythroid specific ALAS), and after several intermediate steps taking place outside the mitochondria, it is transported back in by TMEM14c for the final synthesis reactions [260]. Once ready, heme is transported out of the mitochondria by FLVCR1b [261, 262] for incorporation into haemoproteins of which hemoglobin is the most common. Additionally, Iron also participates in the transcription of Epo by activating PHD2 [263]. At low oxygen and/or iron conditions PHD2 is inactive. By this mechanism erythropoiesis is adjusted based on the iron availability.

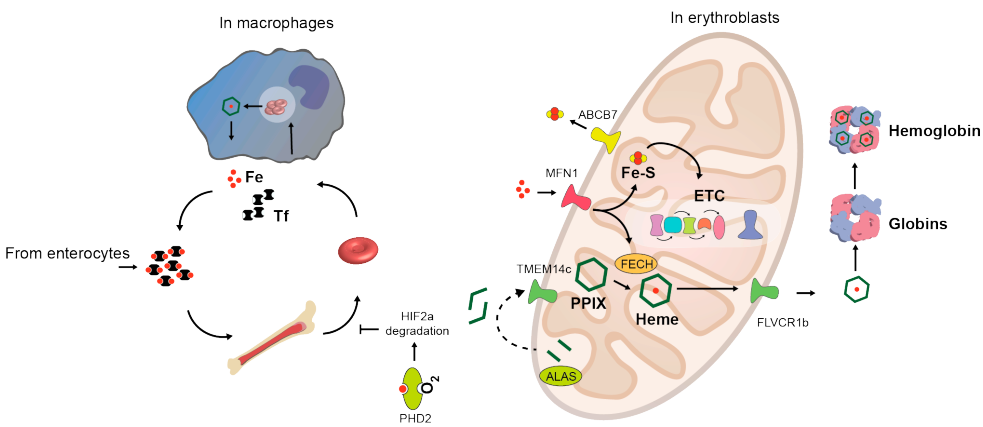

Figure 7. Iron homeostasis and erythropoiesis. Macrophages play an essential part in iron homeostasis by breaking down RBC to recycle iron and heme. The available iron pool is transported to the mitochondria were it participates in essential processes during erythropoiesis. Additionally iron modulates Epo concentrations by activating PHD2.

PPARgamma coactivators

Peroxisome proliferator-activated receptors (PPAR) are ligand-activated TFs that belong to the nuclear receptor superfamily, including members such as estrogen and glucocorticoid receptors. PPARs are known to be involved in regulation of genes associated with energy metabolism, cell differentiation, apoptosis and inflammation [264] **(Figure 8)**. The activation of PPARs is mediated by the binding of ligands and co-regulators (activators and repressors). While the process by which PPAR binding to DNA at the peroxisome proliferator response elements (PPRE) has been extensively review [265, 266], less is known about its ligands and co-regulators. Members of the PPARgamma coactivator-1 (PGC-1) serve as co-regulators of the PPARs by inducing gene transcription. PGC-1a was the first co-activator identified in the brown adipose tissue of mice when exposed to cold [267]. Following the identification of PGC-1a, two related coactivators, PGC-1b and PRC, were discovered [268-270]. While little is known about PRC, the role of PGC-1a and PGC-1b has been extensively studied.

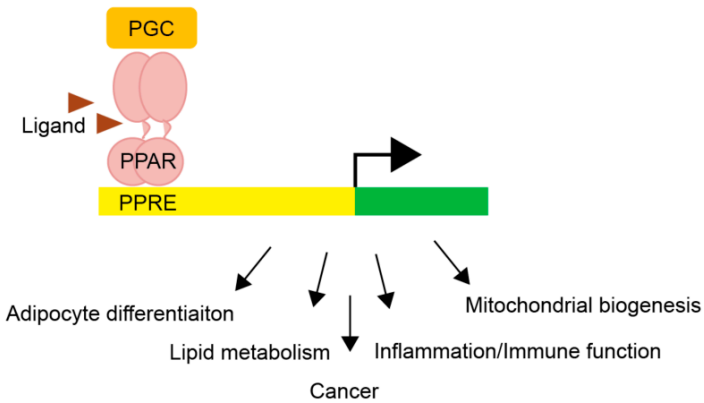

Figure 8. PGCs are inducible cofactors that activate gene transcription

PGC-1a and PGC-1b are preferentially expressed in cells with high oxidative capacity like adipocytes and myocytes where they regulate mitochondrial function and energy metabolism [267, 269, 271-274]. Their role has largely been mapped in adipocytes, hepatocytes and myocytes, while their role in the hematopoietic system remains largely unknown.

To date, only one study has examined the role of PGCs in murine erythropoiesis, demonstrating that PGCa and PGCb deficiency during embryogenesis results in anemia due to deregulation of globin genes [275]. However, the effect on cell cycle, mitochondrial function and role in human erythropoiesis has remained unknown.

4. Anemia

Anemia is a condition characterized by the reduction of circulating RBCs and/or decreased concentration of hemoglobin, the oxygen carrying metalloprotein. The insufficiency in meeting physiological oxygen needs of individuals therefore result in symptoms such as shortness of breath, lethargy, lightness of head, pallor and irregular heartbeats. Anemia has major consequences for human health, contributing to increased morbidity and mortality, impaired development in children, decreased work productivity in adults and general decrease in quality of life. Anemia is estimated to affect approximately one third of the global population [276] with highest prevalence in woman, children [277] and the elderly [278].

The pathophysiology of anemia can be described as the imbalance of RBC production relative to its loss. The most common clinical method of assessing anemia is measuring hemoglobin concentration, but it can also be diagnosed using RBC counts, RBC volume, blood precursor (i.e. reticulocytes) counts or microscopic observation of peripheral blood film. While the diagnosis can be relatively simple based on symptoms, establishing the underlying cause can be complicated.

Since most anemias have characteristic RBC morphology, they can be classified by appearance. However, classification based on morphology alone can be impractical since the same individuals sometimes have multiple causes for the anemia. Therefore, anemias are additionally classified based on the causative biological mechanism. Anemia can be caused by a variety of conditions, including nutritional deficiencies, infections, autoimmune diseases, hereditary hemoglobin/membrane disorders, inflammations due to chronic disease and decreased production due to BM failures [276, 278-283]. The most common cause of anemia is due to nutrition related iron deficiency. The work of this thesis has been focused on two types of anemias associated with genetic alterations, namely refractory anemia associated with myelodysplastic syndromes and RBC membrane disorders.

Red blood cell deficiency in MDS

Myelodysplastic syndromes (MDS) are a group of heterogeneous clonal BM disorders associated with peripheral cytopenias. Anemia is the most common cytopenia, which greatly affecting both the clinical outcome and quality of life [284]. The pathogenesis of MDS is driven by diverse mutations acquired by adult stem cells, including mutations in genes associated with RNA-splicing machinery, DNA methylation, chromatin modification, transcription factors, signal transduction/kinases, RAS pathway, cohesion complex and DNA repair machinery [285-288]. In addition to somatic mutations, cytogenetic aberrations are amongst the most common genetic abnormalities in MDS patients, with the deletion of q arm on chromosome 5 (del(5q) being the most abundant [289]. In some rarer types of MDS with cytogenetic aberrations, patients with elliptocytosis have been observed [290, 291]. Elliptocytosis, or ovalocytes, is abnormally shaped RBC that appear elongated. Elliptocytosis is commonly seen in hereditary conditions where mutations occur on band3, spectrin chains or protein 4.1 which are all cytoskeletal proteins on the RBC membrane.

In addition to del(5q) there are 7 more subtypes of MDS, MDS with single or multi lineage dysplasia (MDS-SLD, MDS-MLD), MDS with excess blast (MDS-EB), MDS, unclassified (MDS-U) and MDS with rind sideroblasts (MDS-RS, MDS-RS SLD and MDS-RS-MLD) [292]. The ring sideroblastic subtypes with anemia (collectively RARS) are particularly fascinating as the erythroblast precursors in these patients have mitochondrial accumulation of iron. The pathogenesis of subtype has been well characterized [293, 294] and will be further discussed in the section covering mitochondria and MDS.

Despite the clonal diversity of recurrently mutated genes and varying cytogenetic abnormalities in MDS patients, anemia is amongst the chief manifestations with concern to peripheral cytopenias [295-300]. Terminal erythropoiesis is disrupted in the majority MDS patients, and is used as a prognostic marker [296].

Current treatments for MDS-related anemia

Approximately 50% of MDS patients require RBC transfusion to alleviated anemia-related symptoms such as fatigue [301]. However, blood transfusions only provide short term benefits and ultimately lead to negative side effects such as iron overload. Erythropoiesis stimulating agents (ESA) are therefore used in conjunction with blood transfusions. However, careful consideration has to be taken when

administering ESA such as Epo or darbepoetin. The treatment route is generally dependent on baseline serum Epo levels in patients, who commonly already have high Epo levels [302, 303]. Additionally, combinations of cytokines are used, such as Epo in combination with G-CSF, to enhance erythroid response [304]. This combinatorial cytokine treatment was shown to inhibit apoptosis in the RARS erythroblasts by inhibiting release of mitochondrial cytochrome c [305-308]. Unfortunately, as is the case with many of the MDS treatment options, patients eventually stop responding to ESAs [309, 310]. In addition to the ESAs, only Lenalidomide is known to give an erythroid response and is mainly limited to the treatment of del(5q) subtype. The response rate to Lenalidome is approximately 50-70% [311, 312]. However, the durability of these responses are uncertain and often with side effects [313, 314].

Mitochondria and MDS

Mitochondrial dysfunction has been implicated in MDS, which is a disease associated with the elderly. Indeed, MDS patients frequently harbours mtDNA mutations [315-320]. The "mitochondrial theory of aging" proposes that aging is associated with reactive oxygen species (ROS) induced damage to mitochondria and its DNA (mtDNA) [321, 322]. However, more recent studies have challenged the notion of ROS and oxidative stress driving aging and have instead proposed that mtDNA mutations primarily affect the respiratory chain [323]. Mitochondrial DNA polymerase gamma (POLG) mutator mice acquire mtDNA mutations and develop an MDS-like anemia due to disrupted erythropoiesis [219]. The specific metabolic requirement of erythroid progenitors has therefore been suggested to be the underlying cause of disrupted erythropoiesis.

The cause for mitochondrial dysfunction in MDS patients is not limited to mtDNA mutations. Of the several somatic mutations in MDS, *SF3B1* mutations are amongst the most common. In the refractory anemia with ring sideroblast (RARS) subtype, *SF3B1* mutations account for 70% of the patients [324]. SF3B1, a component in the RNA splicing machinery, has been implicated in the mis-splicing and deregulation of several genes. The deregulated genes include *ABCB7, ALAS2, MFN1* and *TMEM14C [294, 325]*, all involved in iron and heme homeostasis. While this explains the mechanisms by which heme and iron homeostatis is disturbed, the effect it has on erythroid precursors remains to be elucidated.

Pathogenesis of del(5q) MDS has been attributed to the ribosomal *RPS14 [326]*. It is however questionable whether a single gene out of 40 in the commonly deleted region is responsible for the entire disease phenotype. Notably, *PGC1b* is also located within the commonly deleted region of chromosome 5q, and our work described in Paper I and Paper II indicates that PGC1b could be involved in the disease phenotype of MDS and that mitochondrial function is important for cell cycle exit and mitochondrial metabolism of erythroblasts.

Red cell membrane disorders

RBCs undergo substantial deformation during their passage through the microvasculature. Decreased cellular deformability therefore reduces RBCs ability to deliver oxygen efficiently. Disrupted deformability of RBCs can additionally lead to impounding at the spleen [327] resulting in an untimely degradation. The decreased lifespan of undeformable RCB can therefore lead to anemia. The structural organization of RBC membrane is maintained by associated transmembrane and cytoskeletal proteins. These proteins are essential for the deformability and function of RBCs. Inherited membrane disorders occur due to mutations in genes encoding membrane associated proteins such as ankyrin, spectrin, band 3 and protein 4.1/4.2 [328-334]. Such mutations result in weakened linkages in either vertical or horizontal orientation. Weakening of vertical linkages occur between the lipid bilayer and spectrin-based membrane skeleton and results in membrane loss. In comparison, weakening of horizontal linkages between skeletal proteins results in decreased surface area and membrane fragmentation [335]. The study of these hereditary disorders has led to the defining of structural basis for normal RBC function.

5. Summary of results and discussion

Anemia, can be caused by a variety of mechanisms and is a co-morbidity of both acute and chronic disease states, including bone marrow failures due to clonal disorders. My overall research focus has been in resolving regulatory mechanism that govern terminal erythroid differentiation and to identify new ways to enhance RBC production in the treatment of anemia (**Figure 9**). Below I have summarized the aim and key findings of the papers included in this thesis.

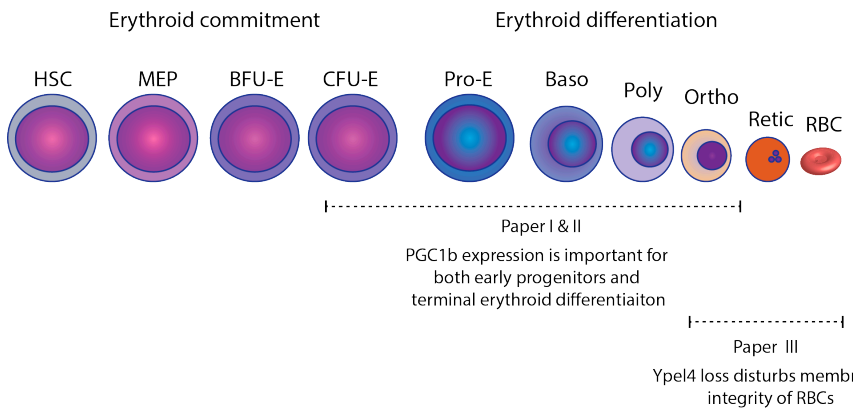

Figure 9 Stages during erythropoiesis in which the published papers add to the development and function of red blood cells. PGC1b is important in both murine and human erythropoiesis in the regulation cell cycle and mitochondrial metabolism. Aberrant expression of Ypel4 results in disrupted RBC membrane

Paper I

Enhancing mitochondrial function in vivo rescues MDS-like anemia induced by pRb deficiency

Taha Sen, Mayur Jain, Magnus Gram, Alexander Mattebo, Shamit Soneji, Carl R. Walkley, Sofie Singbrant

Experimental Hematology, Volume 88, 2020, Pages 28-41
https://doi.org/10.1016/j.exphem.2020.06.006.

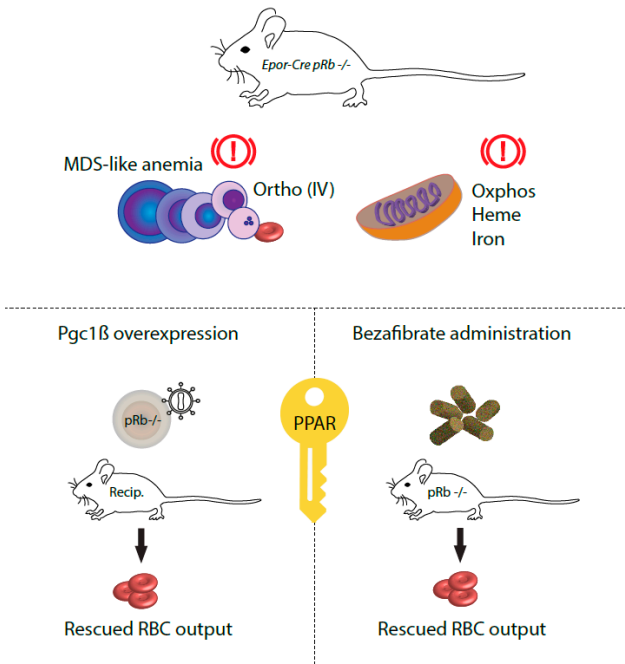

Figure 10 Graphical abstract: Paper I

Background

Erythropoiesis is intimately coupled to cell division, and deletion of the cell cycle regulator retinoblastoma protein (pRb) causes anemia in mice. Erythroid-specific deletion of pRb has been found to result in inefficient erythropoiesis because of deregulated coordination of cell cycle exit and mitochondrial biogenesis. However, the pathophysiology remains to be fully described, and further characterization of the link between cell cycle regulation and mitochondrial function is needed. To this end, our aim was to further assess conditional erythroid-specific deletion of pRb. To

further understand the mechanism of impaired erythroid development caused by pRb deficiency, we used the mouse model previously described by Sankaran and colleagues, where lox-p flanked pRb is deleted specifically in the erythroid lineage using EpoR-driven Cre recombinase (Epor-Cre pRbfl/fl).

Key findings

pRb deficiency results in anemia despite an increase in progenitor frequency. Deletion of pRb in the erythroid lineage resulted in anemia with significantly reduced red blood cell (RBC) counts, hemoglobin (HGB) concentration, and hematocrit (HCT) levels and an increase in mean corpuscular volume (MCV). Deletion of pRb also resulted in reduced platelet counts and an increased total BM white blood cell counts. Measurement of Epo concentration demonstrated a twofold increase in pRb-deficient mice compared with WT animals indicating a maintained physiological response to the anemia.

To accurately determine at what stage erythroid differentiation was impaired, we applied a high fractionation flow cytometry protocol that distinguishes the different myelo/erythroid progenitors including Pre-Meg-E, Pre CFU-E and CFU-E. CFU-E population of pRb-deficient mice were significantly increased. Despite the increase in early progenitors and serum erythropoietin levels, pRb-deficient animals remained anemic due to a developmental block at orthochromatic cells, followed by a decrease in reticulocytes compared to wildtype.

Anemia can induce extramedullary erythropoiesis in the spleen to increase output of erythrocytesduring conditions of stress. The spleen weight of pRb-deficient mice was therefore significantly increased. Similar to the BM, orthochromatic erythroblasts also accumulated in the spleen

Apoptosis analysis demonstrated a switch from increased to decreased cell survival adjacent to the cellular block. Increased survival of early erythroblasts in the pRb knockout is potentially due to the increased circulating levels of Epo.

In summary, detailed phenotypic analysis demonstrated that erythroid specific deletion of pRb resulted in macrocytic anemia in spite of increased frequency of erythroid progenitors and Epo concentration. Terminal differentiation was blocked specifically at the orthochromatic erythroblast stage, which reminds of MDS related anemia.

Transcriptional analysis of erythroblasts at the developmental block revealed five clusters of differentially expressed genes compared to normal erythroid differentiation.

To elucidate mechanisms underlying the inability of pRb deficient orthochromatic erythroblasts to mature into reticulocytes, microarray analysis was performed on three FACS-sorted populations at and adjacent to the block. Differentially expressed genes were clustered into five distinct patterns of deregulation compared to normal expression. Having identified the developmental block we could define sets of genes that were unable to follow normal expression in

pRb deficient orthochromatic erythroblasts fail to exit cell cycle

Gene ontology annotation of clusters of genes that failed to down-regulate or were upregulated mainly associated with cell-cycle related genes. To functionally test the transcriptional profiling cell cycle status of erythroblasts were determined. Cell cycle analysis revealed that pRb deficient cells remained in S-phase. Our results confirm that pRb deletion results in an inability of specifically orthochromatic erythroblasts to properly exit cell cycle therefore extending previous results.

pRb deficient orthochromatic erythroblasts have disrupted mitochondrial related functions

Genes that should be stably expressed but instead were downregulated in pRb deficient erythroblast were mainly related to mitochondrial functions. In agreement, flow cytometry analysis with Mitotracker DeepRed stain demonstrated that pRb-deficiency resulted in reduced mitochondrial activity of erythroblasts. Also, mitochondrial superoxide production, a byproduct of mitochondrial respiration peaked in normal orthochromatic cells. This peak was delayed in pRb deficient erythroblasts and was instead increased in reticulocytes. Collectively, erythroid specific deletion of pRb resulted in decreased expression of mitochondria-related genes, accompanied by a decreased mitochondrial membrane potential and a shift in mitochondria-produced ROS.

Gene clusters that failed to upregulate during terminal differentiation were related to heme synthesis and iron homeostasis. These processes are located at the mitochondria and essential for the function of RBCs. In accordance with perturbed iron homeostasis prussian blue staining of BM cells revealed increased iron accumulation in pRb-deficient erythroid progenitors. Additionally, serum iron

concentrations of KO mice was significantly reduced in the KO mice. Free heme concentration was finally measured in lysed erythroblast as iron is known to regulate heme production [336]. In the normal erythroblasts heme concentration increase however, in the pRb deficient erythroblast heme concentration went from being increased in orthochromatic erythroblasts to reduced in reticulocytes compared to healthy cells. Our data demonstrated that pRb deletion in erythroid cells results in deregulation of heme production and iron metabolism, revealing a new mechanism by which pRb regulates erythropoiesis.

pRb deficient erythroblast exhibit deregulated expression of genes recurrently mutated in MDS

MDS with ring sideroblasts are characterized by mitochondrial iron accumulations. The phenotype has been attributed to mutations in *SF3B1* and downstream aberrant splicing of genes including *ABCB7.* Both *Sf3b1* and *Abcb7* were de-regulated in our pRb-deficient erythroblasts. Heme related genes implicated in MDS-related anemia were also deregulated, including *Tmem14c* and *Alas2*.

pRb-deficient erythroblasts additionally displayed aberrant expression of numerous recurrently mutated genes in MDS including *Srsf2*, *U2af1*, *Mdm2* and *Kras.* Erythroid deletion of pRb therefore results in the altered expression of several genes frequently disrupted in MDS

Enhanced PPARg signalling ameliorates anemia

Mitochondria-related functions were a recurrent theme in the pRb deficient erythroblast. We therefore asked if increased mitochondrial function through the PPARg axis could ameliorate the pRb induced anemia. *Pgc1b* is a transcriptional coactivator of PPARg, which is important for mitochondrial biogenesis and was previously shown to be reduced in Ter119+ erythroblast by Sankaran and colleagues. However, previous studies have not demonstrated if there is a causative link and whether restored Pgc1b expression can rescue the pRb deficiency *in vivo.* To address this, we transduced progenitor cells with *Pgc1b* overexpressing vector and transplanted them into lethally irradiated mice. At 8 weeks post transplantation we could demonstrate a normalization of peripheral blood parameters, including RBC count and MCV, of mice transplanted with KO cells overexpressing *Pgc1β*. While the transplantation experiment provides a proof of principle we asked if pharmacological compounds could deliver the same results. Next we used

Bezafibrate, a pan-PPAR agonist that acts on the same nuclear receptor as PGC1b. Strikingly and consistently with Pgc1b overexpression we could observe an normalization of peripheral blood parameters when compared to healthy animals.

PGC1b overexpression normalizes cell cycle gene expression

To address whether enhanced mitochondrial biogenesis also affected cell cycle, c-kit+ progenitors were transduced with *Pgc1b* overexpressing vector and cultured in erythroid medium. Pgc1b overexpression ameliorated the developmental block in orthochromatic erythroblasts and normalized the expression of cell cycle related genes. Collectively we could demonstrate that enhanced PPAR signalling rescued anemia and normalize the enhanced expression of cell cycle genes in pRb deficient erythroblasts.

Paper II

Decreased PGC1β expression results in disrupted human erythroid differentiation, impaired hemoglobinization and cell cycle exit

Taha Sen, Jun Chen & Sofie Singbrant

Scientific Reports, Volume 11, Article number: 17129 (2021)
https://doi.org/10.1038/s41598-021-96585-0

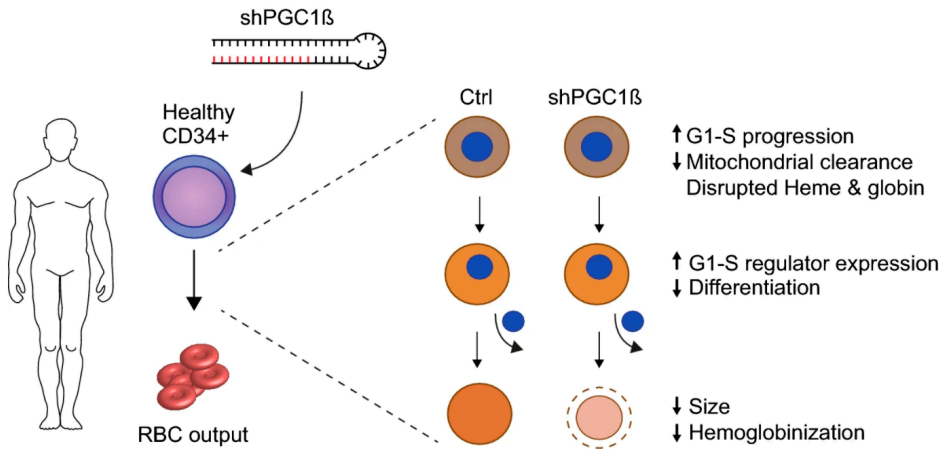

Figure 11 Graphical abstract: Paper II

Background

Production of red blood cells relies on proper mitochondrial function, both for their increased energy demands during differentiation and for proper heme and iron homeostasis. Mutations in genes regulating mitochondrial function have been reported in patients with anemia, yet their pathophysiological role often remains unclear. PGC1b is a critical coactivator of mitochondrial biogenesis, with increased expression during terminal erythroid differentiation. The role of PGC1B has however mainly been studied in skeletal muscle, adipose and hepatic tissues, and its function in erythropoiesis remains largely unknown. We previously demonstrated that enhanced PPARg signaling axis through PGC1b, in a murine setting, was sufficient in rescuing anemia caused by pRb deficiency. We therefore wanted to evaluate *PGC1B* in the human erythroid development.

Key findings

Decreased PGC1b expression results in decreased colony forming potential of early progenitors and delayed terminal differentiation.

Pgc1 coactivators have been indicated to play a role during murine erythropoiesis, while their function in human erythropoiesis remains unknown. To further decipher the role of PGC1b during human erythroid development, we reduced the PGC1b expression using shRNA in human CD34+ progenitors derived from bone marrow (BM) and cord blood (CB). To investigate the role of PGC1b during early erythroid development, transduced CD34+ BM stem/progenitor cells were plated in methyl cellulose and analyzed for formation of erythroid colony forming units (CFU-Es). CFU-E colony forming potential was significantly decreased with reduced expression of PGC1b.

We next wanted to address the requirement of PGC1b in terminal erythropoiesis. Terminal BM derived erythropoiesis was studied by the expression of GPA, Cd49d and Band3 at days 10,14,18,and 21. Formation of GPA + erythroid cells were reduced at day 10 and 14 of analysis. With the onset of more mature erythroid cells further fractionation was achieved by assessing differential expression of surface markers CD49d and Band3. In the more mature cells we could observe a developmental delay at day 18 which then normalized at day 21. In accordance with the flow cytometric results, scoring of of cells stained with giemsa and diaminobenzidine revealed similar developmental delay. Again, the differences were close to normalized at day 21.

Owing to different proliferative and developmental kinetics, Cord blood (CB) derived CD34+ cells differentiated much faster in the erythroid culture and were therefore analysed on days 10, 14 and 16 instead. CB derived cells also exhibited delayed expression of GPA similar to BM derived counterparts at days 10 and 14. PGC1b knock-down resulted in a more pronounced developmental delayed in CB derived erythroblast compared in to BM. Enucleation was analyzed at day 16 using a cell-permeant nucleic acid stain and was significantly reduced with PGC1b knock-down.

In conclusion, reduced expression of PGC1b results in perturbed formation of early erythroid progenitors and impaired terminal erythroid differentiation, a phenotype that is reminiscent of the refractory anemia seen in many MDS patients and the MDS-like anemia we have previously reported on in mouse.

Decreased PGC1b expression in results in deregulation of heme and globin synthesis.

The functional role of the mitochondrial coactivator PGC1β in erythropoiesis remains largely unknown. We recently showed that down-regulation of Pgc1b in response to pRb deletion correlated with decreased expression of genes involved in mitochondrial function, as well as heme synthesis and iron transport in mouse.

To address mitochondrial effects of reduced PGC1b expression we analysed the expression of key genes involved in oxidative phosphorylation, hemoglobin synthesis and iron transport in BM and CB derived erythroblasts. In BM derived erythroblasts gene expression of COX7B, SDHB, NDUFA1 and ATP5s were deregulated. In CB only COX7 had deregulated expression due to reduced PGC1b expression. Since many OXPHOS genes are tightly regulated at the post translational level western blot analysis on key mitochondria related proteins was performed on CB-derived sorted erythroid progenitor populations from day 16.

To investigate the levels of mitochondrial biomass compared to cell mass, the protein level of the mitochondrial marker TOM20 was analyzed in relation to β-Actin in CB derived erythroblasts. In accordance with what has previously shown in mouse, mitochondrial biomass decreases to become virtually non-detectable in mature erythroblasts. Interestingly, TOM20 expression remained in PGC1β transduced CB derived erythroblasts, suggesting a delay in mitochondrial clearance. In Bone marrow this analysis was done by way of flow cytometry and Mitotracker Deep Red stain. Similar to CB, BM derived erythroblast had increased mitochondrial mass.

Next we wanted to determine the involvement of PGC1b in regulation of hemoglobin composition and iron transport, biological processes taking place in mitochondria that are essential for red blood cell function. Transcriptional analysis of BM derived erythroid progenitors on day 18 revealed that the expression of key genes in heme and globin synthesis, including TMEM14c, ABCB7, FECH, HBA and HBB were deregulated in response to PGC1β knock-down. To functionally investigate if reduced expression of genes regulating heme synthesis and iron transport had an effect on hemoglobin content, BM derived erythroid cells from day 21 of culture were stained with hemoglobin staining diaminobenzidine (DAB). DAB analysis revealed that hemoglobin content in reticulocytes decreased with PGC1b knock-down.

Transcriptional analysis in CB erythroblast on day 16 revealed deregulated expression of several of the heme related genes. ALAS2 and FECH were further analyzed using western blot. When compared to total cell numbers (β-ACTIN) FECH protein was significantly increased. However, when taken the increased mitochondrial biomass into account, FECH protein was instead significantly reduced in sh PGC1β transduced cells. In agreement with clearance of mitochondria in later erythroid maturation stages (no detectable TOM20), only FECH had clear bands in more mature erythroblasts. In conclusion, reduced levels of PGC1β results in deregulation of genes involved in hemoglobin composition and iron transport, as well as reduced hemoglobin content during the final stages of erythroid maturation in BM.

Decreased PGC1b expression results in perturbed cell cycle exit and smaller reticulocytes.

Activation of PPAR signaling has been found to be involved in induction of cell cycle arrest in, and inhibition of cell growth cancer cell lines. Additionally, we demonstrated that down-regulation of Pgc1b in response to pRb deletion in the mouse correlated with enhanced cycling and increased expression of cell cycle genes in erythroid progenitors. To further study the direct role of PGC1β in cell cycle regulation of human erythropoiesis, erythroblasts were stained with DAPI and analysed for cell cycle status. In accordance with our previous results, PGC1b knock-down resulted in the perturbed cell cycle exit of BM derived erythroblasts. These erythroblasts continued into S-phase at a time when they are supposed to exit cell cycle. In more mature erythroblasts cell cycle related genes, including E2F7, E2F8, CDK2 and CCNE1 all had increased expression. Gene expression of cell cycle related genes were similarly increased in CB derived erythroblast

It has been shown that erythroblasts that undergo fewer division results in larger erythrocytes. To address if maintained cell cycle entry has an impact on cell size we quantified the size of erythroblasts using flow cytometry and reticulocytes by image analysis. Notably, both erythroblasts and reticulocytes had reduced cell size.

Taken together, our results demonstrate that decreased expression of PGC1β results in perturbed human erythroid differentiation, reduced mitochondrial clearance, disrupted hemoglobin production, inability to properly exit cell cycle, and a consequent reduced cell size of reticulocytes.

Paper III

Yippee like 4 (Ypel4) is essential for normal mouse red blood cell membrane integrity

Alexander Mattebo, Taha Sen, Maria Jassinskaja, Kristýna Pimková, Isabel Prieto González-Albo, Abdul Ghani Alattar, Ramprasad Ramakrishnan, Stefan Lang, Marcus Järås, Jenny Hansson, Shamit Soneji, Sofie Singbrant, Emile van den Akker, and Johan Flygare

Scientific Reports, Volume 11, Article number 15898 (2021).
https://doi.org/10.1038/s41598-021-95291-1

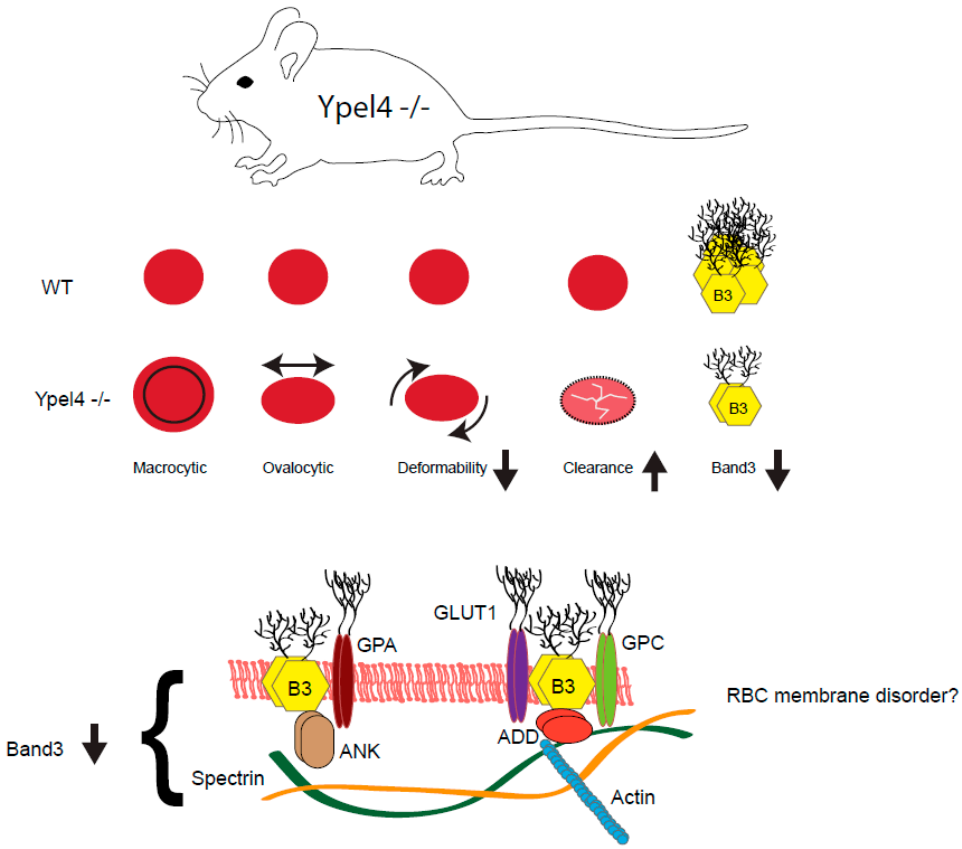

Figure 12 Graphical abstract: Paper III

Background

The YPEL family genes are highly conserved across a diverse range of eukaryotic organisms and are therefore realistically involved in important cellular processes [337, 338]. A common molecular function has not been confirmed for YPEL genes however, studies have examined phenotypic changes to elucidate the gene function. YPEL proteins have been shown to have effects on broad array of biological functions including proliferation, apoptosis and migration. Of published literature, most have studied YPEL in vitro and with cell lines. This could potentially result in overlooking key physiological aspects of a genes function. Ypel4 is specifically and highly expressed in erythroblasts during terminal differentiation. Despite this very specific expression in erythroid cells Ypel4 has yet to be described in erythroid cells. In this regard, we investigated a Ypel4-null mouse to provide insights into its role in erythropoiesis.

Key findings

Ypel null mice display macrocytic secondary polycythemia.

The peripheral blood of Ypel null (-/-) mice were analyzed using hematology analyzer. Ypel4 null mice exhibit a significant increase in hematocrit (HCT), mean corpuscular volume , and frequency of reticulocytes compared to wild type (WT, Ypel4+/+). RBC distribution width was then analyzed to further characterize the observed MCV increase and showed close to elevated variations between RBC in Ypel4 null mice.To determine if the causes of increased HCT and reticulocytosis Epo serum levels were measure. Serum Epo levels were determined to be increased and the mice therefore displayed signs of secondary polycythemia.

Ypel null mice display normal terminal erythroid differentiation.

To define the peripheral blood phenotype bone marrow erythroblasts were analyzed by flow cytometry. Within the fractionated erythroblasts in terminal differentiation population frequencies, cell size, enucleation efficiency and cell cycle status was determined. Despite being highly expressed in orthochromatic erythroblasts no differences could be observed between the WT and Ypel4 null erythroblasts.

To analyze effects of global cellular processes RNA sequencing was performed on sorted polychromatophilic erythroblasts and orthochromatic erythroblast. Together with the expected difference in Ypel4 expression between WT and KO, few other genes were differentially expressed.

In conclusion, Ypel4 deficiency did not affect terminal erythroid differentiation or gene expression profile despite being highly expressed in erythroblasts.

Induced stress erythropoiesis reveals decreased recovering capacity in a transplantation setting.

To determine discrepancy between increased serum Epo levels but a lack in a phenotype of terminal erythroblast, we proposed that mechanisms of Ypel4 deficiency might be accentuated with induced anemia. Stress erythropoiesis was therefore induced in recipient mice by lethal irradiation an transplantation of WT or Ypel4 null BM. The recovering capacity of BM cells were followed by analysis of peripheral blood, spleens and BM. Being the primary organ for stress erythropoiesis, spleens showed rapid expansion of erythroblasts with prolonged expansion of in the mice transplanted with Ypel null BM. In accordance with the prolonged expansion in spleen, frequency of peripheral blood reticulocytes were increased at day 18.

To determine how the initial increased response in spleen translated to overall recovery of anemia, peripheral blood was examined by hematology analyzer. In spite of the increased frequency of erythroid progenitors in spleen and reticulocytes in peripheral blood, mice transplanted with Ypel4 null BM failed to improve their HCT levels, HGB concentration and RBC count. To answer whether this was due to increased clearance of RBCs the rate of longevity or clearance of RBC were determined by In vivo biotinylation of RBCs. As anticipated, circulating RBCs were of Ypel4 null mice were cleared at a higher rate.

Collectively, this demonstrated that Ypel4 null erythroid progenitors are able to expand normally. However, Ypel4 null derived RBC in the circulation were cleared at an increased rate compared.

Ypel4 deficient mice display signs of RBC membrane disorders.

RBC hemolysis can be caused by different mechanisms. We hypothesized that the increased clearance of RBC was due to weaknesses in the membrane as YPEL proteins have been implicated in cytoskeletal changes. To study the morphology RBCs at high resolutions scanning electron microscopy was utilized. Image analysis of RBC revealed abnormally shaped, elongated RBCs from Ypel4 null mice. Abnormally shaped RBCs are indicative of disrupted membrane deformability. The RBCs were therefore analyzed under shear flow and their deformability was determined based on shear forces. In accordance with the morphologic changes RBC of Ypel4 null mice were less deformable.

Membrane associated proteins play an important role in RBCs structure and deformability by anchoring to the cytoskeleton. Band3, a transmembrane protein in RBC membrane, which is one of the most abundantly expressed, was therefore

measured by flow cytometry and SDS-PAGE. Band3 was determined to be decreased when analyzed with both methods.

To address if Ypel4 and Band3 somehow were associated co-immunoprecipitation of erythroid cell lysates was performed to pull protein complexes formed with YPEL4 followed by quantitative liquid chromatography–mass spectrometry. Several proteins were identified as being enriched by the co-immunoprecipitations. However, Band3 could not be confirmed to have protein-protein interactions with Ypel4.

Collectively, Ypel4 deficient RBC are ovalocytic, less deformable and cleared at a faster pace. The Ypel4 null phenotype therefore resembles red cell membrane disorders. We propose that the functional deficiency is attributed to reduced levels of Band3 in Ypel4 null erythroblasts and that Ypel4 loss has an indirect effect on Band3 protein levels in RBC membranes.

Concluding remarks

Cell cycle to mitochondria and back.

Differentiation of most cells are dependent on cell cycle exit. Contrastingly, in erythroid differentiation, cell divisions concomitant with differentiation need to transpire for an additional four divisions. Most likely, an evolutionary mechanism for the increased output of one very specialized cell, constantly being produced. Terminal erythroid differentiation is intimately coupled to cell divisions and deregulation cell cycle regulators have therefore been implicated in disturbed differentiation of erythroblasts numerous times. However, the apparent connection between cell cycle regulation and mitochondrial metabolism has not fully been elucidated yet. In my papers I have provided examples of how mitochondrial biogenesis is regulating cell cycle.

In my first paper we demonstrated that perturbed cell cycle exit could be rescued by increasing mitochondrial biogenesis. Using newer erythroid fractionation protocols, we could define a specific population in which pRb deficient erythropoiesis is disturbed. We identified PGC1b as the factor, in this erythroid differentiation defect, and could rescue the phenotype by enhancing PPARg signaling through PGC1b. We were able to disentangle pRb from the defect and instead provided a proof-of-principle that disturbed mitochondrial function instead is the underlying cause and not necessarily pRb itself. Interestingly, enhanced PPARg signaling seemed to have direct effect on cell cycle regulation. Having many similarities with MDS related anemia we proposed that enhanced mitochondrial function potentially could be a new therapeutic avenue in del(5q) MDS specifically.

However, for our work to be considered in an MDS setting we had to define the role of PGC1b in human terminal erythroid differentiation. To this end, in my second paper we studied the role of PGC1b in human erythropoiesis. In accordance with our previous paper, we could show that PGC1b is important for terminal erythropoiesis, also in the human setting. Disrupted PGC1b expression resulted in phenotype with deregulated cell cycle exit as well as mitochondria related disruptions, which nicely tied back to our first paper.

PPAR-gamma as target in del(5q) MDS

As co-activator of the PPARg transcription factor, PGC1b is important for mitochondrial biogenesis [339-342]. In addition to its coactivator, PPAR signalling pathway is also ligand inducible. Despite intensive research for the past 20 years, identification of a high-affinity endogenous ligand, specific for PPARg has yet to be determined [343, 344]. Presently endogenous ligands for PPARg consists broadly of lipid derivates with low binding affinity and low *in vivo* concentrations. In spite of the uncertainties surrounding the endogenous ligands there are several drugs targeting PPARg including fibrates, thiazolidinediones and other selective PPARg modulators.

My hypothesis is that PGC1b haploinsufficient patients potentially could benefit from the treatment with a PPARg agonist. Enhancing the signalling of this pathway could rescue mitochondrial defects often associated with MDS patients. The drugs are readily available with several already applied in different stages of clinical studies. For these drugs to be considered in a clinical setting, initial experiments could be done with *in vitro* cultures of MDS patient samples.

Outstanding questions

In the first paper we demonstrated that CFU-Es were increased and in the second paper we also demonstrated an effect on earlier progenitors. Importance of PGC1b therefore isn't restricted to terminally differentiating erythroblast. This effect on earlier progenitors is an interesting aspect and one that could be further studied. Glucocorticoids are known to be important for the self-renewal of committed progenitors, BFU-Es [155, 156]. Additionally, PPARa has been shown to synergize with glucocorticoids to promote self-renewal [345]. The question whether PPARg also does that remains unsolved.

Additionally, PGC1 coactivators are known to have tissue specific metabolic actions. Since metabolic requirements changes between HSCs, committed progenitors and terminal progenitors during differentiation the question remains whether PGC1b might have different effect on BFU-E/CFU-Es and more mature erythroid progenitors.

What about the membrane?

Integrity of the RBC membrane is fundamental for their function, as evident by several congenital membrane disorders. In the third paper we described the phenotype of Ypel4 null erythroblasts. While Band3 was decreased in the membrane, it was not enriched in the co-immunoprecipitation. However, there were several enriched genes related to protein translation. Defects in translation are associated with some forms of perturbed erythropoiesis.

Ypel 4 is highly expressed in the orthochromatic cells, which for further maturation needs to enucleate and clear their organelles. During enucleation, erythroblasts undergo intense cytoskeletal and membrane reorganizations. Interestingly, alpha- and beta- tubulin were also consistently enriched in the Co-IP samples that are components of the cell cytoskeleton and this colocalization of YPEL family proteins with microtubule-related structures has previously been reported [346-348]. In addition to translation related and tubulin proteins, Tropomodulin 3 was also enriched. Tropomodulin 3 is known to modify actin filaments and has been shown to be important during erythroblast enucleation [349]. Collectively the Co-IP enriched proteins are interesting candidates for future studies in specifying Ypel4 function.

Ypel4 could potentially have an important function during enucleation that have escaped us for now. Future studies could focus on these aspects of YPEL4 function in erythropoiesis. The faint gene expression differences observed between WT and Ypel4 null mice in the sequencing data could possibly be due to mechanisms of genetic robustness, where genes from the same family sometimes are redundant.

Acknowledgement

This thesis is the product of contributions (in some shape or form) by many people that deserves to be acknowledged. It is therefore with some nervousness that I write this final, very personal, section.

Sofie Singbrant Söderberg, words cannot describe how grateful I am to you. You always knew how to motivate me and were always there for me. You were not satisfied with only the immediate role as a supervisors but have been instrumental in my professional as well as personal development. As you said yourself, it is not about having time for things but rather about what you prioritize. Therefore, I am eternally grateful to you for sharing your "spare time" on me these last couple of years. I am happy to have had you as a supervisor and a mentor. You have a saying "If you haven't regretted doing a PhD at least three time, then you haven't done a PhD". Well, if it were not for you I am sure I would have regretted it more than the three occasions I can think of ☺. Thank you for giving me the opportunity to do this PhD and all your (detailed) feedback throughout my studies. Also thank you for being patient with me at times!

Secondly, I would like to take the opportunity to thank my co-supervisor **Johan Flygare** during the second half of my PhD (main supervisor since 2021). I sincerely feel that I got the best of two worlds with you and Sofie. You are an inspiration and were a pleasure to work with. I really enjoyed our brainstorming sessions in your office and I could not help but feel exhilarated after those meetings (and sometimes overwhelmed at the scope, but mostly excited!).

Stefan Karlsson and **Jonas Larsson**, thank you creating the very special environment at A12.

Mattias Magnusson and **Jill Storry**, thank you for your valuable feedback and suggestions during my half time review.

Christine Karlsson, thank you for always making me feel like I could turn to you for help and checking in on how I was doing. Your support meant a lot.

I would also like to thank my lab members, both past and present. My PhD period would not be the same without you. I have had different office spaces throughout the years and have been blessed with an awesome group of people each time. Thank you **Maria D., Sarah, Roger, Sandra, Shub,** for including us new students and for making difficult times more bearable. **Abdul Ghani**, for never turning me back without having helped me first. Your help was instrumental for my second project. You have a kind soul and a generous personality. I wish you the best. **Jun**, for assisting with experimental work and encouragement especially during some of the hectic days, I am happy to call you a friend. **Alexander M**. Thank you for being a friend, confidant, weapon bearer and a brother. I have very much enjoyed getting to know you and your family over the years. It was a blast working with you throughout the years and thanks for checking in on me from time to time ☺ it means a lot! **Mayur**, thanks for being an amazing colleague and ally. It was nice to get know you a little better during the conference in Frankfurt. I know you are in the region and I look forward to meeting you and your family again☺. To everyone in the new office space **Kris**, **Alexandra**, **Melissa**, **Hooi Min**, **Kiyoka**, **Els,** thank you for the good times and all the help. **Kris** I expect a custom home made fishing lure in going away present! ☺

David Y., I was lucky to have our paths cross early on. It was nice having a mentor in the lab (that I could pester with questions regarding cloning). More importantly, you are someone I look up to and admire. Your work ethic was an encouragement to me and I enjoyed our very interesting discussions (sometimes me just venting, I know). **Roman,** always fun to chat with you, you always crack me up. Also, I wonder how you found the time to game while working so hard, please teach me! **Ludwig,** it has been fun to follow you throughout the years. You are a smart and down to earth. I look forward to following your career.

Thank you **Ineke**, **Xiaojie, and Natsumi** for being the backbone of A12 and making sure everything runs operationally (also sorry for the irregular orders at times). The people involved with core facilities including **Anna**, **Zhi**, **Teona** at FACS facility and **Beata** at Vector facility. **Aurelie BAUDET,** thanks for the smiles and for keeping everyone on their toes.

Everyone who participated in the professional development program, **Sandro**, **Magdalena**, **Maria J**., **Mohamed**, **Ella**, **Parashar**, **Niklas**, **Jonas**, **Ouyang**, **Alexandra**, **Kris** and **Anna**. I wish I had gotten to know you all a little bit sooner, thanks for making that period amazing. Also big thanks to **Christine** and **Jenny**

Hansson for organizing the program. I hope that you can continue with this important program.

I would also like to take the opportunity thank our valuable collaborators, **Shamit Soneji** and **Stefan Lang** for their help with the bioinformatics, **Carl R Walkley** for his speedy yet thorough feedback, **Magnus Gram** for discussions surrounding iron and heme, thank you all.

Also a big thanks to all of you across the hall (B12), I think I have borrowed reagents and gotten help from each groups on several occasions. **Mikael** thank you for being a good friend throughout the years. Magdalena and **Bellodi group** in general for being generous with equipment and reagents. **Stefan Scheding** and group for arranging BM samples from volunteers.

Most importantly my partner **Aysun**, thank you for enduring the late nights, the strange hours and in general being through thick and thin. Sorry for not leaving my work when I left the workplace I wish it was that easy.

Ve en önemlisi ailem, koşulsuz desteğiniz için çok teşekkür ederim.

Thanks everyone!

References

1. Huber TL, Kouskoff V, Fehling HJ, Palis J, Keller G. Haemangioblast commitment is initiated in the primitive streak of the mouse embryo. Nature. 2004;432(7017):625-30.
2. Palis J, Robertson S, Kennedy M, Wall C, Keller G. Development of erythroid and myeloid progenitors in the yolk sac and embryo proper of the mouse. Development. 1999;126(22):5073-84.
3. Sasaki K, Kendall MD. The morphology of the haemopoietic cells of the yolk sac in mice with particular reference to nucleolar changes. J Anat. 1985;140 (Pt 2):279-95.
4. Sankaran VG, Xu J, Orkin SH. Advances in the understanding of haemoglobin switching. Br J Haematol. 2010;149(2):181-94.
5. He Z, Russell JE. Expression, purification, and characterization of human hemoglobins Gower-1 (zeta(2)epsilon(2)), Gower-2 (alpha(2)epsilon(2)), and Portland-2 (zeta(2)beta(2)) assembled in complex transgenic-knockout mice. Blood. 2001;97(4):1099-105.
6. Palis J. Hematopoietic stem cell-independent hematopoiesis: emergence of erythroid, megakaryocyte, and myeloid potential in the mammalian embryo. FEBS Lett. 2016;590(22):3965-74.
7. Ferkowicz MJ, et al. CD41 expression defines the onset of primitive and definitive hematopoiesis in the murine embryo. Development. 2003;130(18):4393-403.
8. Mikkola HK, Fujiwara Y, Schlaeger TM, Traver D, Orkin SH. Expression of CD41 marks the initiation of definitive hematopoiesis in the mouse embryo. Blood. 2003;101(2):508-16.
9. Ito T, Tajima F, Ogawa M. Developmental changes of CD34 expression by murine hematopoietic stem cells. Exp Hematol. 2000;28(11):1269-73.
10. McGrath KE, et al. Distinct Sources of Hematopoietic Progenitors Emerge before HSCs and Provide Functional Blood Cells in the Mammalian Embryo. Cell Rep. 2015;11(12):1892-904.
11. Ottersbach K. Endothelial-to-haematopoietic transition: an update on the process of making blood. Biochem Soc Trans. 2019;47(2):591-601.
12. Bertrand JY, et al. Haematopoietic stem cells derive directly from aortic endothelium during development. Nature. 2010;464(7285):108-11.
13. Boisset JC, et al. In vivo imaging of haematopoietic cells emerging from the mouse aortic endothelium. Nature. 2010;464(7285):116-20.
14. Kissa K, Herbomel P. Blood stem cells emerge from aortic endothelium by a novel type of cell transition. Nature. 2010;464(7285):112-5.

15. Chen MJ, et al. Erythroid/myeloid progenitors and hematopoietic stem cells originate from distinct populations of endothelial cells. Cell Stem Cell. 2011;9(6):541-52.
16. Becker AJ, Mc CE, Till JE. Cytological demonstration of the clonal nature of spleen colonies derived from transplanted mouse marrow cells. Nature. 1963;197:452-4.
17. Till JE, Mc CE. A direct measurement of the radiation sensitivity of normal mouse bone marrow cells. Radiat Res. 1961;14:213-22.
18. Siminovitch L, McCulloch EA, Till JE. The Distribution of Colony-Forming Cells among Spleen Colonies. J Cell Comp Physiol. 1963;62:327-36.
19. Adamo L, Garcia-Cardena G. The vascular origin of hematopoietic cells. Dev Biol. 2012;362(1):1-10.
20. Moore MA, Owen JJ. Chromosome marker studies on the development of the haemopoietic system in the chick embryo. Nature. 1965;208(5014):956 passim.
21. Moore MA, Owen JJ. Chromosome marker studies in the irradiated chick embryo. Nature. 1967;215(5105):1081-2.
22. Moore MA, Metcalf D. Ontogeny of the haemopoietic system: yolk sac origin of in vivo and in vitro colony forming cells in the developing mouse embryo. Br J Haematol. 1970;18(3):279-96.
23. Dieterlen-Lievre F. On the origin of haemopoietic stem cells in the avian embryo: an experimental approach. Journal of embryology and experimental morphology. 1975;33(3):607-19.
24. Dieterlen-Lièvre F, Martin C. Diffuse intraembryonic hemopoiesis in normal and chimeric avian development. Dev Biol. 1981;88(1):180-91.
25. Muller AM, Medvinsky A, Strouboulis J, Grosveld F, Dzierzak E. Development of hematopoietic stem cell activity in the mouse embryo. Immunity. 1994;1(4):291-301.
26. Medvinsky A, Dzierzak E. Definitive hematopoiesis is autonomously initiated by the AGM region. Cell. 1996;86(6):897-906.
27. Boisset J-C, et al. In vivo imaging of haematopoietic cells emerging from the mouse aortic endothelium. Nature. 2010;464(7285):116-20.
28. Zovein AC, et al. Fate tracing reveals the endothelial origin of hematopoietic stem cells. Cell Stem Cell. 2008;3(6):625-36.
29. Chen AT, Zon LI. Zebrafish blood stem cells. Journal of cellular biochemistry. 2009;108(1):35-42.
30. Henninger J, et al. Clonal fate mapping quantifies the number of haematopoietic stem cells that arise during development. Nat Cell Biol. 2017;19(1):17-27.
31. Collin M, Dickinson R, Bigley V. Haematopoietic and immune defects associated with GATA2 mutation. Br J Haematol. 2015;169(2):173-87.
32. Tsai FY, et al. An early haematopoietic defect in mice lacking the transcription factor GATA-2. Nature. 1994;371(6494):221-6.
33. de Pater E, et al. Gata2 is required for HSC generation and survival. J Exp Med. 2013;210(13):2843-50.
34. Gao X, et al. Gata2 cis-element is required for hematopoietic stem cell generation in the mammalian embryo. J Exp Med. 2013;210(13):2833-42.

35. Johnson KD, et al. Cis-element mutated in GATA2-dependent immunodeficiency governs hematopoiesis and vascular integrity. J Clin Invest. 2012;122(10):3692-704.
36. Kruse EA, et al. Dual requirement for the ETS transcription factors Fli-1 and Erg in hematopoietic stem cells and the megakaryocyte lineage. Proc Natl Acad Sci U S A. 2009;106(33):13814-9.
37. Porcher C, et al. The T cell leukemia oncoprotein SCL/tal-1 is essential for development of all hematopoietic lineages. Cell. 1996;86(1):47-57.
38. Robb L, et al. The scl gene product is required for the generation of all hematopoietic lineages in the adult mouse. EMBO J. 1996;15(16):4123-9.
39. Zhu H, et al. Regulation of the lmo2 promoter during hematopoietic and vascular development in zebrafish. Dev Biol. 2005;281(2):256-69.
40. Yamada Y, et al. The T cell leukemia LIM protein Lmo2 is necessary for adult mouse hematopoiesis. Proc Natl Acad Sci U S A. 1998;95(7):3890-5.
41. Nottingham WT, et al. Runx1-mediated hematopoietic stem-cell emergence is controlled by a Gata/Ets/SCL-regulated enhancer. Blood. 2007;110(13):4188-97.
42. Imperato MR, Cauchy P, Obier N, Bonifer C. The RUNX1-PU.1 axis in the control of hematopoiesis. Int J Hematol. 2015;101(4):319-29.
43. Loughran SJ, et al. The transcription factor Erg is essential for definitive hematopoiesis and the function of adult hematopoietic stem cells. Nat Immunol. 2008;9(7):810-9.
44. Speck NA, et al. Core-binding factor: a central player in hematopoiesis and leukemia. Cancer Res. 1999;59(7 Suppl):1789s-93s.
45. Kundu M, et al. Role of Cbfb in hematopoiesis and perturbations resulting from expression of the leukemogenic fusion gene Cbfb-MYH11. Blood. 2002;100(7):2449-56.
46. Chen MJ, Yokomizo T, Zeigler BM, Dzierzak E, Speck NA. Runx1 is required for the endothelial to haematopoietic cell transition but not thereafter. Nature. 2009;457(7231):887-91.
47. North T, et al. Cbfa2 is required for the formation of intra-aortic hematopoietic clusters. Development. 1999;126(11):2563-75.
48. Cai Z, et al. Haploinsufficiency of AML1 affects the temporal and spatial generation of hematopoietic stem cells in the mouse embryo. Immunity. 2000;13(4):423-31.
49. Landry JR, et al. Runx genes are direct targets of Scl/Tal1 in the yolk sac and fetal liver. Blood. 2008;111(6):3005-14.
50. Lim KC, et al. Conditional Gata2 inactivation results in HSC loss and lymphatic mispatterning. J Clin Invest. 2012;122(10):3705-17.
51. Ling KW, et al. GATA-2 plays two functionally distinct roles during the ontogeny of hematopoietic stem cells. J Exp Med. 2004;200(7):871-82.
52. Rodrigues NP, et al. Haploinsufficiency of GATA-2 perturbs adult hematopoietic stem-cell homeostasis. Blood. 2005;106(2):477-84.
53. Johnson KD, et al. Cis-regulatory mechanisms governing stem and progenitor cell transitions. Sci Adv. 2015;1(8):e1500503.

54. Rodrigues NP, et al. GATA-2 regulates granulocyte-macrophage progenitor cell function. Blood. 2008;112(13):4862-73.
55. Mehta C, et al. Integrating Enhancer Mechanisms to Establish a Hierarchical Blood Development Program. Cell Rep. 2017;20(12):2966-79.
56. Kobayashi-Osaki M, et al. GATA motifs regulate early hematopoietic lineage-specific expression of the Gata2 gene. Mol Cell Biol. 2005;25(16):7005-20.
57. Metcalf D. Hematopoietic cytokines. Blood. 2008;111(2):485-91.
58. Thoren LA, et al. Kit regulates maintenance of quiescent hematopoietic stem cells. J Immunol. 2008;180(4):2045-53.
59. Ikuta K, Weissman IL. Evidence that hematopoietic stem cells express mouse c-kit but do not depend on steel factor for their generation. Proc Natl Acad Sci U S A. 1992;89(4):1502-6.
60. Sharma Y, Astle CM, Harrison DE. Heterozygous kit mutants with little or no apparent anemia exhibit large defects in overall hematopoietic stem cell function. Exp Hematol. 2007;35(2):214-20.
61. Cserhati I, Kelemen E. Acute prolonged thrombocytosis in mice induced by thrombocythaemic sera; a possible human thrombopoietin; a preliminary communication. Acta Med Acad Sci Hung. 1958;11(4):473-5.
62. Kelemen E, Cserhati I, Tanos B. Demonstration and some properties of human thrombopoietin in thrombocythaemic sera. Acta Haematol. 1958;20(6):350-5.
63. Wendling F, Varlet P, Charon M, Tambourin P. MPLV: a retrovirus complex inducing an acute myeloproliferative leukemic disorder in adult mice. Virology. 1986;149(2):242-6.
64. Buza-Vidas N, et al. Cytokines regulate postnatal hematopoietic stem cell expansion: opposing roles of thrombopoietin and LNK. Genes Dev. 2006;20(15):2018-23.
65. Qian H, et al. Critical role of thrombopoietin in maintaining adult quiescent hematopoietic stem cells. Cell Stem Cell. 2007;1(6):671-84.
66. Solar GP, et al. Role of c-mpl in early hematopoiesis. Blood. 1998;92(1):4-10.
67. Kaushansky K, et al. Thrombopoietin expands erythroid progenitors, increases red cell production, and enhances erythroid recovery after myelosuppressive therapy. J Clin Invest. 1995;96(3):1683-7.
68. Robb L. Cytokine receptors and hematopoietic differentiation. Oncogene. 2007;26(47):6715-23.
69. Wagemaker G, Burger H, van Gils FC, van Leen RW, Wielenga JJ. Interleukin-3. Biotherapy. 1990;2(4):337-45.
70. Metcalf D, et al. Effects of purified bacterially synthesized murine multi-CSF (IL-3) on hematopoiesis in normal adult mice. Blood. 1986;68(1):46-57.
71. Hercus TR, et al. The granulocyte-macrophage colony-stimulating factor receptor: linking its structure to cell signaling and its role in disease. Blood. 2009;114(7):1289-98.
72. Miller BA. Hematopoietin Receptors. In: William J. Lennarz MDL, editor. Encyclopedia of Biological Chemistry (Second Edition): Academic Press; 2013. p. Pages 526-31.

73. Bennett GD, Kay MM. Homeostatic removal of senescent murine erythrocytes by splenic macrophages. Exp Hematol. 1981;9(3):297-307.
74. Dupire J, Socol M, Viallat A. Full dynamics of a red blood cell in shear flow. Proceedings of the National Academy of Sciences. 2012;109(51):20808.
75. Danielczok JG, et al. Red Blood Cell Passage of Small Capillaries Is Associated with Transient Ca2+-mediated Adaptations. Frontiers in Physiology. 2017;8(979).
76. Palis J. Primitive and definitive erythropoiesis in mammals. Front Physiol. 2014;5:3.
77. Koury MJ, Bondurant MC. Erythropoietin Retards DNA Breakdown and Prevents Programmed Death in Erythroid Progenitor Cells. Science. 1990;248(4953):378-81.
78. Singbrant S, et al. Erythropoietin couples erythropoiesis, B-lymphopoiesis, and bone homeostasis within the bone marrow microenvironment. Blood. 2011;117(21):5631-42.
79. Lu L, Ge Y, Li ZH, Dai MS, Broxmeyer HE. Enhancement of proliferation and differentiation of erythroid progenitors by co-transduction of erythropoietin receptor and H-ras cDNAs into single CD343+ cord blood cells. Bone Marrow Transplantation. 2000;26(8):817-22.
80. Nijhof W, Wierenga PK. Isolation and characterization of the erythroid progenitor cell: CFU-E. J Cell Biol. 1983;96(2):386-92.
81. Wu H, Liu X, Jaenisch R, Lodish HF. Generation of committed erythroid BFU-E and CFU-E progenitors does not require erythropoietin or the erythropoietin receptor. Cell. 1995;83(1):59-67.
82. Chen K, et al. Resolving the distinct stages in erythroid differentiation based on dynamic changes in membrane protein expression during erythropoiesis. Proc Natl Acad Sci U S A. 2009;106(41):17413-8.
83. Borsook H, Lingrel JB, Scaro JL, Millette RL. Synthesis of haemoglobin in relation to the maturation of erythroid cells. Nature. 1962;196:347-50.
84. Au - Koulnis M, et al. Identification and Analysis of Mouse Erythroid Progenitors using the CD71/TER119 Flow-cytometric Assay. JoVE. 2011(54):e2809.
85. Nandakumar SK, Ulirsch JC, Sankaran VG. Advances in understanding erythropoiesis: evolving perspectives. Br J Haematol. 2016;173(2):206-18.
86. Hu J, et al. Isolation and functional characterization of human erythroblasts at distinct stages: implications for understanding of normal and disordered erythropoiesis in vivo. Blood. 2013;121(16):3246-53.
87. Liu J, et al. Quantitative analysis of murine terminal erythroid differentiation in vivo: novel method to study normal and disordered erythropoiesis. Blood. 2013;121(8):e43-e9.
88. Pronk CJ, et al. Elucidation of the phenotypic, functional, and molecular topography of a myeloerythroid progenitor cell hierarchy. Cell Stem Cell. 2007;1(4):428-42.
89. An X, et al. Global transcriptome analyses of human and murine terminal erythroid differentiation. Blood. 2014;123(22):3466-77.
90. Kingsley PD, et al. Ontogeny of erythroid gene expression. Blood. 2013;121(6):e5-e13.

91. de Back DZ, Kostova EB, van Kraaij M, van den Berg TK, van Bruggen R. Of macrophages and red blood cells; a complex love story. Front Physiol. 2014;5:9.
92. Chasis JA, Prenant M, Leung A, Mohandas N. Membrane assembly and remodeling during reticulocyte maturation. Blood. 1989;74(3):1112-20.
93. Malleret B, et al. Significant biochemical, biophysical and metabolic diversity in circulating human cord blood reticulocytes. PLoS One. 2013;8(10):e76062.
94. Waugh RE, et al. Surface area and volume changes during maturation of reticulocytes in the circulation of the baboon. The Journal of laboratory and clinical medicine. 1997;129(5):527-35.
95. Ovchynnikova E, Aglialoro F, von Lindern M, van den Akker E. The Shape Shifting Story of Reticulocyte Maturation. Frontiers in physiology. 2018;9:829-.
96. Franco RS. Measurement of Red Cell Lifespan and Aging. Transfusion Medicine and Hemotherapy. 2012;39(5):302-7.
97. Evans T, Felsenfeld G. The erythroid-specific transcription factor Eryf1: a new finger protein. Cell. 1989;58(5):877-85.
98. Tsai SF, et al. Cloning of cDNA for the major DNA-binding protein of the erythroid lineage through expression in mammalian cells. Nature. 1989;339(6224):446-51.
99. Cheng Y, et al. Erythroid GATA1 function revealed by genome-wide analysis of transcription factor occupancy, histone modifications, and mRNA expression. Genome Res. 2009;19(12):2172-84.
100. Fujiwara T, et al. Discovering hematopoietic mechanisms through genome-wide analysis of GATA factor chromatin occupancy. Mol Cell. 2009;36(4):667-81.
101. Yu M, et al. Insights into GATA-1-mediated gene activation versus repression via genome-wide chromatin occupancy analysis. Mol Cell. 2009;36(4):682-95.
102. Papadopoulos GL, et al. GATA-1 genome-wide occupancy associates with distinct epigenetic profiles in mouse fetal liver erythropoiesis. Nucleic Acids Res. 2013;41(9):4938-48.
103. Gutierrez L, et al. Ablation of Gata1 in adult mice results in aplastic crisis, revealing its essential role in steady-state and stress erythropoiesis. Blood. 2008;111(8):4375-85.
104. Fujiwara Y, Browne CP, Cunniff K, Goff SC, Orkin SH. Arrested development of embryonic red cell precursors in mouse embryos lacking transcription factor GATA-1. Proc Natl Acad Sci U S A. 1996;93(22):12355-8.
105. Pevny L, et al. Development of hematopoietic cells lacking transcription factor GATA-1. Development. 1995;121(1):163-72.
106. Rodriguez P, et al. GATA-1 forms distinct activating and repressive complexes in erythroid cells. The EMBO journal. 2005;24(13):2354-66.
107. Cantor AB, Orkin SH. Transcriptional regulation of erythropoiesis: an affair involving multiple partners. Oncogene. 2002;21(21):3368-76.
108. Kerenyi MA, Orkin SH. Networking erythropoiesis. J Exp Med. 2010;207(12):2537-41.
109. Mancini E, et al. FOG-1 and GATA-1 act sequentially to specify definitive megakaryocytic and erythroid progenitors. EMBO J. 2012;31(2):351-65.

110. Crispino JD, Lodish MB, MacKay JP, Orkin SH. Use of altered specificity mutants to probe a specific protein-protein interaction in differentiation: the GATA-1:FOG complex. Mol Cell. 1999;3(2):219-28.
111. Mikkola HK, et al. Haematopoietic stem cells retain long-term repopulating activity and multipotency in the absence of stem-cell leukaemia SCL/tal-1 gene. Nature. 2003;421(6922):547-51.
112. Robb L, et al. Absence of yolk sac hematopoiesis from mice with a targeted disruption of the scl gene. Proc Natl Acad Sci U S A. 1995;92(15):7075-9.
113. Nuez B, Michalovich D, Bygrave A, Ploemacher R, Grosveld F. Defective haematopoiesis in fetal liver resulting from inactivation of the EKLF gene. Nature. 1995;375(6529):316-8.
114. Love PE, Warzecha C, Li L. Ldb1 complexes: the new master regulators of erythroid gene transcription. Trends Genet. 2014;30(1):1-9.
115. Saleque S, Cameron S, Orkin SH. The zinc-finger proto-oncogene Gfi-1b is essential for development of the erythroid and megakaryocytic lineages. Genes Dev. 2002;16(3):301-6.
116. Suzuki N, et al. Identification and characterization of 2 types of erythroid progenitors that express GATA-1 at distinct levels. Blood. 2003;102(10):3575-83.
117. Pal S, et al. Coregulator-dependent facilitation of chromatin occupancy by GATA-1. Proc Natl Acad Sci U S A. 2004;101(4):980-5.
118. Bresnick EH, et al. Mechanisms of erythrocyte development and regeneration: implications for regenerative medicine and beyond. Development. 2018;145(1).
119. Anderson KP, Crable SC, Lingrel JB. Multiple proteins binding to a GATA-E box-GATA motif regulate the erythroid Kruppel-like factor (EKLF) gene. J Biol Chem. 1998;273(23):14347-54.
120. Hasegawa A, Shimizu R. GATA1 Activity Governed by Configurations of cis-Acting Elements. Front Oncol. 2016;6:269.
121. Borg J, et al. Haploinsufficiency for the erythroid transcription factor KLF1 causes hereditary persistence of fetal hemoglobin. Nat Genet. 2010;42(9):801-5.
122. Drissen R, et al. The erythroid phenotype of EKLF-null mice: defects in hemoglobin metabolism and membrane stability. Mol Cell Biol. 2005;25(12):5205-14.
123. Gnanapragasam MN, et al. EKLF/KLF1-regulated cell cycle exit is essential for erythroblast enucleation. Blood. 2016;128(12):1631-41.
124. Tallack MR, Keys JR, Humbert PO, Perkins AC. EKLF/KLF1 controls cell cycle entry via direct regulation of E2f2. J Biol Chem. 2009;284(31):20966-74.
125. Miller IJ, Bieker JJ. A novel, erythroid cell-specific murine transcription factor that binds to the CACCC element and is related to the Krüppel family of nuclear proteins. Mol Cell Biol. 1993;13(5):2776-86.
126. Tallack MR, et al. A global role for KLF1 in erythropoiesis revealed by ChIP-seq in primary erythroid cells. Genome Res. 2010;20(8):1052-63.
127. Broxmeyer HE, et al. Effect of murine mast cell growth factor (c-kit proto-oncogene ligand) on colony formation by human marrow hematopoietic progenitor cells. Blood. 1991;77(10):2142-9.

128. Broudy VC, Lin NL, Priestley GV, Nocka K, Wolf NS. Interaction of stem cell factor and its receptor c-kit mediates lodgment and acute expansion of hematopoietic cells in the murine spleen. Blood. 1996;88(1):75-81.
129. Perry JM, Harandi OF, Paulson RF. BMP4, SCF, and hypoxia cooperatively regulate the expansion of murine stress erythroid progenitors. Blood. 2007;109(10):4494-502.
130. Broxmeyer HE, et al. Synergistic myelopoietic actions in vivo after administration to mice of combinations of purified natural murine colony-stimulating factor 1, recombinant murine interleukin 3, and recombinant murine granulocyte/macrophage colony-stimulating factor. Proc Natl Acad Sci U S A. 1987;84(11):3871-5.
131. Alexander WS, et al. Studies of the c-Mpl thrombopoietin receptor through gene disruption and activation. Stem Cells. 1996;14 Suppl 1:124-32.
132. Dolznig H, et al. Apoptosis protection by the Epo target Bcl-X(L) allows factor-independent differentiation of primary erythroblasts. Curr Biol. 2002;12(13):1076-85.
133. Zochodne B, et al. Epo regulates erythroid proliferation and differentiation through distinct signaling pathways: implication for erythropoiesis and Friend virus-induced erythroleukemia. Oncogene. 2000;19(19):2296-304.
134. Carroll M, Zhu Y, D'Andrea AD. Erythropoietin-induced cellular differentiation requires prolongation of the G1 phase of the cell cycle. Proc Natl Acad Sci U S A. 1995;92(7):2869-73.
135. Elliott SG, Foote M, Molineux G. Erythropoietins, erythropoietic factors, and erythropoiesis : molecular, cellular, preclinical, and clinical biology. 2nd rev. and ext. ed. Basel ; Boston: Birkhäuser; 2009. xviii, 326 p. p.
136. Cokic VP, et al. JAK-STAT and AKT pathway-coupled genes in erythroid progenitor cells through ontogeny. J Transl Med. 2012;10:116.
137. Lin CS, Lim SK, D'Agati V, Costantini F. Differential effects of an erythropoietin receptor gene disruption on primitive and definitive erythropoiesis. Genes Dev. 1996;10(2):154-64.
138. Jacobson LO, Goldwasser E, Fried W, Plzak L. Role of the Kidney in Erythropoiesis. Nature. 1957;179(4560):633-4.
139. Zon LI, Youssoufian H, Mather C, Lodish HF, Orkin SH. Activation of the erythropoietin receptor promoter by transcription factor GATA-1. Proceedings of the National Academy of Sciences. 1991;88(23):10638-41.
140. Chiba T, Ikawa Y, Todokoro K. GATA-1 transactivates erythropoietin receptor gene, and erythropoietin receptor-mediated signals enhance GATA-1 gene expression. Nucleic Acids Research. 1991;19(14):3843-8.
141. Lodish HF, Ghaffari S, Socolovsky M, Tong W, Zhang J. Intracellular signaling by the erythropoietin receptor. In: Elliott SG, Foote MA, Molineux G, editors. Erythropoietins, Erythropoietic Factors, and Erythropoiesis: Molecular, Cellular, Preclinical, and Clinical Biology. Basel: Birkhäuser Basel; 2009. p. 155-74.
142. Ghaffari S, et al. AKT induces erythroid-cell maturation of JAK2-deficient fetal liver progenitor cells and is required for Epo regulation of erythroid-cell differentiation. Blood. 2006;107(5):1888-91.

143. Socolovsky M, et al. Ineffective erythropoiesis in Stat5a(-/-)5b(-/-) mice due to decreased survival of early erythroblasts. Blood. 2001;98(12):3261-73.
144. Socolovsky M, Fallon AE, Wang S, Brugnara C, Lodish HF. Fetal anemia and apoptosis of red cell progenitors in Stat5a-/-5b-/- mice: a direct role for Stat5 in Bcl-X(L) induction. Cell. 1999;98(2):181-91.
145. Wood AD, et al. ID1 promotes expansion and survival of primary erythroid cells and is a target of JAK2V617F-STAT5 signaling. Blood. 2009;114(9):1820-30.
146. Zhu BM, et al. Hematopoietic-specific Stat5-null mice display microcytic hypochromic anemia associated with reduced transferrin receptor gene expression. Blood. 2008;112(5):2071-80.
147. Yien YY, et al. FAM210B is an erythropoietin target and regulates erythroid heme synthesis by controlling mitochondrial iron import and ferrochelatase activity. J Biol Chem. 2018;293(51):19797-811.
148. Liu X, et al. Regulation of mitochondrial biogenesis in erythropoiesis by mTORC1-mediated protein translation. Nat Cell Biol. 2017;19(6):626-38.
149. KOURY MJ, BONDURANT MC. The molecular mechanism of erythropoietin action. European Journal of Biochemistry. 1992;210(3):649-63.
150. Harandi OF, Hedge S, Wu DC, McKeone D, Paulson RF. Murine erythroid short-term radioprotection requires a BMP4-dependent, self-renewing population of stress erythroid progenitors. J Clin Invest. 2010;120(12):4507-19.
151. Peslak SA, et al. EPO-mediated expansion of late-stage erythroid progenitors in the bone marrow initiates recovery from sublethal radiation stress. Blood. 2012;120(12):2501-11.
152. Singbrant S, Mattebo A, Sigvardsson M, Strid T, Flygare J. Prospective isolation of radiation induced erythroid stress progenitors reveals unique transcriptomic and epigenetic signatures enabling increased erythroid output. Haematologica. 2020;105(11):2561-71.
153. Paulson RF, Shi L, Wu DC. Stress erythropoiesis: new signals and new stress progenitor cells. Curr Opin Hematol. 2011;18(3):139-45.
154. Bauer A, et al. The glucocorticoid receptor is required for stress erythropoiesis. Genes Dev. 1999;13(22):2996-3002.
155. von Lindern M, et al. The glucocorticoid receptor cooperates with the erythropoietin receptor and c-Kit to enhance and sustain proliferation of erythroid progenitors in vitro. Blood. 1999;94(2):550-9.
156. Flygare J, Rayon Estrada V, Shin C, Gupta S, Lodish HF. HIF1alpha synergizes with glucocorticoids to promote BFU-E progenitor self-renewal. Blood. 2011;117(12):3435-44.
157. Kolbus A, et al. Cooperative signaling between cytokine receptors and the glucocorticoid receptor in the expansion of erythroid progenitors: molecular analysis by expression profiling. Blood. 2003;102(9):3136-46.
158. Wessely O, Deiner EM, Beug H, von Lindern M. The glucocorticoid receptor is a key regulator of the decision between self-renewal and differentiation in erythroid progenitors. Embo j. 1997;16(2):267-80.

159. Ganguli G, Back J, Sengupta S, Wasylyk B. The p53 tumour suppressor inhibits glucocorticoid-induced proliferation of erythroid progenitors. EMBO Rep. 2002;3(6):569-74.
160. Norbury C, Nurse P. Animal cell cycles and their control. Annual review of biochemistry. 1992;61:441-70.
161. Hartwell LH, Weinert TA. Checkpoints: controls that ensure the order of cell cycle events. Science. 1989;246(4930):629-34.
162. Zhang HS, Postigo AA, Dean DC. Active transcriptional repression by the Rb-E2F complex mediates G1 arrest triggered by p16INK4a, TGFbeta, and contact inhibition. Cell. 1999;97(1):53-61.
163. Nevins JR. E2F: a link between the Rb tumor suppressor protein and viral oncoproteins. Science. 1992;258(5081):424-9.
164. Lam EW, La Thangue NB. DP and E2F proteins: coordinating transcription with cell cycle progression. Curr Opin Cell Biol. 1994;6(6):859-66.
165. Dyson N. The regulation of E2F by pRB-family proteins. Genes Dev. 1998;12(15):2245-62.
166. Myster DL, Duronio RJ. To differentiate or not to differentiate? Curr Biol. 2000;10(8):R302-4.
167. Ruijtenberg S, van den Heuvel S. Coordinating cell proliferation and differentiation: Antagonism between cell cycle regulators and cell type-specific gene expression. Cell Cycle. 2016;15(2):196-212.
168. Buttitta LA, Edgar BA. Mechanisms controlling cell cycle exit upon terminal differentiation. Curr Opin Cell Biol. 2007;19(6):697-704.
169. Dolznig H, et al. Erythroid progenitor renewal versus differentiation: genetic evidence for cell autonomous, essential functions of EpoR, Stat5 and the GR. Oncogene. 2006;25(20):2890-900.
170. Cadart C, et al. Size control in mammalian cells involves modulation of both growth rate and cell cycle duration. Nature Communications. 2018;9(1):3275.
171. Dolznig H, et al. Establishment of normal, terminally differentiating mouse erythroid progenitors: molecular characterization by cDNA arrays. Faseb j. 2001;15(8):1442-4.
172. von Lindern M, et al. Leukemic transformation of normal murine erythroid progenitors: v- and c-ErbB act through signaling pathways activated by the EpoR and c-Kit in stress erythropoiesis. Oncogene. 2001;20(28):3651-64.
173. Sankaran VG, et al. Cyclin D3 coordinates the cell cycle during differentiation to regulate erythrocyte size and number. Genes Dev. 2012;26(18):2075-87.
174. Ciemerych MA, et al. Development of mice expressing a single D-type cyclin. Genes & development. 2002;16(24):3277-89.
175. Malumbres M, et al. Mammalian cells cycle without the D-type cyclin-dependent kinases Cdk4 and Cdk6. Cell. 2004;118(4):493-504.
176. Kinross KM, Clark AJ, Iazzolino RM, Humbert PO. E2f4 regulates fetal erythropoiesis through the promotion of cellular proliferation. Blood. 2006;108(3):886-95.

177. Pop R, et al. A Key Commitment Step in Erythropoiesis Is Synchronized with the Cell Cycle Clock through Mutual Inhibition between PU.1 and S-Phase Progression. Plos Biology. 2010;8(9).
178. Weinberg RA. The retinoblastoma protein and cell cycle control. Cell. 1995;81(3):323-30.
179. Clark AJ, Doyle KM, Humbert PO. Cell-intrinsic requirement for pRb in erythropoiesis. Blood. 2004;104(5):1324-6.
180. Trimarchi JM, Lees JA. Sibling rivalry in the E2F family. Nat Rev Mol Cell Biol. 2002;3(1):11-20.
181. Bracken AP, Ciro M, Cocito A, Helin K. E2F target genes: unraveling the biology. Trends Biochem Sci. 2004;29(8):409-17.
182. Chen HZ, Tsai SY, Leone G. Emerging roles of E2Fs in cancer: an exit from cell cycle control. Nat Rev Cancer. 2009;9(11):785-97.
183. Dimova DK, Dyson NJ. The E2F transcriptional network: old acquaintances with new faces. Oncogene. 2005;24(17):2810-26.
184. Dick FA, Rubin SM. Molecular mechanisms underlying RB protein function. Nat Rev Mol Cell Biol. 2013;14(5):297-306.
185. Ji P, et al. An Rb-Skp2-p27 pathway mediates acute cell cycle inhibition by Rb and is retained in a partial-penetrance Rb mutant. Mol Cell. 2004;16(1):47-58.
186. Hilgendorf KI, et al. The retinoblastoma protein induces apoptosis directly at the mitochondria. Genes Dev. 2013;27(9):1003-15.
187. Calzone L, Gelay A, Zinovyev A, Radvanyi F, Barillot E. A comprehensive modular map of molecular interactions in RB/E2F pathway. Mol Syst Biol. 2008;4:173.
188. Liu H, Dibling B, Spike B, Dirlam A, Macleod K. New roles for the RB tumor suppressor protein. Curr Opin Genet Dev. 2004;14(1):55-64.
189. Sankaran VG, Orkin SH, Walkley CR. Rb intrinsically promotes erythropoiesis by coupling cell cycle exit with mitochondrial biogenesis. Genes Dev. 2008;22(4):463-75.
190. Clarke AR, et al. Requirement for a functional Rb-1 gene in murine development. Nature. 1992;359(6393):328-30.
191. Jacks T, et al. Effects of an Rb mutation in the mouse. Nature. 1992;359(6393):295-300.
192. Lee EY, et al. Mice deficient for Rb are nonviable and show defects in neurogenesis and haematopoiesis. Nature. 1992;359(6393):288-94.
193. Wu L, et al. Extra-embryonic function of Rb is essential for embryonic development and viability. Nature. 2003;421(6926):942-7.
194. Huh MS, Parker MH, Scime A, Parks R, Rudnicki MA. Rb is required for progression through myogenic differentiation but not maintenance of terminal differentiation. J Cell Biol. 2004;166(6):865-76.
195. Whyatt D, Grosveld F. Cell-nonautonomous function of the retinoblastoma tumour suppressor protein: new interpretations of old phenotypes. EMBO Rep. 2002;3(2):130-5.

196. Maandag EC, et al. Developmental rescue of an embryonic-lethal mutation in the retinoblastoma gene in chimeric mice. EMBO J. 1994;13(18):4260-8.
197. Williams BO, et al. Extensive contribution of Rb-deficient cells to adult chimeric mice with limited histopathological consequences. EMBO J. 1994;13(18):4251-9.
198. de Bruin A, et al. Rb function in extraembryonic lineages suppresses apoptosis in the CNS of Rb-deficient mice. Proc Natl Acad Sci U S A. 2003;100(11):6546-51.
199. Dirlam A, Spike BT, Macleod KF. Deregulated E2f-2 underlies cell cycle and maturation defects in retinoblastoma null erythroblasts. Mol Cell Biol. 2007;27(24):8713-28.
200. Humbert PO, et al. E2F4 is essential for normal erythrocyte maturation and neonatal viability. Mol Cell. 2000;6(2):281-91.
201. Hu T, et al. Concomitant inactivation of Rb and E2f8 in hematopoietic stem cells synergizes to induce severe anemia. Blood. 2012;119(19):4532-42.
202. Kadri Z, et al. Direct binding of pRb/E2F-2 to GATA-1 regulates maturation and terminal cell division during erythropoiesis. PLoS Biol. 2009;7(6):e1000123.
203. Zhang J, et al. pRB and E2F4 play distinct cell-intrinsic roles in fetal erythropoiesis. Cell Cycle. 2010;9(2):371-6.
204. Kinross KM, Clark AJ, Iazzolino RM, Humbert PO. E2f4 regulates fetal erythropoiesis through the promotion of cellular proliferation. Blood. 2006;108(3):886-95.
205. Hsieh FF, et al. Cell cycle exit during terminal erythroid differentiation is associated with accumulation of p27(Kip1) and inactivation of cdk2 kinase. Blood. 2000;96(8):2746-54.
206. Ji P, Yeh V, Ramirez T, Murata-Hori M, Lodish HF. Histone deacetylase 2 is required for chromatin condensation and subsequent enucleation of cultured mouse fetal erythroblasts. Haematologica. 2010;95(12):2013-21.
207. Chen C, Lodish HF. Global analysis of induced transcription factors and cofactors identifies Tfdp2 as an essential coregulator during terminal erythropoiesis. Exp Hematol. 2014;42(6):464-76 e5.
208. Pop R, et al. A key commitment step in erythropoiesis is synchronized with the cell cycle clock through mutual inhibition between PU.1 and S-phase progression. PLoS Biol. 2010;8(9).
209. Rekhtman N, et al. PU.1 and pRB interact and cooperate to repress GATA-1 and block erythroid differentiation. Mol Cell Biol. 2003;23(21):7460-74.
210. Spike BT, et al. The Rb tumor suppressor is required for stress erythropoiesis. EMBO J. 2004;23(21):4319-29.
211. Schultze SM, et al. p38alpha controls erythroblast enucleation and Rb signaling in stress erythropoiesis. Cell Res. 2012;22(3):539-50.
212. Spike BT, Dibling BC, Macleod KF. Hypoxic stress underlies defects in erythroblast islands in the Rb-null mouse. Blood. 2007;110(6):2173-81.
213. Kashatus DF, et al. RALA and RALBP1 regulate mitochondrial fission at mitosis. Nat Cell Biol. 2011;13(9):1108-15.

214. Macleod KF. The role of the RB tumour suppressor pathway in oxidative stress responses in the haematopoietic system. Nat Rev Cancer. 2008;8(10):769-81.
215. Ghazaryan S, et al. Inactivation of Rb and E2f8 synergizes to trigger stressed DNA replication during erythroid terminal differentiation. Mol Cell Biol. 2014;34(15):2833-47.
216. Ito K, Suda T. Metabolic requirements for the maintenance of self-renewing stem cells. Nat Rev Mol Cell Biol. 2014;15(4):243-56.
217. Spencer JA, et al. Direct measurement of local oxygen concentration in the bone marrow of live animals. Nature. 2014;508(7495):269-73.
218. Nombela-Arrieta C, et al. Quantitative imaging of haematopoietic stem and progenitor cell localization and hypoxic status in the bone marrow microenvironment. Nature cell biology. 2013;15(5):533-43.
219. Norddahl GL, et al. Accumulating mitochondrial DNA mutations drive premature hematopoietic aging phenotypes distinct from physiological stem cell aging. Cell Stem Cell. 2011;8(5):499-510.
220. Pfeiffer T, Schuster S, Bonhoeffer S. Cooperation and Competition in the Evolution of ATP-Producing Pathways. Science. 2001;292(5516):504-7.
221. Oburoglu L, et al. Glucose and glutamine metabolism regulate human hematopoietic stem cell lineage specification. Cell Stem Cell. 2014;15(2):169-84.
222. Garate Z, et al. Generation of a High Number of Healthy Erythroid Cells from Gene-Edited Pyruvate Kinase Deficiency Patient-Specific Induced Pluripotent Stem Cells. Stem Cell Reports. 2015;5(6):1053-66.
223. Richard A, et al. Erythroid differentiation displays a peak of energy consumption concomitant with glycolytic metabolism rearrangements. PLoS One. 2019;14(9):e0221472.
224. Huang NJ, et al. Enhanced phosphocholine metabolism is essential for terminal erythropoiesis. Blood. 2018;131(26):2955-66.
225. Chung J, et al. The mTORC1/4E-BP pathway coordinates hemoglobin production with L-leucine availability. Science signaling. 2015;8(372):ra34.
226. Lu Z, et al. pRb is an obesity suppressor in hypothalamus and high-fat diet inhibits pRb in this location. Embo j. 2013;32(6):844-57.
227. Annicotte JS, et al. The CDK4-pRB-E2F1 pathway controls insulin secretion. Nat Cell Biol. 2009;11(8):1017-23.
228. Nicolay BN, et al. Loss of RBF1 changes glutamine catabolism. Genes Dev. 2013;27(2):182-96.
229. Reynolds MR, et al. Control of glutamine metabolism by the tumor suppressor Rb. Oncogene. 2014;33(5):556-66.
230. Blanchet E, et al. E2F transcription factor-1 regulates oxidative metabolism. Nat Cell Biol. 2011;13(9):1146-52.
231. Li B, Gordon GM, Du CH, Xu J, Du W. Specific killing of Rb mutant cancer cells by inactivating TSC2. Cancer Cell. 2010;17(5):469-80.
232. Nicolay BN, et al. Proteomic analysis of pRb loss highlights a signature of decreased mitochondrial oxidative phosphorylation. Genes Dev. 2015;29(17):1875-89.

233. Yamauchi A, Bloom ET. Control of cell cycle progression in human natural killer cells through redox regulation of expression and phosphorylation of retinoblastoma gene product protein. Blood. 1997;89(11):4092-9.
234. Jiang H, et al. The RB-E2F1 pathway regulates autophagy. Cancer research. 2010;70(20):7882-93.
235. Ciavarra G, Zacksenhaus E. Rescue of myogenic defects in Rb-deficient cells by inhibition of autophagy or by hypoxia-induced glycolytic shift. J Cell Biol. 2010;191(2):291-301.
236. Finkel T, Hwang PM. The Krebs cycle meets the cell cycle: mitochondria and the G1-S transition. Proc Natl Acad Sci U S A. 2009;106(29):11825-6.
237. Mitra K, Wunder C, Roysam B, Lin G, Lippincott-Schwartz J. A hyperfused mitochondrial state achieved at G1-S regulates cyclin E buildup and entry into S phase. Proc Natl Acad Sci U S A. 2009;106(29):11960-5.
238. Fontenay M, Cathelin S, Amiot M, Gyan E, Solary E. Mitochondria in hematopoiesis and hematological diseases. Oncogene. 2006;25(34):4757-67.
239. Chandel NS, et al. Reactive oxygen species generated at mitochondrial complex III stabilize hypoxia-inducible factor-1alpha during hypoxia: a mechanism of O2 sensing. J Biol Chem. 2000;275(33):25130-8.
240. Zhao B, Mei Y, Yang J, Ji P. Erythropoietin-regulated oxidative stress negatively affects enucleation during terminal erythropoiesis. Exp Hematol. 2016;44(10):975-81.
241. Carraway MS, et al. Erythropoietin activates mitochondrial biogenesis and couples red cell mass to mitochondrial mass in the heart. Circ Res. 2010;106(11):1722-30.
242. Boultwood J, et al. The role of the iron transporter ABCB7 in refractory anemia with ring sideroblasts. PLoS One. 2008;3(4):e1970.
243. Nikpour M, et al. The transporter ABCB7 is a mediator of the phenotype of acquired refractory anemia with ring sideroblasts. Leukemia. 2013;27(4):889-96.
244. Bellelli R, et al. NCOA4 Deficiency Impairs Systemic Iron Homeostasis. Cell Rep. 2016;14(3):411-21.
245. Davuluri G, et al. Inactivation of 3-hydroxybutyrate dehydrogenase 2 delays zebrafish erythroid maturation by conferring premature mitophagy. Proc Natl Acad Sci U S A. 2016;113(11):E1460-9.
246. Liu Z, Ciocea A, Devireddy L. Endogenous siderophore 2,5-dihydroxybenzoic acid deficiency promotes anemia and splenic iron overload in mice. Mol Cell Biol. 2014;34(13):2533-46.
247. Chen W, et al. Abcb10 physically interacts with mitoferrin-1 (Slc25a37) to enhance its stability and function in the erythroid mitochondria. Proc Natl Acad Sci U S A. 2009;106(38):16263-8.
248. Chung J, et al. Iron regulatory protein-1 protects against mitoferrin-1-deficient porphyria. J Biol Chem. 2014;289(11):7835-43.
249. Troadec MB, et al. Targeted deletion of the mouse Mitoferrin1 gene: from anemia to protoporphyria. Blood. 2011;117(20):5494-502.

250. Shaw GC, et al. Mitoferrin is essential for erythroid iron assimilation. Nature. 2006;440(7080):96-100.
251. Wingert RA, et al. Deficiency of glutaredoxin 5 reveals Fe-S clusters are required for vertebrate haem synthesis. Nature. 2005;436(7053):1035-39.
252. Ye H, et al. Glutaredoxin 5 deficiency causes sideroblastic anemia by specifically impairing heme biosynthesis and depleting cytosolic iron in human erythroblasts. J Clin Invest. 2010;120(5):1749-61.
253. Bruno M, De Falco L, Iolascon A. How I Diagnose Non-thalassemic Microcytic Anemias. Semin Hematol. 2015;52(4):270-8.
254. Nilsson R, et al. Discovery of genes essential for heme biosynthesis through large-scale gene expression analysis. Cell Metab. 2009;10(2):119-30.
255. Ponka P. Tissue-specific regulation of iron metabolism and heme synthesis: distinct control mechanisms in erythroid cells. Blood. 1997;89(1):1-25.
256. Morgan EH. Transferrin, biochemistry, physiology and clinical significance. Molecular Aspects of Medicine. 1981;4(1):1-123.
257. Wu CK, et al. The 2.0 A structure of human ferrochelatase, the terminal enzyme of heme biosynthesis. Nature structural biology. 2001;8(2):156-60.
258. Pondarré C, et al. The mitochondrial ATP-binding cassette transporter Abcb7 is essential in mice and participates in cytosolic iron-sulfur cluster biogenesis. Hum Mol Genet. 2006;15(6):953-64.
259. Ferreira GC, Gong J. 5-Aminolevulinate synthase and the first step of heme biosynthesis. Journal of bioenergetics and biomembranes. 1995;27(2):151-9.
260. Yien YY, et al. TMEM14C is required for erythroid mitochondrial heme metabolism. J Clin Invest. 2014;124(10):4294-304.
261. Chiabrando D, et al. The mitochondrial heme exporter FLVCR1b mediates erythroid differentiation. The Journal of clinical investigation. 2012;122(12):4569-79.
262. Keel SB, et al. A heme export protein is required for red blood cell differentiation and iron homeostasis. Science. 2008;319(5864):825-8.
263. Wang GL, Semenza GL. Desferrioxamine induces erythropoietin gene expression and hypoxia-inducible factor 1 DNA-binding activity: implications for models of hypoxia signal transduction. Blood. 1993;82(12):3610-5.
264. Houseknecht KL, Cole BM, Steele PJ. Peroxisome proliferator-activated receptor gamma (PPARgamma) and its ligands: a review. Domest Anim Endocrinol. 2002;22(1):1-23.
265. Debril MB, Renaud JP, Fajas L, Auwerx J. The pleiotropic functions of peroxisome proliferator-activated receptor gamma. J Mol Med (Berl). 2001;79(1):30-47.
266. Willson TM, Brown PJ, Sternbach DD, Henke BR. The PPARs: from orphan receptors to drug discovery. J Med Chem. 2000;43(4):527-50.
267. Puigserver P, et al. A cold-inducible coactivator of nuclear receptors linked to adaptive thermogenesis. Cell. 1998;92(6):829-39.
268. Andersson U, Scarpulla RC. Pgc-1-related coactivator, a novel, serum-inducible coactivator of nuclear respiratory factor 1-dependent transcription in mammalian cells. Mol Cell Biol. 2001;21(11):3738-49.

269. Lin J, Puigserver P, Donovan J, Tarr P, Spiegelman BM. Peroxisome proliferator-activated receptor gamma coactivator 1beta (PGC-1beta), a novel PGC-1-related transcription coactivator associated with host cell factor. J Biol Chem. 2002;277(3):1645-8.
270. Kressler D, Schreiber SN, Knutti D, Kralli A. The PGC-1-related protein PERC is a selective coactivator of estrogen receptor alpha. J Biol Chem. 2002;277(16):13918-25.
271. Wu Z, et al. Mechanisms controlling mitochondrial biogenesis and respiration through the thermogenic coactivator PGC-1. Cell. 1999;98(1):115-24.
272. St-Pierre J, et al. Bioenergetic analysis of peroxisome proliferator-activated receptor gamma coactivators 1alpha and 1beta (PGC-1alpha and PGC-1beta) in muscle cells. J Biol Chem. 2003;278(29):26597-603.
273. Kamei Y, et al. PPARgamma coactivator 1beta/ERR ligand 1 is an ERR protein ligand, whose expression induces a high-energy expenditure and antagonizes obesity. Proc Natl Acad Sci U S A. 2003;100(21):12378-83.
274. Lin J, Handschin C, Spiegelman BM. Metabolic control through the PGC-1 family of transcription coactivators. Cell Metabolism. 2005;1(6):361-70.
275. Cui S, et al. PGC-1 coactivator activity is required for murine erythropoiesis. Mol Cell Biol. 2014;34(11):1956-65.
276. Kassebaum NJ, et al. A systematic analysis of global anemia burden from 1990 to 2010. Blood. 2014;123(5):615-24.
277. WHO. WHO Global Anaemia estimates. https://wwwwhoint/data/gho/data/themes/topics/anaemia_in_women_and_children. 2021.
278. Patel KV. Epidemiology of anemia in older adults. Semin Hematol. 2008;45(4):210-7.
279. Moore CA, Krishnan K. Bone Marrow Failure. StatPearls. Treasure Island (FL): StatPearls Publishing

280. McLean E, Cogswell M, Egli I, Wojdyla D, de Benoist B. Worldwide prevalence of anaemia, WHO Vitamin and Mineral Nutrition Information System, 1993-2005. Public Health Nutr. 2009;12(4):444-54.
281. Barcellini W, et al. Hereditary red cell membrane defects: diagnostic and clinical aspects. Blood Transfus. 2011;9(3):274-7.
282. Weiss G, Goodnough LT. Anemia of chronic disease. N Engl J Med. 2005;352(10):1011-23.
283. Cascio MJ, DeLoughery TG. Anemia: Evaluation and Diagnostic Tests. Med Clin North Am. 2017;101(2):263-84.
284. Zivot A, Lipton JM, Narla A, Blanc L. Erythropoiesis: Insights into pathophysiology and treatments in 2017. Molecular Medicine. 2018;24(1).
285. Ganguly BB, Kadam NN. Mutations of myelodysplastic syndromes (MDS): An update. Mutat Res Rev Mutat Res. 2016;769:47-62.

286. Sperling AS, Gibson CJ, Ebert BL. The genetics of myelodysplastic syndrome: from clonal haematopoiesis to secondary leukaemia. Nat Rev Cancer. 2017;17(1):5-19.
287. Walter MJ, et al. Clonal diversity of recurrently mutated genes in myelodysplastic syndromes. Leukemia. 2013;27(6):1275-82.
288. Papaemmanuil E, et al. Clinical and biological implications of driver mutations in myelodysplastic syndromes. Blood. 2013;122(22):3616-27; quiz 99.
289. Komrokji RS, Padron E, Ebert BL, List AF. Deletion 5q MDS: molecular and therapeutic implications. Best Pract Res Clin Haematol. 2013;26(4):365-75.
290. Baweja M, Moreno-Aspitia A, Menke DM, Roy V, Zubair A. Marked Elliptocytosis in Myelodysplastic Syndromes (MDS) Is Associated to Deletion of Chromosome 20q. Blood. 2005;106(11):4927-.
291. Manthri S, Vasireddy NK, Bandaru S, Pathak S. Acquired Elliptocytosis as a Manifestation of Myelodysplastic Syndrome Associated with Deletion of Chromosome 20q. Case reports in hematology. 2018;2018:6819172-.
292. Hong M, He G. The 2016 Revision to the World Health Organization Classification of Myelodysplastic Syndromes. J Transl Int Med. 2017;5(3):139-43.
293. Conte S, et al. Aberrant splicing of genes involved in haemoglobin synthesis and impaired terminal erythroid maturation in SF3B1 mutated refractory anaemia with ring sideroblasts. Br J Haematol. 2015;171(4):478-90.
294. Dolatshad H, et al. Disruption of SF3B1 results in deregulated expression and splicing of key genes and pathways in myelodysplastic syndrome hematopoietic stem and progenitor cells. Leukemia. 2015;29(5):1092-103.
295. Santini V. Anemia as the Main Manifestation of Myelodysplastic Syndromes. Semin Hematol. 2015;52(4):348-56.
296. Ali AM, et al. Severely impaired terminal erythroid differentiation as an independent prognostic marker in myelodysplastic syndromes. Blood Adv. 2018;2(12):1393-402.
297. Fontenay-Roupie M, et al. Ineffective erythropoiesis in myelodysplastic syndromes: correlation with Fas expression but not with lack of erythropoietin receptor signal transduction. Br J Haematol. 1999;106(2):464-73.
298. Malcovati L. Red blood cell transfusion therapy and iron chelation in patients with myelodysplastic syndromes. Clin Lymphoma Myeloma. 2009;9 Suppl 3:S305-11.
299. Stein RS. The role of erythropoietin in the anemia of myelodysplastic syndrome. Clin Lymphoma. 2003;4 Suppl 1:S36-40.
300. Greenberg PL. Current therapeutic approaches for patients with myelodysplastic syndromes. Br J Haematol. 2010;150(2):131-43.
301. Heptinstall K. Quality of life in myelodysplastic syndromes. A special report from the Myelodysplastic Syndromes Foundation, Inc. Oncology (Williston Park, NY). 2008;22(2 Suppl Nurse Ed):13-8; discussion 9.
302. Nakazaki K, Nannya Y, Kurokawa M. Distribution of serum erythropoietin levels in lower risk myelodysplastic syndrome cases with anemia. Int J Hematol. 2014;99(1):53-6.

303. Stasi R, Abruzzese E, Lanzetta G, Terzoli E, Amadori S. Darbepoetin alfa for the treatment of anemic patients with low- and intermediate-1-risk myelodysplastic syndromes. Ann Oncol. 2005;16(12):1921-7.
304. Hellström-Lindberg E, et al. Erythroid response to treatment with G-CSF plus erythropoietin for the anaemia of patients with myelodysplastic syndromes: proposal for a predictive model. Br J Haematol. 1997;99(2):344-51.
305. Hellström-Lindberg E, et al. Treatment of anemia in myelodysplastic syndromes with granulocyte colony-stimulating factor plus erythropoietin: results from a randomized phase II study and long-term follow-up of 71 patients. Blood. 1998;92(1):68-75.
306. Jädersten M, Montgomery SM, Dybedal I, Porwit-MacDonald A, Hellström-Lindberg E. Long-term outcome of treatment of anemia in MDS with erythropoietin and G-CSF. Blood. 2005;106(3):803-11.
307. Tehranchi R, et al. Granulocyte colony-stimulating factor inhibits spontaneous cytochrome c release and mitochondria-dependent apoptosis of myelodysplastic syndrome hematopoietic progenitors. Blood. 2003;101(3):1080-6.
308. Tehranchi R, et al. Aberrant mitochondrial iron distribution and maturation arrest characterize early erythroid precursors in low-risk myelodysplastic syndromes. Blood. 2005;106(1):247-53.
309. Kelaidi C, et al. Long-term outcome of anemic lower-risk myelodysplastic syndromes without 5q deletion refractory to or relapsing after erythropoiesis-stimulating agents. Leukemia. 2013;27(6):1283-90.
310. Park S, et al. Outcome of Lower-Risk Patients With Myelodysplastic Syndromes Without 5q Deletion After Failure of Erythropoiesis-Stimulating Agents. J Clin Oncol. 2017;35(14):1591-7.
311. List A, et al. Lenalidomide in the myelodysplastic syndrome with chromosome 5q deletion. N Engl J Med. 2006;355(14):1456-65.
312. Fenaux P, et al. A randomized phase 3 study of lenalidomide versus placebo in RBC transfusion-dependent patients with Low-/Intermediate-1-risk myelodysplastic syndromes with del5q. Blood. 2011;118(14):3765-76.
313. Volpe VO, Komrokji RS. Treatment options for lower-risk myelodysplastic syndromes. Where are we now? Ther Adv Hematol. 2021;12:2040620720986641-.
314. Sekeres MA, et al. Relationship of treatment-related cytopenias and response to lenalidomide in patients with lower-risk myelodysplastic syndromes. J Clin Oncol. 2008;26(36):5943-9.
315. Gattermann N. From sideroblastic anemia to the role of mitochondrial DNA mutations in myelodysplastic syndromes. Leuk Res. 2000;24(2):141-51.
316. Gupta M, et al. Mitochondrial DNA variations in myelodysplastic syndrome. Ann Hematol. 2013;92(7):871-6.
317. Kim HR, et al. Mitochondrial DNA aberrations and pathophysiological implications in hematopoietic diseases, chronic inflammatory diseases, and cancers. Ann Lab Med. 2015;35(1):1-14.
318. Shin MG, Kajigaya S, Levin BC, Young NS. Mitochondrial DNA mutations in patients with myelodysplastic syndromes. Blood. 2003;101(8):3118-25.

319. Schildgen V, Wulfert M, Gattermann N. Impaired mitochondrial gene transcription in myelodysplastic syndromes and acute myeloid leukemia with myelodysplasia-related changes. Exp Hematol. 2011;39(6):666-75 e1.
320. Wulfert M, et al. Analysis of mitochondrial DNA in 104 patients with myelodysplastic syndromes. Exp Hematol. 2008;36(5):577-86.
321. Loeb LA, Wallace DC, Martin GM. The mitochondrial theory of aging and its relationship to reactive oxygen species damage and somatic mtDNA mutations. Proceedings of the National Academy of Sciences of the United States of America. 2005;102(52):18769-70.
322. Harman D. Aging: a theory based on free radical and radiation chemistry. J Gerontol. 1956;11(3):298-300.
323. Trifunovic A, et al. Somatic mtDNA mutations cause aging phenotypes without affecting reactive oxygen species production. Proceedings of the National Academy of Sciences of the United States of America. 2005;102(50):17993-8.
324. Papaemmanuil E, et al. Somatic SF3B1 mutation in myelodysplasia with ring sideroblasts. N Engl J Med. 2011;365(15):1384-95.
325. Dolatshad H, et al. Cryptic splicing events in the iron transporter ABCB7 and other key target genes in SF3B1-mutant myelodysplastic syndromes. Leukemia. 2016;30(12):2322-31.
326. Ebert BL, et al. Identification of RPS14 as a 5q- syndrome gene by RNA interference screen. Nature. 2008;451(7176):335-9.
327. Safeukui I, et al. Quantitative assessment of sensing and sequestration of spherocytic erythrocytes by the human spleen. Blood. 2012;120(2):424-30.
328. Da Costa L, Galimand J, Fenneteau O, Mohandas N. Hereditary spherocytosis, elliptocytosis, and other red cell membrane disorders. Blood Rev. 2013;27(4):167-78.
329. Miragliadel Giudice E, et al. Ankyrin Napoli: a de novo deletional frameshift mutation in exon 16 of ankyrin gene (ANK1) associated with spherocytosis. British Journal of Haematology. 1996;93(4):828-34.
330. Agre P, Casella JF, Zinkham WH, McMillan C, Bennett V. Partial deficiency of erythrocyte spectrin in hereditary spherocytosis. Nature. 1985;314(6009):380-3.
331. Jarolim P, et al. Characterization of 13 novel band 3 gene defects in hereditary spherocytosis with band 3 deficiency. Blood. 1996;88(11):4366-74.
332. Hassoun H, et al. Characterization of the Underlying Molecular Defect in Hereditary Spherocytosis Associated With Spectrin Deficiency. Blood. 1997;90(1):398-406.
333. Eber S, Lux SE. Hereditary spherocytosis—defects in proteins that connect the membrane skeleton to the lipid bilayer. Seminars in Hematology. 2004;41(2):118-41.
334. Huang YS, et al. Circulating primitive erythroblasts establish a functional, protein 4.1R-dependent cytoskeletal network prior to enucleating. Sci Rep. 2017;7(1):5164.
335. Narla J, Mohandas N. Red cell membrane disorders. Int J Lab Hematol. 2017;39 Suppl 1:47-52.
336. Kafina MD, Paw BH. Intracellular iron and heme trafficking and metabolism in developing erythroblasts. Metallomics. 2017;9(9):1193-203.

337. Roxström-Lindquist K, Faye I. The Drosophila gene Yippee reveals a novel family of putative zinc binding proteins highly conserved among eukaryotes. Insect molecular biology. 2001;10(1):77-86.
338. Farlie P, et al. Ypel1: a novel nuclear protein that induces an epithelial-like morphology in fibroblasts. Genes Cells. 2001;6(7):619-29.
339. Scarpulla RC. Metabolic control of mitochondrial biogenesis through the PGC-1 family regulatory network. Biochim Biophys Acta. 2011;1813(7):1269-78.
340. Villena JA. New insights into PGC-1 coactivators: redefining their role in the regulation of mitochondrial function and beyond. FEBS J. 2015;282(4):647-72.
341. Liu C, et al. Pparg promotes differentiation and regulates mitochondrial gene expression in bladder epithelial cells. Nat Commun. 2019;10(1):4589.
342. Hernandez-Quiles M, Broekema MF, Kalkhoven E. PPARgamma in Metabolism, Immunity, and Cancer: Unified and Diverse Mechanisms of Action. Frontiers in endocrinology. 2021;12:624112.
343. Grygiel-Górniak B. Peroxisome proliferator-activated receptors and their ligands: nutritional and clinical implications--a review. Nutr J. 2014;13:17-.
344. Schupp M, Lazar MA. Endogenous ligands for nuclear receptors: digging deeper. J Biol Chem. 2010;285(52):40409-15.
345. Lee HY, et al. PPAR-α and glucocorticoid receptor synergize to promote erythroid progenitor self-renewal. Nature. 2015;522(7557):474-7.
346. Hosono K, Sasaki T, Minoshima S, Shimizu N. Identification and characterization of a novel gene family YPEL in a wide spectrum of eukaryotic species. Gene. 2004;340(1):31-43.
347. Liang P, et al. MVP interacts with YPEL4 and inhibits YPEL4-mediated activities of the ERK signal pathway. Biochemistry and cell biology = Biochimie et biologie cellulaire. 2010;88(3):445-50.
348. Hosono K, et al. YPEL5 protein of the YPEL gene family is involved in the cell cycle progression by interacting with two distinct proteins RanBPM and RanBP10. Genomics. 2010;96(2):102-11.
349. Sui Z, et al. Tropomodulin3-null mice are embryonic lethal with anemia due to impaired erythroid terminal differentiation in the fetal liver. Blood. 2014;123(5):758-67.

Paper I

ELSEVIER

Experimental Hematology

Experimental Hematology 2020;88:28–41

REGULAR SUBMISSION

Enhancing mitochondrial function *in vivo* rescues MDS-like anemia induced by pRb deficiency

Taha Sen[a], Mayur Jain[a], Magnus Gram[b], Alexander Mattebo[a], Shamit Soneji[c], Carl R. Walkley[d,1], and Sofie Singbrant[a,1]

[a]*Division of Molecular Medicine and Gene Therapy, Lund Stem Cell Center, Lund University, Lund, Sweden;* [b]*Department of Clinical Sciences Lund, Pediatrics, Lund University, Skane University Hospital Lund, Lund, Sweden;* [c]*Division of Molecular Hematology, Lund Stem Cell Center, Lund University, Lund, Sweden;* [d]*St. Vincent's Institute of Medical Research and Department of Medicine, University of Melbourne, Fitzroy, VIC, Australia*

(Received 28 March 2020; revised 25 June 2020; accepted 30 June 2020)

Erythropoiesis is intimately coupled to cell division, and deletion of the cell cycle regulator retinoblastoma protein (pRb) causes anemia in mice. Erythroid-specific deletion of pRb has been found to result in inefficient erythropoiesis because of deregulated coordination of cell cycle exit and mitochondrial biogenesis. However, the pathophysiology remains to be fully described, and further characterization of the link between cell cycle regulation and mitochondrial function is needed. To this end we further assessed conditional erythroid-specific deletion of pRb. This resulted in macrocytic anemia, despite elevated levels of erythropoietin (Epo), and an accumulation of erythroid progenitors in the bone marrow, a phenotype strongly resembling refractory anemia associated with myelodysplastic syndromes (MDS). Using high-fractionation fluorescence-activated cell sorting analysis for improved phenotypic characterization, we illustrate that erythroid differentiation was disrupted at the orthochromatic stage. Transcriptional profiling of sequential purified populations revealed failure to upregulate genes critical for mitochondrial function such as *Pgc1β*, *Alas2*, and *Abcb7* specifically at the block, together with disturbed heme production and iron transport. Notably, deregulated *ABCB7* causes ring sideroblastic anemia in MDS patients, and the mitochondrial co-activator PGC1β is heterozygously lost in del5q MDS. Importantly, the anemia could be rescued through enhanced PPAR signaling in vivo via either overexpression of *Pgc1β* or bezafibrate administration. In conclusion, lack of pRb results in MDS-like anemia with disrupted differentiation and impaired mitochondrial function at the orthochromatic erythroblast stage. Our findings reveal for the first time a role for pRb in heme and iron regulation, and indicate that pRb-induced anemia can be rescued in vivo through therapeutic enhancement of PPAR signaling.

Erythropoiesis, the formation of red blood cells (RBCs), is a tightly regulated multistep process fundamental to life because RBCs transport oxygen to all cells and tissues. RBCs are continuously replenished from the bone marrow (BM), where multipotent hematopoietic stem cells (HSCs) differentiate through intermediates including megakaryocytic-erythroid progenitors (MegEs), erythroid burst-forming-units (BFU-Es), and erythroid colony-forming units (CFU-Es) [1]. This expansion phase of erythroid commitment is followed by terminal differentiation, in which CFU-Es generate erythroblasts that undergo stepwise morphological changes, including gradual accumulation of

[1]SoSi and CRW conceived the study. TS, MG, and SoSi designed the experiments. TS, MJ, MG, AM, and SoSi performed experiments. TS, MG, ShSo, and SoSi analyzed data. CRW provided the mouse model and intellectual input. TS and SoSi wrote the article. All authors commented on the final draft.

Supplementary material associated with this article can be found in the online version at https://doi.org/10.1016/j.exphem.2020.06.006.

https://doi.org/10.1016/j.exphem.2020.06.006

hemoglobin, progressive decrease in cell size and nuclear condensation, and finally enucleation to become reticulocytes that mature in the bloodstream into biconcave erythrocytes [1]. Disruption at any stage of the process can result in anemia, a condition that results in reduced quality of life and impaired clinical outcome from a diverse set of diseases including chronic inflammation, cancer, and bone marrow disorders such as myeloid myelodysplastic syndrome (MDS) [2].

Erythropoiesis is intimately coupled to cell division; early erythroid progenitors are required to proliferate and self-renew to maintain the pool of more mature precursors, whereas late erythroid progenitors are dependent on cell cycle progression to initiate and progress through their terminal differentiation program [3]. Retinoblastoma protein (pRb) is a key cell cycle regulator controlling the G1-to-S phase transition [4], which is of particular importance for erythropoiesis. In a key commitment step from CFU-Es to terminal differentiation, erythroid progenitors are synchronized in S phase through downregulation of cyclin-dependent kinase (CDK) inhibitor $p57^{KIP2}$ [5]. This leads to inhibition of PU.1 and activation of the erythroid master transcriptional regulator GATA-1 and the erythropoietin receptor (EpoR), which locks the cell cycle clock to the erythroid differentiation program. During the final steps of maturation, orthochromatic erythroblasts undergo cell cycle exit and are arrested in G1 phase [5].

During the G1-to-S phase transition, pRb is hyperphosphorylated by CDKs, which in turn release E2F transcription factors necessary for cell cycle progression [6]. Deletion of pRb in hematopoietic stem cells (HSCs) using MxCre induces myeloproliferative disease. This is, however, not intrinsic to HSCs, but rather the consequence of an pRb-dependent interaction between myeloid-derived cells and the microenvironment caused by dual deletion in stem/progenitor cells and the bone marrow stroma [7]. Rb-deficient embryos have profound anemia, and cell-specific deletion has revealed an intrinsic requirement for pRb and several of its downstream E2F mediators for proper erythroid development [8]. Furthermore, erythroid-specific deletion of pRb was reported by Sankaran et al. [9] to result in inefficient terminal differentiation because of deregulated coordination of cell cycle exit and mitochondrial biogenesis. However, because of the methods available at the time, it remained unclear at what specific stage erythroid development was disrupted, and further characterization of the link between cell cycle regulation and mitochondrial function is needed.

To further decipher mechanisms downstream of pRb deficiency that cause anemia we took advantage of the erythroid-specific pRb conditional knockout mouse described by Sankaran et al. [9]. Herein we report that lack of pRb results in MDS-like macrocytic anemia despite elevated levels of Epo and accumulation of erythroid progenitors in the bone marrow, with a developmental block at the orthochromatic erythroblast stage. Detailed transcriptional profiling of purified erythroid progenitor populations immediately around the differentiation block revealed that pRb-deficient erythroblasts in final maturation stages failed to upregulate large clusters of genes critical for mitochondrial function, heme synthesis, and iron metabolism. Importantly, we report that the in vivo overexpression of peroxisome proliferator-activated receptor γ co-activator 1β (PGC1β), an essential co-activator of mitochondrial biogenesis [10], successfully rescued anemia induced by pRb deficiency. Treatment with bezafibrate [11], a small molecule activator of the same nuclear complex as PGC1β, normalized the blood parameters in a similar fashion, indicating that enhanced mitochondrial function rescues MDS-like anemia induced by pRb deficiency.

Methods

Mice, sampling, and transplantations

Epor-Cre *Rosa26*-eYFP$^{ki/ki}$ *Rb1*$^{fl/fl}$ conditional knockout mice (referred to as *Epor*-Cre *pRb*$^{fl/fl}$) were bred in the clinical research center at Lund University and maintained at BMC Lund University, Lund, Sweden. All experiments were performed under ethical guidelines approved by the Animal Ethics Committee of Lund, Sweden.

Steady-state parameters were analyzed using littermate mice aged 8–9 months. Peripheral blood (PB) from tail vein punctures was collected in EDTA tubes and analyzed using Sysmex KX-21N (Sysmex Corp., Kobe, Japan). Bone marrow (BM) was flushed from femurs, spleens were weighed, and then crushed and single-cell suspensions were counted using Sysmex.

For transplantation studies, donor BM from femur, tibia, and iliac crest was harvested (*pRb*$^{-/-}$ or Cre-*pRb*$^{fl/fl}$, CD45.2), counted, and depleted for lineage markers and Sca1. Cells were transduced with PGC1β overexpressing lentivirus or control for 12 hours and transplanted into lethally irradiated recipients (CD45.1, 2×500 cGy) together with 100,000 whole BM cells from congenic wild-type (WT) mice (CD45.1) for support. PB was analyzed 4 and 8 weeks post transplant and in BM and spleen on termination at 8 weeks.

Cohorts of *Epor*-Cre *pRb*$^{fl/fl}$ conditional knockout mice and Cre negative WT littermates were fed custom feed containing 0.5% bezafibrate (w/w, ssniff Spezialdiäten GmbH, Soest, Germany) or control feed without bezafibrate. PB samples were collected at days 0, 30, and 60 and analyzed on the Sysmex.

Flow cytometry

Four separate flow cytometry antibody stains were performed to analyze (i) early myelo-erythroid/erythroid progenitors in BM using Sca1, c-Kit, CD150, CD105, CD41, and lineage markers B220, CD3, Gr-1, and Mac-1; (ii) terminal erythroid differentiation in BM and spleen using Ter119, CD44, and FSC-A; (iii) lymphoid/myeloid lineages in BM using B220, CD3, Gr-1, and Mac-1; and (iv) donor-derived lineages in

PB using CD45.2, Ter119, B220, CD3, and Gr1. DAPI; or 7-AAD was used to exclude dead cells, and MitoTracker deep red (Thermo Fisher Scientific, Waltham, MA, USA) was included to measure mitochondrial activity. Samples were sorted and analyzed on a FACS Aria III (Becton Dickinson).

In vitro erythroid differentiation

C-kit$^+$ bone marrow cells from WT and pRb-deficient mice were enriched using CD117 MicroBeads (Miltenyi Biotec, Bergish Gladbach, Germany) and transduced with PGC1β overexpressing lentivirus or control vector in SFEM (StemSpan Stemcell Technologies, Vancouver, BC, Canada) erythroid culture medium with 3 U Epo/mL, 30% fetal bovine serum, 0.3 mg/mL holo-transferrin (Sigma Aldrich), and 0.4 μg/mL protamine sulfate. Cells were cultured for 36 hours before analysis.

Transcriptional analysis

For microarray analysis, 80,000 erythroid progenitors from the polychromatic (III), orthochromatic (IV), and reticulocyte (V) populations were sorted into RLT buffer (1% β-mercaptoethanol) and snap-frozen. RNeasy Plus micro kit (Qiagen, Hilden, Germany) was used for RNA extraction followed by the NuGEN high-yield RNA amplification protocol. The microarray was performed by Kompetenzzentrum Fluoreszente Bioanalytik (KFB, Regensburg Germany) using a single-cartridge array (Affymetrix, mouse gene 2.0 ST).

For quantitative reverse transcription polymerase chain reaction (RT-qPCR), 20,000 erythroid progenitors from populations IV and V (from in vitro cultures 5,000–10,000 population IV cells) were sorted into RLT buffer. The RNeasy Micro Kit (Qiagen) was used for RNA extraction. cDNA synthesis was performed according to the manufacturer's protocol using the SuperScript III First-Strand Synthesis kit (Thermo Fisher). RT-qPCR assays were performed using the TaqMan Gene expression master mix protocol (Thermo Fisher) with pre-designed probe-based primers (Integrated DNA Technologies, Coralville, IA, USA) (Supplementary Table E1, online only, available at www.exphem.org).

Apoptosis assay

BM cells were stained with antibodies against Ter119 (APC, BioLegend, San Diego, CA, USA) and CD44 (APC-Cy7, BD Bioscience), the PE Annexin V kit (BD Bioscience), and DAPI (4′,6-diamidino-2-phenylindole, Sigma Aldrich) to analyze erythroid progenitors (IV and V). Annexin V was added to each sample, gently vortexed and incubated at room temperature for 15 min in the dark, and analyzed on the LSRII (BD Bioscience).

Cell cycle assay

Two hundred fifty thousand to four hundred thousand sorted erythroid progenitors (III, IV, V) were fixed with ice-cold 70% ethanol, incubated at −20°C overnight, washed with PBS, and stained individually with propidium iodide staining buffer (10 μg/mL, Sigma Aldrich). PI intensity in the sorted populations was analyzed on the LSR II.

Heme assay

Five hundred thousand sorted erythroid progenitors (IV and V) were lysed in 500 μL of Cell Extraction Buffer (Thermo Fisher) and snap-frozen. Free heme was detected according to protocol using the Hemin Colorimetric Assay Kit (BioVision, Milpitas, CA, USA).

Serum iron assay

Serum supernatant from PB was collected and analyzed according to protocol using the Iron Colorimetric Assay kit (Sigma Aldrich).

Morphology and iron stain

Cytospin slides with 15,000 BM cells were stained with May–Grünwald (Merck) for 5 min and counterstained with 3% Giemsa (Merck) for 15 min. For analysis of iron accumulations slides were stained with potassium ferrocyanide (20%) and hydrochloric acid (10%) at a 1:1 ratio for 20 min, and counterstained with eosin (0.2%) for 10 min.

Statistical analysis

Statistical analysis was done using GraphPad Prism 7.00 (GraphPad Software, San Diego, CA, USA); significance was analyzed using Student's unpaired parametric *t*-test when comparing WT with knockout groups, if not stated otherwise. Ordinary one-way analysis of variance (ANOVA) was used for analysis of the in vivo bezafibrate experiment and in vitro erythroid differentiation experiment. Pairwise comparisons were done where applicable.

A detailed description of all methods is available online in the Supplementary Data (online only, available at www.exphem.org).

Results

Erythroid-specific deletion of pRb results in MDS-like anemia with a developmental block at the orthochromatic erythroblast stage

To further understand the mechanism of impaired erythroid development caused by pRb deficiency, we used the mouse model previously described by Sankaran and colleagues, where *lox-p* flanked *pRb* is deleted specifically in the erythroid lineage using EpoR-driven Cre recombinase (*Epor*-Cre $pRb^{fl/fl}$) [9]. To enable tracing of nucleated pRb-deficient cells, the mice were further crossed with Rosa26 yellow fluorescent protein (eYFP) mice with a *lox-p* flanked stop codon after the promoter, resulting in YFP labeling and pRb deletion in EpoR-expressing cells (Figure 1A) [12,13]. Erythroid specific pRb deletion was confirmed using qPCR in FACS-sorted erythroid, B, T, and myeloid cells (Supplementary Figure E1A,B, online only, available at www.exphem.org). Only erythroid cells became YFP+ consistent with our previously analysis of eYFP expression using *Epor*-Cre [12] (Supplementary Figure E1C). In line with Sankaran et al. [9], intrinsic deletion of pRb in the erythroid lineage resulted in anemia with

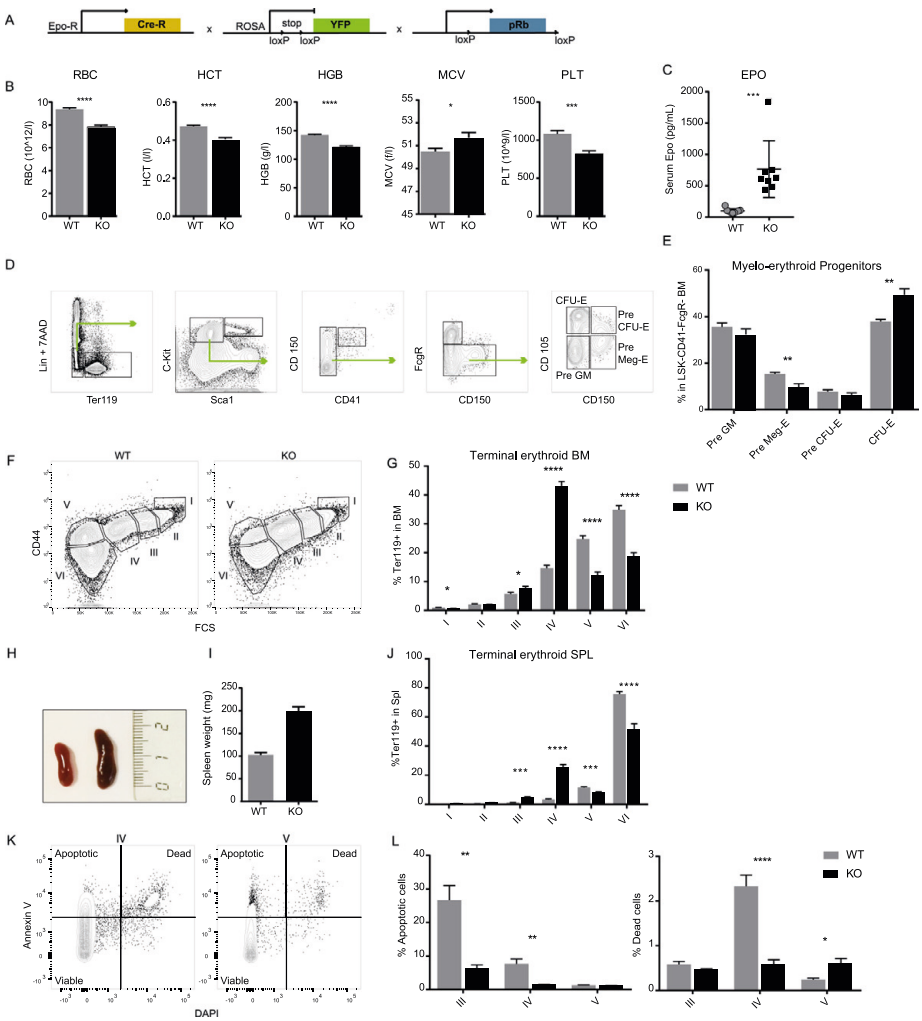

Figure 1. Erythroid specific knockout of pRb results in anemia despite the increased progenitors in bone marrow and spleen. **(A)** Schematic outline of erythroid-specific conditional YFP knockin and *pRB* knockout model driven by the Epo receptor (Epo-R) promotor. **(B)** Sysmex analysis on peripheral blood measuring red blood cell count (RBC), hemoglobin concentration (HGB), hematocrit levels (HCT), mean corpuscular volume (MCV), and platelets (PLT) ($n = 6$). **(C)** Enzyme-linked immunosorbent assay measuring Epo serum concentrations ($n = 8$ or 9). **(D)** The gating strategy used to fractionate myelo-erythroid progenitors with indicated surface markers ($n = 5$). **(E)** Quantification of Pre granulocyte−macrophage (Pre GM), Pre megakaryocyte−erythroid (Pre Meg-E), Pre erythroid colony-forming units (Pre CFU-E), and erythroid colony-forming units (CFU-E cell) from freshly isolated bone marrow (BM), as determined by flow cytometry ($n = 5$) [14]. **(F)** Representative flow cytometry plots of terminal erythroid differentiation in BM, using cell size (FSC-A), CD44, and Ter119 to fractionate BM cells into pro-erythroblasts (I), basophilic erythroblasts (II), polychromatic erythroblasts (III), orthochromatic erythroblasts (IV), reticulocytes (V), and erythrocytes (VI) [15]. **(G)** Quantification of terminal erythroid populations in BM ($n = 19$ or 20). **(H)** Representative images (WT left, KO right) and **(I)** quantification of spleen (Spl) weight ($n = 25–26$). **(J)** Quantification of terminal erythroid populations in spleen ($n = 10$). **(K)** Representative flow cytometry plots for populations IV (left) and V (right) from WT mice, and **(L)** quantification of cell viability using Annexin V, DAPI, and flow cytometry ($n = 4$). Data are expressed as the mean ± SEM. $*p \leq 0.05$, $**p \leq 0.01$, $***p \leq 0.001$.

significantly reduced red blood cell (RBC) counts, hemoglobin (HGB) concentration, and hematocrit (HCT) levels (Figure 1B). In addition, pRb-deficient erythroid cells exhibited an increase in mean corpuscular volume (MCV) (Figure 1B). Deletion of pRb also resulted in reduced platelet numbers (Figure 1B) and an increased total number of bone marrow cells (Supplementary Figure E1D). Measurement of serum EPO concentration using enzyme-linked immunosorbent assay (ELISA) revealed a twofold increase in pRb-deficient mice compared with WT animals (Figure 1C), indicating a maintained physiological response to the anemia.

Previous analysis of *Epor*-Cre $pRb^{fl/fl}$ mice utilized only CD71 and Ter119 staining to provide an overview of erythroid development. More recently developed phenotyping strategies provide greatly improved fractionation of the erythroid populations and define distinct stages within the differentiation trajectory of murine erythropoiesis. To accurately determine at what stage erythroid differentiation was impaired, we applied a high-fractionation flow cytometry protocol efficiently distinguishing the different myelo-erythroid/erythroid progenitors in the bone marrow [14] including Pre-Meg-E, Pre CFU-E, and CFU-E (Figure 1D), revealing a 44% increase in the CFU-E population of pRb-deficient mice (Figure 1E; for absolute numbers see Supplementary Figure E1E). Despite an increased number of erythroid progenitors in the BM and elevated serum erythropoietin levels, pRb-deficient animals remained anemic. Analyses of terminal erythroid differentiation using the surface marker CD44 in conjunction with forward scatter (FSC-A) [15], separating Ter119+ BM erythroblasts into pro-erythroblasts (I), basophilic (II), polychromatic (III), orthochromatic (IV) erythroblast, reticulocytes (V), and mature RBCs (VI) (Figure 1F), revealed that pRb deficiency resulted in a 2.9-fold increase in orthochromatic (IV) cells, followed by a 51% decrease in reticulocytes (V) compared with wild type (Figure 1G).

Steady-state erythropoiesis occurs at a constant rate in the BM, while anemia induces an extramedullary stress response in the spleen to rapidly produce large numbers of new erythrocytes [16,17]. The spleen weight of pRb-deficient mice was increased 2-fold compared with wild type (Figure 1H,I). Similar to that observed in BM, orthochromatic erythroblasts accumulated in the spleen (5.3-fold increase), with compromised ability to differentiate into reticulocytes (Figure 1J). Even though absolute numbers of reticulocytes are compensated for by the vast increase in numbers of total white blood cells per femur and spleen (Supplementary Figure E1F,G), mice lacking pRb remain anemic.

Apoptosis analysis within each differentiation step using Annexin V and DAPI (Figure 1K), demonstrated a switch from increased to decreased cell survival adjacent to the cellular block (Figure 1L). Increased survival of early erythroblasts in the pRb knockout is potentially due to the increased circulating levels of Epo [18]. In summary, detailed phenotypic analysis revealed that erythroid-specific deletion of pRb resulted in macrocytic anemia despite enhanced levels of circulating erythropoietin and increased numbers of erythroid progenitors in the BM, with disturbed terminal differentiation specifically at the orthochromatic erythroblast stage. Such inefficient erythropoiesis is characteristic of anemia associated with MDS, a group of heterogeneous diseases characterized by abnormal and ineffective hematopoiesis [19].

Transcriptional analysis around the maturation block reveals multiple distinct patterns of gene deregulation compared with normal terminal erythroid differentiation

Transcriptional complexity is high during terminal erythroid development, with large changes in gene expression in each step of maturation accompanying the morphological transformation [20]. To elucidate mechanisms underlying the inability of pRb-deficient orthochromatic erythroblasts (IV) to mature into reticulocytes (V), microarray analysis was performed on FACS-sorted populations at and adjacent to the block (III, IV, and V) (Figure 2A; for morphology see Supplementary Figure E2, online only, available at www.exphem.org). Transcriptome analysis revealed that very few genes were significantly different compared with WT before the block (III), followed by a gradual increase in numbers of deregulated genes (Figure 2B). Analysis using Genesis [21] revealed that differentially expressed genes clustered into five distinct patterns of deregulation compared with the expected expression during the final stages of terminal erythroid differentiation in the WT: clusters of genes that (I) should be downregulated but failed to downregulate (Figure 2C); (II) should be downregulated but were upregulated (Figure 2D); (III) should have stable expression through differentiation but were downregulated (Figure 2E); (IV) should be upregulated but failed to upregulate either at the block (Figure 2F) (V) or in the final maturation to reticulocytes (Figure 2G; for gene lists per cluster, see Supplementary Table E2, online only, available at www.exphem.org). Having identified where the developmental block induced by pRb deficiency occurred allowed us to define sets of genes that were unable to adhere to normal expression patterns during terminal erythroid differentiation.

Cell cycle exit is perturbed in pRb-deficient orthochromatic erythroblasts

Analysis using the Database for Annotation, Visualization and Integrated Discovery (DAVID) [22] revealed

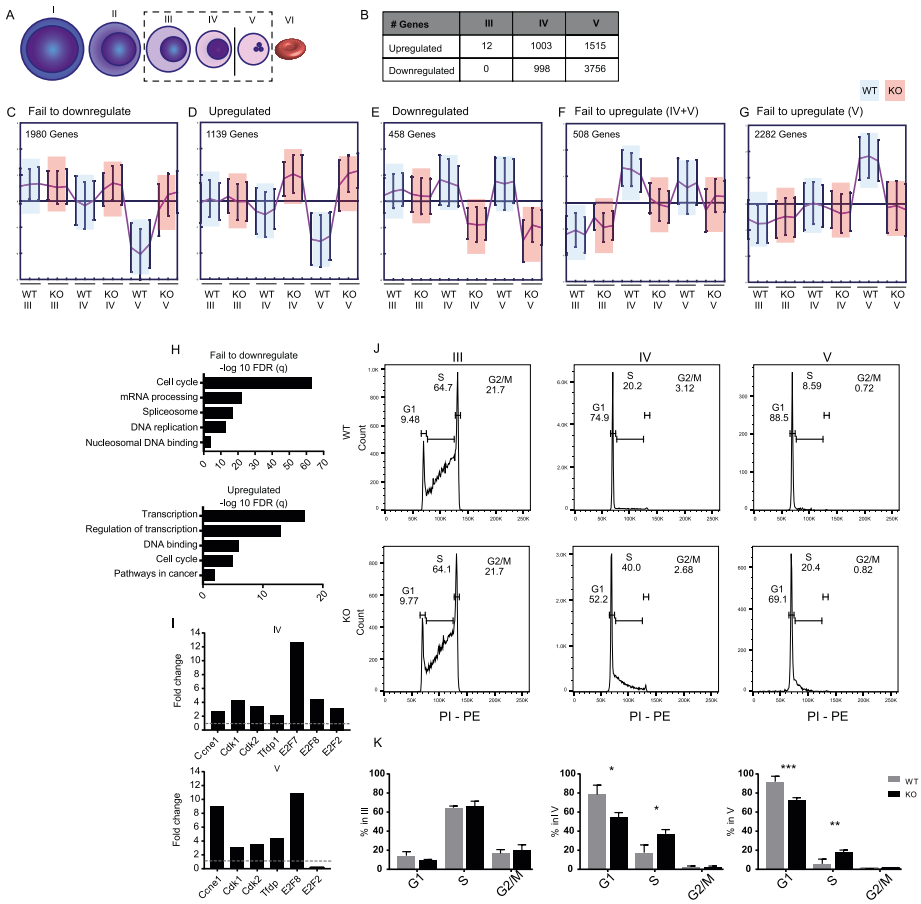

Figure 2. Cell cycle exit is perturbed in pRb-deficient orthochromatic erythroblasts. **(A)** Schematic description of erythroid populations around the maturation block during terminal erythroid differentiation sorted out for microarray analysis ($n = 3$). **(B)** Number of differentially expressed genes in each population (false discovery rate [FDR] <0.03). **(C–G)** Genesis (Version 1.7.7, developed by Alexander Sturn and Rene Snajder) analysis of differentially expressed genes, revealing clusters of genes following five distinct patterns of deregulation compared with WT: **(C)** Fail to downregulate, **(D)** upregulate, **(E)** downregulate, **(F)** fail to upregulate in IV, and **(G)** fail to upregulate in V. **(H)** DAVID analysis of genes contained in cluster B (fail to downregulate) and cluster C (upregulated), revealing associated Gene Ontology (GO) Project terms, including cell cycle and transcription. **(I)** Verification of deregulated genes from clusters B and C, critical for cell cycle transitions and repression of transcriptional activity, using qPCR. Gene expression was normalized to GAPDH and is depicted as fold change compared with WT ($n = 2$). **(J)** Representative plots and **(K)** quantification of cell cycle status within individually sorted erythroid progenitors (III–V, left to right) using propidium iodide ($n = 4$). Data are expressed as the mean ± SEM. $*p \leq 0.05$, $**p \leq 0.01$, $***p \leq 0.001$.

that the clusters of genes that failed to downregulate or were upregulated (Figure 2C,D) associated mainly with cell-cycle related functions (Figure 2H). A 2- to 12-fold increased expression of cell cycle-related genes compared with WT was confirmed in both populations IV and V using qPCR, including genes critical for cell cycle transitions (*Ccne1, Cdk1, Cdk2, Tfdp1*) and transcriptional repression (*E2f7, E2f8*) (Figure 2I). Notably, the expression of *E2f2*, a transcriptional activator normally increased during terminal differentiation [23], was decreased in pRb-deficient reticulocytes. In line with the transcriptional profiling, analysis using propidium iodide and FACS revealed that the cell cycle status of polychromatic erythroblasts (III) was

unchanged, while orthochromatic erythroblasts (IV) and reticulocytes (V) lacking pRb exhibited a 2-fold increase in cells remaining in S phase (Figure 2J,K). Taken together, our results confirm that pRb deletion results in an inability to properly exit cell cycle and extends previous findings to demonstrate that the defect is specific to the orthochromatic erythroblasts.

pRb deficiency results in deregulation of mitochondrial function including heme production and iron metabolism

DAVID analysis of genes that should remain stably expressed during terminal erythroid differentiation, but were downregulated in Rb-deficient progenitors (Figure 2E), revealed that these clusters were highly related to mitochondrial function, with gene ontology terms including oxidative phosphorylation and NADH dehydrogenase activity (Figure 3A). Decreased expression of key genes involved in oxidative phosphorylation, such as *Ndufa1* (complex1, OXPHOS), *Atp5s* (ATP synthesis), and *Cox7b* (electron transfer), was confirmed using qPCR (Figure 3B). Furthermore, in line with reactive oxygen species (ROS) being a byproduct of mitochondrial respiration, the expression of mitochondrial antioxidant *Prdx3*, which is important for ROS homeostasis, was also decreased at the developmental block (Figure 3B). In accordance, flow cytometry analysis using Mitotracker DeepRed revealed that pRb deficiency resulted in reduced mitochondrial membrane potential in the populations around the maturation block (Figure 3C). Furthermore, analysis of mitochondrial ROS levels using MitoSox revealed a delay in the peak of MitoSox^{high} cells (Figure 3D,E). Collectively, erythroid-specific deletion of pRb resulted in decreased expression of mitochondria-related genes, accompanied by a decreased mitochondrial membrane potential and a shift in mitochondria-produced ROS.

The clusters that failed to upregulate during terminal erythroid maturation (Figure 2F,G) included genes involved in heme synthesis and iron transport (Figure 3F), biological processes taking place in the mitochondria that are fundamental for proper RBC function. These included *Fech,* which catalyzes insertion of iron into heme [24], and *Alas2,* which encodes the rate-limiting enzyme in erythroid-specific heme synthesis [25]. Furthermore, the iron transporter *Abcb7* and protoporphyrinogen IX transporter *Tmem14c* exhibited decreased gene expression (Table 1), which was verified using qPCR (Figure 3G). In accordance with perturbed expression of iron transporters, Prussian blue staining of BM cells revealed increased iron accumulation in pRb-deficient erythroid progenitors compared with wild type (Figure 3H), consistent with previous observations in the spleen [9]. Furthermore, total iron concentration in the serum of KO mice was significantly decreased (Figure 3I). Coordination of iron acquisition and heme synthesis is required for effective erythropoiesis, and iron availability is known to regulate heme production [26]. Measuring heme concentration in sorted IV and V progenitor populations revealed that wild-type cells increased their heme concentration from the orthochromatic erythroblast (IV) to reticulocyte (V) stage (Figure 3J). In contrast, pRb-deficient cells had 1.9-fold higher heme concentrations in the orthochromatic erythroblasts compared with WT, followed by decreased heme concentrations in reticulocytes (Figure 3J). Collectively, our data indicate that erythroid-specific deletion of pRb resulted in deregulation of heme production and iron metabolism, uncovering a previously unrecognized mechanism by which pRb regulates erythropoiesis.

pRb-deficient erythroid cells exhibit aberrant expression of genes that are recurrently deregulated in human MDS

Subtypes of MDS are characterized by mitochondrial iron accumulations resulting in refractory anemia with ring sideroblasts (RARS), which are caused by mutated *SF3B1* [27] and downstream aberrant splicing of genes including *Abcb7* [28]. Both *Sf3b1* and *Abcb7* were deregulated in pRb-deficient erythroid progenitors together with other genes involved in MDS-related anemia such as *Tmem14c* and *Alas2* (Table 1). pRb-Deficient cells also displayed aberrant expression of several of the most recurrently mutated genes in MDS involved in other disease phenotypes [19], including *Srsf2* and *U2af1* affecting pre-mRNA splicing [29], *Mdm2* promoting enhanced cancer susceptibility [30], and *Kras* promoting survival and proliferation [31] (Table 1). Collectively, our data indicate that erythroid-specific deletion of pRb results in deregulation of a large number of genes frequently altered in human MDS.

Improving mitochondrial function via an enhanced PPAR signaling pathway rescues MDS-like anemia in pRb-deficient animals

Because of the impairment of mitochondria-related genes and function, we next asked if increased mitochondrial function could rescue the MDS-like anemia induced by intrinsic pRb deficiency. PGC1β is a transcriptional co-activator of mitochondrial biogenesis [10], which has previously been reported to be reduced in Ter119+ erythroblasts of pRb-deficient mice and when knockdown resulted in impaired erythroid maturation of G1E-ER cells [9]. Previous data, however, did not address whether there was a causative link, and if restoration of PGC1β expression could rescue the phenotype of pRb deficiency in vivo. Analyzing its expression in purified erythroid progenitor populations, we confirmed that PGC1β was downregulated

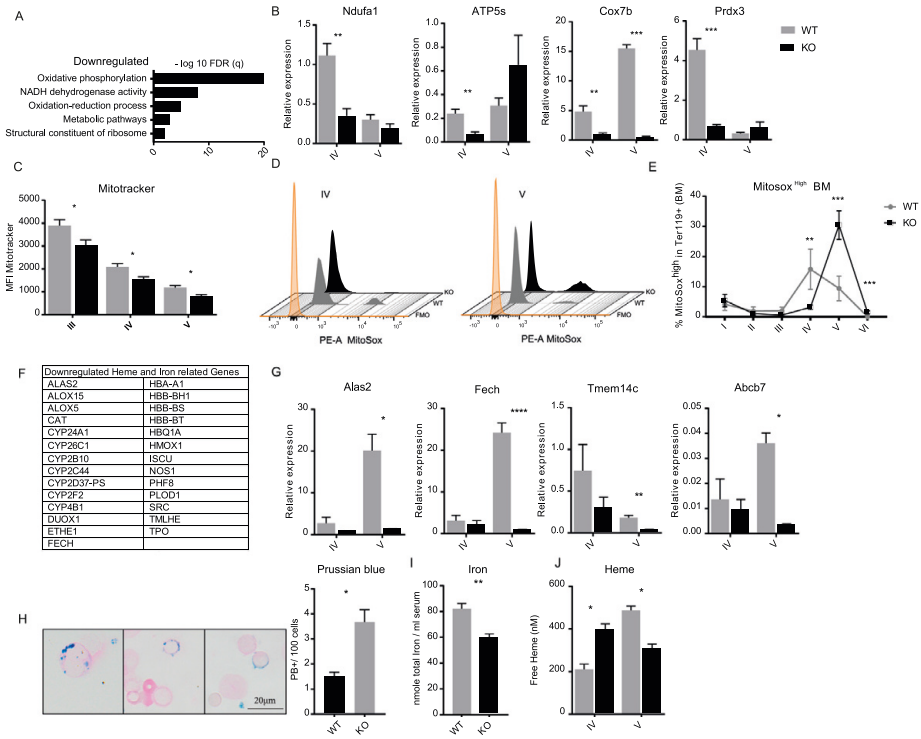

Figure 3. pRb-deficient cells have reduced mitochondrial function specifically around the developmental block. **(A)** DAVID analysis of genes contained in cluster D revealed associated Gene Ontology Project (GO) terms related to mitochondrial oxidative phosphorylation (OXPHOS). **(B)** Verification of deregulated genes from cluster D, confirming downregulation of genes related to OXPHOS. Gene expression normalized to GAPDH ($n = 4$). **(C)** Quantification of mitochondrial membrane potential as measured by the mitochondria-specific dye MitoTracker DeepRed and flow cytometry depicted as mean fluorescence intensity (MFI) ($n = 5$). **(D)** Representative plots of MitoSox stain, measuring mitochondrial ROS in populations IV (left) and V (right): *orange peak* denotes fluorochrome minus one (FMO) for Mitosox, *gray peak* denotes WT, and *black peak* denotes KO. **(E)** Quantification of MitoSox high cells in individual erythroid progenitor populations during terminal differentiation ($n = 5$ or 6). **(F)** Heme- and iron-associated genes downregulated in population V. **(G)** Verification of deregulated genes from clusters E and F (fail to upregulate) using qPCR, confirming decreased expression of genes involved in heme production and iron metabolism ($n = 2–4$). **(H)** Representative images (left) and quantification (right) of iron accumulation within nucleated BM cells, as indicated by staining positive with Prussian blue ($n = 3$). **(I)** Quantification of total iron (Fe^{2+} and Fe^{3+}) in serum ($n = 7$ or 8). **(J)** Quantification of (free) heme concentration in lysates of erythroid populations IV and V. Data are expressed as the mean ± SEM. $*p \leq 0.05$, $**p \leq 0.01$, $***p \leq 0.001$.

specifically in the orthochromatic erythroblasts where the developmental block occurs (Figure 4A). To determine if restoring expression of PGC1β could rescue the anemic phenotype in vivo, we created a lentiviral vector efficiently overexpressing PGC1β under the SFFV promotor (Figure 4B; Supplementary Figure E3A–D, online only, available at www.exphem.org). Transduced progenitor-enriched BM cells (initial transduction efficiency of 70%–80%, Supplementary Figure E3B) together with whole BM support cells were transplanted into lethally irradiated mice that were followed for recovery over time (Figure 4C). Strikingly, analyses of PB parameters after 8 weeks revealed complete normalization of the RBC count in mice transplanted with KO cells overexpressing PGC1β, whereas mice treated with the control vector remained anemic (Figure 4D). Equivalent improvements were seen for hemoglobin concentration and hematocrit volumes (Figure 4D). In addition, the increase in mean cellular volume resulting from intrinsic pRb deletion was close to normalized by overexpression of PGC1β (Figure 4D). Spleens remained enlarged (data not shown), indicating that extramedullary stress erythropoiesis is still required at 8 weeks to ameliorate the anemia. Further analysis of

Table 1. Genes commonly associated with MDS are deregulated in the pRb-deficient mouse model

Gene deregulated in mouse model	IV Log_2 KO/WT	IV FDR	V Log_2 KO/WT	V FDR	Function of gene	Function in MDS	Role in human MDS
Sf3b1	0.53	9.00E-02	0.84	2.65E-03	Spliceosomal machinery	Deregulated pre-mRNA splicing, RARS phenotype	Malcovati et al. [27]
Srsf2	1.19	1.17E-03	3.20	4.78E-08	Spliceosomal machinery	Deregulated pre-mRNA splicing, frequently mutated in MDS	Smeets et al. [60]
U2af1	1.06	8.00E-02	2.68	6.90E-05	Spliceosomal machinery	Deregulated pre-mRNA splicing, frequently mutated in MDS	Shirai et al. [56]
Mdm2	1.58	5.22E-06	2.09	1.05E-05	E3 ubiquitin–protein ligase	SNPs within p53—MDM2 leads to cancer susceptibility	McGraw et al. [30]
p53	0.70	4.82E-02	0.80	9.24E-03	Tumor suppressor	SNPs within p53—MDM2 leads to cancer susceptibility	McGraw et al. [30]
Fancc	ns	ns	1.11	7.96E-03	DNA repair	Genomic stability, deregulated in RARS	Nikpour et al. [43]
Map3k7	ns	ns	2.05	2.41E-03	MAP kinase pathway	Negative regulation of apoptosis, deregulated in RARS	Nikpour et al. [43]
Jak2	0.69	2.24E-02	0.96	7.75E-04	Tyrosine signaling pathway	Activating mutations in MDS, promotes survival and expansion	Steensma et al. [61]
Kras	1.38	2.35E-02	4.29	6.75E-07	Tyrosine signaling pathway	Activating mutations in MDS, promotes survival and expansion	Bejar et al. [31]
Cbl	1.50	1.41E-02	0.82	9.29E-02	Tyrosine signaling pathway	Negative regulator of receptor tyrosine kinase	Bejar et al. [31]
Asxl1	1.08	4.46E-03	1.89	1.00E-05	Epigenetic regulator	Frequently mutated in MDS	Chen et al. [57]
Ezh2	1.39	1.09E-03	2.09	6.30E-06	Epigenetic regulator	Inactivating mutation in myeloid disorders	Ernst et al. [58]
Tmem14c	−1.55	3.57E-02	ns	ns	Heme metabolism	Altered splicing in RARS	Conte et al. [32]
Alas2	ns	ns	−0.74	4.53E-03	Heme biosynthesis	Deregulated in RARS progenitors	Malcovati et al. [59]
Abcb7	−1.04	4.3002	−1.22	6.87E-03	Iron transport from mitochondria	Mediator of RARS phenotype	Nikpour et al. [28]

FDR = false discovery rate; ns = not significant.
Gene expression analysis revealed that genes that are known to be frequently deregulated in human MDS [27,28,30–32,43,56–61] were also deregulated in the pRb-deficient mouse model. Gene expression is expressed as the log_2 fold change in KO/WT in erythroid populations IV and V of pRb-deficient mice. Gene biological function and proposed role in MDS pathophysiology are indicated.

erythroid progenitors in the BM revealed that the accumulation of orthochromatic erythroblasts (IV) observed in untreated KOs was significantly decreased by PGC1β overexpression (Figure 4E). This is particularly encouraging as previous experiments have determined that mice transplanted with wild-type and *Epor*-Cre*pRb*$^{-/-}$ BM at a 1:1 ratio remained anemic, indicating that pRb-deficient erythroid progenitors are able to outcompete wild-type progenitors [9]. Although it is unlikely that downregulation of PGC1β is solely responsible for the mitochondrial dysfunction seen in pRb-deficient cells, our results clearly indicate that overexpression of PGC1β alone is sufficient to reverse the phenotype in vivo and rescue the MDS-like anemia induced by pRb deficiency. This indicates that the mitochondrial defect is causative for a significant percentage of the anemia.

Although overexpression of PGC1β provides proof-of-principle that impaired mitochondrial function is causally linked to the erythroid differentiation defect, it is not a treatment relevant for clinical application. We therefore asked if we could ameliorate the anemia by pharmacological enhancement of mitochondrial function. To this end, we used bezafibrate, a pan-PPAR agonist acting on the same nuclear receptors that are activated by PGCs [11]. Strikingly, and consistent with the PGC1β overexpression, treating nontransplanted WT and KO mice with 0.5% bezafibrate in the food or control diet for 2 months resulted in amelioration of the refractory anemia with normalization of RBC count and HCT and MCV levels as compared with WT, as well as a trend toward normalization of HGB concentrations (Figure 4F; Supplementary Figure E4, online only, available at www.exphem.org).

To determine if enhanced mitochondrial function also affected the cell cycle, c-kit$^+$ bone marrow cells from WT and pRb-knockout mice were transduced with PGC1β overexpressing lentivirus or a control vector and cultured in erythroid culture medium for 36 hours (Figure 5A). Pgc-1β was efficiently overexpressed (Figure 5B) and resulted in increased mitochondrial membrane potential in orthochromatic erythroblasts (IV), as measured with Mitotracker Deep Red and FACS (Figure 5C). Pgc-1β overexpression in vitro reversed the developmental block at the orthochromatic erythroblasts stage (IV) in the same way as seen in vivo (Figure 5D). Furthermore, transcriptional analysis within transduced population IV progenitors revealed that cell cycle genes were deregulated in pRb-deficient cells in a similar fashion in vitro and in vivo (Figure 5E). Interestingly, Pgc-1β overexpression normalized the expression of cell cycle genes critical for both cell cycle transitions and repression of transcriptional activity, including Cdk1, Cdk2, Ccne1, E2f7, and E2f8 (Figure 5E). In conclusion, improved

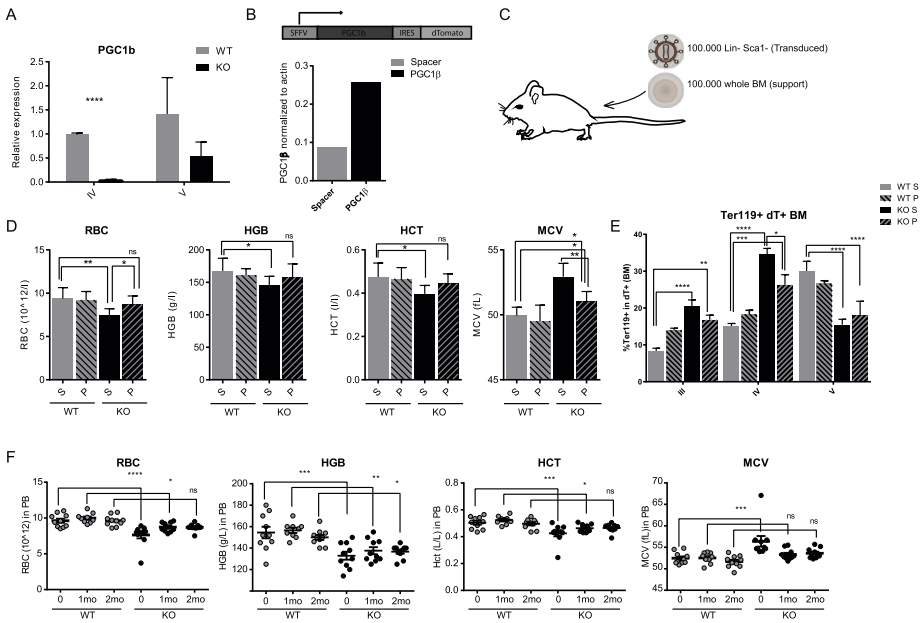

Figure 4. Increased activation of the PPAR pathway through PGC-1β overexpression and bezafibrate treatment ameliorates pRb deficiency-induced anemia. **(A)** mRNA expression of PGC1β in erythroid populations IV and V using qPCR, revealing reduced expression in pRb-deficient cells ($n = 2$). **(B)** Schematic representation of PGC1β overexpressing lentiviral vector containing a spleen focus-forming virus (SFFV) promoter, internal ribosome entry site (IRES) element, and dTomato fluorescent reporter, and Western blot analysis of PGC1β protein expression in 3T3 cells transduced with spacer or PGC1b overexpression vector ($n = 1$). **(C)** Experimental layout of transplantation experiment in which lethally irradiated mice were transplanted with 100,000 transduced progenitor-enriched cells together with 100,000 whole bone marrow support cells. **(D)** Sysmex analysis at 8 weeks post transplant on peripheral blood from mice transplanted with WT or KO donor BM treated with spacer or PGC1β overexpression vector, measuring red blood cell (RBC) count, hemoglobin (HGB) concentration, hematocrit (HCT) levels, and mean corpuscular volume (MCV). **(E)** Quantification of flow cytometric analysis of dTomato$^+$ and Ter119$^+$ erythroid cells within the BM at 8 weeks. **(F)** Quantification of Sysmex analysis on peripheral blood at start, 1 month, and 2 months of 0.5% (w/w) bezafibrate chow treatment ($n = 9$ or 10). Data are expressed as the mean ± SEM. *$p \leq 0.05$, **$p \leq 0.01$, ***$p \leq 0.001$.

mitochondrial function through an enhanced PPAR signaling pathway rescued MDS-like anemia, as well as normalized the enhanced expression of cell cycle genes induced by pRb deficiency.

Discussion

Deletion of *pRb* causes anemia in mice [9]. However, the precise stage of erythroid development when pRb is important and the underlying mechanisms have not been clearly defined. Using high-fractionation FACS protocols [14,15], we found that erythroid-specific deletion of *pRb* results in inefficient erythropoiesis reminiscent of MDS-related anemia, with a developmental block at the orthochromatic erythroblast stage similar to that reported in human MDS patients [32]. Chronic refractory anemia is present in more than 85% of MDS patients [33] and severely impairs the quality of life of patients [33,34], affects their clinical outcome [35], and correlates with increased risk of transformation into acute myeloid leukemia [36].

Consistent with pRb being a potent inhibitor of the G1-to-S phase transition [4] Rb-deficient erythroblasts failed to repress S-phase genes and to properly exit the cell cycle at the orthochromatic erythroblasts. Our results are in line with ex vivo studies indicating that *pRb*-null terminal erythroid cells from fetal liver continue to cycle in culture [37]. Previous analysis using the same mouse model did not detect a difference in proliferation [9]. This is likely due to the use of a heterogeneous phenotypic population of erythroblasts before the differentiation block (CD71^{high}/Ter-119^{high}), whereas we detected increased cycling in the populations after the maturation block. In agreement with the finding by Spike et al. [38] that pRb deficiency results in decreased enucleation in red cells from fetal liver [38], we detected propidium iodide-positive

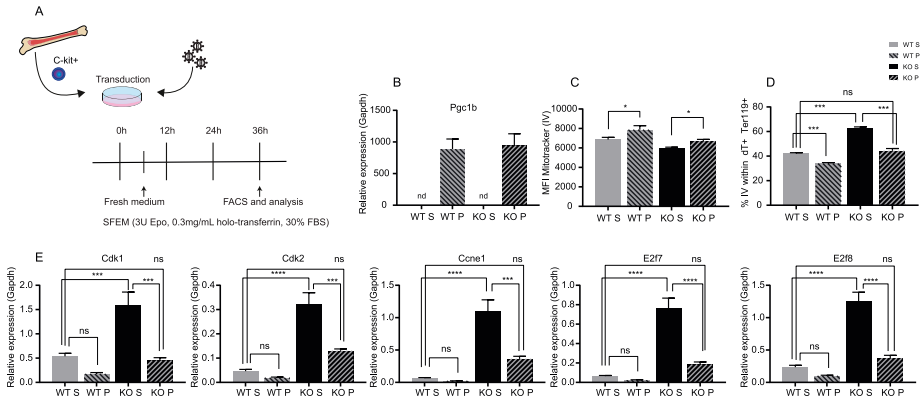

Figure 5. PGC1β overexpression normalizes cell cycle gene expression. **(A)** Schematic outline of the in vitro culture; c-kit+ bone marrow cells from wild-type and pRb-deficient mice were transduced with a control vector spacer (S) or a PGC1β-overexpressing vector (*p*) and cultured in medium promoting erythroid differentiation. **(B)** Relative mRNA expression of PGC1β in transduced (dTomato$^+$) Ter119$^+$ orthochromatic erythroblasts (IV) at 36 hours ($n = 5$). **(C)** Quantification of mitochondrial membrane potential within population IV, as measured by MitoTracker DeepRed and flow cytometry. Results depicted as mean fluorescence intensity (MFI) ($n = 5$). **(D)** Quantification of flow cytometric analysis of orthochromatic erythroblasts (IV) within transduced (dTomato$^+$) Ter119$^+$ cells at 36 hours of in vitro culture ($n = 5$). **(E)** mRNA expression relative to Gapdh of genes critical for cell cycle transitions and repression of transcriptional activity ($n = 5$). Data are expressed as the mean ± SEM. *$p \leq 0.05$, **$p \leq 0.01$, ***$p \leq 0.001$.

reticulocytes in bone marrow from pRb-deficient mice, indicating less efficient enucleation. This effect was, however, transient as RBCs in PB from KO mice displayed normal enucleation.

Interestingly, our results indicate that activation of PPAR signaling through overexpression of PGC1β normalized the enhanced expression of cell cycle genes induced by pRb deficiency. In line with these results, activation of PPAR-γ in Rb-deficient mouse embryo fibroblasts has been reported to induce adipocyte terminal differentiation, which also requires cell cycle exit to occur [39]. Furthermore, activation of PPAR signaling has been found to inhibit cell growth in human colorectal cancer cell lines [40]. Further studies are required to conclusively establish the link between pRb-induced cell cycle arrest and PPAR signaling.

Apart from being a cell cycle regulator, pRb has recently been reported to also control various aspects of cell metabolism, including nucleotide synthesis, glutathione synthesis, glycolysis, and oxidative metabolism [41]. Coupling of cell cycle regulation to mitochondrial function has been observed in various cell types, including erythroid cells [9]. However, the specific stage of erythroid maturation at which pRb is important for metabolic control has not been previously defined. Here we report that pRb deficiency results in impaired oxidative phosphorylation and ROS regulation specifically at the final differentiation step from orthochromatic erythroblast to reticulocyte. This is the same stage at which erythroid differentiation becomes compromised, suggesting these are closely coupled features of the mechanism. This was accompanied by decreased mitochondrial membrane potential and deregulated mitochondrial production of ROS. Although a previous study using the same mouse model [9] did not detect a difference in ROS, our analysis of more highly purified phenotypic populations has now detected the shift in ROS production. Every division during terminal erythroid differentiation results in daughter cells that are significantly different from the mother cell. This emphasizes the importance of performing mechanistic studies in highly purified, stage-specific cell populations.

Mutations in mitochondrial genes have been reported in MDS patients [42], and somatic *SF3B1* mutations, which are common in subtypes of MDS, are associated with downregulation of core mitochondrial pathways [32,43]. These include genes related to iron and heme homeostasis [27,32], suggesting that iron and heme homeostasis could play a role in the disease phenotype. Loss of the mitochondrial matrix chaperone Hspa9b in zebrafish recapitulates ineffective hematopoiesis including anemia, dysplasia, and increased cell apoptosis caused by compromised mitochondrial function and oxidative stress [44]. Furthermore, mice with accumulating mitochondrial mutations caused by defective Polg proofreading activity exhibit MDS-like macrocytic anemia [45], further suggesting a role for deregulated mitochondrial function in MDS pathogenesis.

Whereas pRb has previously been implicated in regulation of mitochondrial function [9,41], this is the first

time that pRb is described as important for functional heme synthesis and iron transport. We and others [46,47] have found that heme and iron metabolism genes are strongly upregulated during terminal erythroid differentiation. Furthermore, we found that pRb deficiency results in failure to enhance the expression of several genes required for heme production and iron transport. Interestingly, many of these genes are known to be involved in refractory anemia with ring sideroblasts (RARS) [28,48], a subtype of MDS characterized by iron accumulations in perinuclear mitochondria in the form of mitochondrial ferritin [27]. The formation of ring sideroblasts has proven very difficult to reproduce in mouse models of MDS [49]. Our results indicate that intracellular iron accumulations are significantly more frequent in BM cells from mice lacking pRb in the erythroid compartment, although at low frequency. The phenomenon was occasionally also observed, albeit at markedly lower frequency, in WT BM.

It is interesting to note that although *RB* itself is not commonly mutated in MDS, many of the genes that are deregulated in response to its deletion are known to be involved in MDS pathogenesis, as outlined in Table 1. In addition, PGC1β, which is downregulated specifically where the developmental block occurs, is located within the commonly deleted region of chromosome 5 of the del(5q) subtype of MDS [50]. Impaired erythropoiesis in del(5q) MDS has previously been linked to heterozygous deletion of RPS14 [51]. It is, however, unlikely that the full disease phenotype is attributed to loss of a single gene out of the entire commonly deleted region. Supporting that PGC1β deficiency potentially also contributes to the disease phenotype, patients with del(5q) MDS exhibit inefficient erythropoiesis, with increased levels of heme in the progenitors before the block and decreased levels of ALAS2 in later progenitor stages after the block [52], in a fashion very similar to that we report here. Furthermore, knockdown of PGC1β in G1E-ER cells resulted in inefficient erythroid differentiation [9]. Importantly, we report that in vivo overexpression of PGC1β ameliorates MDS-like anemia, which was reproduced using a small molecule therapy with the mitochondria function-enhancing drug bezafibrate [53].

In line with the pRb-deficient mice, many MDS patients already have high levels of circulating EPO [54], and the majority of MDS patients do not respond efficiently to treatment with erythropoietin and develop transfusion dependency during the course of their disease [34]. Regular transfusion therapy has severe side effects from the iron overload [55]. It is therefore important to find new ways to treat MDS-related anemia. Here we report that erythroid-specific deletion of pRb results in refractory anemia that phenocopies several of the hallmarks of MDS-related anemia, indicating that this model could be valuable for mechanistic studies. We further report that the anemia could be ameliorated by enhanced PPAR pathway signaling in vivo either genetically or therapeutically, suggesting that improved mitochondrial function could be beneficial—a potentially important step in finding new ways to treat MDS-related anemia. Further studies are needed to investigate if these findings can be translated to the human setting.

Acknowledgments

We thank Dr. Johan Flygare for intellectual input, Dr. Eva Hellström-Lindberg for expert advice regarding MDS-related anemia, Dr. David Thorburn for valuable discussions regarding the use of bezafibrate, Dr. Abdul G. Alattar for kindly assisting in experimental work, and the Lund Stem Cell Center FACS Core for expert assistance with cell sorting. This research was supported by the Swedish Cancer Society (fellowship to SoSi), the Swedish Society for Medical Research (fellowship to SoSi), the Crafoordska Foundation, the Åke Wiberg Foundation, the Clas Groschinsky's Memory Foundation, the Gunnar Nilsson Cancer Foundation, the Royal Physiographic Society of Lund, and the Harald & Greta Jeansson Foundation.

References

1. Lodish H, Flygare J, Chou S. From stem cell to erythroblast: regulation of red cell production at multiple levels by multiple hormones. IUBMB Life. 2010;62:492–496.
2. Zivot A, Lipton JM, Narla A, Blanc L. Erythropoiesis: insights into pathophysiology and treatments in 2017. Mol Med. 2018;24:11.
3. von Lindern M, Deiner EM, Dolznig H, et al. Leukemic transformation of normal murine erythroid progenitors: v- and c-ErbB act through signaling pathways activated by the EpoR and c-Kit in stress erythropoiesis. Oncogene. 2001;20:3651–3664.
4. Bartek J, Lukas J. Pathways governing G1/S transition and their response to DNA damage. FEBS Lett. 2001;490:117–122.
5. Pop R, Shearstone JR, Shen QC, et al. A key commitment step in erythropoiesis is synchronized with the cell cycle clock through mutual inhibition between PU.1 and S-phase progression. Plos Biology. 2010;8:e100484.
6. Dyson N. The regulation of E2F by pRB-family proteins. Genes Dev. 1998;12:2245–2262.
7. Walkley CR, Shea JM, Sims NA, Purton LE, Orkin SH. Rb regulates interactions between hematopoietic stem cells and their bone marrow microenvironment. Cell. 2007;129:1081–1095.
8. Walkley CR, Sankaran VG, Orkin SH. Rb and hematopoiesis: stem cells to anemia. Cell Div. 2008;3:13.
9. Sankaran VG, Orkin SH, Walkley CR. Rb intrinsically promotes erythropoiesis by coupling cell cycle exit with mitochondrial biogenesis. Genes Dev. 2008;22:463–475.
10. Kelly DP, Scarpulla RC. Transcriptional regulatory circuits controlling mitochondrial biogenesis and function. Genes Dev. 2004;18:357–368.
11. Bastin J, Aubey F, Rotig A, Munnich A, Djouadi F. Activation of peroxisome proliferator-activated receptor pathway stimulates the mitochondrial respiratory chain and can correct deficiencies

in patients' cells lacking its components. J Clin Endocrinol Metab. 2008;93:1433–1441.
12. Singbrant S, Russell MR, Jovic T, et al. Erythropoietin couples erythropoiesis, B-lymphopoiesis, and bone homeostasis within the bone marrow microenvironment. Blood. 2011;117:5631–5642.
13. Heinrich AC, Pelanda R, Klingmuller U. A mouse model for visualization and conditional mutations in the erythroid lineage. Blood. 2004;104:659–666.
14. Pronk CJ, Rossi DJ, Mansson R, et al. Elucidation of the phenotypic, functional, and molecular topography of a myeloerythroid progenitor cell hierarchy. Cell Stem Cell. 2007;1:428–442.
15. Liu J, Zhang J, Ginzburg Y, et al. Quantitative analysis of murine terminal erythroid differentiation in vivo: novel method to study normal and disordered erythropoiesis. Blood. 2013;121:e43–e49.
16. Singbrant S, Mattebo A, Sigvardsson M, Strid T, Flygare J. Prospective isolation of radiation induced erythroid stress progenitors reveals unique transcriptomic and epigenetic signatures enabling increased erythroid output. Haematologica. 2020. https://doi.org/10.3324/haematol.2019.234542. in press.
17. Paulson RF, Shi L, Wu DC. Stress erythropoiesis: new signals and new stress progenitor cells. Curr Opin Hematol. 2011;18:139–145.
18. Lacombe C, Mayeux P. Biology of erythropoietin. Haematologica. 1998;83:724–732.
19. Lindsley RC, Ebert BL. Molecular pathophysiology of myelodysplastic syndromes. Annu Rev Pathol. 2013;8:21–47.
20. An X, Schulz VP, Li J, et al. Global transcriptome analyses of human and murine terminal erythroid differentiation. Blood. 2014;123:3466–3477.
21. Sturn A, Quackenbush J, Trajanoski Z. Genesis: cluster analysis of microarray data. Bioinformatics. 2002;18:207–208.
22. Huang da W, Sherman BT, Lempicki RA. Systematic and integrative analysis of large gene lists using DAVID bioinformatics resources. Nat Protoc. 2009;4:44–57.
23. Swartz KL, Wood SN, Murthy T, et al. E2F-2 promotes nuclear condensation and enucleation of terminally differentiated erythroblasts. Mol Cell Biol. 2017;37. e00274-16.
24. Chen W, Dailey HA, Paw BH. Ferrochelatase forms an oligomeric complex with mitoferrin-1 and Abcb10 for erythroid heme biosynthesis. Blood. 2010;116:628–630.
25. Ajioka RS, Phillips JD, Kushner JP. Biosynthesis of heme in mammals. Biochim Biophys Acta. 2006;1763:723–736.
26. Kafina MD, Paw BH. Intracellular iron and heme trafficking and metabolism in developing erythroblasts. Metallomics. 2017;9:1193–1203.
27. Malcovati L, Karimi M, Papaemmanuil E, et al. SF3B1 mutation identifies a distinct subset of myelodysplastic syndrome with ring sideroblasts. Blood. 2015;126:233–241.
28. Nikpour M, Scharenberg C, Liu A, et al. The transporter ABCB7 is a mediator of the phenotype of acquired refractory anemia with ring sideroblasts. Leukemia. 2013;27:889–896.
29. Yoshida K, Sanada M, Shiraishi Y, et al. Frequent pathway mutations of splicing machinery in myelodysplasia. Nature. 2011;478:64–69.
30. McGraw KL, Cluzeau T, Sallman DA, et al. TP53 and MDM2 single nucleotide polymorphisms influence survival in non-del (5q) myelodysplastic syndromes. Oncotarget. 2015;6:34437–34445.
31. Bejar R, Stevenson K, Abdel-Wahab O, et al. Clinical effect of point mutations in myelodysplastic syndromes. N Engl J Med. 2011;364:2496–2506.
32. Conte S, Katayama S, Vesterlund L, et al. Aberrant splicing of genes involved in haemoglobin synthesis and impaired terminal erythroid maturation in SF3B1 mutated refractory anaemia with ring sideroblasts. Br J Haematol. 2015;171:478–490.
33. Ryblom H, Hast R, Hellstrom-Lindberg E, Winterling J, Johansson E. Self-perception of symptoms of anemia and fatigue before and after blood transfusions in patients with myelodysplastic syndromes. Eur J Oncol Nurs. 2015;19:99–106.
34. Hellstrom-Lindberg E, van de Loosdrecht A. Erythropoiesis stimulating agents and other growth factors in low-risk MDS. Best Pract Res Clin Haematol. 2013;26:401–410.
35. Kao JM, McMillan A, Greenberg PL. International MDS risk analysis workshop (IMRAW)/IPSS reanalyzed: impact of cytopenias on clinical outcomes in myelodysplastic syndromes. Am J Hematol. 2008;83:765–770.
36. Balducci L. Transfusion independence in patients with myelodysplastic syndromes: impact on outcomes and quality of life. Cancer. 2006;106:2087–2094.
37. Clark AJ, Doyle KM, Humbert PO. Cell-intrinsic requirement for pRb in erythropoiesis. Blood. 2004;104:1324–1326.
38. Spike BT, Dirlam A, Dibling BC, et al. The Rb tumor suppressor is required for stress erythropoiesis. EMBO J. 2004;23:4319–4329.
39. Hansen JB, Petersen RK, Larsen BM, Bartkova J, Alsner J, Kristiansen K. Activation of peroxisome proliferator-activated receptor gamma bypasses the function of the retinoblastoma protein in adipocyte differentiation. J Biol Chem. 1999;274:2386–2393.
40. Lin MS, Chen WC, Bai X, Wang YD. Activation of peroxisome proliferator-activated receptor gamma inhibits cell growth via apoptosis and arrest of the cell cycle in human colorectal cancer. J Dig Dis. 2007;8:82–88.
41. Nicolay BN, Dyson NJ. The multiple connections between pRB and cell metabolism. Curr Opin Cell Biol. 2013;25:735–740.
42. Wulfert M, Kupper AC, Tapprich C, et al. Analysis of mitochondrial DNA in 104 patients with myelodysplastic syndromes. Exp Hematol. 2008;36:577–586.
43. Nikpour M, Pellagatti A, Liu A, et al. Gene expression profiling of erythroblasts from refractory anaemia with ring sideroblasts (RARS) and effects of G-CSF. Br J Haematol. 2010;149:844–854.
44. Craven SE, French D, Ye W, de Sauvage F, Rosenthal A. Loss of Hspa9b in zebrafish recapitulates the ineffective hematopoiesis of the myelodysplastic syndrome. Blood. 2005;105:3528–3534.
45. Chen ML, Logan TD, Hochberg ML, et al. Erythroid dysplasia, megaloblastic anemia, and impaired lymphopoiesis arising from mitochondrial dysfunction. Blood. 2009;114:4045–4053.
46. Nilsson R, Schultz IJ, Pierce EL, et al. Discovery of genes essential for heme biosynthesis through large-scale gene expression analysis. Cell Metab. 2009;10:119–130.
47. Yien YY, Robledo RF, Schultz IJ, et al. TMEM14C is required for erythroid mitochondrial heme metabolism. J Clin Invest. 2014;124:4294–4304.
48. Cotter PD, Rucknagel DL, Bishop DF. X-linked sideroblastic anemia: identification of the mutation in the erythroid-specific delta-aminolevulinate synthase gene (ALAS2) in the original family described by Cooley. Blood. 1994;84:3915–3924.
49. Beachy SH, Aplan PD. Mouse models of myelodysplastic syndromes. Hematol Oncol Clin North Am. 2010;24:361–375.
50. Horrigan SK, Arbieva ZH, Xie HY, et al. Delineation of a minimal interval and identification of 9 candidates for a tumor suppressor gene in malignant myeloid disorders on 5q31. Blood. 2000;95:2372–2377.
51. Schneider RK, Schenone M, Ferreira MV, et al. Rps14 haploinsufficiency causes a block in erythroid differentiation mediated by S100A8 and S100A9. Nat Med. 2016;22:288–297.

52. Yang Z, Keel SB, Shimamura A, et al. Delayed globin synthesis leads to excess heme and the macrocytic anemia of Diamond Blackfan anemia and del(5q) myelodysplastic syndrome. Sci Transl Med. 2016;8. 338ra367.
53. Augustyniak J, Lenart J, Gaj P, et al. Bezafibrate upregulates mitochondrial biogenesis and influence neural differentiation of human-induced pluripotent stem cells. Mol Neurobiol. 2019; 56:4346–4363.
54. Aul C, Arning M, Runde V, Schneider W. Serum erythropoietin concentrations in patients with myelodysplastic syndromes. Leuk Res. 1991;15:571–575.
55. Cazzola M, Della Porta MG, Malcovati L. Clinical relevance of anemia and transfusion iron overload in myelodysplastic syndromes. Hematology Am Soc Hematol Educ Program. 2008: 166–175.
56. Shirai CL, Ley JN, White BS, et al. Mutant U2AF1 Expression alters hematopoiesis and pre-mRNA splicing in vivo. Cancer Cell. 2015;27:631–643.
57. Chen TC, Hou HA, Chou WC, et al. Dynamics of ASXL1 mutation and other associated genetic alterations during disease progression in patients with primary myelodysplastic syndrome. Blood Cancer J. 2014;4:e177.
58. Ernst T, Chase AJ, Score J, et al. Inactivating mutations of the histone methyltransferase gene EZH2 in myeloid disorders. Nat Genet. 2010;42:722–726.
59. Malcovati L, Della Porta MG, Pietra D, et al. Molecular and clinical features of refractory anemia with ringed sideroblasts associated with marked thrombocytosis. Blood. 2009;114:3538–3545.
60. Smeets MF, Tan SY, Xu JJ, et al. Srsf2(P95H) initiates myeloid bias and myelodysplastic/myeloproliferative syndrome from hemopoietic stem cells. Blood. 2018;132:608–621.
61. Steensma DP, Dewald GW, Lasho TL, et al. The JAK2 V617F activating tyrosine kinase mutation is an infrequent event in both "atypical" myeloproliferative disorders and myelodysplastic syndromes. Blood. 2005;106:1207–1209.

Supplemental Methods

Mice, sampling and transplantation

The *Epor*-Cre *Rosa26*-eYFP$^{ki/ki}$ *Rb1*$^{fl/fl}$ conditional knockout mice were bred in the clinical research center at Lund university and maintained at BMC Lund University, Sweden. All experiments were performed under ethical guidelines approved by the Animal Ethics Committee of Lund.

Steady state parametres were analyzed using littermate mice, age 8-9 months old. Bone marrow (BM) was flushed with PBS/2% FCS (GE Healthcare Life Sciences, Pittsburgh, PA USA) through a 23G needle/1mL syringe or crushed using a mortar and pestle. Whole spleens where weighted and crushed through a 70µm filter with a syringe into petri dishes and flushed with 10ml PBS/2% FCS. Peripheral blood (PB) was taken from tail vein punctures, collected into EDTA tubes. PB, BM and spleen cell suspensions were counted on a hematologic analyzer Sysmex KX-21N (Sysmex corporation, Kobe, Japan). RBCs in PB were lysed with ammonium chloride (Stem cell technologies) before antibody staining and FACS analysis.

For transplantation bone marrow (BM) from femur, tibia and iliac crest was harvested from donor transgenic mice (*pRb*$^{-/-}$ or Cre- *pRb*$^{fl/fl}$ controls, CD45.2), and subsequently filtered, counted and depleted for lineage markers FcγR, CD4, CD8, Gr1, Mac1, B220 and Ter119-biotin (Biolegend, San Diego, CA USA) using MACS separator columns (Miltenyi Biotec, Bergisch Gladbach, Germany). Donor BM was also depleted for Sca1 to not affect the mitochondrial function of hematopoietic stem cells. Each Lin-/Sca1- donor BM was resuspended in StemSpan SFEM (Stemcell Technologies, Vancouver Canada) medium supplemented with 1% P/S (Invitrogen, Carlsbad CA USA), 50ng/ml mSCF, 10ng/ml mIL-3, 50ng/ml hIL-6, (Pepro Tech, London UK) 0.4µg/ml proteamine sulfate (Sigma Aldrich), and divided in two for transduction with control vector or PGC-1β over-expressing vector. Transduced cells were incubated overnight, resuspended in PBS (GE Healthcare Life Sciences) with 2% FCS (GE Healthcare Life Sciences) and transplanted into lethally irradiated recipients (CD45.1, 2x 500cGy) together with 100,000 whole BM cells from congenic WT mice (CD45.1+) for support. Peripheral blood (PB) was harvested through tail vein puncture and collected in tubes with EDTA (Sigma Aldrich). Reconstitution and blood parameters were analyzed in PB at 4 and 8 weeks post-transplant and in BM and spleen upon termination at 8 weeks.

Cohorts of *Epor*-Cre *Rosa26*-eYFP$^{ki/ki}$ *Rb1*$^{fl/fl}$ conditional knockout mice and Cre- WT littermates were fed custom feed (SF10-034, Ssniff Spezialdiäten GmbH, Soest Germany) with or without 0.5% Bezafibrate (w/w) (Sigma Aldrich, St. Louis, Missouri, United States). PB samples were taken at day 0 (baseline), 30 and 60 of treatment and blood parameters including red blood cell (RBC) counts, hemoglobin (Hgb) concentration, hematocrit (Hct) and mean corpuscular volume (MCV) was analyzed using Sysmex KX-21N.

Cloning of PGC1b vector

The PGC-1β construct was cloned into a pRLL backbone lentiviral vector for co-expression with dTomato. The empty vector was digested with the fast digest BamHI restriction enzyme (Thermo Fisher Scientific, Waltam, MA USA) for 15minutes in 37°C. Terminal 5'-phosphatases were removed by incubating the digested plasmid with 1.5µl Fast AP (Thermo Fisher Scientific) for 20 minutes at 37°C. A two-step PCR program was used for the complementary DNA (cDNA) of PGC1β, with primers specifically designed for Gibson assembly. The vector and insert were separated on a 1% Seakem GTG (Lonza, Basel, Switzerland) agarose gel and purified using a QIAquick (Qiagen, Hilden Germany) gel extraction kit. The Gibson ligation reaction was done with 10µl GA master mix (New England Biolabs, Ipswich, MA USA) at 50°C for 1 hour.

Flow cytometry

Four separate flow cytometry antibody stains were performed to analyze (1) early myelo/erythroid progenitors in BM using Sca1 (BV421, Biolegend), c-Kit (APC780, Biolegend), CD32/16 (PerCP5.5, Becton Dickinson, Franklin Lakes, NJ USA), CD41 (BV605, Becton Dickinson), CD150 (PeCy7, Biolegend), CD105 (Biotin/StrAv-Qdot655, Thermo Fisher/Nordic BioSite AB, Täby, Sweden), and the lineage markers B220 (PeCy5, Biolegend), CD3 (PeCy5, Biolegend), Gr-1 (PeCy5, Biolegend), Mac-1 (PeCy5, Biolegend), (2) terminal erythroid differentiation in BM and spleen using Ter119 (BV510 or PeCy7, Biolegend), CD44 (APCCy7, BD bioscience) and size, (3) lymphoid/myeloid lineages in BM using CD3 (PeCy5, Biolegend), B220 (PeCy5, Biolegend), Gr-1(Biolegend), and Mac-1 (Biotin/StrAv-Qdot605, Biolegend/Invitrogen), and (4) donor derived lineages in PB using Ter119 (PeCy7, Biolegend), Gr1 (Biotin/StrAv-Qdot605,

Biolegend/Invitrogen), CD45.2 (APC-eFL780, eBioscience/Thermo Fisher Scientific). 4',6-diamidino-2-phenylindole (DAPI, Thermo Fisher Scientific) or 7-Aminoactinomycin D (7-AAD, Sigma Aldrich) was used to exclude dead cell, and MitoTracker deep red (Thermo Fisher Scientific) was used to measure mitochondrial activity. Samples were sorted and analyzed on FACS Aria III (Becton Dickinson) and FACS data was analyzed with FlowJo software (Becton Dickinson).

Microarray

For microarray analysis, 80,000 erythroid progenitors from the polychromatic erythroblast (III), orthochromatic eryhtroblast(IV) and reticulocyte (V) populations respectively were sorted from 3 Cre- (WT) and 3 *pRb*$^{-/-}$ (KO) mice into RLT buffer (1% β-mercaptoethanol) using FACS Aria III (Becton Dickinson) and snap frozen. RNeasy Plus micro kit (Qiagen) was used for RNA extraction followed by NuGEN high-yield RNA amplification protocol. The microarray was performed by Kompetenzzentrum Fluoreszente Bioanalytik (KFB, Regensburg Germany) using single cartridge array (Affymetrix, mouse gene 2.0 ST) and the array data was normalised using RMA. Probe/gene expression was called differential between WT and KO using a cut off at FDR<0.003. The resulting 7282 genes were k-means clustered into 6 clusters using Genesis. Differentially expressed probes/genes were further identified using limma package for R. Tables comparing different erythroid populations pairwise within WT and KO groups were also created (cut off of FDR<0,06, no cut off for fold-change)

In vitro erythroid differentiation

C-kit+ cells were enriched using CD117 MicroBeads (Miltenyi Biotec, Bergish Gladbach, Germany) according to manufacturer protocol. C-kit+ were cultured in SFEM (Stemcell technologies, Vancouver, Canada) erythroid culture medium with 3U EPO/ml, 30% FBS, 0,3mg/ml holo-transferrin (Sigma Aldrich) and 0.4µg/ml Protamine sulphate (Sigma Aldrich) and transduced with Pgc1β overexpressing lentivirus. Medium was changed to fresh SFEM erythroid culture medium without Protamine sulphate after 6h of transduction. After 36h of culture cells were stained with Ter119 (PeCy7, Biolegend) CD44 (BV711, Biolegend), Mitotracker Deep Red (Thermo Fisher Scientific) and DAPI (Thermo Fisher Scientific). 5.000-10.000 dTomato+

erythroid progenitors (IV) were sorted using Aria III (BD bioscience) into 350µl of RLT buffer (Qiagen) with 1% β-mercaptoethanol.

Quantitative Real-Time PCR

20,000 erythroid progenitors (fractions IV and V) were sorted into RLT buffer (1% β-mercaptoethanol) and snap frozen. RNA was purified using RNeasy mini kit according to instructions (Qiagen) and cDNA was prepared using SuperScript III reverse transcriptase (Thermo Fisher Scientific). RT-qPCR assays were performed according to the TaqMan Gene expression master mix protocol and pre-designed probe based primers (Integrated DNA Technologies, Coralville, IA USA) (**Supplemental table 1**).

Apoptosis assay

BM from WT and KO's was and stained for erythroid terminal populations using Ter119 (APC, Biolegend) and CD44 (APC-Cy7, BD bioscience) antibodies for 30 minutes on ice. Cells were washed and resuspended with 100µl 1x Binding buffer diluted with distilled water (Becton Dickinson, PE, 10X Annexin V binding buffer 0.1M Hepes/NaOH (pH7.4), 1.4M NaCl, 25 mM $CaCl_2$). 5µl of Annexin V was added to each sample, gently vortexed, incubated at RT for 15 minutes in the dark, and analyzed on LSR II (Becton Dickinson).

Cell cycle assay

Since erythroid cells are sensitive to permeabilization and fixation, 250,000-400,000 erythroid progenitors (fractions III, IV and V), were sorted based on Ter119 (BV510, Biolegend) and CD44 (PE, Biolegend) and size (FSC-A) using Aria III (Becton Dickinson), prior to fixation. Cell pellets were fixed with ice cold 70% Ethanol in PBS (GE Healthcare Life Sciences) while vortexing and incubated at -20ºC overnight. The fixed cells were washed with PBS and stained with PI staining buffer (0.1% TritonX100 (Sigma Aldrich), 0.1% Sodium citrate (Sigma Aldrich), 10µg/mL Propidium iodide (Sigma Aldrich), 500µg/ml RNase A (Sigma Aldrich) for 30 minutes at 37ºC. PI intensity was analyzed individually in the sorted populations on LSR II (Becton Dickinson).

Heme-assay

500,000 erythroid progenitors from populations IV and V were sorted (Aria III, Becton Dickinson) based on Ter119 (BV510, BioLegend) and CD44 (PE, biolegend) and size (FSC-A). 100µl Cell Extraction Buffer (Thermo Fisher Scientific) was added per 100,000 sorted cells and snap-frozen on dry ice. Free heme was detected using the Hemin Colorimetric Assay kit according to protocol (BioVision, Milpitas, CA, USA), and OD was measured at 570nm.

Serum Iron assay

PB was collected through tail vein puncturing into Eppendorf tubes without anticoagulant, and left at room temperature for 1 hour prior to being centrifuged at 2000g. Serum supernatant was collected and analyzed using the Iron Assay kit (Sigma Aldrich) according to manufacturer protocol. The colorimetric product was measured with an OD of 593nm.

Morphology and iron stain

15,000 whole BM cells were spun down on micro slides, at 550RPM for 3 minutes using pre-wet filters. Air dried slides were stained with May-Grünwald (Merck) for 5 minutes and counterstained with 3% Giemsa (Merck) for 15 minutes. The slides were washed in MilliQ water 2 times 1 minute and air dried.

For analysis of iron accumulations slides were stained with newly mixed Potassium ferrocyanide (20%) and hydrochloric acid (10%) at a 1:1 ratio for 20 minutes, washed with distilled water and counterstained with Eosin (0.2%) for 10 minutes, rinsed in distilled water and air dried. Slides were manually graded for iron accumulation and pictures were taken with microscope (BX50, Olympus) using 60x magnification.

Statistical analysis

Statistical analysis was done using GraphPad Prism 7.00 (GraphPad Software, San Diego, CA USA), significance was analyzed using students unpaired parametric t-test when comparing WT to KO groups, if not stated otherwise. Ordinary 1way ANOVA, corrected for multiple comparisons using Tukey's test, was used for the analysis of the *in vivo* Bezafibrate experiment and In vitro erythroid differentiation experiment. 2way ANOVA was used for In vivo transplantation flow cytometry data from BM, corrected for multiple comparisons using Tukey's test. Pairwise comparisons were done were applicable.

Supplemental Table 1. Primers (Integrated DNA Technologies, Coralville, Iowa, USA) used for the RT-qPCR assays. Sequence names are included which are specific the manufacturer predesigned primers.

Sequence name	Gene
Mm.PT.39a.1	Gapdh
Mm.PT.58.29564054	Ccne1
Mm.PT.58.5595112	Cdk1
Mm.PT.58.30168441	Cdk2
Mm.PT.58.13028991	Tfdp1
Mm.PT.58.12540977	E2f8
Mm.PT.58.43528160	E2f2
Mm.PT.58.11914043	E2f7
Mm.PT.58.10646197	Fech
Mm.PT.58.17288666	Alas2
Mm.PT.58.10787436	Abcb7
Mm.PT.56a.43099224	Tmem14c
Mm.PT.58.16950406	Ndufa1
Mm.PT.58.32779333	Prdx3
Mm.PT.56a.32210284	Cox7b
Mm.PT.58.31008765	Atp5s
Hs.PT.58.40035104	GAPDH
Hs.PT.58.38577994	PPARGC1B
Mm.PT.58.29600686	ppargc1b

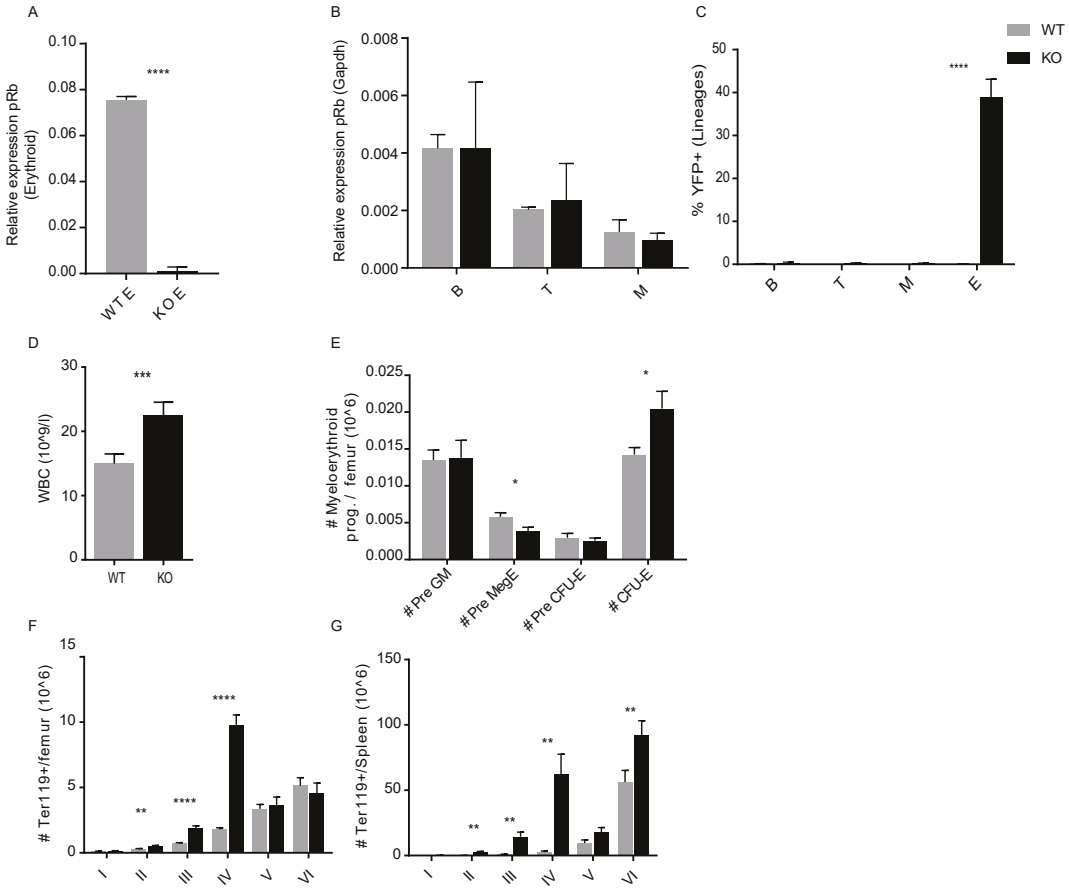

Supplemental figure 1. pRb is efficiently and specifically deleted in erythroid cells.
A) pRb specifically deleted in KO erythroid cells (n=3) B) Relative expression of pRb within B, T and Myeloid cell lineages is not affected in KO animals. C) Frequency of YFP expressing cells within lineages (B,T, Myeloid & Erythroid), YFP specifically expressed within KO erythroid cells (n=3). D) White blood cell count was significantly increased in BM of KO animals (n=15). E) Absolute numbers of Myeloeryhtroid progenitors per femur (n=5). F) Absolute numbers of Terr19+ eryhtroid populations per femur (n=12) and G) spleen (n=5). Data is presented as mean ± SEM (*P ≤ 0.05, **P ≤ 0.01, ***P ≤ 0.001,****P ≤ 0.0001).

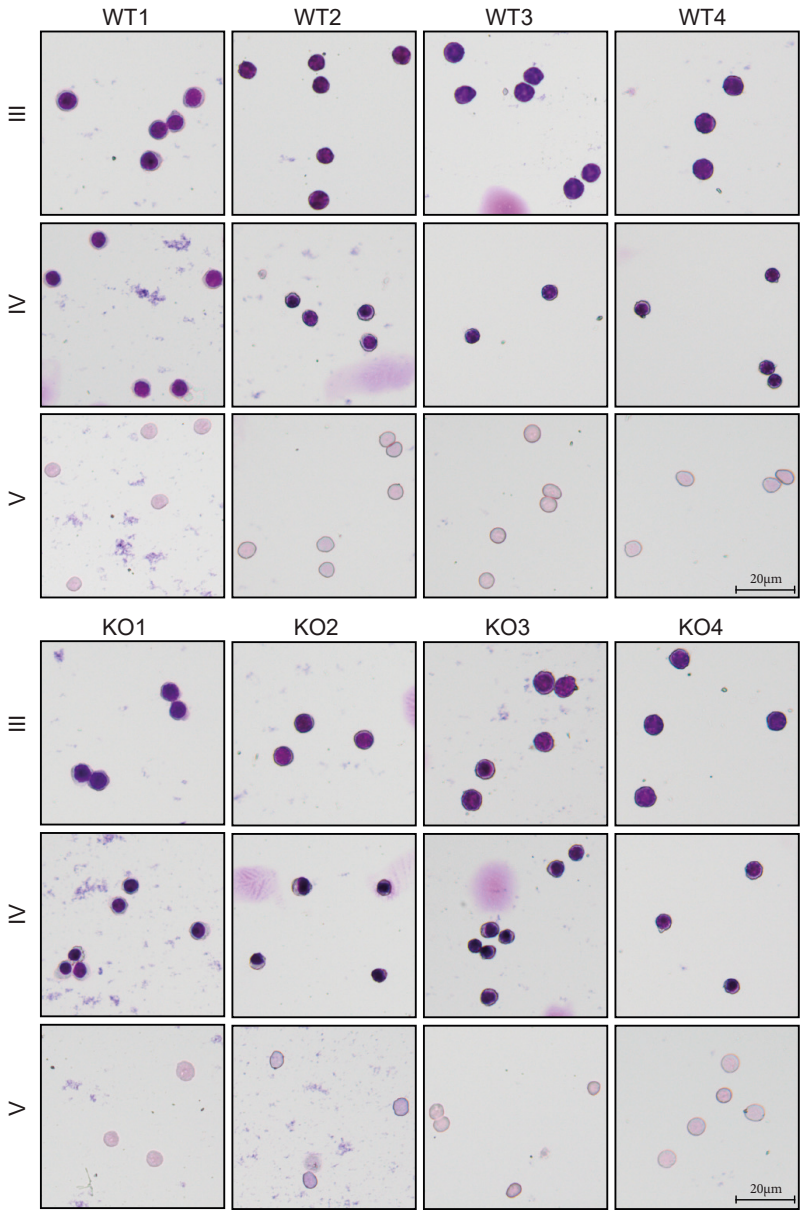

Supplemental figure 2. Cytospins of sorted erythroid polychromatic erythroblasts (III), orthocromatic erythroblasts and reticulocytes, stained with May-Grünwald Giemsa. 10.000 Ter119+ erythroid progenitors were sorted based on CD44 expression and FSC (size). Morphologically distinct populations for their respective gate could be observed, shown here from 8 different animals.

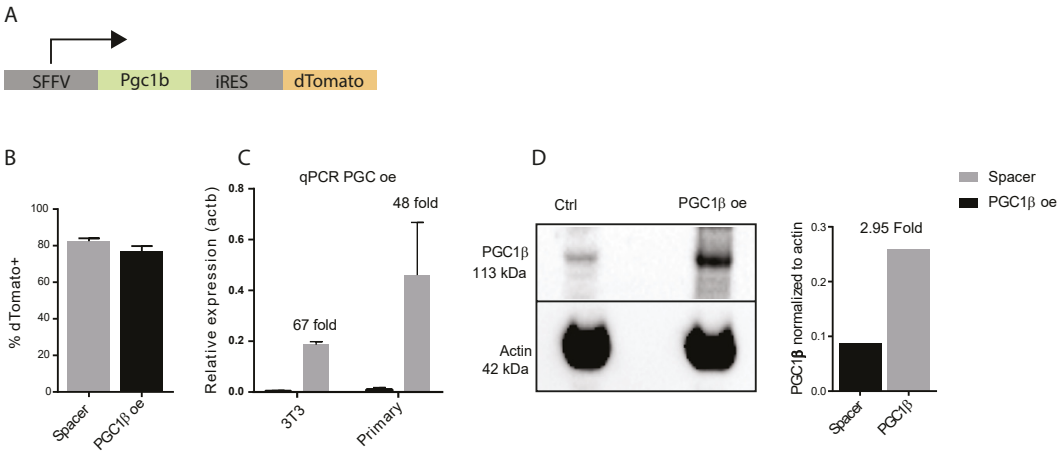

Supplemental figure 3. Efficient overexpression of Pgc1ß using lentiviral vector A) Schematic representation of lentiviral overexpression vector. B) Frequency of initial transduction efficiency measured as % dTomato+ using FACS at 48 hours after transduction. C) Relative expression of Pgc1ß in 3T3 cell line and primary cells measured by qPCR. D) Images (left) and quantification (right) of western blot analysis of Pgc1ß overexpression in sorted transduced 3T3 cells demonstrating 2.95 fold increase in Pgc1ß expression.

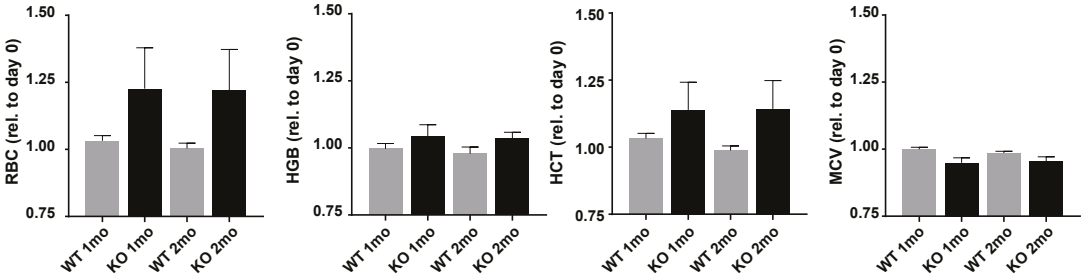

Supplemental figure 4. Bezafibrate treatment increases RBC, HGB and HCT in KO animals but not in WT. Sysmex readout from Bezafibrate in vivo experiment, shown here normalized to day 0 as baseline.

Paper II

scientific reports

Check for updates

OPEN

Decreased PGC1β expression results in disrupted human erythroid differentiation, impaired hemoglobinization and cell cycle exit

Taha Sen, Jun Chen & Sofie Singbrant✉

Production of red blood cells relies on proper mitochondrial function, both for their increased energy demands during differentiation and for proper heme and iron homeostasis. Mutations in genes regulating mitochondrial function have been reported in patients with anemia, yet their pathophysiological role often remains unclear. PGC1β is a critical coactivator of mitochondrial biogenesis, with increased expression during terminal erythroid differentiation. The role of PGC1β has however mainly been studied in skeletal muscle, adipose and hepatic tissues, and its function in erythropoiesis remains largely unknown. Here we show that perturbed PGC1β expression in human hematopoietic stem/progenitor cells from both bone marrow and cord blood results in impaired formation of early erythroid progenitors and delayed terminal erythroid differentiation in vitro, with accumulations of polychromatic erythroblasts, similar to MDS-related refractory anemia. Reduced levels of PGC1β resulted in deregulated expression of iron, heme and globin related genes in polychromatic erythroblasts, and reduced hemoglobin content in the more mature bone marrow derived reticulocytes. Furthermore, PGC1β knock-down resulted in disturbed cell cycle exit with accumulation of erythroblasts in S-phase and enhanced expression of G1-S regulating genes, with smaller reticulocytes as a result. Taken together, we demonstrate that PGC1β is directly involved in production of hemoglobin and regulation of G1-S transition and is ultimately required for proper terminal erythroid differentiation.

Mammalian red blood cells (RBC) are the most abundant cells in the body, with the primary function to transport oxygen and clear distal tissues of carbon dioxide. RBCs have a finite lifetime of approximately 120 days[1] and require continuous production through erythropoiesis, a step-wise process requiring delicate coordination of intrinsic and extrinsic regulators[2]. Imbalanced coordination drives the pathogenesis of various anemia related disorders. During erythropoiesis pluripotent hematopoietic stem cells differentiate through a series of tightly regulated intermediate steps into mature RBC[2]. The first erythroid committed colony forming progenitors BFU-E's and the subsequent CFU-E's have activated expression of the receptor for erythropoietin (EPO)[3], the main hormone responsible for maintenance and proliferation of erythroid committed progenitors during definitive erythropoiesis[4,5]. During the subsequent terminal differentiation erythroblasts undergo stepwise maturation, becoming smaller and increasingly hemoglobinized with each division, condense their nuclei, autophagocytize mitochondria and other organelles, and finally exit cell cycle and extrude their nuclei[6,7].

Mitochondrial biogenesis is enhanced through post-transcriptional modifications in human erythropoiesis[8], and recent advances have implicated that mitochondrial dysfunction leads to impaired erythropoiesis[8–15], indicating that proper mitochondrial function is critical for erythroid development. Differentiating erythroblasts have increased energy demands, which mitochondria supply by ramping up oxidative phosphorylation (OXPHOS). Additionally, mitochondria are responsible for heme and iron metabolism, two components critical for proper function of erythrocytes. The PPAR-gamma coactivator-1 (PGC-1) family of transcriptional coactivators have been shown to regulate mitochondrial capacity and energy metabolism through various nuclear receptors and

Division of Molecular Medicine and Gene Therapy, Lund Stem Cell Center, Lund University, Lund, Sweden. ✉email: sofie.singbrant@med.lu.se

recruitment of protein complexes to specific DNA sequences[16]. They are preferentially expressed in tissues with high OXPHOS needs, and the first member, PGC1α was identified in brown adipose tissue where it was shown to regulate mitochondrial biogenesis[17,18]. The PGC1α homologs, PGC1β and PGC-1-related coactivator (PRC), exert similar downstream effects[19,20]. However, due to tissue-specific expression patterns, the various PGC1 coactivators have distinct physiological roles dependent on the availability of the numerous nuclear receptors through which cellular metabolism is controlled[16].

Pgc-1β display increased expression during terminal erythroid differentiation[21]. However, its function has mainly been studied in adipocytes, hepatic-, cardiac and skeletal tissues[19,22–25], while the role of PGC-1β in erythropoiesis remains largely unknown. The only study to date directly evaluating the role of PGC-1 coactivators during RBC development demonstrates that compound deletion of the related *Pgc1α* and *Pgc1β* during embryonic development in mouse results in anemia due to deregulation of globin genes[26]. Furthermore, we recently demonstrated that perturbed PGC1β expression in response to pRb-deletion in mice results in a developmental block during terminal erythropoiesis and anemia reminiscent of that reported in Myelodysplastic syndrome (MDS)[21,27]. Importantly, the MDS-like anemia could be rescued by enhanced PPAR-signaling, either through PGC1β over-expression or Bezafibrate treatment[21], indicating that PGC1β plays a functional role in the anemic phenotype. Notably, PGC1β is haplo-insufficient in the chromosome 5q deletion subtype of MDS (del(5q) MDS)[28] and deregulation of core mitochondrial pathways and acquired mtDNA mutations have been reported in MDS-patients with anemia[29], generally in genes related to iron and heme homeostasis[12,30,31]. However, the role of PGC1β in regulation of human erythropoiesis is yet to be determined.

To decipher the role of PGC1β in human erythropoiesis, PGC1β was knocked down in bone marrow derived $CD34^+$ hematopoietic stem/progenitor cells and investigated for its effects during erythroid differentiation. Here we show that PGC1β is required for proper human erythroid development, and that perturbed expression results in delayed differentiation in vitro, with accumulations of polychromatic erythroblasts similar to what is seen in MDS-related refractory anemia. Transcriptional and functional analysis revealed that reduced levels of PGC1β resulted in perturbed hemoglobin production, as well as disturbed cell cycle exit with smaller reticulocytes as a result.

Results. *Pgc1* coactivators have been indicated to play a role during murine erythropoiesis[26], while their function in human erythropoiesis remains unknown. To further decipher the role of PGC1β during human erythroid development, we reduced the PGC1β expression in human $CD34^+$ bone marrow (BM) and cord blood (CB) progenitors using lentiviral knock-down with two different shRNAs (sh3, sh5) to reduce the risk of off-target effects (Fig. 1A), and investigated its effects during erythroid differentiation in vitro. High initial transduction efficiency, on average 65%, was achieved with both vectors (data not shown), with sh3 consequently resulting in more efficient knock-down of PGC1β expression than sh5, averaging 48% and 26% respectively for BM (Fig. 1B, n = 4 biological replicates times 3 and 2 separate transductions for sh3 and sh5 respectively), and 55% and 25% respectively for CB (Fig. 1C). PGC1β knock-down efficiency was further assessed at the protein level in CB derived $CD34^+$ cells. Surprisingly, sh5 with less efficient mRNA knock-down at the transcriptional level displayed a more effective reduction at the protein level (Fig. 1D, full blot in Fig. S1). Transduced (GFP^+) $CD34^+$ BM and CB cells were sorted and the effects of perturbed PGC1β expression were analyzed using a three-phase culture system that over 21 days effectively recapitulates human erythroid development from hematopoietic stem/progenitor cells to reticulocytes, including all intermediate erythroid precursors (Fig. 1E, modified from Hu et al. 2013)[32], with some differences in kinetics in proliferation and differentiation between $CD34^+$ progenitors derived from fetal and adult sources [33].

Decreased expression of PGC1β results in perturbed formation of early erythroid progenitors and delayed terminal differentiation. To investigate the role of PGC1β during early erythroid development, transduced $CD34^+$ BM stem/progenitor cells were plated in methyl cellulose and analyzed for formation of erythroid colony forming units (CFU-Es) on day 14. Decreased expression of PGC1β severely affected the capacity of multipotent $CD34^+$ progenitors to form CFU-Es, with a striking 8.8 and 25.5-fold reduced CFU-E-formation for sh3 and sh5 respectively (Fig. 2A). To further understand the importance of PGC1β during terminal erythroid differentiation, we took advantage of the pan-erythroid surface marker Glycophorin A/CD235a (GPA) in combination with differential expression of surface markers Cd49d and Band3[32], and increased hemoglobin availability naturally occurring during stepwise erythroid maturation (Fig. 2B). Flowcytometric analysis of transduced, cultured BM cells on day 10 (GPA^+ cell emergence), day 14 (early erythroid differentiation), day 18 and day 21 (terminal erythroid differentiation) revealed that decreased expression of PGC1β resulted in a significant reduction in the overall formation of erythroid cells (GPA^+) on day 10 and day 14, which was normalized by day 18 and day 21 (Fig. 2C,D).

Further fractionation of GPA^+ erythroid progenitors demonstrated that reduced expression of PGC1β resulted in delayed erythroid maturation, with increasing accumulation of basophilic/polychromatic erythroblasts ($Cd49d^+/Band3^-$) and impaired formation of more mature polychromatic/orthochromatic erythroblasts ($Cd49d^+/Band3^+$) on day 14 and day 18 of culture respectively (Fig. 2C,D). Erythroid differentiation was close to normalized on day 21, when the majority of cells in the culture had reached final maturation (orthochromatic erythroblasts/Reticulocytes, $Cd49d^-/Band3^+$). Terminal erythroid maturation was further analyzed morphologically, allowing more detailed fractionation. Morphological scoring demonstrated that the surface markers Cd49d and Band3 mark a continuum of differentiating erythroblasts. Furthermore, the intensity of Band3 doesn't increase substantially between day 14 and day 18, although the cells contained in the $Cd49d^+/Band3^-$ compartment are significantly more mature on d18 (polychromatic erythroblasts) than on day 14 (basophilic). In accordance with the flowcytometric results, scoring of cells stained with Giemsa together with hemoglobin-marking

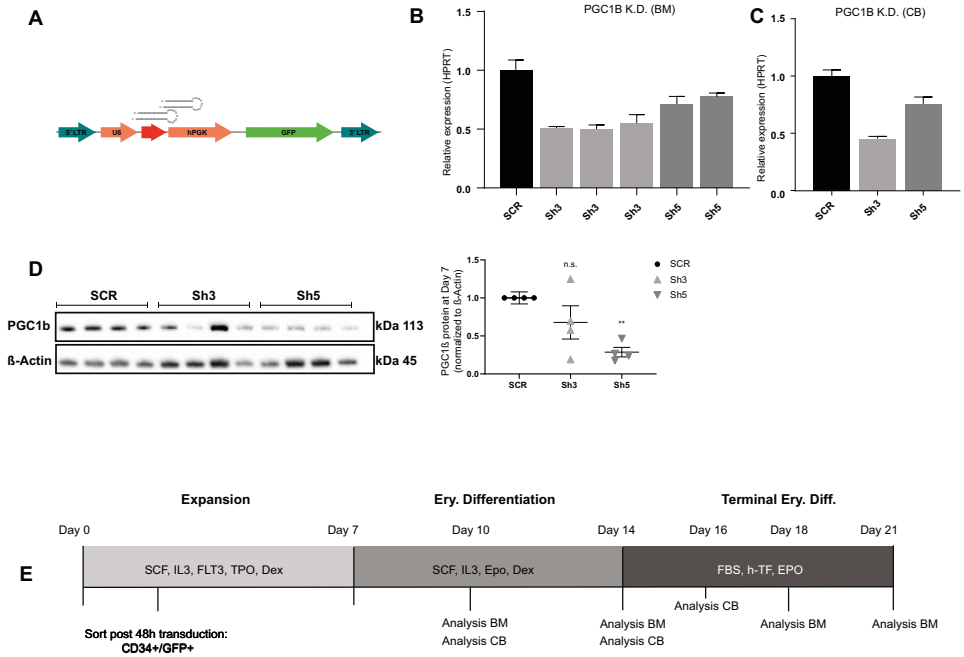

Figure 1. Experimental setup to study perturbed PGC1β signaling during human erythroid development. (**A**) Description of the pLKO lentiviral vector used, expressing a scrambled control vector (Scr) or two different short hairpin RNA for PGC1β, sh3 and sh5. Initial transduction efficiency was on average 65% on day3 (SCR: 62%, sh3: 66%, sh5 66%). (**B**) Quantification of knock-down efficiency in transduced cells at the transcriptional level in B) bone marrow derived CD34 + cells and (**C**) cord blood derived CD34 + cells. (n = SCR:4, Sh3:12, Sh5:6 for BM and n = 4 for CB). (**D**) Knock-down efficiency of PGCβ at the protein level in cord blood derived progenitors on day7 as assessed by western blot. Quantification of PGC1β protein was normalized to ß-ACTIN. (**E**) Schematic outline of the 3-phase erythroid culturing system of human $CD34^+$ cells (modified from Hu et al. 2013)[32]. 25,000 transduced CD34 + BM cells or 100,000 transduced CD34 + CB cells were seeded on day 3, and split on days of medium switching, with average cell concentrations of 9×10^5 cells/ml, 3.5×10^6 cells/ml and 2×10^5 cells/ml on days 14, 18 and 21 respectively. Data is presented as mean ± SEM (*P ≤ 0.05, **P ≤ 0.01, ***P ≤ 0.001).

3,3′-Diaminobenzidine (DAB) (Fig. 2E) demonstrated a delay in maturation with accumulations of basophilic erythroblasts (II) on day 14, and at the polychromatic erythroblast stage (III) on day 18 (Fig. 2F). Again, the formation of more mature orthochromatic erythroblasts and reticulocytes (IV, V) was close to normalized by day 21 (Fig. 2F). The DAB-Giemsa quantification was not possible on day 10, since GPA^+ and GPA^- progenitors could not be distinguished morphologically.

Differentiation from $CD34^+$ cells to mature erythroid progenitors occurs faster in CB compared to BM. As a result, analyses for CB were done on day 10, 14 and 16, with day 16 corresponding to between day 18 and day 21 of BM differentiation. Knock-down of PGC1β in CB derived $CD34^+$ cells resulted in a developmental delay that was even more pronounced compared to BM, with remaining significantly reduced levels of $Cd49d^-/Band3^+$ progenitors on day 16 (Fig. 3A,B). The more pronounced reduction of formed GPA^+ cells during early erythropoiesis using sh5 as compared to sh3 can likely be attributed to the lower PGC1β protein levels caused by sh5-mediated knock-down. Analysis of enucleation using the nucleic acid stain Syto62 demonstrated that knock-down of PGC1β also resulted in significantly reduced enucleation in mature GPA^+ cells compared to control (Fig. 3C). In conclusion, reduced expression of PGC1β results in perturbed formation of early erythroid progenitors and impaired terminal erythroid differentiation with an accumulation of polychromatic erythroblasts and a subsequent reduction of more mature erythroblasts, a phenotype that is reminiscent of the refractory anemia seen in many MDS patients[27] and the MDS-like anemia we have previously reported on in mouse[21].

PGC1β knock-down results in deregulated hemoglobinization of erythroid progenitors. The functional role of the mitochondrial coactivator PGC1β in erythropoiesis remains largely unknown. However,

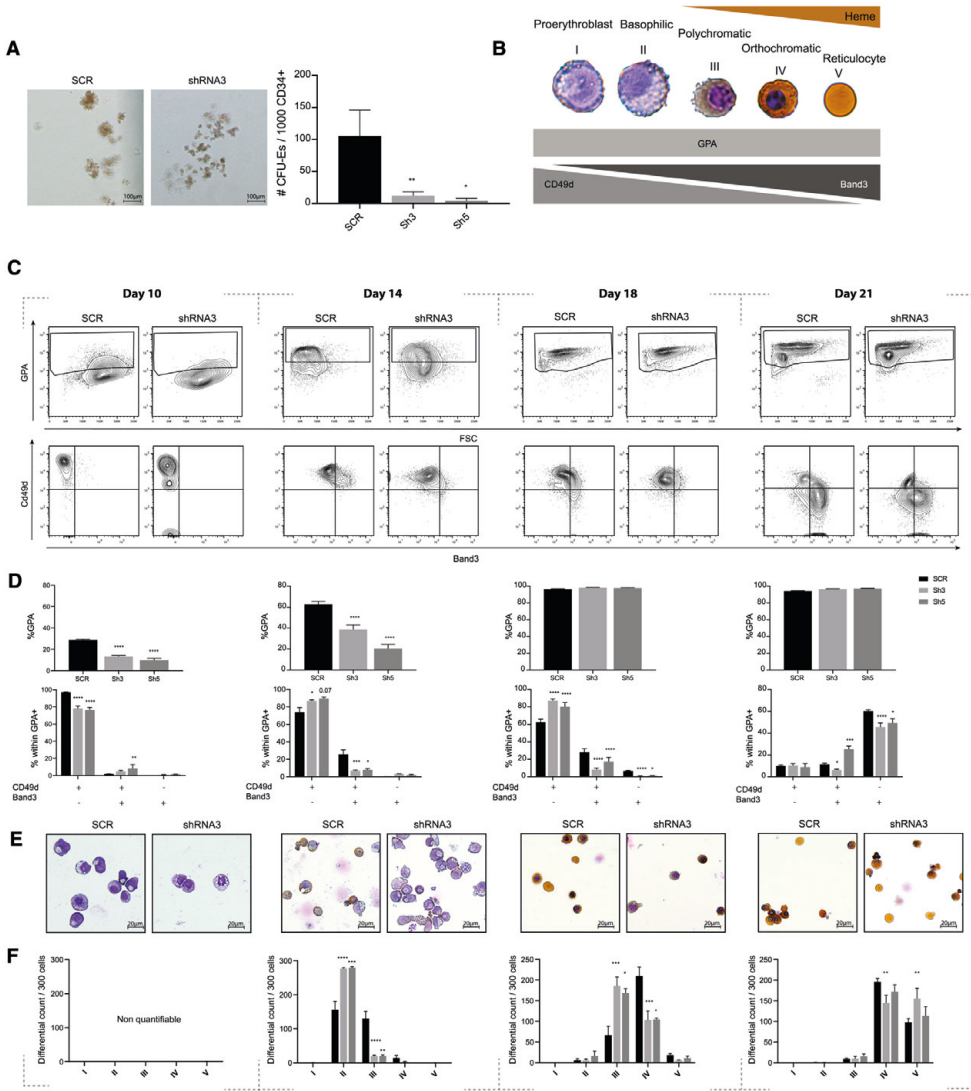

Figure 2. Decreased expression of PGC1β results in perturbed formation of early erythroid progenitors and delayed terminal differentiation in BM. (**A**) Representative pictures (left) and quantification (right) of CFU-E colonies at day 14 (n = SCR:4, Sh3:12, Sh5:6). (**B**) Schematic description of the cell morphology, cell surface markers and heme availability during terminal erythroid differentiation. The representative pictures are of erythroid progenitors from the erythroid culture, stained with DAB-Giemsa. (**C**) Representative plots and (**D**) quantification of flow cytometry analysis of GPA (top) and CD49d/Band3 within GPA^+ (bottom) on day 10, 14, 18 and 21 of erythroid in vitro differentiation (n = SCR:4, Sh3:12, Sh5:6). (**E**) Representative pictures at 40 × magnification and (**F**) quantification of progenitors from cytospins stained with DAB-Giemsa (n = 3–4). Quantification was not possible on day 10 as GPA^+ and GPA^- progenitors cannot be differentiated. Data is presented as mean ± SEM (*P ≤ 0.05, **P ≤ 0.01, ***P ≤ 0.001, ****P ≤ 0.0001).

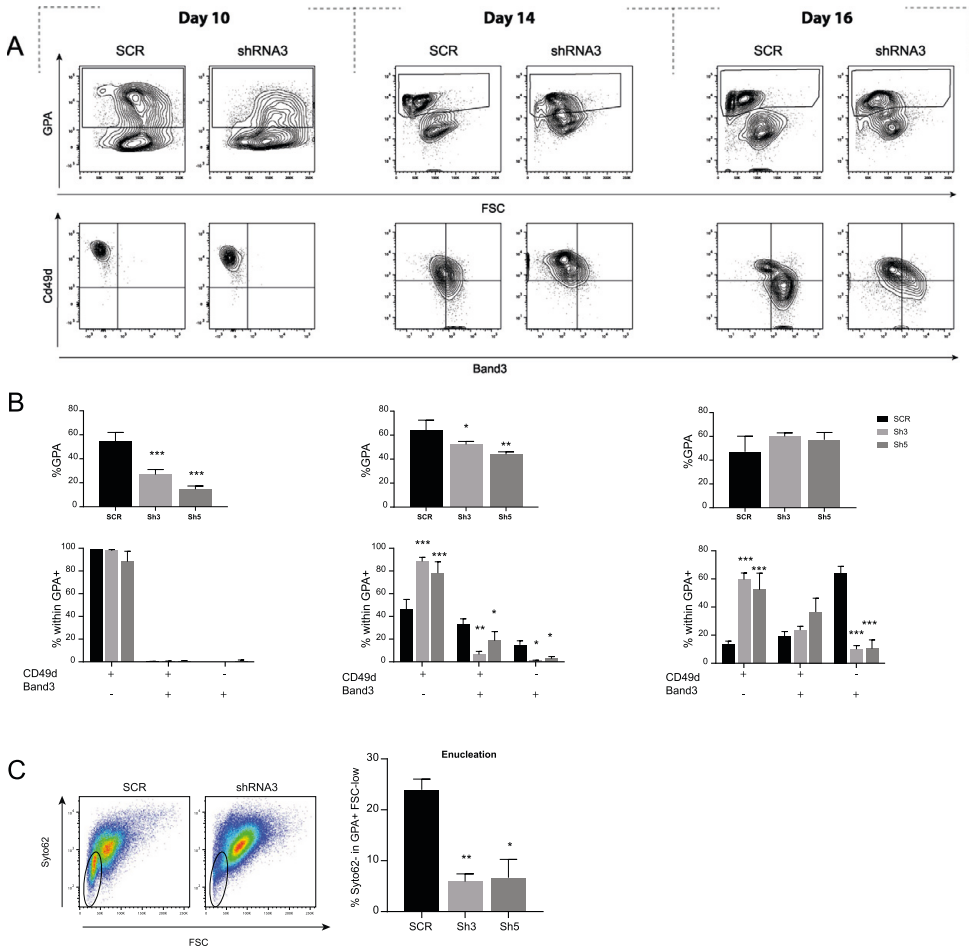

Figure 3. Decreased expression of PGC1β in CB derived CD34 + cells results in perturbed formation of early erythroid progenitors and impaired enucleation. (**A**) Representative plots and (**B**) quantification of flow cytometry analysis of GPA (top) and CD49d/Band3 (bottom) on day 10, 14 and 16 of CB derived CD34 + erythroid in vitro differentiation (n = 4). (**C**) Representative plots (left) and quantification (right) of enucleation efficiency based on Syto62 nucleic acid stain within mature GPA$^+$ cells (n = 4). Data is presented as mean ± SEM (*P ≤ 0.05, **P ≤ 0.01, ***P ≤ 0.001).

we recently showed that down-regulation of *pgclβ* in response to *pRb* deletion correlated with decreased expression of genes involved in mitochondrial function, as well as heme synthesis and iron transport in mouse[21], and compound deletion of the related *Pgc1α* and *Pgc1β* genes in mouse has indicated that PGC1 coactivators might be able to affect globin gene transcription during fetal development[26]. Furthermore, mitochondrial clearance has been shown to be important for human terminal erythroid differentiation, with mitochondrial retention due to deregulated mitophagy resulting in perturbed enucleation[14,15]. To investigate mitochondrial effects of reduced PGC1β expression during human erythroid differentiation, we analyzed the expression of key genes involved in oxidative phosphorylation (OXPHOS) in BM derived erythroid progenitors on day 18 (Fig. 4A–C) and CB derived erythroid progenitors on day 16 (Fig. 4D–F). In BM, decreased PGC1β expression resulted in decreased expression of *COX7B* (Cytochrome C Oxidase, respiratory electron transport[34]), *SDHB* (CII: respiratory electron transport[35]), *NDUFA1* (CI: respiratory electron transport[36]) and *ATP5S* (ATP synthesis[37]) in polychromatic erythroblasts (Fig. 4B). In contrast, the expression of *COX7B* and *SDHB* were increased while

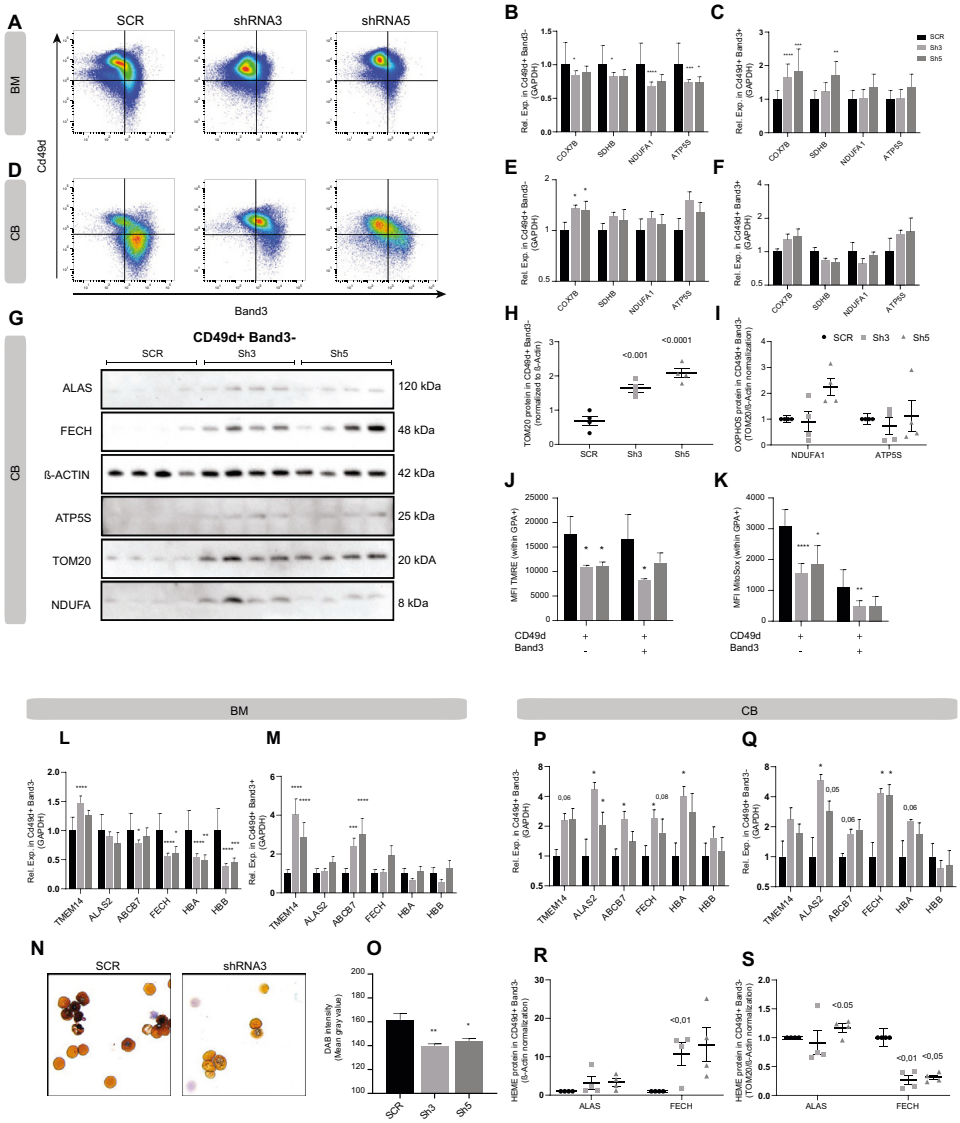
A
SCR
shRNA3
shRNA5
BM
CD49d
D
CB
Band3
B
C
SCR
Sh3
Sh5
COX7B
SDHB
NDUFA1
ATP5S
E
F
G
CD49d+ Band3-
SCR
Sh3
Sh5
ALAS
FECH
ß-ACTIN
ATP5S
TOM20
NDUFA
120 kDa
48 kDa
42 kDa
25 kDa
20 kDA
8 kDa
H
I
J
K
BM
CB
L
M
P
Q
N
O
R
S
ALAS
FECH
HBA
HBB
TMEM14
ABCB7

◂**Figure 4.** PGC1β knock-down results in deregulated hemoglobinization of erythroid progenitors. (**A**) Representative flow cytometry plots of bone marrow derived erythroid progenitors within GPA$^+$ (SCR). (**B**, **C**) RT-qPCR analysis of gene expression relative to GAPDH on day 18 of genes important for Oxidative phosphorylation (OXPHOS) in bone marrow derived (**B**) polychromatic erythroblasts and (**C**) orthochromatic erythroblasts respectively (n = SCR:4, Sh3:12, Sh5:6). (**D**) Representative flow cytometry plots of cord blood derived erythroid progenitors within GPA$^+$ (SCR). (**E**, **F**) RT-qPCR analysis of gene expression relative to GAPDH on day 16 of genes important for Oxidative phosphorylation (OXPHOS) in cord blood derived (**E**) polychromatic erythroblasts and (**F**) orthochromatic erythroblasts respectively (n = 4). (**G**) Mitochondria related protein levels were evaluated by western blot in sorted cord blood derived polychromatic erythroblasts from day 16 of culture (ALAS2 (65 kDa) specific bands appear at 120 kDa, likely due to protein dimers). Western blot quantification of (**H**) TOM20 relative to β-Actin as a marker for mitochondrial mass in relation to cell number, and (**I**) OXPHOS related ATP5S and NDUFA1 relative to TOM20/β-Actin to account for differences in mitochondrial mass. Expression depicted as normalized to control (SCR, n = 4). (**J**) Quantification of mitochondrial membrane potential of cord blood derived polychromatic erythroblasts measured on day 16 of differentiation using TMRE and flow cytometry (n = 4). (**K**) Quantification of ROS production by mitochondria in cord blood derived polychromatic erythroblasts measured on day 16 of differentiation using MitoSox and flow cytometry (n = 4). (**L**, **M**) RT-qPCR analysis of gene expression relative to GAPDH on day 18 of genes important for hemoglobin and heme synthesis of bone marrow derived polychromatic erythroblasts (left) and orthochromatic erythroblasts (right) respectively (n = SCR:4, Sh3:12, Sh5:6). (**N**) Representative images of DAB-Giemsa stained erythroblasts from d21 of culture at 40 × magnification and (**O**) quantification of hemoglobin content using ImageJ software (n = SCR:4, Sh3:12, Sh5:6). (**P**, **Q**) RT-qPCR analysis of gene expression relative to GAPDH on day 16 of genes important for hemoglobin and heme synthesis in cord blood derived polychromatic erythroblasts and orthochromatic erythroblasts respectively (n = 4). (**R**) Western blot quantification of heme related ALAS2 and FECH relative to β-Actin and (**S**) TOM20/β-Actin to account for differences in mitochondrial mass (n = 4). Expression depicted as normalized to control (SCR. Data is presented as mean ± SEM (*P ≤ 0.05, **P ≤ 0.01, ***P ≤ 0.001, ****P ≤ 0.0001).

NDUFA1 and *ATP5S* were unchanged in the more mature orthochromatic erythroblasts (Fig. 4C). In CB derived progenitors (Fig. 4D), displaying a similar developmental delay, the transcriptional profile of OXPHOS genes in polychromatic erythroblasts more resembled that of later maturation stages in the BM (Fig. 4C), with increased expression of only *COX7B* (Fig. 4E), while none of the investigated genes were differentially expressed in the orthochromatic erythroblasts (Fig. 4F). This fits well with that CB derived progenitors have differentiated further on day 16 than BM progenitors on d18 (Fig. 4A,D).

As many OXPHOS genes are tightly regulated at the post translational level western blot analysis on key mitochondria related proteins was performed on CB-derived sorted erythroid progenitor populations from day 16 (Fig. 4G and S4A, full blots in Figs. S2, S3). To investigate the levels of mitochondrial biomass compared to cell mass, the protein level of the mitochondrial marker TOM20 was analyzed in relation to β-Actin. In accordance with what we have previously shown in mouse[21] and Moras et al., have demonstrated in human cells[14], mitochondrial biomass decreased during the final maturation steps of unperturbed terminal erythroid differentiation, to become virtually non-detectable at the orthochromatic stage (Scr in Figs. 4G,H and S4A), indicating that a significant portion of the mitochondria have been cleared at that stage. Interestingly, TOM20 was detected at significantly increased levels in the sh PGC1β transduced polychromatic erythroblasts (Fig. 4H). A difference that was no longer apparent in the orthochromatic erythroblasts (Fig. S4A), suggesting a delay in mitochondrial clearance. This delay was also apparent in BM derived erythroid progenitors, where knock-down of PGC1β resulted in increased mitochondrial biomass in all progenitor populations during early differentiation (day 14) as analyzed by flow cytometry and Mitotracker Deep Red (MTDR) (Fig. S4B), which was less pronounced on day 18 (Fig. S4B).

Further analysis of OXPHOS related proteins revealed that NDUFA1 and ATP5S were not significantly altered in sh PGC1β transduced cells, when taking into account the increased mitochondrial biomass (Fig. 4I). However, if instead comparing to cell numbers (β-ACTIN), sh3 transduced cells had significantly increased NDUFA1 protein (Fig. S4C). To evaluate mitochondrial function, CB derived erythroid progenitors were stained with TMRE and MitoSox on day 14 and 16 of differentiation, to measure mitochondrial membrane potential and mitochondrially produced reactive oxygen species (ROS) respectively. While decreased expression of PGC1β resulted in increased mitochondrial membrane potential on day 14, especially using sh3, (Fig. S4D), the mitochondrial membrane potential was significantly reduced at day 16 in both sh PGC1β transduced polychromatic erythroblasts, and in the sh3 transduced orthochromatic erythroblasts (Fig. 4J), in spite of having more mitochondrial mass per cell (Fig. 4h). At day 16 of differentiation, the mitochondrial membrane potential nicely correlated with the level of mitochondrial ROS production (Fig. 4K). This was also true for the control cells on day 14 (Fig. S4D,E), while the levels of mitochondrial ROS increased significantly with differentiation in cells transduced with sh3, despite decreasing membrane potential (Fig. S4E). In conclusion, reduced levels of PGC1β results in disruption of mitochondrial clearance. Furthermore, PGC1β knock-down leads to reduced expression of key OXPHOS genes in earlier erythroid progenitors, but increased expression in more mature progenitors. Notably, mitochondrial function is reduced in both polychromatic and orthochromatic erythroblasts despite increased mitochondrial biomass.

We next sought to understand the involvement of PGC1β in regulation of hemoglobin composition and iron transport, biological processes taking place in the mitochondria that are fundamental for proper red blood cell function. Transcriptional analysis of BM derived erythroid progenitors on day 18 revealed that the expression of *TMEM14C* (transporter of protoporphyrinogen[38]) was increased, *ALAS2* (the rate-limiting enzyme in heme

synthesis[39]) remained unchanged, while the levels *ABCB7* and *FECH* (catalyzing insertion of iron into heme[40]), were decreased in response to PGC1β knock-down in polychromatic erythroblasts (Fig. 4L). Furthermore, in accordance with Cui et al.[26], gene expression of both globin *HBA* and *HBB* subunits was significantly reduced (Fig. 4L). In the more mature orthochromatic erythroblasts, the expression of *ALAS2*, *FECH*, *HBA* and *HBB* was unchanged, while *TMEM14C* and *ABCB7* had increased expression compared to control (Fig. 4M). To functionally investigate if reduced expression of genes regulating heme synthesis and iron transport had an effect on hemoglobin content, erythroid cells from day 21 of culture were stained with hemoglobin-marking DAB (Fig. 4N). Analysis of DAB-intensity as a proxy for heme content revealed a 13% and 11% decrease in the mature reticulocytes with sh3 and sh5 knock-down respectively compared to control (Fig. 4O). Transcriptional analysis in CB derived polychromatic erythroblast on day 16 instead revealed an increased expression of several of the heme related genes, which was especially prominent in sh3 transduced cells (only a significant for *ALAS2* using sh5) (Fig. 4P), potentially reflecting that CB derived progenitors have differentiated further on day 16 than BM progenitors on d18 (Fig. 4A,D). In the orthochromatic erythroblasts only *ALAS2* and *FECH* remained significantly increased (Fig. 4Q). ALAS2 and FECH were further analyzed using western blot (Figs. 4G, S4A). When compared to total cell numbers (β-ACTIN) FECH protein was significantly increased in sh3 transduced polychromatic erythroblasts (Fig. 4R), in agreement with the transcriptional data. However, when taken the increased mitochondrial biomass into account, FECH protein was instead significantly reduced in sh PGC1β transduced cells, while ALAS2 remained slightly increased in sh5 transduced polychromatic erythroblasts (Fig. 4S). In agreement with clearance of mitochondria in later erythroid maturation stages (no detectable TOM20), only FECH had clear bands in orthochromatic erythroblasts (Fig. S4A) with a trend towards increased protein compared to control (Fig. S4F). In conclusion, reduced levels of PGC1β results in deregulation of genes involved in hemoglobin composition and iron transport, as well as reduced hemoglobin content during the final stages of erythroid maturation in BM.

PGC1β knock-down results in disturbed cell cycle exit and smaller reticulocytes. Activation of PPAR signaling has been found to be involved in induction of cell cycle arrest in adipocytes[41] and inhibition of cell growth in human colorectal cancer cell lines[42]. In addition, we recently demonstrated in mouse that down-regulation of PGC1β in response to *pRb* deletion correlated with enhanced cycling and increased expression of cell cycle genes in erythroid progenitors[21]. Importantly, overexpression of *Pgc1β* could normalize the deregulated expression of cell cycle genes induced by pRb deficiency[21]. To further study the direct role of PGC1β in cell cycle regulation in human erythropoiesis, polychromatic erythroblasts from day 18 of culture were stained with DAPI and analyzed for cell cycle status using FACS (Fig. 5A). Since erythroid cells are sensitive to permeabilization and fixation, the polychromatic erythroblasts were sorted prior to fixation and staining. In accordance with our previous results in mouse[21], decreased expression of PGC1β resulted in fewer polychromatic erythroblasts in G1-phase and a 1.5- and twofold increase in cells remaining in S-phase for sh3 and sh5 respectively compared to control (Fig. 5A). Transcriptional analysis on day 18 of genes involved in G1 to S progression revealed that, while the expression of these genes was largely unchanged polychromatic erythroblasts (Fig. 5B), the expression of *E2F7* and *E2F8* (repression of G1/S-regulated genes[43]), *CDK2* (G1/S transition[44]), and *CCNE1* (regulator of *CDK2*[45]) were greatly upregulated in the slightly more mature orthochromatic erythroblasts (Fig. 5C). The same cell cycle related genes were also up-regulated in CB derived erythroblasts on day 16 already at the polychromatic erythroblasts stage (Fig. S5), demonstrating that reduced levels of PGC1β affects cell cycle regulation in both BM and CB erythropoiesis, in spite of known differences in cell cycle status between these hematopoietic tissues[46].

It has been shown that erythroid precursors that undergo fewer cell divisions result in larger erythrocytes[47]. To investigate if enhanced cycling resulted in reduced cell size, we quantified the size of the orthochromatic erythroblasts/Reticulocytes ($CD49d^{-}$ $Band3^{+}$) on day 21 using Forward Scatter Area (FSC-A) and flow cytometry. Results clearly demonstrated that reduced expression of PGC1β resulted in a 13.6% (sh3) and 8.4% (sh5) decrease in median FSC-A compared to cells transduced with control vector (Fig. 5D). Similarly, quantification of the 2D area of reticulocytes from cytospin images at day 21 of culture using ImageJ[48,49] demonstrated a 10% decrease in cell area using the more efficient sh3, while there was no significant difference in reticulocyte size observed using sh5 (Fig. 5E). Taken together, our results demonstrate that decreased expression of PGC1β results in perturbed human erythroid differentiation, reduced mitochondrial clearance, disrupted hemoglobin production, inability to properly exit cell cycle, and a consequent reduced cell size of reticulocytes (Fig. 6).

Discussion

Multiple pathways involved in cell cycle regulation, organelle clearance, apoptosis and iron homeostasis are crucial for functional erythropoiesis[50–53]. A central player for several of these pathways is the mitochondria. However, mechanisms regulating mitochondrial function during erythropoiesis remains elusive. Here we demonstrate that decreased expression of PGC1β a critical coactivator of mitochondrial biogenesis, results in perturbed formation of early erythroid progenitors and delayed human erythroid differentiation, reduced reticulocyte size, disturbed cell cycle regulation and deregulated hemoglobinization. Knock-down of PGC1β expression resulted in a substantial and similar phenotype with both short hairpins used, in spite of their different and relatively low knock-down efficiencies (sh3: 50%, sh5: 20%), demonstrating the importance of unperturbed levels of PGC1β for both early and terminal erythroid development. shRNA mediated gene silencing can either degrade mRNA or inhibit protein translation. The weaker effect on mRNA transcription, but stronger reduction at the protein level detected using sh5, could hence potentially be due to sh5 exerting its effect mainly through stronger inhibition of protein translation.

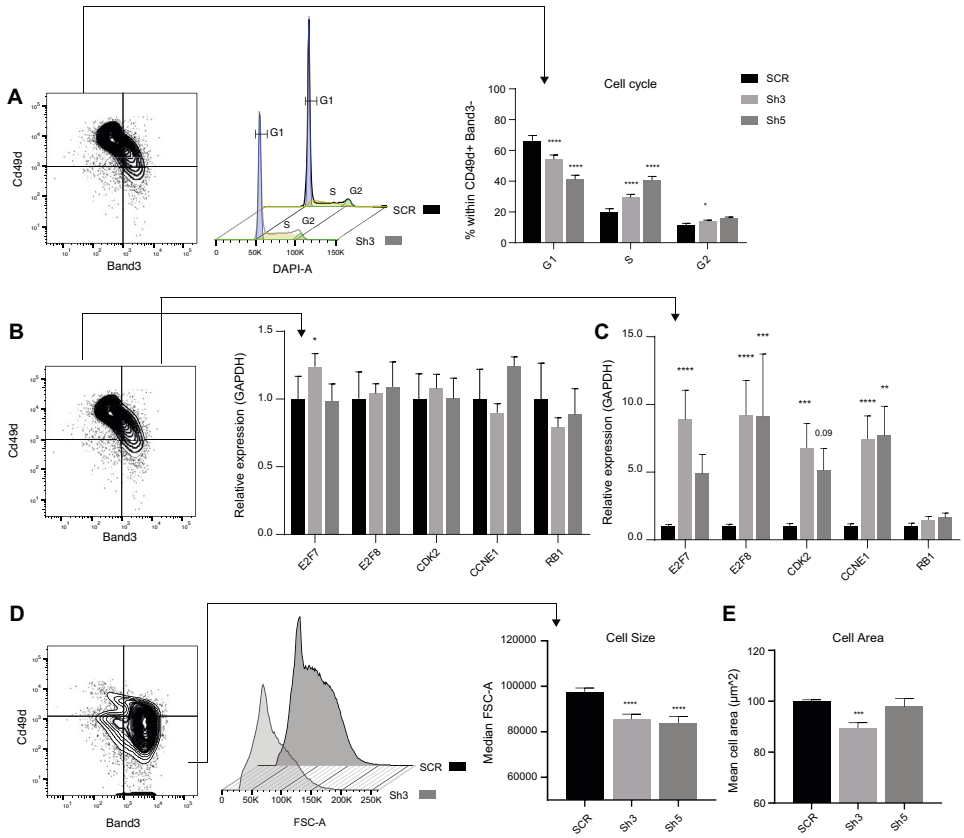

Figure 5. PGC1β knock-down results in perturbed cell cycle exit and smaller reticulocytes. (**A**) Representative plots indicating populations analyzed (SCR, left) and cell cycle profile (middle), and quantification (right) of the cell cycle status on d18 within bone marrow derived polychromatic erythroblast (CD49d$^+$ Band3$^-$), using flow cytometry and DAPI (n = SCR:4, Sh3:12, Sh5:6). (**B**, **C**) Analysis of expression relative to GAPDH on day 18 of cell cycle related genes involved in G1 to S phase progression in (**B**) polychromatic erythroblasts (CD49d$^+$ Band$^-$), and (**C**) orthochromatic erythroblasts (CD49d$^+$ Band$^+$) using RT-qPCR (n = SCR:4 , Sh3:12, Sh5:6). (**D**) Representative plot indicating populations analyzed (SCR, left) and quantification (right) of cell size using flow cytometry and FSC-A within orthochromatic erythroblasts (CD49d$^-$ Band$^+$) on day 21 at the final stage in terminal differentiation. (**E**) 2D cell area quantification of enucleated cells (day 21) stained with DAB-Giemsa, using cytospin microscopy images and ImageJ software, (n = SCR:4, Sh3:12, Sh5:6). Data is presented as mean ± SEM (*P ≤ 0.05, **P ≤ 0.01, ***P ≤ 0.001, ****P ≤ 0.0001).

PGC1α has been shown to have a compensatory effect in other tissues in Pgc1β KO mice[54]. We therefore investigated if reduced expression of PGC1β resulted in a compensatory increase in PGC1α in the human setting. PGC1α expression, which was undetectable in wildtype ortho/poly chromatic erythroblasts, was however not upregulated in response to reduced levels of PGC1β (data not shown), ruling out compensatory mechanisms between the two homologs in the erythroid compartment.

Being a coactivator of mitochondrial biogenesis, it could be expected that reduced expression of PGC1β would result in decreased expression of OXPHOS related genes and proteins. In contrast, mitochondrial biomass was increased in all BM derived erythroblast populations on day 14 as measured by MTDR. This is likely due to disrupted mitophagy. During terminal erythroid differentiation mitochondria undergo mitophagy leading to decreased MTDR intensity[14,55], which is also evident by our data, demonstrating a stepwise reduction of MFI in maturing erythroblasts in the control cells (Fig. S4B, SCR black bars). This is also in agreement with our data showing that the mitochondrial housekeeping protein TOM20 is present in polychromatic erythroblasts (Fig. 4G,H), but no longer detectable in orthochromatic erythroblasts (Fig. S4A). That PGC1β likely plays a functional role in mitochondrial clearance was further strengthened by that knock-down of PGC1β resulted in

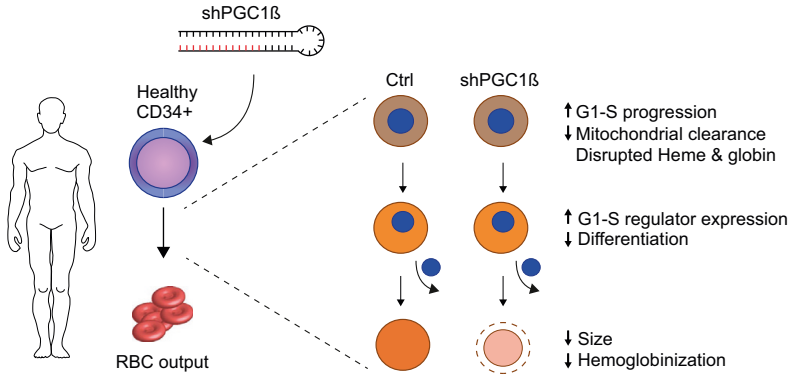

Figure 6. PGC1β is directly involved in mitochondrial clearance, production of hemoglobin and regulation of G1-S transition and is ultimately required for proper terminal erythroid differentiation.

retention of TOM20 expression in CB derived polychromatic progenitors compared to control (Fig. 4G,H). However, the fact that the same cell populations display reduced TMRE and MitoSox intensity in spite of increased mitochondrial cell mass, indicate that the retained mitochondria are not fully functional. We further demonstrate that knock-down of PGC1β results in significantly reduced enucleation in mature GPA$^+$ cells compared to control. Interestingly, it was recently shown that late-stage erythroblasts sustain mitochondrial metabolism and subsequent enucleation, and that metabolic fueling of mitochondria is critical for the erythroid enucleation process[56].

The perturbed formation of erythroid cells from BM was the most prominent during early differentiation, whereas the formation of mature reticulocytes was close to normalized by day 21 of culture. The recovery noted on day 21 indicate that PGC1β might be less important during the final maturation steps of adult erythropoiesis. It could however also be due to cell intrinsic attempts to compensate. For example, the decreased expression of heme-, globin- and some OXPHOS-related genes seen in response to PGC1β knock-down in polychromatic erythroblasts, was normalized or even increased in the more mature orthochromatic erythroblasts. Erythroid development from CB progenitors was even more affected by the decreased levels of PGC1β indicating that PGC1β plays a more prominent role during earlier ontogeny. In contrast to what was seen in adult erythroblasts, CB derived erythroblasts, displayed increase expression of heme- and globin related-genes. This could potentially be due to the retention of mitochondria, or a cell intrinsic attempt to compensate for deregulated heme-regulation at earlier stages of differentiation, as seen in BM.

Erythropoiesis is intimately coupled to cell cycle regulation, and erythroblasts undergo initial self-renewal divisions, followed by a series of quick divisions during terminal differentiation to give rise to the immense amounts of mature RBCs each day[57,58]. In addition to its more established role as regulator of mitochondrial biogenesis and energy metabolism, PGC1β has been implicated in cell cycle regulation of cancer cells[42]. Furthermore, we recently showed that enhanced Pgc1β expression alone was enough to normalize the disrupted expression of cell cycle related genes in pRb-deficient murine erythroblasts[21]. Here we show that multiple genes involved in G1 to S progression were greatly increased in response to PGC1β knock-down in both BM and CB derived erythroblasts, demonstrating a direct involvement of PGC1β in cell cycle regulation. While the total expression of *pRB*, a G1-S master regulator[59], was unchanged, *CDK2* that targets pRB for phosphorylation[60] was significantly increased. Hence, hyper-phosphorylation of pRB by CDK2 could potentially contribute to increased cell cycle progression in PGC1β-deficient cells. Furthermore, in line with a previous publication showing that erythroid precursors that undergo fewer cell divisions result in larger erythrocytes[47], we here demonstrate that increased cell cycle progression results in smaller reticulocytes.

The disrupted terminal erythroid differentiation with accumulations of polychromatic and orthochromatic erythroblasts that we see in response to decreased levels of PGC1β is reminiscent of the impaired terminal erythroid differentiation seen in MDS[27]. The majority of MDS patients are transfusion dependent, which negatively affect their quality of life, clinical outcome and correlates with increased risk of leukemic transformations[61–64]. A high frequency of acquired mutations in mitochondrial DNA has been reported in MDS patients[29]. For example, subtypes of MDS with somatic SF3B1 mutations are associated with downregulation of core mitochondrial pathways[30,31]. This includes deregulation of genes important for iron and heme homeostasis[31,65], suggesting that these biological processes could contribute to the disease phenotype. Notably, PGC1β is located within the commonly deleted region of chromosome 5 of the del(5q) subtype of MDS[66]. While the pathogenesis of del(5q) MDS has been attributed to heterozygous deletion of RPS14[67], it is unlikely that the full disease phenotype is caused by the loss of a single gene out of the 40 coding genes included in the commonly deleted region[66]. Patients with del(5q) MDS exhibit a similar inefficient erythropoiesis[68] to that described here, indicating that PGC1β deficiency potentially also contributes to the disease phenotype. In addition, reduced PGC1β expression result in disrupted heme and globin coordination, which is also reported in del(5q) MDS[68]. Furthermore, Lenalidomide, which is

used to treat del(5q) MDS patients[69], has been shown to also affect mitochondrial homeostasis[70]. However, further studies are needed to determine if disturbed PPAR-signaling is involved in MDS-related anemia pathogenesis.

Materials and methods

Human BM cells. Human bone marrow (BM) cells were supplied by Lonza or collected at the Hematology Department, University of Lund, Sweden. Informed consent was obtained from all participants. All work on BM samples was done according to ethical guidelines approved by the Institutional Review Board of the University of Lund and in accordance with the Declaration of Helsinki.

Vector design and transduction. Bacterial glycerol stocks with shPGC1β inserts from MISSION® sh3: TRCN0000008600 and sh5: TRCN0000429958 clones (Sigma Aldrich, St. Louis, MO, USA) or scrambled for control, as described in Supplemental Table 1, were cloned into pLKO lentiviral vector with eGFP reporter gene using NdeI and BamHI restriction enzymes. Control digestions on plasmid were done with NdeI and BamHI prior to sequencing. Cloned plasmids were sent with U6 FWD primer to Eurofins Scientific (Luxembourg) for plasmid sequence confirmation.

Approximately 100,000 $CD34^+$ cells were transduced with shPGC1β lentiviral vectors or scramble control vector in phase I medium (see below) supplemented with 0.4 µg/mL Protamine sulphate. Upon validation of different shPGC1β vectors, variance was observed in knock-down efficiency between transduction replicates of the same vector and donor. To ensure sufficient knock-down efficiency for all donor samples, more transductions were performed with the shPGC1β vectors as compared to the control Scramble vector. This was done to avoid losing biological replicates to inefficient transductions Transduced (GFP^+) $CD34^+$ (APC-eFluor780, Thermo Fisher Scientific, Waltham, MA, USA) cells were sorted into RLT buffer (1% β-mercaptoethanol) 48 h after transduction for analysis of PGC1β knockdown efficiency.

Erythroid culture. Transduced $CD34^+$ bone marrow cells (Lonza, Basel, Switzerland) were sorted 48 h post transduction on Aria III based on GFP and CD34 (4H-11, APC-eFluor780, Thermo Fisher Scientific) expression and cultured in a 3-phase erythroid culturing system; 5 days in phase 1 medium, consisting of SFEM supplemented with 1% penicillin streptomycin , 50 ng/ml SCF, 10 ng/ml IL-3, 50 ng/ml FLT3, 20 ng/ml TPO and 100 nM Dexamethasone, followed by 7 days in phase 2 medium (SFEM with 1% penicillin streptomycin, 50 ng/ml SCF, 10 ng/ml IL-3, 50 ng/ml, 2U/ml EPO and 100 nM Dexamethasone) for differentiation of erythroid committed progenitors. On Day 14 the medium was switched to phase 3 medium (SFEM with 1% penicillin streptomycin, 30% heat inactivated FBS and 3U/ml EPO) for terminal erythroid differentiation. Cells were collected on day 10, 14, 18 and 21 (BM) and day 10, 14 and 16 (CB) for morphologic and flow cytometric analysis. Cells collected on day 18 for BM and day 16 for CB were also sorted for RT-qPCR, Western analysis (CB) and cell cycle analysis (BM).

Erythroid colony formation assay. 1000 transduced $CD34^+$ cells were plated in MethoCult™ (H4230, Stemcell Technologies) supplemented with 20 ng/ml SCF, 10 ng/ml IL3, 50 ng/ml GM-CSF, 3U/ml EPO, incubated at 37 °C and 5% CO_2 and scored for CFU-E colonies after 14 days.

Morphologic scoring of diaminobenzidine (DAB) stained BM derived erythroid progenitors. Approximately 10,000–15,000 cells were spun down on cytospins slides and fixed with methanol at − 20 °C for 2 min. The slides were air-dried and stained with Diaminobenzidine hydrochloride (DAB) solution (10 mg/ml in PBS, Sigma Aldrich) including freshly added H_2O_2 (3 ppm, Sigma Aldrich). DAB solution was applied on the slides with the help of a PAP pen to cover all cells. The slides were washed with DH2O, stained with Giemsa (1:20 dilution in distilled water) for 15 min, wash with DH2O, and air-dried. 300 cells per transduction were visually scored into five different developmental stages based on known morphologic characteristics including presence and size of nucleus, hemoglobin content and general cell size, using an Olympus BX43 microscope (Olympus Corporation, Tokyo, Japan) and 40 × magnification. Apoptotic cell displaying blebbing and or fragmentation were excluded.

Cell area and hemoglobin stain intensity was scored using ImageJ[48,49] (v1.153c). For quantification of cell size, images were converted to grayscale by changing type to 8-bit and converted to binary format. Cell area was quantified using 'Analyze particles' with a threshold of 50–150 μm^2. For quantification of hemoglobin content, reticulocytes were marked with selection tool, followed by subtraction of noise, grayscale conversion and inversion of image. Reticulocytes were then analyzed for DAB color intensity by measuring integrated density. For more detail see Supplemental Methods.

Flow cytometric analysis. Cultured transduced cells were collected on days 10, 14, 18, 21 (BM) and days 10, 14, 16 (CB) for FACS analysis. The cells were washed with PBS (GE Healthcare Life Sciences) with 2% FCS (GE Healthcare Life Sciences) and stained with the cell surface markers GPA (GA-R2, BV421, BD), CD49d (9F10, PeCy7, BioLegend) and Band3 (Bric 6, PE/APC, IBGRL Research Products). Mitotracker Deep Red (50 nM, Thermo Fisher Scientific), TMRE (100 nM, Thermo Fisher Scientific) and MitoSox (250 nM, Thermo Fisher Scientific) was included to measure mitochondrial biomass, membrane potential and ROS production respectively. Nucleic Acid Stain Syto62 (25 nM) was included to assess enucleation. 7-Aminoactinomycin D (7-AAD, Sigma Aldrich) was used to exclude dead cells. Samples were analyzed and sorted on FACS Aria III, FACS Aria II and LSR Fortessa.

Cell cycle analysis. Since erythroid cells are sensitive to permeabilization and fixation, 200,000–400,000 polychromatic erythroblasts were sorted based on their GPA, CD49d and Band3 expression prior to fixation. Cell pellets were fixed with ice cold 70% Ethanol in PBS (GE Healthcare Life Sciences) while vortexing and incubated at − 20 °C overnight. Fixed cells were washed with PBS and stained with DAPI staining buffer (0.1% TritonX100 (Sigma Aldrich), 0.1% Sodium citrate (Sigma Aldrich), 10 µg/ml DAPI (Sigma Aldrich) for 30 min at 37 °C. DAPI intensity was analyzed individually in the sorted erythroid progenitor populations on LSR Fortessa (Becton Dickinson).

Gene expression. 5000–20,000 polychromatic ($Cd49d^+$, $Band3^-$) and orthochromatic ($Cd49d^+$, $Band3^+$) erythroid progenitors were sorted into RLT buffer (1% β-mercaptoethanol) and snap frozen. RNA was purified using RNeasy mini kit according to instructions (Qiagen) and cDNA was prepared using SuperScript IV reverse transcriptase (Thermo Fisher Scientific). RT-qPCR assays were performed according to the TaqMan Gene expression master mix protocol and pre-designed probe-based primers (Supplemental Table 2) (Integrated DNA Technologies, Coralville, IA USA and Thermo Fisher Scientific).

SDS-PAGE and immunoblotting. Whole cell lysates of transduced cord blood derived cells on day7 were used for analysis of knock-down efficiency, and GPA^+, $CD49d^+/Band3^-$ and $CD49d^+/Band3^+$ populations were sorted on day 16 for analysis of OXHPOS and cell cycle proteins. Sorted cells were prepared with RIPA lysis and extraction buffer (Fischer scientific). Protein concentration of lysates were quantified with Pierce™ BCA Protein Assay Kit (Thermo Fisher Scientific) and proteins were separated using NuPAGE® 4–12% Bis–Tris gels. Proteins were transferred to nitrocellulose membrane using Trans-Blot Turbo Transfer System (BioRad, Hercules, CA, USA). Immunoblotting was done with following antibodies and dilutions overnight at 4 °C: Rabbit Anti-PGC1 beta Ab (ab176328, 1:1000, Abcam, Cambridge UK), Rabbit Anti-NDUFA1 Ab (ab176563, 1:1000, Abcam), Mouse Anti-TOM20 Ab (sc-17764, 1:1000, Santa Cruz Biotechnology, Dallas, TX, USA) ,Mouse Anti-ALAS-E Ab (sc-166739, 1:1000, Santa Cruz Biotechnology), Mouse Anti-Ferrochelatase Ab (sc-377377, 1:1000, Santa Cruz Biotechnology) Rabbit Anti-ATP5S Ab (PA5-101443, 1:1000, Fisher Scientific), Mouse Anti-Actin (Ab-5, 1:1000, Biosciences), HRP coupled anti-rabbit IgG (NA9340-1ML, 1:5000, Cytiva), HRP coupled anti-mouse IgG (NA9310-1ML, 1:5000, Cytiva). Proteins of interest were exposed using Amersham ECL Prime Western Blotting Detection Reagent (Cytiva, Marlborough, MA, USA). Images were acquired by ChemiDoc™ Imaging Systems (Bio-Rad) and bands intensity were quantified with Image Lab software (v6.0, Bio-Rad).

Statistics. Statistical analysis was done using GraphPad Prism 8.00 or 9.00 (GraphPad Software, San Diego, CA USA). Significance was analyzed with 2way ANOVA test, corrected for multiple comparisons, using Sidak's or two-stage step-up method of Benjamini, Krieger and Yekutieli (False discovery rate), if not stated otherwise. Students paired t-test was used for analyzing RT-qPCR, Enucleation, DAB intensity and Cell size analyses, when only comparing two groups.

Received: 16 March 2021; Accepted: 10 August 2021
Published online: 24 August 2021

References

1. Palis, J. Primitive and definitive erythropoiesis in mammals. *Front. Physiol.* **5**, 3 (2014).
2. Hattangadi, S. M., Wong, P., Zhang, L., Flygare, J. & Lodish, H. F. From stem cell to red cell: Regulation of erythropoiesis at multiple levels by multiple proteins, RNAs, and chromatin modifications. *Blood* **118**(24), 6258–6268 (2011).
3. Singbrant, S. *et al.* Erythropoietin couples erythropoiesis, B-lymphopoiesis, and bone homeostasis within the bone marrow microenvironment. *Blood* **117**(21), 5631–5642 (2011).
4. Koury, M. J. & Bondurant, M. C. Maintenance by erythropoietin of viability and maturation of murine erythroid precursor cells. *J. Cell Physiol.* **137**(1), 65–74 (1988).
5. Kelley, L. L. *et al.* Apoptosis in erythroid progenitors deprived of erythropoietin occurs during the G1 and S phases of the cell cycle without growth arrest or stabilization of wild-type p53. *Mol. Cell Biol.* **14**(6), 4183–4192 (1994).
6. An, X., Schulz, V. P., Mohandas, N. & Gallagher, P. G. Human and murine erythropoiesis. *Curr. Opin. Hematol.* **22**(3), 206–211 (2015).
7. Chen, K. *et al.* Resolving the distinct stages in erythroid differentiation based on dynamic changes in membrane protein expression during erythropoiesis. *Proc. Natl. Acad. Sci. USA* **106**(41), 17413–17418 (2009).
8. Liu, X. *et al.* Regulation of mitochondrial biogenesis in erythropoiesis by mTORC1-mediated protein translation. *Nat. Cell Biol.* **19**(6), 626–638 (2017).
9. Fontenay, M., Cathelin, S., Amiot, M., Gyan, E. & Solary, E. Mitochondria in hematopoiesis and hematological diseases. *Oncogene* **25**(34), 4757–4767 (2006).
10. Zhang, S. *et al.* HRI coordinates translation necessary for protein homeostasis and mitochondrial function in erythropoiesis. *Elife* **8**, 1–10 (2019).
11. Jensen, E. L. *et al.* Copper deficiency-induced anemia is caused by a mitochondrial metabolic reprograming in erythropoietic cells. *Metallomics* **11**(2), 282–290 (2019).
12. Papaemmanuil, E. *et al.* Somatic SF3B1 mutation in myelodysplasia with ring sideroblasts. *N. Engl. J. Med.* **365**(15), 1384–1395 (2011).
13. Gonzalez-Menendez, P. *et al.* An IDH1-vitamin C crosstalk drives human erythroid development by inhibiting pro-oxidant mitochondrial metabolism. *Cell Rep.* **34**(5), 108723 (2021).
14. Moras, M. *et al.* Human erythroid differentiation requires VDAC1-mediated mitochondrial clearance. *Haematologica* (2021).
15. Moras, M. *et al.* Downregulation of mitochondrial TSPO inhibits mitophagy and reduces enucleation during human terminal erythropoiesis. *Int. J. Mol. Sci.* **21**, 23 (2020).

16. Finck, B. N. & Kelly, D. P. PGC-1 coactivators: Inducible regulators of energy metabolism in health and disease. *J. Clin. Invest.* **116**(3), 615–622 (2006).
17. Puigserver, P. *et al.* A cold-inducible coactivator of nuclear receptors linked to adaptive thermogenesis. *Cell* **92**(6), 829–839 (1998).
18. Nicholls, D., Cunningham, S. & Wiesinger, H. Mechanisms of thermogenesis in brown adipose tissue. *Biochem. Soc. Trans.* **14**(2), 223–225 (1986).
19. Lin, J., Puigserver, P., Donovan, J., Tarr, P. & Spiegelman, B. M. Peroxisome proliferator-activated receptor gamma coactivator 1beta (PGC-1beta), a novel PGC-1-related transcription coactivator associated with host cell factor. *J. Biol. Chem.* **277**(3), 1645–1648 (2002).
20. Kressler, D., Schreiber, S. N., Knutti, D. & Kralli, A. The PGC-1-related protein PERC is a selective coactivator of estrogen receptor alpha. *J. Biol. Chem.* **277**(16), 13918–13925 (2002).
21. Sen, T. *et al.* Enhancing mitochondrial function in vivo rescues MDS-like anemia induced by pRb deficiency. *Exp. Hematol.* **88**, 28–41 (2020).
22. Lehman, J. J. *et al.* Peroxisome proliferator-activated receptor gamma coactivator-1 promotes cardiac mitochondrial biogenesis. *J. Clin. Invest.* **106**(7), 847–856 (2000).
23. St-Pierre, J. *et al.* Bioenergetic analysis of peroxisome proliferator-activated receptor gamma coactivators 1alpha and 1beta (PGC-1alpha and PGC-1beta) in muscle cells. *J. Biol. Chem.* **278**(29), 26597–26603 (2003).
24. Wu, Z. *et al.* Mechanisms controlling mitochondrial biogenesis and respiration through the thermogenic coactivator PGC-1. *Cell* **98**(1), 115–124 (1999).
25. Spiegelman, B. M., Puigserver, P. & Wu, Z. Regulation of adipogenesis and energy balance by PPARgamma and PGC-1. *Int. J. Obes. Relat. Metab. Disord.* **24**(Suppl 4), S8-10 (2000).
26. Cui, S. *et al.* PGC-1 coactivator activity is required for murine erythropoiesis. *Mol. Cell Biol.* **34**(11), 1956–1965 (2014).
27. Ali, A. M. *et al.* Severely impaired terminal erythroid differentiation as an independent prognostic marker in myelodysplastic syndromes. *Blood Adv.* **2**(12), 1393–1402 (2018).
28. Giagounidis, A. A., Germing, U. & Aul, C. Biological and prognostic significance of chromosome 5q deletions in myeloid malignancies. *Clin. Cancer Res.* **12**(1), 5–10 (2006).
29. Wulfert, M. *et al.* Analysis of mitochondrial DNA in 104 patients with myelodysplastic syndromes. *Exp. Hematol.* **36**(5), 577–586 (2008).
30. Nikpour, M. *et al.* Gene expression profiling of erythroblasts from refractory anaemia with ring sideroblasts (RARS) and effects of G-CSF. *Br. J. Haematol.* **149**(6), 844–854 (2010).
31. Conte, S. *et al.* Aberrant splicing of genes involved in haemoglobin synthesis and impaired terminal erythroid maturation in SF3B1 mutated refractory anaemia with ring sideroblasts. *Br. J. Haematol.* **171**(4), 478–490 (2015).
32. Hu, J. *et al.* Isolation and functional characterization of human erythroblasts at distinct stages: Implications for understanding of normal and disordered erythropoiesis in vivo. *Blood* **121**(16), 3246–3253 (2013).
33. Yan, H. *et al.* Developmental differences between neonatal and adult human erythropoiesis. *Am. J. Hematol.* **93**(4), 494–503 (2018).
34. Fontanesi, F., Soto, I. C., Horn, D. & Barrientos, A. Assembly of mitochondrial cytochrome c-oxidase, a complicated and highly regulated cellular process. *Am. J. Physiol. Cell Physiol.* **291**(6), C1129–C1147 (2006).
35. Bezawork-Geleta, A., Rohlena, J., Dong, L., Pacak, K. & Neuzil, J. Mitochondrial complex II: At the crossroads. *Trends Biochem. Sci.* **42**(4), 312–325 (2017).
36. Au, H. C., Seo, B. B., Matsuno-Yagi, A., Yagi, T. & Scheffler, I. E. The NDUFA1 gene product (MWFE protein) is essential for activity of complex I in mammalian mitochondria. *Proc. Natl. Acad. Sci. USA.* **96**(8), 4354–4359 (1999).
37. Belogrudov, G. I. & Hatefi, Y. Factor B and the mitochondrial ATP synthase complex. *J. Biol. Chem.* **277**(8), 6097–6103 (2002).
38. Yien, Y. Y. *et al.* TMEM14C is required for erythroid mitochondrial heme metabolism. *J. Clin. Invest.* **124**(10), 4294–4304 (2014).
39. Ajioka, R. S., Phillips, J. D. & Kushner, J. P. Biosynthesis of heme in mammals. *Biochim. Biophys. Acta.* **1763**(7), 723–736 (2006).
40. Maio, N., Kim, K. S., Holmes-Hampton, G., Singh, A. & Rouault, T. A. Dimeric ferrochelatase bridges ABCB7 and ABCB10 homodimers in an architecturally defined molecular complex required for heme biosynthesis. *Haematologica* **104**(9), 1756–1767 (2019).
41. Hansen, J. B. *et al.* Activation of peroxisome proliferator-activated receptor gamma bypasses the function of the retinoblastoma protein in adipocyte differentiation. *J. Biol. Chem.* **274**(4), 2386–2393 (1999).
42. Lin, M. S., Chen, W. C., Bai, X. & Wang, Y. D. Activation of peroxisome proliferator-activated receptor gamma inhibits cell growth via apoptosis and arrest of the cell cycle in human colorectal cancer. *J. Dig. Dis.* **8**(2), 82–88 (2007).
43. Li, J. *et al.* Synergistic function of E2F7 and E2F8 is essential for cell survival and embryonic development. *Dev. Cell.* **14**(1), 62–75 (2008).
44. Berthet, C. *et al.* Combined loss of Cdk2 and Cdk4 results in embryonic lethality and Rb hypophosphorylation. *Dev. Cell.* **10**(5), 563–573 (2006).
45. Geng, Y. *et al.* Cyclin E ablation in the mouse. *Cell* **114**(4), 431–443 (2003).
46. De Bruyn, C., Delforge, A., Lagneaux, L. & Bron, D. Characterization of $CD34^+$ subsets derived from bone marrow, umbilical cord blood and mobilized peripheral blood after stem cell factor and interleukin 3 stimulation. *Bone Marrow Transplant.* **25**(4), 377–383 (2000).
47. Sankaran, V. G. *et al.* Cyclin D3 coordinates the cell cycle during differentiation to regulate erythrocyte size and number. *Genes Dev.* **26**(18), 2075–2087 (2012).
48. Schindelin, J. *et al.* Fiji: An open-source platform for biological-image analysis. *Nat. Methods.* **9**(7), 676–682 (2012).
49. Schneider, C. A., Rasband, W. S. & Eliceiri, K. W. NIH Image to ImageJ: 25 years of image analysis. *Nat. Methods.* **9**(7), 671–675 (2012).
50. Gnanapragasam, M. N. *et al.* EKLF/KLF1-regulated cell cycle exit is essential for erythroblast enucleation. *Blood* **128**(12), 1631–1641 (2016).
51. Moras, M., Lefevre, S. D. & Ostuni, M. A. From erythroblasts to mature red blood cells: Organelle clearance in mammals. *Front. Physiol.* **8**, 1076 (2017).
52. Testa, U. Apoptotic mechanisms in the control of erythropoiesis. *Leukemia* **18**(7), 1176–1199 (2004).
53. Ganz, T. & Nemeth, E. Iron metabolism: Interactions with normal and disordered erythropoiesis. *Cold Spring Harb. Perspect Med.* **2**(5), 011668 (2012).
54. Sonoda, J., Mehl, I. R., Chong, L. W., Nofsinger, R. R. & Evans, R. M. PGC-1beta controls mitochondrial metabolism to modulate circadian activity, adaptive thermogenesis, and hepatic steatosis. *Proc. Natl. Acad. Sci. USA.* **104**(12), 5223–5228 (2007).
55. Mauro-Lizcano, M. *et al.* New method to assess mitophagy flux by flow cytometry. *Autophagy* **11**(5), 833–843 (2015).
56. Liang, R. *et al.* Mitochondrial localization and moderated activity are key to murine erythroid enucleation. *Blood Adv.* **5**(10), 2490–2504 (2021).
57. von Lindern, M. *et al.* Leukemic transformation of normal murine erythroid progenitors: V- and c-ErbB act through signaling pathways activated by the EpoR and c-Kit in stress erythropoiesis. *Oncogene* **20**(28), 3651–3664 (2001).
58. Pop, R. *et al.* A key commitment step in erythropoiesis is synchronized with the cell cycle clock through mutual inhibition between PU.1 and S-phase progression. *PLoS Biol.* **8**(9), e1000484 (2010).
59. Classon, M. & Harlow, E. The retinoblastoma tumour suppressor in development and cancer. *Nat. Rev. Cancer.* **2**(12), 910–917 (2002).

60. Foster, J. S., Henley, D. C., Bukovsky, A., Seth, P. & Wimalasena, J. Multifaceted regulation of cell cycle progression by estrogen: Regulation of Cdk inhibitors and Cdc25A independent of cyclin D1-Cdk4 function. *Mol. Cell Biol.* **21**(3), 794–810 (2001).
61. Ryblom, H., Hast, R., Hellstrom-Lindberg, E., Winterling, J. & Johansson, E. Self-perception of symptoms of anemia and fatigue before and after blood transfusions in patients with myelodysplastic syndromes. *Eur. J. Oncol. Nurs.* **19**(2), 99–106 (2015).
62. Hellstrom-Lindberg, E. & van de Loosdrecht, A. Erythropoiesis stimulating agents and other growth factors in low-risk MDS. *Best Pract Res Clin Haematol.* **26**(4), 401–410 (2013).
63. Kao, J. M., McMillan, A. & Greenberg, P. L. International MDS risk analysis workshop (IMRAW)/IPSS reanalyzed: Impact of cytopenias on clinical outcomes in myelodysplastic syndromes. *Am. J. Hematol.* **83**(10), 765–770 (2008).
64. Balducci, L. Transfusion independence in patients with myelodysplastic syndromes: Impact on outcomes and quality of life. *Cancer* **106**(10), 2087–2094 (2006).
65. Malcovati, L. *et al.* SF3B1 mutation identifies a distinct subset of myelodysplastic syndrome with ring sideroblasts. *Blood* **126**(2), 233–241 (2015).
66. Jadersten, M. & Karsan, A. Clonal evolution in myelodysplastic syndromes with isolated del(5q): The importance of genetic monitoring. *Haematologica* **96**(2), 177–180 (2011).
67. Schneider, R. K. *et al.* Rps14 haploinsufficiency causes a block in erythroid differentiation mediated by S100A8 and S100A9. *Nat. Med.* **22**(3), 288–297 (2016).
68. Yang, Z. *et al.* Delayed globin synthesis leads to excess heme and the macrocytic anemia of Diamond Blackfan anemia and del(5q) myelodysplastic syndrome. *Sci. Transl. Med.* **8**(338), 338–367 (2016).
69. Talati, C., Sallman, D. & List, A. Lenalidomide: Myelodysplastic syndromes with del(5q) and beyond. *Semin. Hematol.* **54**(3), 159–166 (2017).
70. Pearson, G. & Soleimanpour, S. A. A ubiquitin-dependent mitophagy complex maintains mitochondrial function and insulin secretion in beta cells. *Autophagy* **14**(7), 1160–1161 (2018).

Acknowledgements
We are grateful to project students Kristina Munke and Mathilda Wessman for laboratory assistance during initial pilot experiments of this study, and to Dr. Abdul Ghani Alattar and Dr. Carl Walkley for intellectual input. This research was supported by the Swedish Society for Medical Research (fellowship SS), the Crafoordska Foundation (Grant No. 20170902), the Åke Wiberg Foundation (Grant No. M17/0252), the Clas Groschinsky's Memory Foundation (Grant No. M1789), the Gunnar Nilsson Cancer Foundation (Grant No. GN-2017-38), the Royal Physiographic Society of Lund, and the Harald & Greta Jeansson Foundation (SS).

Author contributions
T.S. and S.S. conceived the study, T.S. and S.S. designed experiments, T.S. and J.C. performed experiments and T.S. and S.S. analyzed data, T.S. and S.S. wrote the manuscript, and all authors have commented on the final draft.

Funding
Open access funding provided by Lund University.

Competing interests
The authors declare no competing interests.

Additional information
Supplementary Information The online version contains supplementary material available at https://doi.org/10.1038/s41598-021-96585-0.

Correspondence and requests for materials should be addressed to S.S.

Reprints and permissions information is available at www.nature.com/reprints.

Publisher's note Springer Nature remains neutral with regard to jurisdictional claims in published maps and institutional affiliations.

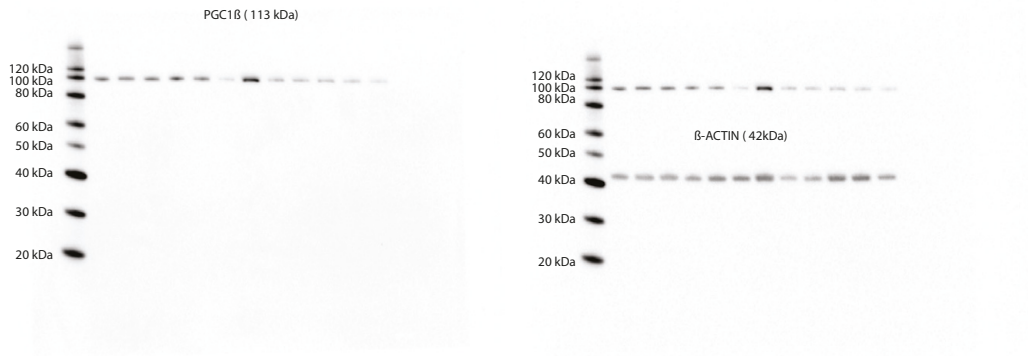

Figure S1. Full size blot images used in Figure 1 to determine PGC1ß knock-down efficiency. Anti-PGC1ß immunoblotting (left) was done prior to immunoblotting with Anti-ß-ACTIN (right).

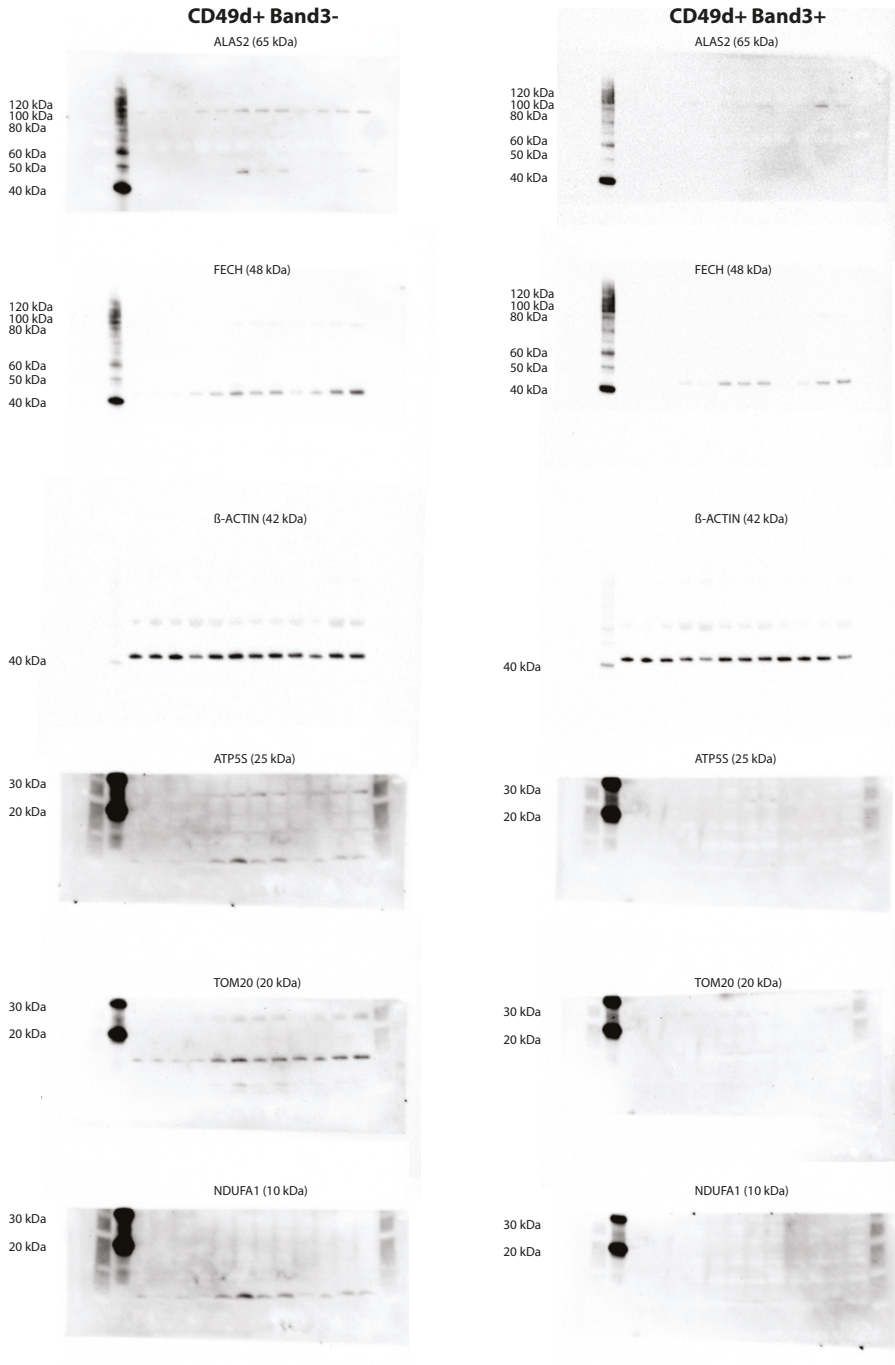

Figure S2. Full size blot images of the OXPHOS and heme realted proteins used in Figure 4 and Figure S1. CD49d+ Band3- (polychromatic erythroblasts, left) and CD49d+ Band3+(orthochromatic erythroblats, right) sorted at day 16 of differentiation. Blots were cut at 35kDa and stained with different antibodies. ALAS2 (65kDa) specific bands appear at 120 kDa, likely due to protein dimers.

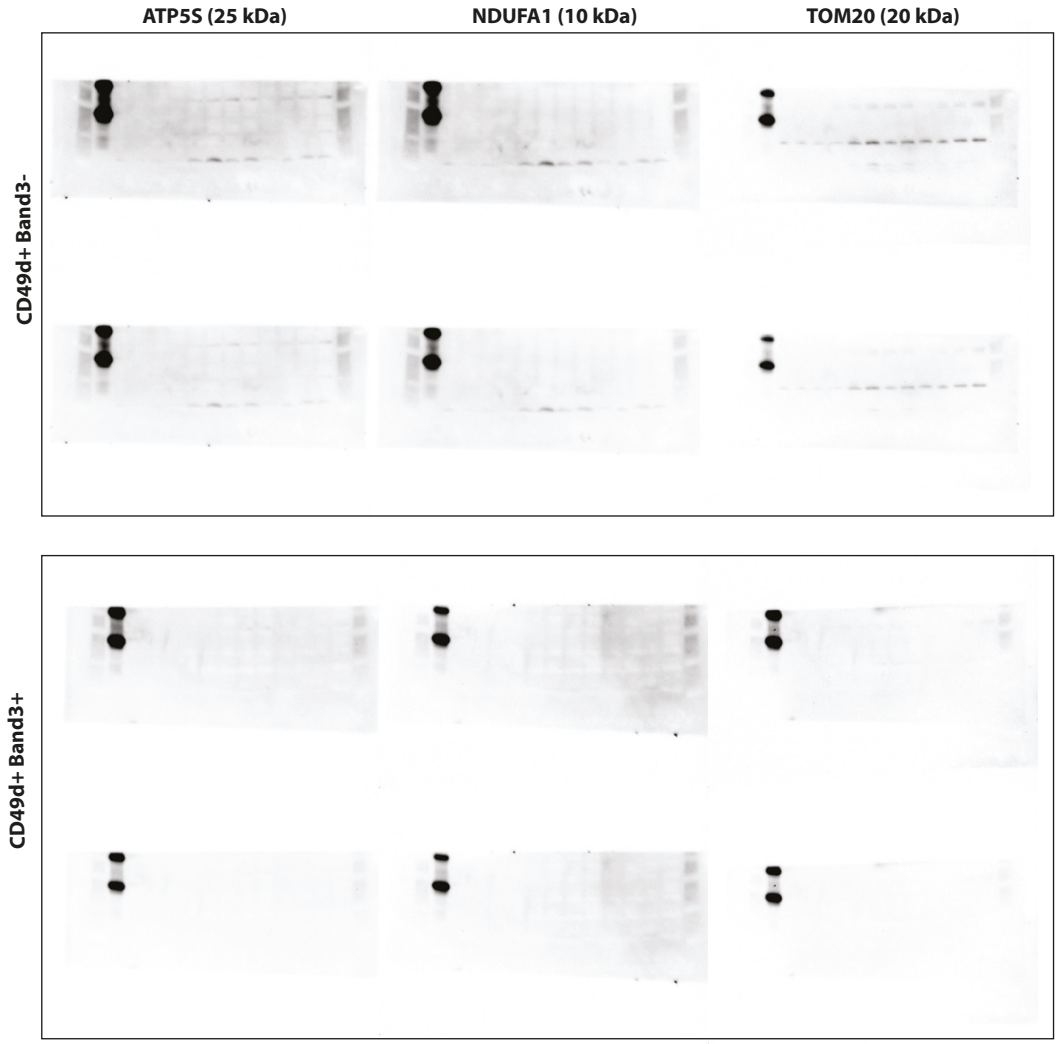

Figure S3. Full size blot images of the OXPHOS realted proteins with 2 additional lower exposed images (compared to Figure 4 and Figure S1). Due to higher contrast on ATP5S, TOM20 and NDUFA blots in figure 4G we include here same blots with lower exposure to compliment the high contrast images in Figure 4G.

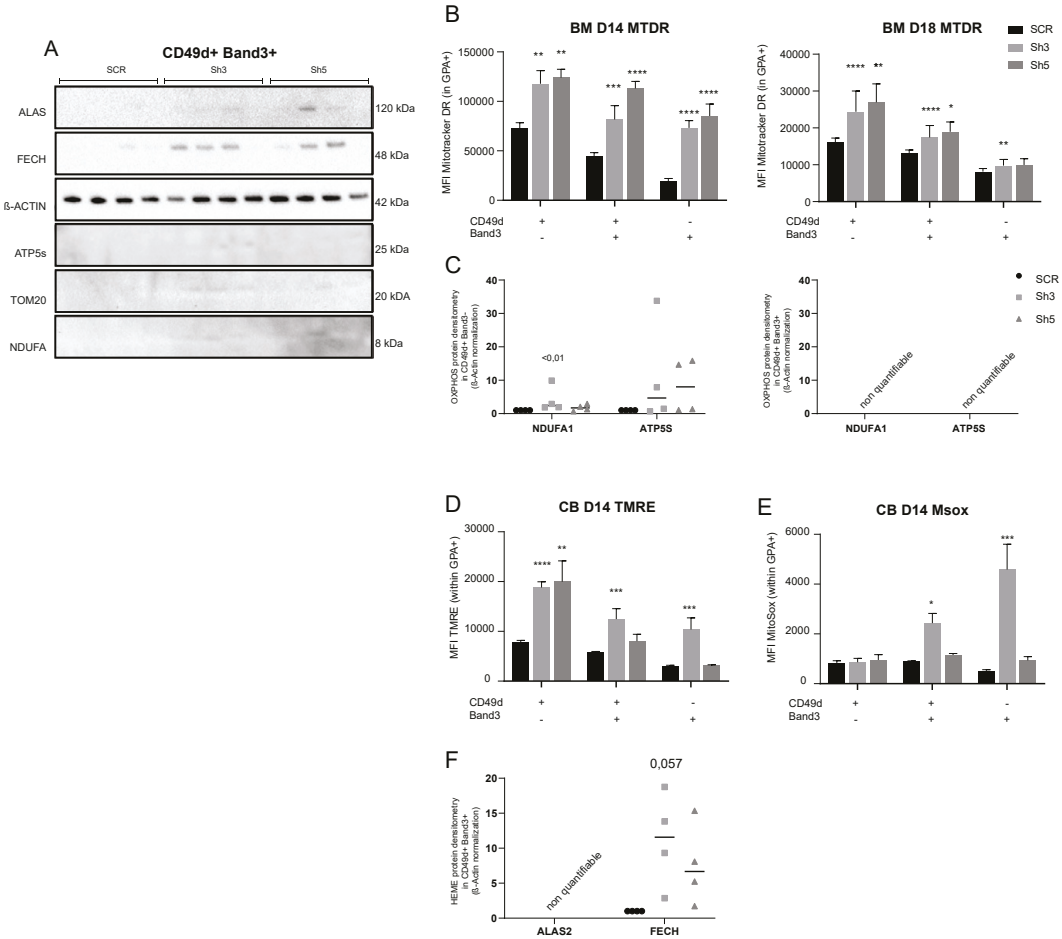

Figure S4. PGC1ß knock-down reults in retained mitochondrial biomass and increased activity on day 14. A) Mitochondria related protein levels are close to non-detectable on day 16 , in CB derived orthochromatic erythroblasts, as analayzed by western blot (n=4). **B)** Quantification of mitochondrial biomass using Mitotracker Deep Red at day 14 (left) and 18 (right) in bone marrow derived erythroid progenitors (n= SCR:4, Sh3:12, Sh5:6). **C)** Western blot quantification of OXPHOS related ATP5S and NDUFA1 normalized to ß-ACTIN in polychromatic erythroblasts (left). Bands too faint to quantify protein in orthochromatic erythroblasts (right) , SCR arbitrarily set to "1", data shown as median (n=4). **D)** Quantification of mitochondrial membrane potential using TMRE on day 14 in CB derived erythroid progenitors (n=4). **E)** Quantification of mitochondrial ROS using MitoSox on day 14 in CB derived erythroid progenitors (n=4). **F)** Western blot quantification of heme related ALAS2 and FECH normalized to ß-ACTIN on day 16 in orthochromatic erythroblasts, SCR arbitrarily set to "1", data shown as median (n=4). Data is presented as mean ± SEM (*P ≤ 0.05, **P ≤ 0.01, ***P ≤ 0.001, ****P ≤ 0.0001).

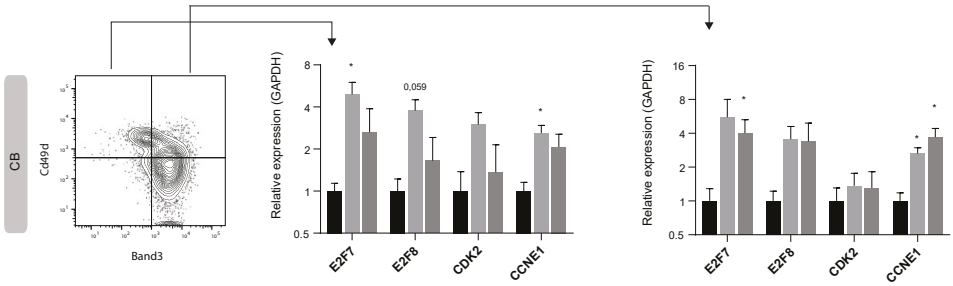

Figure S5. PGC1ß knock-down reults in increased expression of cell cycle regulating genes in CB derived eryhtroid progenitors.
Representative plot of SCR transduced cells indicating populations analyzed for gene expression of cell cycle related genes involved in G1 to S phase progression. Quantification of expression relative to GAPDH on day 16 of polychromatic erythroblasts (left) and orthochromatic erythroblasts (right) (n=4) Data is presented as mean ± SEM (*P ≤ 0.05).

Sen et al Supplemental tables

Supplemental table 1. shRNA's used for the knockdown of PGC1B.
TRC number for specfic shPGC1B clones with corresponding shRNA sequence.

sh#	Clones	Sequence
sh3	TRCN0000008600	CCGGGCATAGTCTAGGCAAAGAAATCTCGAGATTTCTTTGCCTAGACTATGCTTTTT
sh5	TRCN0000429958	CCGGAGCAACTCTATGCTGACTTTCCTCGAGGAAAGTCAGCATAGAGTTGCTTTTTTTG
SCR	Control	CCGGCAACAAGATGAAGAGCACCAACTCGAGTTGGTGCTCTTCATCTTGTTGTTTTT

Supplemental table 2. Primers from IDT and TaqMan, used for RT-qPCR assays.
Included assay names are specific to manufacturer predesigned primers.

Gene	Assay name	Manufacturer
GAPDH	Hs.PT.39a.22214836	IDT
PPARGC1B	Hs.PT.58.38577994	IDT
PPARGC1A	Hs.PT.58.14965839	IDT
COX7B	Hs.PT.58.27185131	IDT
SDHB	Hs.PT.58.39555113	IDT
NDUFA1	Hs.PT.58.20113449	IDT
ATP5S	Hs.PT.58.25982660	IDT
TMEM14C	Hs.PT.58.1926884	IDT
ALAS2	Hs.PT.56a.1433425.g	IDT
ABCB7	Hs.PT.58.2334204	IDT
FECH	Hs.PT.58.25999059	IDT
E2F7	Hs.PT.58.39751342	IDT
E2F8	Hs.PT.58.22500779	IDT
CDK2	Hs.PT.58.302089	IDT
CCNE1	Hs.PT.56a.27776605	IDT
RB1	Hs.PT.58.785814	IDT
HBA	Hs00361191_g1	TaqMan
HBB	Hs00758889_s1	TaqMan

Supplemental Methods

Morphologic scoring DAB stained slides

Cytospin slides were visually scored with Olympus BX43 microscope (Olympus Corporation, Tokyo, Japan), using 40x magnification, into five different developmental stages based on presence and size of nucleus, hemoglobin content and general cell size. Apoptotic cell displaying blebbing and or fragmentation were excluded. 300 cells were counted and scored based on known morphologic characteristics.

Cell size and hemoglobin stain intensity was scored using ImageJ (v1.153c). Scale was set to 8.55pixels/µm using in figure scale bar from ImageView software (v 3.7, YSC Technologies, Fremont CA, USA). Nucleated cells were manually excluded. For quantification of cell size, images were converted to grayscale by changing type to 8-bit and further converted to binary format. Cell size was quantified using 'Analyze particles' with a size threshold of 50-150µm^2 and unadjusted circularity (0.00-1.00). At least 20 intact reticulocytes were scored per transduction.

For quantification of hemoglobin content, at least 20 intact reticulocytes were manually selected with multi-point tool per transduction, followed by subtraction of image noise, grayscale conversion and inversion of image. Inversion is done to avoid white background giving highest intensity. Reticulocytes were then analyzed for DAB color intensity by measuring mean grey value.

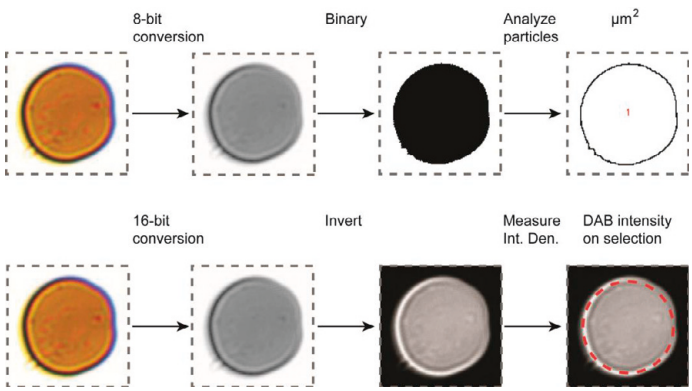

Paper III

scientific reports

Check for updates

OPEN

Yippee like 4 (*Ypel4*) is essential for normal mouse red blood cell membrane integrity

Alexander Mattebo[1], Taha Sen[1], Maria Jassinskaja[2], Kristýna Pimková[2], Isabel Prieto González-Albo[1], Abdul Ghani Alattar[1], Ramprasad Ramakrishnan[3], Stefan Lang[2], Marcus Järås[3], Jenny Hansson[2], Shamit Soneji[2], Sofie Singbrant[1], Emile van den Akker[4] & Johan Flygare[1]✉

The YPEL family genes are highly conserved across a diverse range of eukaryotic organisms and thus potentially involved in essential cellular processes. *Ypel4*, one of five YPEL family gene orthologs in mouse and human, is highly and specifically expressed in late terminal erythroid differentiation (TED). In this study, we investigated the role of *Ypel4* in murine erythropoiesis, providing for the first time an in-depth description of a *Ypel4*-null phenotype in vivo. We demonstrated that the *Ypel4*-null mice displayed a secondary polycythemia with macro- and reticulocytosis. While lack of *Ypel4* did not affect steady-state TED in the bone marrow or spleen, the anemia-recovering capacity of *Ypel4*-null cells was diminished. Furthermore, *Ypel4*-null red blood cells (RBC) were cleared from the circulation at an increased rate, demonstrating an intrinsic defect of RBCs. Scanning electron micrographs revealed an ovalocytic morphology of *Ypel4*-null RBCs and functional testing confirmed reduced deformability. Even though Band 3 protein levels were shown to be reduced in *Ypel4*-null RBC membranes, we could not find support for a physical interaction between YPEL4 and the Band 3 protein. In conclusion, our findings provide crucial insights into the role of *Ypel4* in preserving normal red cell membrane integrity.

The YPEL (Yippee like) family genes were discovered in 2001 when orthologs to the *Drosophila Yippee* gene were identified in a diverse range of eukaryotic organisms[1,2]. Interaction experiments, cloning and sequence analysis of *Yippee* revealed a putative zinc binding RING finger protein with self-interacting properties[1]. The earliest designated human gene ortholog *YPEL1*, "Yippee like 1", was in comparative analysis found to have four paralogs in the human genome, subsequently named *YPEL2-5*. Mouse gene orthologs (*Ypel1* through *Ypel5*) were also identified with 99.2–100% similarity. Further analysis identified 100 YPEL family genes from 68 species, including mammal, bird, fish, insect and fungus. High homology was detected in all species and a consensus sequence was designated as the Yippee domain[3]. Several studies have implicated localization of the YPEL family proteins to nuclear and perinuclear structures such as the centrosome and mitotic spindle, but also to microtubules[3–5]. Functionally, a common molecular function has not been demonstrated, but studies using reverse genetics approaches have shown effects on proliferation, apoptosis, senescence, cell adhesion and migration[2,5–9]. Most published studies to date have been performed in vitro with cell lines, thereby potentially missing relevant physiological features crucial to the understanding of a common molecular function.

The *Ypel4/YPEL4* gene has been reported to be highly upregulated during terminal erythroid differentiation (TED) in both murine and human erythropoiesis[10–12], reaching exceptionally high expression levels when compared to other tissues[13]. Erythropoiesis is a tightly regulated process in which red blood cells (RBC) are produced from hematopoietic stem cells (HSC), through a multistep cellular differentiation program involving several intermediate progenitor cells[14,15]. Briefly, rapidly dividing erythroid-restricted progenitors[16–18] mature, become erythropoietin (EPO)-dependent and upregulate the transferrin receptor CD71. This maturation step initiates TED by synchronization of cell cycle to differentiation, in which each division generates two daughter cells with distinct morphologies, transcriptomes and proteomes[11,12,19,20]. The locking of cell cycle to terminal

[1]Division of Molecular Medicine and Gene Therapy, Lund Stem Cell Center, Lund University, Lund, Sweden. [2]Division of Molecular Hematology, Lund Stem Cell Center, Lund University, Lund, Sweden. [3]Division of Clinical Genetics, Faculty of Medicine, Lund University, Lund, Sweden. [4]Sanquin Research, Department of Hematopoiesis and Landsteiner Laboratory, Amsterdam UMC, University of Amsterdam, Amsterdam, The Netherlands. ✉email: johan.flygare@med.lu.se

differentiation allows for timely expression of erythroid genes in a chronological manner and explains the stepwise acquisition of RBC characteristics such as reduction of cell size, hemoglobinization, synthesis and assembly of red cell membrane components as well as end stage enucleation[21].

Two decades into YPEL family gene-related research, more studies are still needed to highlight the roles of these genes in different biological processes. *Ypel4* has been shown to be a promising gene to study in murine erythropoiesis. Due to this fact and the complex nature of RBC physiology, we hypothesized that *Ypel4* loss-of-function in vivo would generate a phenotype that could elucidate the role of *Ypel4* in RBC-related cellular processes. To evaluate this assumption, we utilized the advantages of reverse genetics techniques and acquired a conventional knockout mouse model[22]. We showed that *Ypel4*-null mice displayed a secondary polycythemia due to an increased clearance of circulating RBCs. Furthermore, *Ypel4*-null RBCs had an ovalocytic morphology and reduced deformability. Band 3 protein levels were slightly reduced in RBC membranes, providing support for a mild red cell membrane disorder in the *Ypel4*-null mice. In conclusion, we for the first time identify *Ypel4* as a regulator of RBC morphology and red cell membrane protein composition.

Results

Disruption of the *Ypel4* gene results in a macrocytic secondary polycythemia. To study how *Ypel4* affects erythropoiesis, we obtained a conventional knockout mouse model in which a targeted trap allele disrupts transcription of the protein-coding exons (Fig. 1A). The genotype was verified by PCR using primer combinations for allele-specific amplification (Supplementary Figure S1A). The *Ypel4*-null allele (–) was validated by RNA sequencing (Supplementary Figure S1B).

Ypel4-null (–/–) mice were born viable in Mendelian ratio, demonstrating that *Ypel4* is not essential for embryonic development (Fig. 1B, $p = 0.74$).

Peripheral blood (PB) from wild-type (+/+) and *Ypel4*-null mice was analyzed and blood values quantified in a hematology analyzer. *Ypel4*-null mice displayed a significant increase in hematocrit (HCT) (Fig. 1C) but not in hemoglobin concentration (HGB) or red blood cell count (RBC) (Fig. 1D,E). This was accompanied with a significant increase in mean corpuscular volume (MCV) (Fig. 1F), while mean corpuscular hemoglobin (MHC) (Fig. 1G) and mean corpuscular hemoglobin concentration (MCHC) (Fig. 1H) remained unaltered. Neither white blood cell count (WBC) (Supplementary Figure S1C) nor platelet count (Supplementary Figure S1D) was significantly changed.

To evaluate the characteristics of the observed macrocytosis, the RBC distribution width (RDW-SD) and reticulocyte count were measured using a hematology analyzer and flow cytometer, respectively. A trend towards relative anisocytosis, i.e. unequally sized RBCs, was observed in *Ypel4*-null mice (Fig. 1I), together with a slight but significant reticulocytosis (Fig. 1J).

To determine if the detected polycythemia, i.e. increase in HCT, and reticulocytosis had a primary or secondary cause, serum EPO concentration was measured using ELISA. Serum EPO concentration was significantly increased in *Ypel4*-null mice (Fig. 1K).

Taken together, our data demonstrates that the *Ypel4*-null mice disrupts transcription of the *Ypel4* gene, and that this disruption leads to a macrocytic secondary polycythemia.

***Ypel4* is upregulated during terminal erythropoiesis but deficiency does not affect normal erythroid precursor functionality in bone marrow.** To determine the cause of the peripheral blood phenotype, steady-state erythropoiesis in the bone marrow was examined using fluorescent activated cell sorting (FACS) and antibodies against the erythroid-specific marker Ter119. Inclusion of anti-CD44 antibodies allows for further subfractionation of the Ter119+ cells into proerythroblasts (Pro-E), basophilic erythroblasts (Baso-E), polychromatic erythroblasts (Poly-E), orthochromatic erythroblasts (Ortho-E), reticulocytes (Retics) and RBCs[23]. Within those populations, cell size, enucleation efficiency and cell cycle differences were analyzed (Fig. 2A).

Transcriptional analysis of the different Ter119+ subpopulations using FACS and qPCR revealed that *Ypel4* expression increased markedly by differentiation to peak in the Ortho-E population before enucleation. *Ypel4* mRNA was not detected in *Ypel4*-null populations (Fig. 2B).

In spite of being highly expressed during terminal erythropoiesis, total Ter119+ erythroid fraction in *Ypel4*-null bone marrow was not significantly different when quantified by flow cytometry (Fig. 2C). Neither could any significant differences in subpopulation frequencies within this fraction be detected (Fig. 2D). This was further confirmed with morphologic analysis of sorted erythroblast subpopulations stained with May-Grünwald-Giemsa (MGG) (Supplementary Figure S2A).

To analyze if *Ypel4*-deficiency affected normal erythroid precursor functionality, flow cytometry-based analyses to assess cell size, enucleation efficiency and cell cycle differences was carried out. Differences in cell size was analyzed by comparing the mean fluorescent intensity (MFI) of the forward scatter area (FSC-A) within the *Ypel4*-expressing Ter119+ subpopulations and RBCs. In spite of the observed macrocytosis in PB, no significant differences were detected between the compared groups (Fig. 2E). Neither could any differences be detected in the earlier erythroblast populations (Supplementary Figure S2B). Enucleation efficiency was analyzed by measuring positivity of a cell-permeant DNA dye (Hoechst 33342) in the reticulocyte and RBC populations. None of the compared groups displayed significant differences in enucleation rates (Fig. 2F). Cell cycle differences were analyzed in the *Ypel4*-expressing nucleated erythroblast populations using FACS and measurement of total DNA content using PI. No significant cell cycle differences could be detected between the groups (Fig. 2G,H). Neither could any difference be detected in earlier erythroblast populations (Supplementary Figure S2C).

In order to further analyze the effects on cellular processes, RNA-sequencing was performed on sorted Poly-E (Fig. 2I) and Ortho-E (Fig. 2J) populations from *Ypel4*+/+ and *Ypel4*–/– mice. The quality of the data was

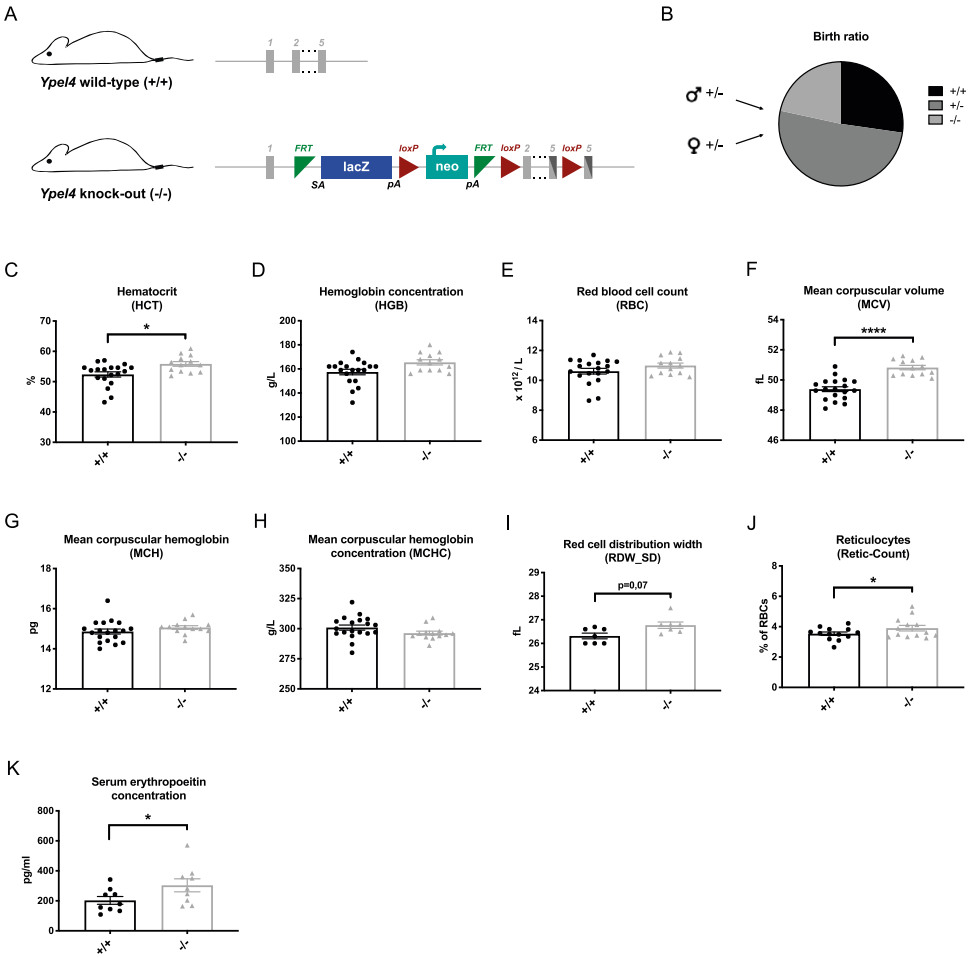

Figure 1. Disruption of the *Ypel4* gene results in a macrocytic secondary polycythemia. (**A**) Schematic of the *Ypel4* wild-type (+) and knockout (−) allele in the mouse model (image adapted from https://www.mousephenotype.org[49]). (**B**) Breeding statistics of breeding pairs carrying one wild-type and one knock-out allele (+/−) each (n = 19–45). (**C**) Peripheral blood analysis of hematocrit (HCT) (n = 13–19); (**D**) Hemoglobin concentration (HGB) (n = 13–19); (**E**) Red blood cell count (RBC) (n = 13–19); (**F**) Mean corpuscular volume (MCV) (n = 13–19); (**G**) Mean corpuscular hemoglobin (MCH) (n = 13–19); (**H**) Mean corpuscular hemoglobin concentration (MCHC) (n = 13–19) and (**I**) Red cell distribution width (RDW_SD) (n = 7) by utilization of a hematology analyzer. (**J**) Percentage of reticulocytes in total red blood cells as quantified by flow cytometry (n = 13). (**K**) Erythropoietin concentration in serum as detected by enzyme-linked immunosorbent assay (ELISA) (n = 9). Data displayed as average ± SEM, *P ≤ 0.05, ****P ≤ 0.0001.

confirmed by a principal component analysis. Of note, corresponding wild-type and *Ypel4*-null samples did not cluster separate (Supplementary Figure S2D). In line with these findings, except for the expected changes in expression of *Ypel4* and the gene trapping splice acceptor *En2*, only three genes were significantly differentially expressed (P ≤ 0.05) in either population (Supplementary Table S1). Two of these genes were considered to be straight-forward false positive discoveries (Supplementary Figure S2E–G).

To analyze extra-medullary hematopoiesis, spleens were examined by weight which showed no significant difference in *Ypel4*-null mice (Supplementary Figure S2H). To investigate extra-medullary erythropoiesis in

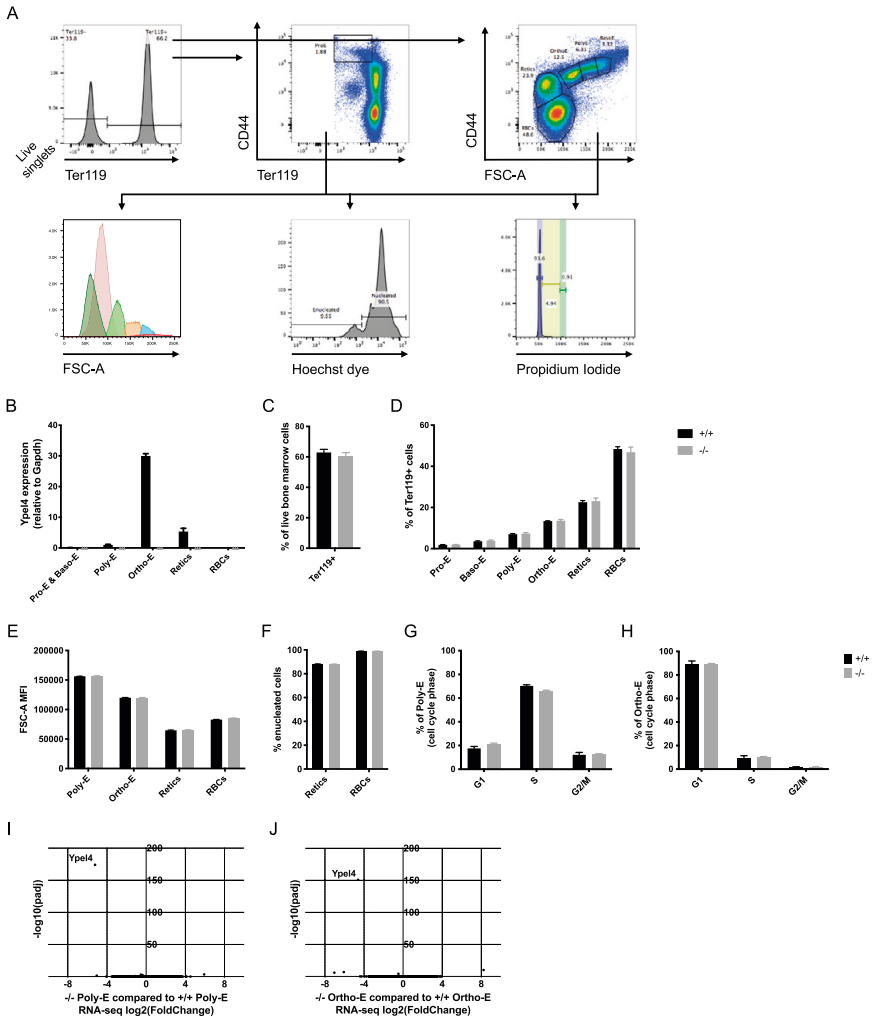

Figure 2. *Ypel4* is upregulated during terminal erythropoiesis but deficiency does not affect normal erythroid precursor functionality in bone marrow. (**A**) FACS gating strategy for bone marrow (BM) terminal erythroid cell populations in wild-type (+/+) and *Ypel4*-null (−/−) mice together with their forward scatter area (FSC-A) mean fluorescence intensity (MFI), Hoechst 33342 dye positivity and Propidium Iodide (PI) positivity after fixation. (**B**) *Ypel4* quantitative Polymerase Chain Reaction (qPCR) expression relative to *Gapdh* in sorted subpopulations (n = 3). (**C**) Total live erythroid cell (n = 4) and (**D**) subpopulation frequencies in BM (n = 4). (**E**) FSC-A MFI measurements as approximations of cell size in *Ypel4*-expressing subpopulations (n = 4). (**F**) Total enucleation efficiency as measured by lack of DNA staining using the cell-permeant Hoechst 33342 dye (n = 4). Cell cycle analysis by measurement of total DNA content (PI positivity) in the *Ypel4*-expressing (**G**) Poly-E (n = 3) and (**H**) Ortho-E (n = 3) populations after fixation. RNA-sequencing was conducted on sorted (**I**) Poly-E (n = 4) or (**J**) Ortho-E (n = 4) populations and differential gene expression presented using log2(fold change) and − log10(padj). Data displayed as average ± SEM. *Pro-E* proerythroblast, *Baso-E* basophilic erythroblast, *Poly-E* polychromatic erythroblast, *Ortho-E* orthochromatic erythroblast, *Retics* reticulocyte, *RBCs* red blood cells, *padj* adjusted p value.

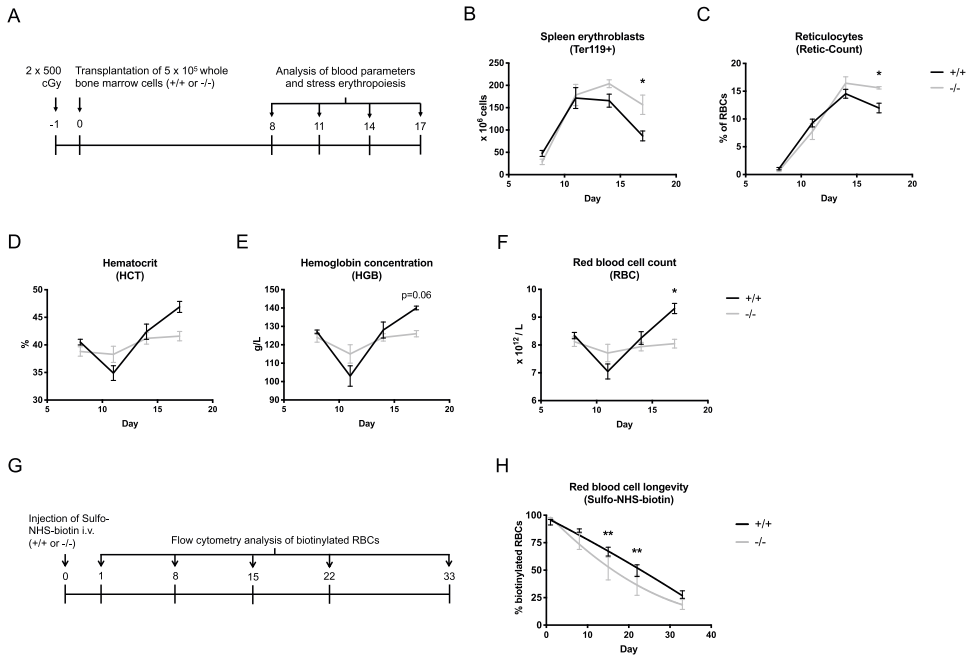

Figure 3. *Ypel4*-null hematopoietic cells display reduced anemia-recovering capacity due to an increased clearance of circulating erythrocytes. (**A**) Stress erythropoiesis was induced using lethal irradiation followed by transplantation of unfractionated wild-type (+/+) or *Ypel4*-null (−/−) bone marrow (BM) cells to +/+ recipients, followed by analysis of anemia recovery in spleen and peripheral blood (PB) at day 8, 11, 14 and 17. (**B**) Expansion of the Ter119+ erythroid fraction in spleen as quantified by cell counting and flow cytometry (n = 3). (**C**) Percentage of reticulocytes of total red blood cells as quantified by flow cytometry (n = 3). PB analysis of (**D**) hematocrit (HCT) (n = 3), (**E**) hemoglobin concentration (HGB) (n = 3) and (**F**) red blood cell (RBC) count (n = 3) by utilization of a hematology analyzer. (**G**) RBC longevity was analyzed by i.v. injection of Sulfo-NHS-biotin followed by flow cytometric quantification of biotinylated RBCs in PB at day 1, 8, 15, 22 and 33. (**H**) Percentage of biotinylated RBCs in PB over time with estimated clearance rates of wild-type (+/+) and *Ypel4*-null (−/−) RBCs (n = 5). Data displayed as average ± SEM, *P ≤ 0.05, **P ≤ 0.01, *i.v.* intravenous.

particular, flow cytometry and antibodies against Ter119 and CD71 were performed on spleens (Supplementary Figure S2I). Neither frequencies (Supplementary Figure S2J) nor total cell numbers (Supplementary Figure S2K) of early (CD71+Ter119+) or late (CD71−Ter119+) erythroid cells were significantly changed in *Ypel4*-null mice.

Taken together, in spite of high expression of *Ypel4* during late TED, disruption of *Ypel4* gene transcription does not significantly alter the late TED gene expression profile, erythroid precursor development, cell cycle or enucleation efficiency during steady-state erythropoiesis.

***Ypel4*-null hematopoietic cells display reduced anemia-recovering capacity due to an increased clearance of circulating erythrocytes.** Due to the increased serum erythropoietin levels but lack of distinct phenotype in steady-state TED, we hypothesized that the kinetics of *Ypel4*-deficiency might be accentuated in a situation of induced anemia. Stress-erythropoiesis was therefore induced using a lethal dose of whole-body irradiation followed by transplantation of 5×10^5 *Ypel4*+/+ or *Ypel4*−/− unfractionated BM cells (Ly5.2) to wild-type recipients (Ly5.1 + Ly5.2). Recovery was followed by analysis of PB, BM and spleen at day 8, 11, 14 and 17 after transplantation (Fig. 3A). Since spleen is the primary organ for stress-erythropoiesis in mice, we expected an early and robust response from spleen followed by a slower repopulation of the BM erythroid fraction[24].

Using flow cytometry and cell counting, the Ter119+ erythroid fraction in spleen and BM was analyzed and quantified. As expected, a rapid expansion of the erythropoietic activity in spleen was observed between day 8 and day 11 in both groups of mice. Interestingly, mice transplanted with *Ypel4*−/− BM however displayed a prolonged expansion phase, generating more erythroid progenitors in the spleen compared to the control (Fig. 3B). As expected, the BM displayed a slower recovery rate than that seen in the spleen, with no significant difference between *Ypel4*+/+ and −/−-transplanted mice (Supplementary Figure S3A).

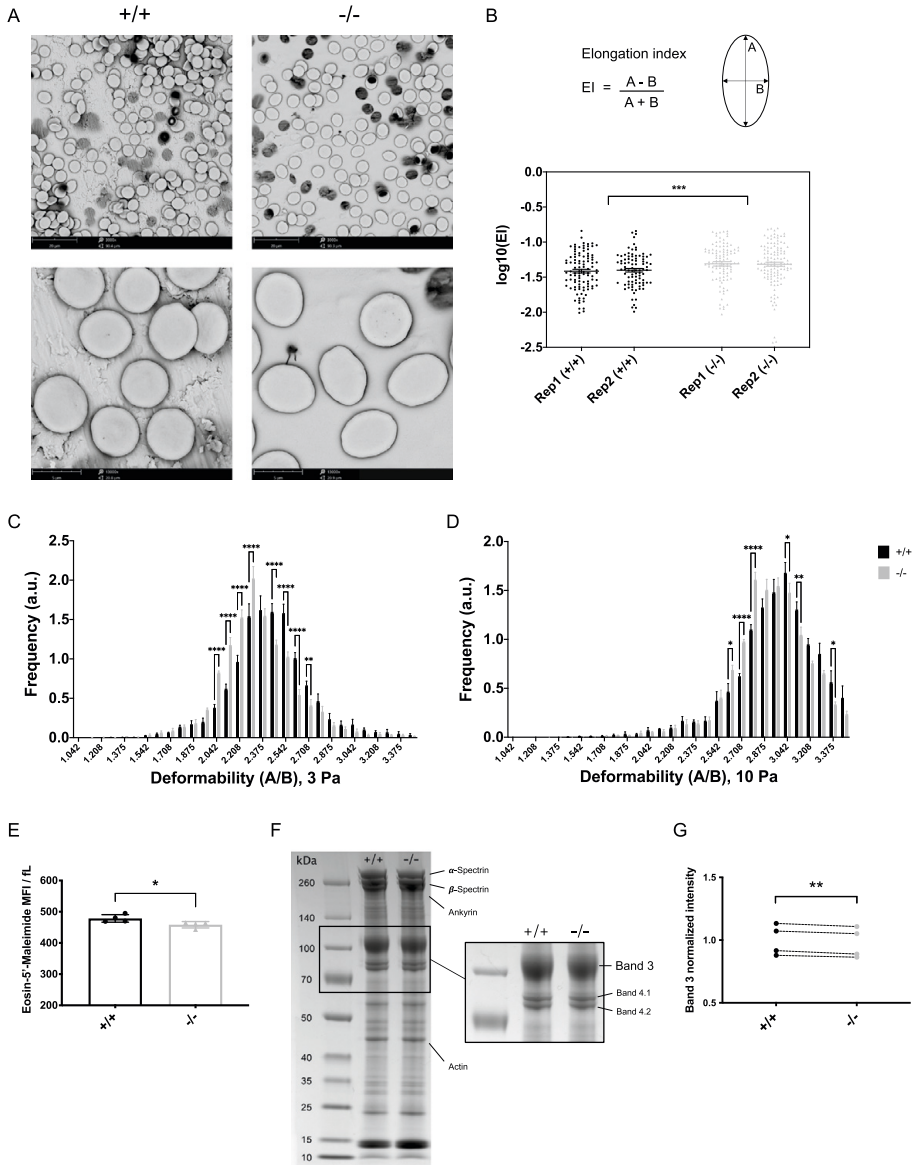
A
+/+
-/-
B
Elongation index
EI = (A - B) / (A + B)
A
B
log10(EI)
***
Rep1 (+/+)
Rep2 (+/+)
Rep1 (-/-)
Rep2 (-/-)
C
Frequency (a.u.)
Deformability (A/B), 3 Pa
D
Frequency (a.u.)
Deformability (A/B), 10 Pa
+/+
-/-
E
Eosin-5'-Maleimide MFI / fL
F
kDa
+/+
-/-
α-Spectrin
β-Spectrin
Ankyrin
Band 3
Band 4.1
Band 4.2
Actin
G
Band 3 normalized intensity

◂**Figure 4.** Erythrocytes from mice deficient in *Ypel4* are ovalocytic, less deformable and have reduced Band 3 protein levels. (**A**) Representative scanning electron micrographs of peripheral blood (PB) from wild-type (+/+) and *Ypel4*-null (−/−) mice. Micrographs taken at 3000× and 13,000× original magnification. (**B**) Isolated red blood cell (RBC) long and short axes were measured using ImageJ software and RBC elongation calculated using the elongation index (EI) formula $EI = (A - B)/(A + B)$ (n = 2). (**C**,**D**) Deformability of RBCs was measured using an Automated Rheoscope and Cell Analyzer (ARCA) applying 3 Pa (**C**; n = 4) or 10 Pa (**D**; n = 4) shear stress. The graphs show the frequency of cells (y-axis) with a specific deformability index, this index is measured as the ratio between length over width (x-axis). (**E**) PB analysis of Eosin-5′-Maleimide mean fluorescence intensity (MFI) in RBCs measured by flow cytometry. MFI values are normalized to mean corpuscular volume (MCV), as determined by a hematology analyzer, in each sample for accurate density assessment of Band 3 protein levels in the RBC membranes (n = 4). (**F**) RBCs were hemoglobin-depleted using hypotonic lysis. Membrane protein concentrations were measured and equal amounts of protein solubilized and separated by sodium dodecyl sulphate (SDS)-polyacrylamide gel electrophoresis (PAGE). Gels were fixed in ethanol and stained with Coomassie Blue G-250 dye to visualize proteins. Representative images of one +/+ and one −/− sample is shown, first with all visible bands and then with only Bands 3, 4.1 and 4.2 visible after further separation to emphasize the visible differences in band intensities. (**G**) Band 3 intensities were analyzed and normalized by total protein normalization using ImageJ software. Data displayed normalized to average wild-type ratio and a paired Student's *t* test was used to compare the means. Connecting lines depict age and gender matched +/+ and −/− samples (n = 4). All other data displayed as average ± SEM, *P ≤ 0.05, ** P ≤ 0.01, ***P ≤ 0.001, ****P ≤ 0.0001, *a.u.* arbitrary unit, *kDa* kilodalton.

To analyze the output of reticulocytes, peripheral blood was stained with Retic-Count reagent and RNA/DNA-positive red blood cells detected by flow cytometry. In line with the increased stress-erythropoiesis observed in the spleen, the *Ypel4*−/−-transplanted mice kept producing more reticulocytes for a significantly longer time compared to *Ypel4*+/+-transplanted mice (Fig. 3C).

In order to trace the development and recovery of the anemia after irradiation, blood parameters were quantified using a hematology analyzer. In spite of the increased output of erythroid progenitors in spleen and reticulocytes in PB, mice transplanted with *Ypel4*−/− BM failed to recover their HCT (Fig. 3D), HGB (Fig. 3E) and RBC (Fig. 3F) over time compared to *Ypel4*+/+-transplanted mice, indicating an increased clearance of *Ypel4*−/− erythrocytes. The WBC count recovered at a similar rate (Supplementary Figure S3B), while the platelet count recovery rate was significantly decreased in the *Ypel4*−/− compared to the *Ypel4*+/+-transplanted mice (Supplementary Figure S3C).

To directly measure RBC longevity and rate of clearance, wild-type and *Ypel4*-null mice were injected with Sulfo-NHS-biotin that binds to and biotinylates RBCs. Mice were bled at day 1, 8, 15, 22 and 33 and the percentage of biotinylated RBCs was measured by flow cytometry (Fig. 3G). As expected, the wild-type mice had an estimated linear clearance rate of RBCs (Fig. 3H, black line), while RBCs in *Ypel4*-null mice were cleared at a significantly higher rate (Fig. 3H).

Taken together, *Ypel4*-null hematopoietic cells are equally able to expand the erythroid progenitor pool and form reticulocytes during stress-erythropoiesis as their wild-type counterparts. However, when they reach the circulation, *Ypel4*-null RBCs are cleared from the blood at a much higher rate compared to wild-type RBCs, indicating a lesion linked to the functionality of RBCs rather than erythroid precursors.

Erythrocytes from mice deficient in *Ypel4* are ovalocytic, less deformable and have reduced Band 3 protein levels. Increased clearance of RBCs can be caused by different mechanisms[25]. Since YPEL family proteins have been observed to induce changes in cell morphology and the cytoskeleton[2,9], we hypothesized that the increased clearance could be caused by a defect in the red cell membrane skeleton. To study the morphology, scanning electron microscopy was utilized to obtain high resolution micrographs of single RBC surface topographies. Examination of the micrographs revealed the presence of abnormally shaped erythrocytes in the *Ypel4*-null samples, identified as ovalocytes (Fig. 4A). Indeed, when calculating the elongation index for isolated RBCs in the samples, the majority of *Ypel4*-null RBCs displayed increased elongation compared to wild-type RBCs. There were no indications of RBC subpopulations (Fig. 4B).

The presence of abnormally elongated RBCs in the blood is indicative of both increased clearance of RBCs and reduced membrane deformability[26,27]. An Automated Rheoscope and Cell Analyzer (ARCA) was therefore utilized to evaluate the ability of individual RBCs to deform during shear stress. Deformability was evaluated at two different shear forces: 3 Pa and 10 Pa. At 3 Pa, differences between groups are often most prominent while at 10 Pa cells become more deformed. In accordance with the morphological observations, *Ypel4*-null RBCs were significantly less deformable than wild-type RBCs at 3 Pa and there were no detected subpopulations in the different groups (Fig. 4C). Similarly, a significant difference was detected even at 10 Pa when cells were much more uniformly deformed (Fig. 4D). The area of individual RBCs was also measured, demonstrating that *Ypel4*-null RBCs had a significantly larger area compared to wild-type RBCs (Supplementary Figure S4A), confirming the MCV results from the hematology analyzer.

The red cell membrane skeleton is built from cytoskeletal proteins anchored to Band 3 multiprotein complexes in the RBC membrane[28]. Flow cytometric analysis of Eosin-5′-maleimide (EMA) predominant binding to the Band 3 protein on intact RBCs is a routinely used first-line diagnostic screening test for hereditary red cell membrane disorders[29]. In disorders such as Hereditary Spherocytosis a clear reduction in EMA MFI is normally detected, while variants of Hereditary Elliptocytosis generally display a lower degree of reduction. The volume of RBCs affects the MFI, so the ratio between EMA MFI and MCV is a critical comparison[29,30]. An EMA binding

test was therefore conducted together with hematology analyzer measurements of MCV. A slight but significant reduction in the EMA MFI to MCV ratio in *Ypel4*-null RBCs was detected (Fig. 4E).

The gold-standard technique to quantify relative membrane protein content is separation of solubilized and hemoglobin-depleted RBCs, so called RBC ghosts, by sodium dodecyl sulphate (SDS)-polyacrylamide gel electrophoresis (PAGE). The membrane proteins are visualized in the gel by Coomassie Brilliant Blue dye. Equal amounts of packed *Ypel4*-null and wild-type cells were loaded, and normalized intensities compared between matched samples (Fig. 4F, all samples shown in Supplementary Figure S4B). As indicated, Band 3 protein abundance in *Ypel4*-null RBC membranes was indeed slightly but significantly reduced compared to wild-type RBCs, confirming the results from the EMA binding test (Fig. 4G).

To elucidate if YPEL4 binds to the Band 3 protein directly, co-immunoprecipitation (Co-IP) was utilized to pull out YPEL4 protein complexes from primary erythroid cell lysates followed by quantitative liquid chromatography–mass spectrometry (LC–MS) analysis. Hematopoietic stem and progenitor (c-Kit+) cells from *Ypel4*−/− BM were transduced with either SFFV-FLAG-YPEL4 or SFFV-YPEL4-HA lentiviral overexpression vectors (Supplementary Figure S4C) and transplanted to lethally irradiated wild-type recipients. At day 16 after transplantation, recipients were sacrificed and total primary and erythroid cells in spleen recovered. Co-IPs cross-performed on cell lysates were analyzed by nano liquid chromatography–mass spectrometry (LC–MS) using a tandem mass tag (TMT) quantitative approach (Supplementary Figure S4D). Many proteins, including YPEL4, were detected as consistently enriched in the tagged compared to the control samples. The Band 3 protein however, even though detectable, was not amongst those (Supplementary Figure S4E, all detected proteins in Supplementary Table S2). These results provide support for the lack of physical interaction between YPEL4 and the Band 3 protein.

Taken together, erythrocytes from mice deficient in *Ypel4* are ovalocytic and less deformable than wild-type erythrocytes. This functional deficiency is associated with slightly reduced levels of Band 3 protein in the *Ypel4*-null RBC membranes, providing combined evidence for the presence of a mild red cell membrane disorder in the *Ypel4*-null mice. Lastly, strong indications are provided for an indirect effect of *Ypel4*-deficiency on Band 3 protein levels in RBC membranes.

Discussion

The roles of the highly conserved YPEL family genes in mammals have for a long time been elusive. Most previous studies have been performed in vitro in cell lines. Here we describe in detail the role of *Ypel4* during erythroid development using a knockout mouse model, providing for the first time insights into the physiological processes governed by *Ypel4* in vivo.

We demonstrated that *Ypel4*-deficiency leads to a secondary polycythemia in mice, with a slight increase in MCV that is accompanied by reticulocytosis. Since murine reticulocytes have around 45% more volume than erythrocytes[31], the observed reticulocytosis likely contributes to the increase seen in MCV. However, the increase in reticulocyte numbers alone is not sufficient to explain the observed macrocytosis, since it would have required that the *Ypel4*−/− mice had more than 10% reticulocytes, compared to the 3.90 ± 0.18% observed. This conclusion is also supported by data from the ARCA experiment, showing a general shift in size of the whole RBC population. The secondary polycythemia displayed in the mice relates to a clinical condition, where an increase in RBC mass is seen together with increased serum EPO concentration. This condition is considered either physiologically appropriate, if there is decreased tissue oxygenation, or physiologically inappropriate, if there is abnormal overproduction of EPO[32]. In bone marrow transplantation and RBC longevity assays, we demonstrated an intrinsic RBC lesion and increased clearance of *Ypel4*-null erythrocytes. Mice transplanted with *Ypel4*-null cells also failed to recover platelet counts at the same rate as controls, an expected side-effect to the lingering anemia since megakaryocytopenia occurs naturally during situations of hypoxia and active erythropoiesis[33]. Our findings together provide evidence for a physiologically appropriate secondary polycythemia in the *Ypel4*-null mice.

YPEL4 and all other YPEL family proteins have previously been hypothesized to affect cell cycle regulation and progression due to their localization to mitosis-related structures[3–5]. In this study, even though we show that *Ypel4*-deficiency leads to macrocytosis, which can be due to cell cycle defects[34], we do not detect a cell cycle defect in *Ypel4*-null erythroblasts. Our results, together with those from previous studies showing conflicting results regarding the effect of YPEL family proteins on cell cycle[5,35], shows that this gene family might emerge as one with a much wider range of mechanisms than originally predicted.

YPEL4 has also been shown to affect Elk-1 activity[4]. We, however, could not detect differences in Elk-1 target gene transcription in *Ypel4*-expressing bone marrow erythroblast populations. This negative finding is important for future studies aiming to investigate exactly how *YPEL4* affect Elk-1 activity. Of note, Elk-1 has been reported to acquire alternative functions during evolution[36]. It has also been uniquely reported to interact with neuronal microtubules[37], relating to previous findings of YPEL family proteins to co-localize with microtubule-related structures[3–5].

Despite the apparent lack of phenotype during TED, we could instead demonstrate that *Ypel4*-null RBCs were more elongated compared to normal RBCs with a resulting ovalocytic morphology. A discovery of changes in RBC morphology is a routine finding in the clinic when investigating a suspected red cell membrane disorder in a patient[26]. When further investigating the function of these altered RBCs, we found that they were cleared from the circulation at an increased rate and that they had reduced deformability. The Band 3 protein is fundamental in providing mechanical stability and deformability to the RBC, due to it being a major component in the macromolecular complexes serving as attachment points between the membrane and underlying cytoskeleton[38]. In various red cell membrane disorders, the Band 3 EMA MFI is affected negatively[39]. The results from the EMA binding test indicated a slight relative reduction of Band 3 protein levels in *Ypel4*-null RBC membranes. This reduction was confirmed by separation of solubilized RBC ghosts by SDS-PAGE. It remains an open question

if the observed 2.2–4.4% reduction in Band 3 protein levels is sufficient to cause the pathologic alterations seen in *Ypel4*-null RBCs. Of note, it has been shown that the Band 3 EMA MFI is negatively correlated with osmotic fragility, implying that disease severity correlates with the degree of signal reduction[40]. It is therefore possible that a slight relative reduction in Band 3 protein levels could cause a mild red cell membrane disorder, especially considering the concurrent existence of abnormal RBC morphology in the *Ypel4*-null mice. A full investigation of the RBC membrane protein composition, including known Band 3 interacting proteins, was not conducted and is a delimitation of this study that should be taken into consideration.

We could not identify evidence of a physical interaction between YPEL4 and the Band 3 protein when performing two different Co-IPs, suggesting an indirect effect of YPEL4 on Band 3 protein levels. The remaining candidate binding partners could provide clues for future studies. Even though not verified as physical binding partners, the consistent enrichment of both alpha- and beta-tubulin in all Co-IP samples could be of special interest in the light of previous reports of YPEL family proteins to co-localize with microtubule-related structures[3–5]. Our findings further relate to previous studies showing that *Ypel1* induces changes in cell morphology, the cytoskeleton and cell adhesion machinery[2], and *Ypel3* to be important for proper migration and morphology of perineural glia cells during neural development[9]. It is possible that redundancy between these highly similar YPEL proteins could attenuate the observed phenotype, although no changes in expression of other YPEL family genes could be detected in *Ypel4*-null erythroblasts.

In conclusion, we show that *Ypel4* is a highly specialized gene important for the integrity of the red cell membrane. We propose that through a putative indirect effect of *Ypel4*-deficiency, Band 3 protein levels are reduced in RBC membranes, likely contributing to the reduced membrane deformability, altered RBC morphology and increased clearance of RBCs in peripheral blood. These findings explain the observed secondary polycythemia in the *Ypel4*-null mice and provide evidence that the increase in hematocrit is a compensatory mechanism to secure proper tissue oxygenation. Further in-depth studies on the RBC membrane protein composition of the *Ypel4*-null mice might provide critical insights into the molecular function of *Ypel4* and the Yippee domain.

Methods

Mice. Mice were bred and maintained at the BMC animal facilities, Lund University, Sweden. The C57BL/6N-A^{tm1Brd} Ypel4$^{tm1a(EUCOMM)Wtsi}$/WtsiIeg (Ly5.2) knockout mouse model was obtained from the European Mouse Mutant Archive.

Anemia was induced by subjecting age and gender matched adult recipient mice (C57BL/6xB6SJL; Ly5.1 + Ly5.2) to a single or split dose of lethal irradiation of 1×900 or 2×500 cGy, followed by bone marrow (BM) transplantation to rescue and trigger stress erythropoiesis. For analysis of recovery after anemia, 5×10^5 unfractionated wild-type (+/+) or knockout (−/−) BM cells were transplanted intravenously (i.v.) by tail vein injection. The recipients were bled and sacrificed at either 8, 11, 14 or 17 days after transplantation for analysis of peripheral blood (PB), spleen and BM. For analysis of YPEL4 binding partners, 10^5 transduced cKit + BM cells (−/−) were transplanted i.v. by tail vein injection. The recipients were sacrificed at day 16 after transplantation for recovery of primary erythroid cells in spleen.

For all types of blood analysis, PB was collected from the tail vein and analyzed according to described procedure.

For determination of blood parameters, PB was collected to EDTA coated Microvette tubes (Sarstedt, Nümbrecht, Germany) and analyzed on a KX-21N hematology analyzer (Sysmex, Kobe, Japan).

For determination of RBC longevity, an EZ-Link Sulfo-NHS-Biotin (Thermo Fisher Scientific, Waltham, MA, USA) solution was prepared in PBS, sterile-filtered and 3 mg administered i.v. by tail vein injection to each recipient at day 0. At day 1, 8, 15, 22 and 33 after injection, recipients were bled for analysis.

All procedures involving mice were approved by the Animal Ethics Committee of Malmö/Lund, Sweden and all experiments were performed in accordance with relevant guidelines and regulations. The reporting in the manuscript follows the recommendations in the ARRIVE guidelines.

Enzyme-linked immunosorbent assay (ELISA). The Mouse Erythropoietin Quantikine® ELISA Kit (R&D Systems, Minneapolis, MN, USA) was used to detect serum erythropoietin (EPO) levels. Blood was collected to Eppendorf tubes without anticoagulant, and left at room temperature for one hour prior to being centrifuged at 2000*g*. Serum supernatant was collected and prepared according to manufacturer's protocol. Samples were analyzed on SPECTROstar nano (BMG Labtech, Ortenberg, Germany). A standard curve was generated by four parameter logistic (4-PL) curve-fit to determine protein concentration of samples. Optical density was determined at 450 nm with a correction at 570 nm.

Cell preparations and flow cytometry. BM and spleens were homogenized and filtered to single cell suspensions prior to cell culture, flow cytometry analysis or cell sorting (FACS).

For flow cytometry and FACS, the following conjugated antibodies against murine epitopes were used: CD44 (Clone IM7, APC) (BioLegend, San Diego, CA, USA), CD71 (Clone C2, PE) (BD Biosciences, San Jose, CA, USA), Ter119 (PE-Cy7) (eBioscience; Thermo Fisher Scientific), CD3 (Clone 145-2C11, PE-Cy5) (BioLegend), B220 (Clone RA3-6B2, PE-Cy5) (BioLegend) and Gr-1 (Clone RB6-8C5, PE-Cy5) (BioLegend). Fc receptor block (BD Biosciences) was used for sorting samples, dead cells were excluded using propidium iodide (PI) and enucleation was determined using Hoechst 33342 (Thermo Fisher Scientific).

Reticulocyte levels were determined by resuspending PB in BD Retic-Count (BD Biosciences) according to manufacturer's protocol.

Biotinylated RBCs were detected with Streptavidin-conjugated PE-Cy7 (BioLegend).

Eosin-5′-Malemide (EMA) binding test was performed by resuspension of PB in EMA dye (Sigma-Aldrich, Saint Louis, MO, USA) according to manufacturer's protocol.

Since erythroid precursors are very sensitive to fixation, cells from each of the nucleated erythroblast populations were sorted using FACS prior to fixation and staining for cell cycle analysis. Cell pellets were fixed with ice cold 70% ethanol in PBS while vortexing and incubated at − 20 °C overnight. The fixed cells were washed with PBS and stained with PI staining buffer [0.1% TritonX100 (Sigma-Aldrich), 0.1% Sodium citrate, 40 µg/ml PI, 500 µg/ml RNase A (Sigma-Aldrich)] for 30 min at 37 °C. PI intensity was analyzed individually in the sorted populations by flow cytometry analysis.

Flow cytometry analyses were performed on BD FACS Calibur or LSR II (BD Biosciences). FACS was performed on BD FACS Aria IIu or III (BD Biosciences). Results were analyzed with FlowJo 10 software (Tree Star, Ashland, OR, USA).

RNA isolation and gene expression analysis. Total RNA was extracted from cells using RNeasy Kit (QIAGEN, Hilden, Germany) according to manufacturer's protocol. Genomic DNA was removed using DNase I on-column digestion (QIAGEN).

For quantitative PCR (qPCR), complementary DNA from the isolated RNA was synthesized using the Superscript III Reverse Transcriptase (Invitrogen; Thermo Fisher Scientific) with random hexamers (Invitrogen; Thermo Fisher Scientific). Quantitation was performed on a 7900HT RT-PCR instrument (Applied Biosystems; Thermo Fisher Scientific) using the Mm.PT.58.9019795 (*Ypel4*) and Mm.PT.39a.1 (*Gapdh*) probes (Integrated DNA Technologies, Coralville, IA, USA).

For global gene expression, RNA concentration and integrity were measured using Agilent RNA Pico Kit on a Bioanalyzer Instrument (Agilent Genomics, Santa Clara, CA, USA). RNA sequencing libraries were prepared using TruSeq RNA Library Preparation Kit v2 (Illumina, San Diego, CA, USA) according to manufacturer's standard protocol and the sequencing was performed using NextSeq 500/550 Mid Output v2 Kit, 150 cycle (Illumina). Fastq files were processed using the nf-core Nextflow pipeline for RNAseq *nf-core/rnaseq* v1.4.2[41,42]. Reads were mapped against GRCm38 reference genome. Differentially expressed genes were found using DESeq2[43]. Visual exploration and analysis of normalized sequencing data was performed using the Integrative Genomics Viewer software[44].

Scanning electron microscopy (SEM). PB specimens were fixed with 2.5% glutaraldehyde in 150 mM sodium cacodylate pH 7.2 and adhered to a poly-L-lysine coated surface. They were washed with cacodylate buffer and dehydrated with an ascending ethanol series from 50% (v/v) to absolute ethanol. The specimens were then subjected to critical-point drying with carbon dioxide and absolute ethanol was used as an intermediate solvent. The tissue samples were mounted on aluminum holders, sputtered with 20 nm palladium/gold, and examined in a DELPHI correlative light and scanning electron microscope. Isolated RBC long and short axes were measured using ImageJ software[45] and RBC elongation calculated using the elongation index (EI) formula $EI = (A - B)/(A + B)$.

Automated Rheoscope and Cell Analyzer (ARCA). RBC deformability was measured with an ARCA and analyzed using automated cell framing software as described previously[46]. In short, morphological response to shear stress was measured at 3 Pa and 10 Pa. A minimum of 3000–4000 cells were measured and grouped in 30 bins according to increasing elongation or cell projection area (as a measure of membrane surface area). The elongation was calculated as the major cell radius divided by minor cell radius.

Preparation of hemoglobin-depleted RBC ghosts. Equal volumes of packed cells were resuspended in ice cold PBS with added Halt Protease and Phosphatase Inhibitor Cocktail (Thermo Fisher Scientific), centrifuged cold at 2000*g* for 20 min and resuspended in 5 mM Na-Phosphate solution with added cOmplete Protease Inhibitor Cocktail (Sigma-Aldrich) to induce hypotonic lysis and generate RBC ghosts. The centrifugation and resuspension steps were repeated six times with the final centrifugation step prolonged with 10 min. The resulting hemoglobin-depleted RBC ghosts were resuspended in appropriate amount of Na-Phosphate solution with added protease inhibitors and membrane protein concentration determined using the Pierce 660 nm protein assay (Thermo Fisher Scientific) on a Nanodrop 1000 Spectrophotometer (Thermo Fisher Scientific).

Sodium dodecyl sulphate (SDS)-polyacrylamide gel electrophoresis (PAGE) and staining. Equal amounts of protein were solubilized and boiled in 2× Laemmli sample buffer (Bio-Rad Laboratories, Hercules, CA, USA) with 5% 2-Mercaptoethanol, then separated by sodium dodecyl sulphate (SDS)-polyacrylamide gel electrophoresis (PAGE). Gels were fixed in 30% ethanol, 2% v/v of 85% phosphoric acid overnight, washed 2 × 10 min in 2% (v/v) of 85% phosphoric acid and equilibrated for 30 min in 2% (v/v) of 85% phosphoric acid, 18% ethanol and 15% (w/v) ammonium sulphate. Equilibrated gels were stained with 0.2% Coomassie Blue G-250 dye (Sigma-Aldrich) for at least 30 min until proteins were visualized, analyzed in a ChemiDoc XRS+ with ImageLab software (Bio-Rad Laboratories) and band intensities quantified using ImageJ software[45].

Statistical analysis. All statistical significance, except where else stated, has been analyzed using either paired or non-paired Student's *t* tests, Chi-square goodness of fit tests, nested *t* tests, one-way ANOVAs or 2-way ANOVAs followed by Tukey's multiple comparisons test depending on experiments and groups compared. P values were adjusted for multiple comparisons where applicable. $^{*}P \leq 0.05$, $^{**}P \leq 0.01$, $^{***}P \leq 0.001$, $^{****}P \leq 0.0001$.

Additional methods. For details about genotyping, staining procedures, molecular cloning and lentivirus production, cell culture, co-immunoprecipitation and proteomics, please refer to Supplementary Methods.

Data availability

The RNA-seq data discussed in this publication have been deposited in NCBI's Gene Expression Omnibus[47] and are accessible through GEO Series accession number GSE171959. The mass spectrometry proteomics data have been deposited to the ProteomeXchange Consortium via the PRIDE[48] partner repository with the dataset identifier PXD025242.

Received: 7 May 2021; Accepted: 22 July 2021
Published online: 05 August 2021

References

1. Roxstrom-Lindquist, K. & Faye, I. The Drosophila gene Yippee reveals a novel family of putative zinc binding proteins highly conserved among eukaryotes. *Insect Mol. Biol.* **10**, 77–86. https://doi.org/10.1046/j.1365-2583.2001.00239.x (2001).
2. Farlie, P. *et al.* Ypel1: A novel nuclear protein that induces an epithelial-like morphology in fibroblasts. *Genes Cells* **6**, 619–629. https://doi.org/10.1046/j.1365-2443.2001.00445.x (2001).
3. Hosono, K., Sasaki, T., Minoshima, S. & Shimizu, N. Identification and characterization of a novel gene family YPEL in a wide spectrum of eukaryotic species. *Gene* **340**, 31–43. https://doi.org/10.1016/j.gene.2004.06.014 (2004).
4. Liang, P. *et al.* MVP interacts with YPEL4 and inhibits YPEL4-mediated activities of the ERK signal pathway. *Biochem. Cell Biol.* **88**, 445–450. https://doi.org/10.1139/o09-166 (2010).
5. Hosono, K. *et al.* YPEL5 protein of the YPEL gene family is involved in the cell cycle progression by interacting with two distinct proteins RanBPM and RanBP10. *Genomics* **96**, 102–111. https://doi.org/10.1016/j.ygeno.2010.05.003 (2010).
6. Kelley, K. D. *et al.* YPEL3, a p53-regulated gene that induces cellular senescence. *Cancer Res.* **70**, 3566–3575. https://doi.org/10.1158/0008-5472.CAN-09-3219 (2010).
7. Lee, J. Y. *et al.* Pro-apoptotic role of the human YPEL5 gene identified by functional complementation of a yeast moh1Delta mutation. *J. Microbiol. Biotechnol.* **27**, 633–643. https://doi.org/10.4014/jmb.1610.10045 (2017).
8. Zhang, J. *et al.* YPEL3 suppresses epithelial–mesenchymal transition and metastasis of nasopharyngeal carcinoma cells through the Wnt/beta-catenin signaling pathway. *J. Exp. Clin. Cancer Res.* **35**, 109. https://doi.org/10.1186/s13046-016-0384-1 (2016).
9. Blanco-Sanchez, B. *et al.* Yippee like 3 (ypel3) is a novel gene required for myelinating and perineurial glia development. *PLoS Genet.* **16**, e1008841. https://doi.org/10.1371/journal.pgen.1008841 (2020).
10. Flygare, J., Rayon Estrada, V., Shin, C., Gupta, S. & Lodish, H. F. HIF1alpha synergizes with glucocorticoids to promote BFU-E progenitor self-renewal. *Blood* **117**, 3435–3444. https://doi.org/10.1182/blood-2010-07-295550 (2011).
11. An, X. *et al.* Global transcriptome analyses of human and murine terminal erythroid differentiation. *Blood* **123**, 3466–3477. https://doi.org/10.1182/blood-2014-01-548305 (2014).
12. Kingsley, P. D. *et al.* Ontogeny of erythroid gene expression. *Blood* **121**, e5–e13. https://doi.org/10.1182/blood-2012-04-422394 (2013).
13. Hruz, T. *et al.* Genevestigator v3: A reference expression database for the meta-analysis of transcriptomes. *Adv Bioinform.* **2008**, 420747. https://doi.org/10.1155/2008/420747 (2008).
14. Dzierzak, E. & Philipsen, S. Erythropoiesis: Development and differentiation. *Cold Spring Harb. Perspect. Med.* **3**, a011601. https://doi.org/10.1101/cshperspect.a011601 (2013).
15. Hattangadi, S. M., Wong, P., Zhang, L., Flygare, J. & Lodish, H. F. From stem cell to red cell: Regulation of erythropoiesis at multiple levels by multiple proteins, RNAs, and chromatin modifications. *Blood* **118**, 6258–6268. https://doi.org/10.1182/blood-2011-07-356006 (2011).
16. Stephenson, J. R., Axelrad, A. A., McLeod, D. L. & Shreeve, M. M. Induction of colonies of hemoglobin-synthesizing cells by erythropoietin in vitro. *Proc. Natl. Acad. Sci. U.S.A.* **68**, 1542–1546. https://doi.org/10.1073/pnas.68.7.1542 (1971).
17. Gregory, C. J. & Eaves, A. C. Three stages of erythropoietic progenitor cell differentiation distinguished by a number of physical and biologic properties. *Blood* **51**, 527–537 (1978).
18. Gregory, C. J. & Eaves, A. C. Human marrow cells capable of erythropoietic differentiation in vitro: Definition of three erythroid colony responses. *Blood* **49**, 855–864 (1977).
19. Pop, R. *et al.* A key commitment step in erythropoiesis is synchronized with the cell cycle clock through mutual inhibition between PU.1 and S-phase progression. *PLoS Biol.* https://doi.org/10.1371/journal.pbio.1000484 (2010).
20. Gautier, E. F. *et al.* Comprehensive proteomic analysis of human erythropoiesis. *Cell Rep.* **16**, 1470–1484. https://doi.org/10.1016/j.celrep.2016.06.085 (2016).
21. An, X. & Mohandas, N. Erythroblastic islands, terminal erythroid differentiation and reticulocyte maturation. *Int. J. Hematol.* **93**, 139–143. https://doi.org/10.1007/s12185-011-0779-x (2011).
22. Hardy, S., Legagneux, V., Audic, Y. & Paillard, L. Reverse genetics in eukaryotes. *Biol. Cell* **102**, 561–580. https://doi.org/10.1042/BC20100038 (2010).
23. Liu, J. *et al.* Quantitative analysis of murine terminal erythroid differentiation in vivo: Novel method to study normal and disordered erythropoiesis. *Blood* **121**, e43–e49. https://doi.org/10.1182/blood-2012-09-456079 (2013).
24. Singbrant, S., Mattebo, A., Sigvardsson, M., Strid, T. & Flygare, J. Prospective isolation of radiation induced erythroid stress progenitors reveals unique transcriptomic and epigenetic signatures enabling increased erythroid output. *Haematologica* **105**, 2561–2571. https://doi.org/10.3324/haematol.2019.234542 (2020).
25. Phillips, J. & Henderson, A. C. Hemolytic anemia: Evaluation and differential diagnosis. *Am. Fam. Physician* **98**, 354–361 (2018).
26. Narla, J. & Mohandas, N. Red cell membrane disorders. *Int. J. Lab. Hematol.* **39**(Suppl 1), 47–52. https://doi.org/10.1111/ijlh.12657 (2017).
27. Huisjes, R. *et al.* Squeezing for life—Properties of red blood cell deformability. *Front. Physiol.* **9**, 656. https://doi.org/10.3389/fphys.2018.00656 (2018).
28. van den Akker, E., Satchwell, T. J., Williamson, R. C. & Toye, A. M. Band 3 multiprotein complexes in the red cell membrane; of mice and men. *Blood Cells Mol. Dis.* **45**, 1–8. https://doi.org/10.1016/j.bcmd.2010.02.019 (2010).
29. King, M. J. *et al.* Using the eosin-5-maleimide binding test in the differential diagnosis of hereditary spherocytosis and hereditary pyropoikilocytosis. *Cytom. B Clin. Cytom.* **74**, 244–250. https://doi.org/10.1002/cyto.b.20413 (2008).
30. Ciepiela, O., Adamowicz-Salach, A., Bystrzycka, W., Lukasik, J. & Kotula, I. Mean corpuscular volume of control red blood cells determines the interpretation of eosin-5′-maleimide (EMA) test result in infants aged less than 6 months. *Ann. Hematol.* **94**, 1277–1283. https://doi.org/10.1007/s00277-015-2377-0 (2015).
31. de Jong, K. *et al.* Short survival of phosphatidylserine-exposing red blood cells in murine sickle cell anemia. *Blood* **98**, 1577–1584. https://doi.org/10.1182/blood.v98.5.1577 (2001).

32. Hocking, W. G. & Golde, D. W. Polycythemia: Evaluation and management. *Blood Rev.* **3**, 59–65. https://doi.org/10.1016/0268-960x(89)90026-x (1989).
33. Cullen, W. C. & McDonald, T. P. Effects of isobaric hypoxia on murine medullary and splenic megakaryocytopoiesis. *Exp. Hematol.* **17**, 246–251 (1989).
34. Sankaran, V. G. *et al.* Cyclin D3 coordinates the cell cycle during differentiation to regulate erythrocyte size and number. *Genes Dev.* **26**, 2075–2087. https://doi.org/10.1101/gad.197020.112 (2012).
35. Baker, S. J. Small unstable apoptotic protein, an apoptosis-associated protein, suppresses proliferation of myeloid cells. *Cancer Res.* **63**, 705–712 (2003).
36. Somma, M. P. *et al.* Moonlighting in mitosis: Analysis of the mitotic functions of transcription and splicing factors. *Cells* https://doi.org/10.3390/cells9061554 (2020).
37. Demir, O., Korulu, S., Yildiz, A., Karabay, A. & Kurnaz, I. A. Elk-1 interacts with neuronal microtubules and relocalizes to the nucleus upon phosphorylation. *Mol. Cell. Neurosci.* **40**, 111–119. https://doi.org/10.1016/j.mcn.2008.10.004 (2009).
38. Salomao, M. *et al.* Protein 4.1R-dependent multiprotein complex: New insights into the structural organization of the red blood cell membrane. *Proc. Natl. Acad. Sci. U.S.A.* **105**, 8026–8031. https://doi.org/10.1073/pnas.0803225105 (2008).
39. King, M. J. *et al.* Rapid flow cytometric test for the diagnosis of membrane cytoskeleton-associated haemolytic anaemia. *Br. J. Haematol.* **111**, 924–933 (2000).
40. Stoya, G., Gruhn, B., Vogelsang, H., Baumann, E. & Linss, W. Flow cytometry as a diagnostic tool for hereditary spherocytosis. *Acta Haematol.* **116**, 186–191. https://doi.org/10.1159/000094679 (2006).
41. Ewels, P. A. *et al.* The nf-core framework for community-curated bioinformatics pipelines. *Nat. Biotechnol.* **38**, 276–278. https://doi.org/10.1038/s41587-020-0439-x (2020).
42. Di Tommaso, P. *et al.* Nextflow enables reproducible computational workflows. *Nat. Biotechnol.* **35**, 316–319. https://doi.org/10.1038/nbt.3820 (2017).
43. Love, M. I., Huber, W. & Anders, S. Moderated estimation of fold change and dispersion for RNA-seq data with DESeq2. *Genome Biol.* **15**, 550. https://doi.org/10.1186/s13059-014-0550-8 (2014).
44. Robinson, J. T. *et al.* Integrative genomics viewer. *Nat. Biotechnol.* **29**, 24–26. https://doi.org/10.1038/nbt.1754 (2011).
45. Schneider, C. A., Rasband, W. S. & Eliceiri, K. W. NIH Image to ImageJ: 25 years of image analysis. *Nat. Methods* **9**, 671–675. https://doi.org/10.1038/nmeth.2089 (2012).
46. Dobbe, J. G., Streekstra, G. J., Hardeman, M. R., Ince, C. & Grimbergen, C. A. Measurement of the distribution of red blood cell deformability using an automated rheoscope. *Cytometry* **50**, 313–325. https://doi.org/10.1002/cyto.10171 (2002).
47. Edgar, R., Domrachev, M. & Lash, A. E. Gene Expression Omnibus: NCBI gene expression and hybridization array data repository. *Nucleic Acids Res.* **30**, 207–210. https://doi.org/10.1093/nar/30.1.207 (2002).
48. Perez-Riverol, Y. *et al.* The PRIDE database and related tools and resources in 2019: Improving support for quantification data. *Nucleic Acids Res.* **47**, D442–D450. https://doi.org/10.1093/nar/gky1106 (2019).
49. Dickinson, M. E. *et al.* High-throughput discovery of novel developmental phenotypes. *Nature* **537**, 508–514. https://doi.org/10.1038/nature19356 (2016).

Acknowledgements

This work was supported by grants from the Ragnar Söderberg Foundation (M96/13) and the Swedish Research Council (2017-02483). AM and TS are Ph.D. candidates at Lund University. This work is submitted in partial fulfillment of the requirement for the Ph.D. The authors would like to thank the personnel at the Lund Stem Cell Center FACS Core and Vector Facilities, Sven Kjellström and Hong Yan at the BioMS Lund node and Maria Baumgarten at the IQ Biotechnology Platform at Lund University, Lund, Sweden, for their expert technical assistance. We would also like to thank Rob van Zwieten and Martijn Veldthuis at Sanquin Diagnostics, Amsterdam, The Netherlands, for the expert technical assistance with the ARCA. Lastly, we would like to thank Jörg Cammenga and Björn Nilsson for intellectual input.

Author contributions

J.F. and A.M. conceived the study; A.M., Ma.Jä., J.H., Sh.So., So.Si., E.A. and J.F. designed experiments; A.M., T.S., Ma.Ja., K.P., I.P.G.-A., A.G.A. and R.R. performed experiments; A.M. analyzed the data and performed statistical analysis; S.L. and Sh.So. performed statistical analysis on the sequencing data; Ma.Ja. and K.P. performed initial proteomic data analysis, A.M. wrote the manuscript and all authors have commented on the final draft.

Funding

Open access funding provided by Lund University.

Competing interests

The authors declare no competing interests.

Additional information

Supplementary Information The online version contains supplementary material available at https://doi.org/10.1038/s41598-021-95291-1.

Correspondence and requests for materials should be addressed to J.F.

Reprints and permissions information is available at www.nature.com/reprints.

Publisher's note Springer Nature remains neutral with regard to jurisdictional claims in published maps and institutional affiliations.

Yippee like 4 (*Ypel4*) is essential for normal mouse red blood cell membrane integrity

Alexander Mattebo,[1] Taha Sen,[1] Maria Jassinskaja,[2] Kristýna Pimková,[2] Isabel Prieto González-Albo,[1] Abdul Ghani Alattar,[1] Ramprasad Ramakrishnan,[3] Stefan Lang,[2] Marcus Järås,[3] Jenny Hansson,[2] Shamit Soneji,[2] Sofie Singbrant,[1] Emile van den Akker,[4] and Johan Flygare*[1]

[1]Division of Molecular Medicine and Gene Therapy, Lund Stem Cell Center, Lund University, Sweden; [2]Division of Molecular Hematology, Lund Stem Cell Center, Lund University, Sweden; [3]Division of Clinical Genetics, Faculty of Medicine, Lund University, Sweden; and [4]Sanquin Research, Department of Hematopoiesis, Amsterdam, The Netherlands, and Landsteiner Laboratory, Academic University Medical Center, University of Amsterdam, Amsterdam, The Netherlands

*Correspondence: Johan Flygare, BMC A12, 221 84 Lund, Sweden; e-mail: johan.flygare@med.lu.se; phone number: +46 46 222 06 87; fax number: +46 46 222 05 68.

Supplementary Appendix

Supplementary Methods

DNA isolation and genotyping

Genomic DNA was prepared from mice ear marking samples and used as template for genotyping by PCR. A combination of one forward and two reverse primer oligonucleotides (5' to 3') were used to assess the genotype of mice progeny: Ypel4_222829_F GACCAGAGGACCAGATGCTAGG, Ypel4_222829_R GCCTTGAGTGCAACATCACC and CAS_R1_Term TCGTGGTATCGTTATGCGCC. The Ypel4_222829_F and Ypel4_222829_R primers amplifies a 406 basepair (bp) fragment with the wild-type (+) allele as template but fails to amplify a PCR fragment with the Ypel4$^{tm1a(EUCOMM)Wtsi}$ mutant (-) allele due to the inserted LacZ cassette. The Ypel4_222829_F and CAS_R1_Term primers amplifies a 292 bp fragment with the Ypel4$^{tm1a(EUCOMM)Wtsi}$ mutant allele but not with the wild-type allele, since the reverse primer anneals to a sequence in the inserted LacZ cassette. Gel electrophoresis was utilized for visualization of PCR products.

Cytospin and May-Grünwald-Giemsa staining

Cells were cytocentrifuged using Shandon Cytospin 3 (Block Scientific, Inc., NY, USA) at 350 rpm for 2 minutes. Giemsa solution was prepared by diluting Giemsa stock solution (Histolabs, Gothenburg, Sweden) to 5% in distilled water. Air-dried slides were stained in May-Grünwald solution (Merck, Darmstadt, Germany) for 5 minutes and then transferred to the Giemsa solution for 10 minutes. The slides were finally washed twice in distilled water and allowed to dry before examination under the microscope.

Molecular cloning and production of lentiviral vectors

The self-inactivating lentiviral vectors used in this study were derived from the SFFV-RPS19 vector.[1] *Ypel4* cDNA from murine fetal liver was inserted downstream of the spleen focus-forming virus (SFFV) promoter, either with FLAG (SFFV-FLAG-YPEL4) or HA (SFFV-YPEL4-HA) tag fused to the N-terminus or C-terminus of the protein coding sequence, respectively. Following the *Ypel4* cDNA, an internal

ribosomal entry site (IRES) and the protein coding sequence for EGFP was used as reporter of gene expression. Lentiviral vectors were produced by the Vector Unit at Lund University as described previously.[1]

Cell culture and lentiviral transductions

Singularized BM cell suspensions were enriched for cKit+ cells using CD117 MicroBeads and a magnetic-activated cell sorting (MACS) separation column (Miltenyi Biotech, Bergisch Gladbach, Germany) according to manufacturer's instructions. Purified cKit+ cells were resuspended in StemSpan serum-free expansion medium (SFEM) (Stem Cell Technologies, Vancouver, Canada) supplemented with 1% penicillin/streptomycin (P/S) (Cytiva, Marlborough, MA, USA), 20 ng/mL murine interleukin-3 (mIL-3) (PeproTech, Rocky Hill, NJ, USA), 20 ng/mL human thrombopoietin (hTPO) (PeproTech), 100 ng/mL murine stem cell factor (mSCF) (PeproTech), 2 U/mL human erythropoietin (EPO) (LEO Pharma, Ballerup, Denmark) and 100 nM Dexamethason (Sigma-Aldrich, Saint Louis, MO, USA).

Newly seeded cells were transduced at a multiplicity of infection (MOI) of 7.5 using 5 μg/mL polybrene transfecting agent (Merck Millipore, Burlington, MA, USA), incubated for 6 hours at 37°C and 5% CO_2 and transduced a second time with the same MOI before continued incubation overnight. The next day, samples were washed twice with PBS supplemented with 2% fetal bovine serum (FBS) (Thermo Fisher Scientific, Waltham, MA, USA) before transplantation.

Co-immunoprecipitation (Co-IP)

$4x10^7$ snap-frozen spleen cells were dissolved in ice-cold lysis buffer consisting of PBS, 0.5% Igepal CA-630 (Sigma-Aldrich) and added Halt Protease and Phosphatase Inhibitor Cocktail (Thermo Fisher Scientific). Cell remnants and nuclei were removed by centrifugation at 10 000g for 5 minutes and supernatant taken in equal volumes for Co-IP. Anti-HA magnetic beads (Thermo Fisher Scientific) and Anti-FLAG M2 magnetic beads (Sigma-Aldrich) were used for Co-IP according to manufacturer's instructions. The protein complexes were eluted from the beads by resuspension in 2x Laemmli sample buffer (Bio-Rad Laboratories, Hercules, CA, USA) with 5% 2-Mercaptoethanol (Sigma-Aldrich). Samples were boiled for 10 minutes at 95°C, then

separated by sodium dodecyl sulphate (SDS)-polyacrylamide gel electrophoresis (PAGE) for a short time until all samples were 1-2 cm in the gels. Gels were fixed and stained in 1:4:5 v/v of acetic acid: Milli-Q H_2O: methanol with 0.1% Coomassie Blue R-250 dye (Sigma-Aldrich) for 2 hours in room temperature (RT) before destaining in 1:3:6 v/v of acetic acid: methanol: Milli-Q H_2O overnight in 4°C. After destaining, each sample was cut out from the gel separately into 1x1 mm^2 cubes and transferred to new tubes, then centrifuged briefly before processing for proteomics analysis.

Proteomics sample preparation

In the presented study we combined in-gel digestion with chemical TMT labeling. The method was adapted from Schmidt et al.[2] with slight modifications. Gel pieces were washed with acetonitrile (ACN) and 200 mM triethylammonium bicarbonate TEAB/ACN (1:1 v/v) until they became colorless. Gel pieces were dried in a speed-vac and re-hydrated in 50 mM TEAB/10 mM dithiothreitol. Samples were incubated in a thermomixer for 50 minutes at 56°C to reduce disulfide bonds. Reduced thiols were blocked by addition of iodoacetamide (final concentration 22.5 mM) and incubation at RT for 30 minutes in the dark. Gel pieces were washed several times in 50 mM TEAB to remove remaining reagents. Washed pieces were dried and rehydrated in 25 mM TEAB. Trypsin was added at a final concentration of 0.02 $\mu g/\mu l$ and proteins were digested overnight at 37°C. Tryptic peptides were extracted by washing gel-pieces with 1% formic acid/2% ACN (v/v) followed by 50% ACN in LC-MS grade water. Peptide concentration was estimated using NanoDrop. Supernatant containing tryptic peptides was dried completely. Extracted peptides were dissolved in 50 mM TEAB. TMT labeling using TMT6plex reagents was performed in accordance with manufacturer's protocol. Immediately before use, TMT label reagents were equilibrated to room temperature. Vials containing 0.8 mg of TMT label were dissolved in 41 μL of anhydrous ACN. Dissolved TMT labels were added to the dissolved peptides at the ratio recommended by the supplier. Samples were incubated for 1 hour at 37°C. Reaction was stopped by addition of 5% hydroxylamine to the samples. Samples representing biological replicate and their negative controls were combined, dried completely, re-dissolved in 0.1% TFA and

cleaned-up using C18 micro-spin columns. Desalted samples were dissolved in 4% ACN/0.1% formic acid and 1 μg was injected for nanoLC-MS.

Liquid Chromatography- Mass Spectrometry (LC-MS) analysis

MS analyses were carried out on an Orbitrap Fusion Tribrid MS system (Thermo Scientific) equipped with a Proxeon Easy-nLC 1000 (Thermo Fisher) on a 120-minute linear gradient separation followed by synchronous precursor selection MS3 (SPS-MS3) method. Each sample was injected twice. Injected peptides were trapped on an Acclaim PepMap C18 column (3 μm particle size, 75 μm inner diameter x 20 mm length, nanoViper fitting). After trapping, gradient elution of peptides was performed on an Acclaim PepMap RSLC C18 100 Å column (2 μm particle size, 75 μm inner diameter x 250 mm length, nanoViper fitting). The mobile phases for LC separation were 0.1% (v/v) formic acid in LC-MS grade water (solvent A) and 0.1% (v/v) formic acid in ACN (solvent B). Peptides were first loaded with a constant flow of solvent A at 9 µl/min onto the trapping column. Subsequently, peptides were eluted via the analytical column at a constant flow of 300 nl/min. During the elution step, the percentage of solvent B was increased in a linear fashion from 5% to 10% in 2 minutes, then increased to 25% in 85 minutes and finally to 60% in an additional 20 minutes. The peptides were introduced into the mass spectrometer via a stainless steel nano-bore emitter (150 μm OD x 30 μm ID; 40 mm length; Thermo Fisher Scientific) and a spray voltage of 2.0 kV was applied. The capillary temperature was set at 275°C.

The mass spectrometer was operated in data-dependent mode. First full MS scan was performed in the Orbitrap in the range of m/z 380 to 1580 and at resolution 120000 FWHM using automatic gain control (AGC) setting 4.0e5 and a maximum ion accumulation time of 50 ms. The top ten most intense ions selected in first MS scan were isolated for ion trap collision-induced dissociation MS2 (CID-MS2) at a precursor isolation window width of 0.7 m/z using AGC setting 1.5e4 and a maximum ion accumulation time of 50ms. The CID energy was set to 35%. Directly following each MS2 experiment, the top ten most intense fragment ions in an m/z range of 400-1200 were selected for high energy collisional-induced dissociation MS3 (HCD-MS3). The MS3 scan range was 100-500 m/z, the fragment ion isolation

width was set to 2 m/z, the AGC was 1.0e5 and the maximum ion time 120 ms. Normalized collision energy was set to 55%.

Proteomic data analysis

MS raw data were processed using Proteome Discoverer (version 2.2; Thermo Scientific). All raw files were processed together in a single run. Enzyme was set to trypsin and a maximum of two missed cleavages were allowed. Carbamidomethylation was set as a fixed modification; methionine oxidation and acetylation of protein amino-terminus were selected as variable modifications. The derived peak list was searched using the Sequest HT node against the Swissprot mouse database (version 2017.07.05; 25 170 protein entries) together with commonly observed contaminants and reversed sequences for all entries. Precursor and fragment mass tolerance were set to 10 ppm and 0.6 Da, respectively. Unique and razor peptides were used for quantification. The co-isolation threshold was set to 75. A 1% false discovery rate (FDR) was required at both the protein level and the peptide level. Contaminants and reverse hits were excluded. Protein quantification was evaluated based on corrected TMT reporter ion intensities.

References

1 Jaako, P. *et al*. Gene therapy cures the anemia and lethal bone marrow failure in a mouse model of RPS19-deficient Diamond-Blackfan anemia. *Haematologica* **99**, 1792-1798, doi:10.3324/haematol.2014.111195 (2014).

2 Schmidt, C. & Urlaub, H. iTRAQ-labeling of in-gel digested proteins for relative quantification. *Methods Mol Biol* **564**, 207-226, doi:10.1007/978-1-60761-157-8_12 (2009).

3 Boehm, J. S. *et al*. Integrative genomic approaches identify IKBKE as a breast cancer oncogene. *Cell* **129**, 1065-1079 (2007).

4 Robinson, J. T. *et al*. Integrative genomics viewer. *Nat Biotechnol* **29**, 24-26, doi:10.1038/nbt.1754 (2011).

Supplementary Table Legends

Supplementary Table S1. RNA-seq of poly- and orthochromatic bone marrow erythroblasts in wild-type and *Ypel4*-null mice. The spreadsheet contains lists of expressed genes in the different sequenced erythroblast populations as well as information about differentially expressed between wild-type and *Ypel4*-null samples found using DESeq2. Gene symbol, log2 Fold Change (*Ypel4*-/- compared to *Ypel4*+/+), p value, adjusted p value and -log10 (adjusted p value) are shown in the gene lists.

Supplementary Table S2. Proteins detected in quantitative LC-MS analysis after co-immunoprecipitation of YPEL4 tagged by FLAG and HA. The spreadsheet contains a list of all detected proteins in the proteomic data analysis together with comparable protein abundance measurements from all analyzed samples.

Supplementary Figure Legends

Supplementary Figure S1. *Ypel4* transcription is efficiently disrupted in *Ypel4*-null mice and affects red blood cell parameters only. (A) Representative separation of gel electrophoresis genotype Polymerase Chain Reaction products: a single 406 basepair (bp) band represents a wild-type (+/+) genotype, one 406 and one 292 bp band represents a heterozygous (+/-) genotype and a single 292 bp band represents a homozygous (-/-) genotype. (B) Visual exploration and analysis of the *Ypel4* gene disruption using RNA sequencing of orthochromatic erythroblasts and Integrative Genomics Viewer software[3] (n=4). Peripheral blood analysis of (C) white blood cell count (WBC) (n=13-19) and (D) platelet count (PLT) (n=13-19). Data displayed as average ± SEM.

Supplementary Figure S2. Erythroblast morphology and transcriptomes are unaffected in *Ypel4*-null mice. (A) Representative light microscopy images of May-Grünwald-Giemsa stained cytospins of sorted Ter119+ erythroblast subpopulations from wild-type (+/+) or *Ypel4*-null (-/-) bone marrow. Original magnification x1000. (B) Forward scatter area mean fluorescence intensity measurements as approximations of cell size in early Ter119+ subpopulations (n=4). (C) Cell cycle analysis by measurement of total DNA content (Propidium Iodide positivity) in early Ter119+ subpopulations after fixation. (D) Principal Component Analysis of RNA sequenced samples (n=4). Visualization of mapped RNA sequencing reads from *Ypel4*-expressing erythroblast populations to the (E, F) *Gm19426* and (G) *Lrrc8d* gene loci using Integrative Genomics Viewer software (n=4).[4] (H) Spleen weight as percentage of total body weight (n=5). (I) Flow cytometry gating strategy for analysis of extra-medullary erythropoiesis in *Ypel4*-null mouse spleen. (J) Frequencies and (K) total cell numbers of early (CD71+Ter119+) and late (CD71-Ter119+) erythroid cells (n=5). Data displayed as average ± SEM, Pro-E: proerythroblast, Baso-E: basophilic erythroblast, Poly-E: polychromatic erythroblast, Ortho-E: orthochromatic erythroblast.

Supplementary Figure S3. Ter119+ bone marrow and white blood cell count recover normally after transplantation of *Ypel4*-null hematopoietic cells. (A) Expansion of the Ter119+ erythroid niche in bone marrow (BM) after transplantation

of unfractionated wild-type (+/+) or *Ypel4*-null (-/-) BM cells to lethally irradiated mice at day 8, 11, 14 and 17, as quantified by cell counting and flow cytometry (n=3). Peripheral blood analysis of (B) white blood cell (WBC) and (C) platelet (PLT) count recovery after transplantation, by utilization of a hematology analyzer (n=3). Data displayed as average ± SEM, *P≤0.05.

Supplementary Figure S4. The Band 3 protein is not detected as a binding partner to YPEL4. (A) Red blood cells (RBC) were subjected to shear stress (10 Pa) using an Automated Rheoscope and Cell Analyzer with single cell resolution. Masking software (See Methods) was used to calculate the area (μM) of the deformed RBC (n=4). (B) RBCs were hemoglobin-depleted using hypotonic lysis. Membrane protein concentrations were measured and equal amounts of protein solubilized and separated by sodium dodecyl sulphate (SDS)-polyacrylamide gel electrophoresis (PAGE). Gels were fixed in ethanol and stained with Coomassie Blue G-250 dye to visualize proteins (n=4). (C) Plasmid maps of the SFFV-FLAG-YPEL4 and SFFV-YPEL4-HA overexpression vectors used for the co-immunoprecipitation (Co-IP) experiments, visualized using SnapGene® software (from Insightful Science; available at snapgene.com). (D) Stress erythropoiesis was induced using lethal irradiation followed by transplantation of 10^5 transduced c-Kit+ *Ypel4*-null (-/-) bone marrow (BM) cells to wild-type recipients. At day 16 after transplantation, recipients were sacrificed and primary erythroid cells in spleen recovered, Co-IPs cross-performed on cell lysates and tandem mass tag (TMT) chemical labeling performed to utilize the possibility of quantitative liquid chromatography- mass spectrometry (LC-MS) analysis through synchronous precursor selection (SPS)-MS3 method. (E) Enriched proteins in tagged compared to control Co-IP samples, filtered based on positive enrichment in all biological replicates. Mean imputation was utilized to replace missing values (n=3 for anti-FLAG, n=2 for anti-HA). Data displayed as average ± SEM, **P≤0.01, ***P≤0.001.

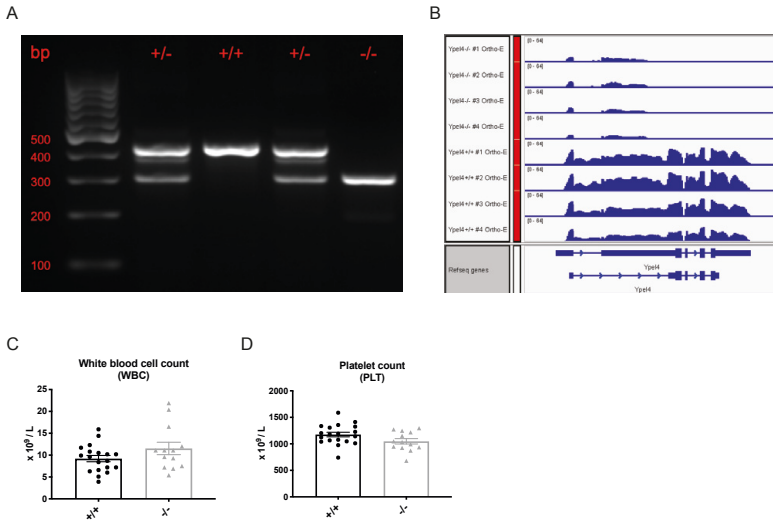

Supplementary Figure S1. ***Ypel4*** **transcription is efficiently disrupted in** ***Ypel4*****-null mice and affects red blood cell parameters only.**

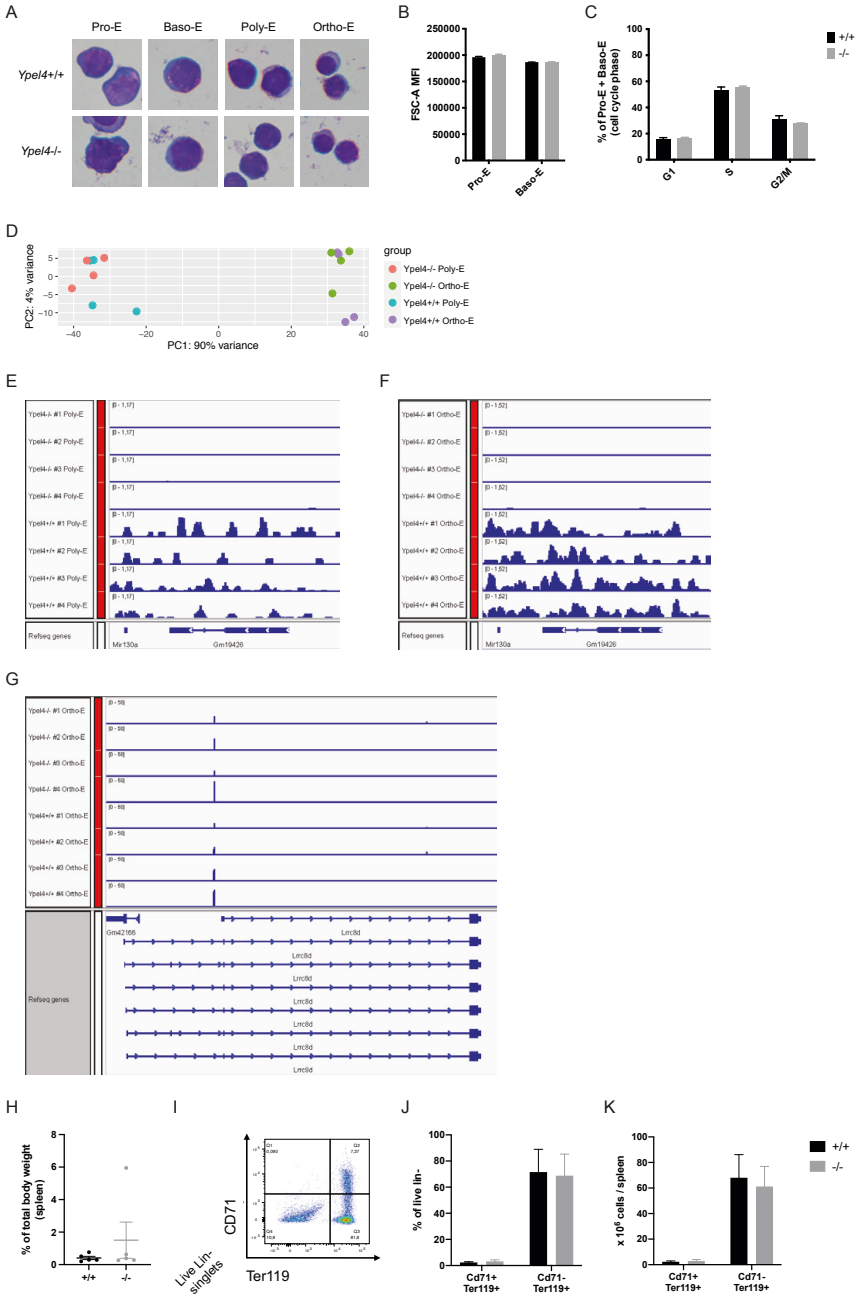

Supplementary Figure S2. Erythroblast morphology and transcriptomes are unaffected in *Ypel4*-null mice.

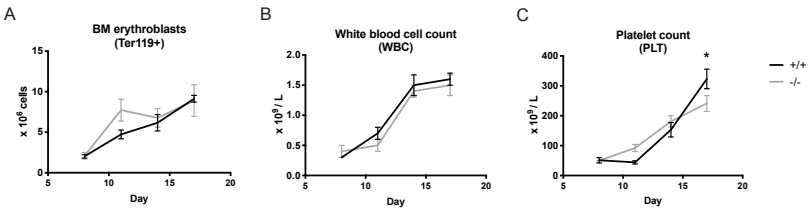

Supplementary Figure S3. Ter119+ bone marrow and white blood cell count recover normally after transplantation of *Ypel4*-null hematopoietic cells.

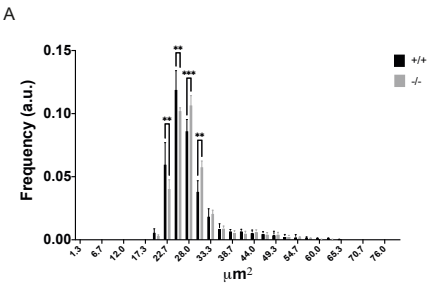

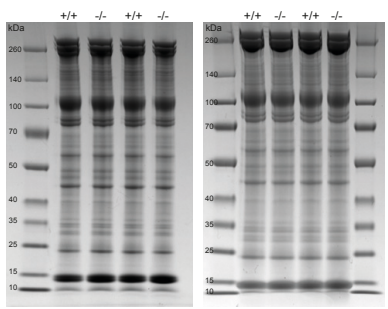

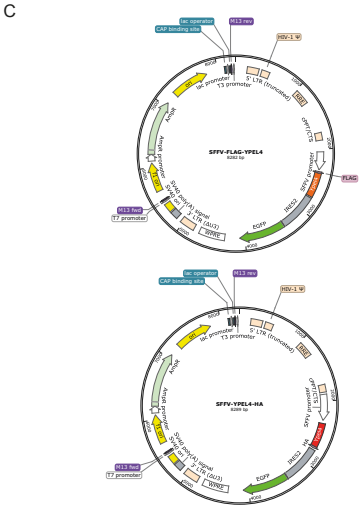

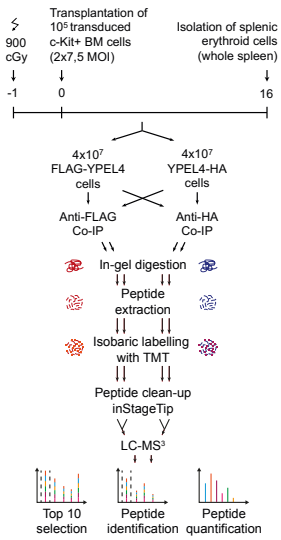

E

Accession	Gene name	Average log2(FLAG/HA) Anti-FLAG Co-IP	Average log2(HA/FLAG) Anti-HA Co-IP
Q0VEE5	**Ypel4**	**1,921**	**0,837**
Q6ZWV7	Rpl35	0,162	0,925
Q03265	Atp5a1	0,122	0,523
Q8BMJ3	Eif1ax	0,226	0,383
D3YYV8	Rpl5	0,234	0,423
Q6ZWZ6	Rps12	0,294	0,347
Q3V3K3	Taok3	0,066	0,539
Q9JHJ0	Tmod3	0,520	0,068
G5E8R2	Tpm1	0,274	0,342
P99024	Tubb5	0,172	0,401
Q54AH9	Hbb-b2	0,209	0,331
Q5U222	Ddx5	0,147	0,408
P05213	Tuba1b	0,142	0,385
Q3UW40	Rpl24	0,019	0,348
Q9CWI9	Rps23	0,159	0,318
Q9WUM5	Suclg1	0,275	0,135
P51175	Ppox	0,113	0,288
Q9DB77	Uqcrc2	0,358	0,088
Q642K0	Myl6	0,233	0,094
Q3UDS0	Hspa8	0,182	0,167
S4R1N6	Rps18	0,123	0,232
P14206	Rpsa	0,207	0,085
Q99LE6	Abcf2	0,139	0,074

Supplementary Figure S4. The Band 3 protein is not detected as a binding partner to YPEL4